EPA 910-R-15-001c

United States Environmental Protection Agency
Region 10
1200 Sixth Avenue
Seattle WA 98101
Alaska
Idaho
Oregon
Washington
Office of Environmental Assessment

October 2015

Combined WRF/MMIF/ AERCOARE/AERMOD Overwater Modeling Approach for Offshore Emission Sources

Volume 3 – Analysis of AERMOD Performance Using Weather Research and Forecasting Model Predicted Meteorology and Measured Meteorology in the Arctic

Combined WRF/MMIF/ AERCOARE/AERMOD Overwater Modeling Approach for Offshore Emission Sources

Volume 3 – Analysis of AERMOD Performance Using Weather Research and Forecasting Model Predicted and Measured Meteorology in the Arctic

EPA Contract No. EP-W09-028
Work Assignment No. M12PG00033R

Prepared for:
U.S. Environmental Protection Agency
Region 10
1200 Sixth Avenue
Seattle, WA 98101

and

U.S. Department of the Interior
Bureau of Ocean Energy Management
45600 Woodland Road
Sterling, VA 20166

Prepared by:
Ramboll Environ US Corporation
773 San Marin Drive, Suite 2115
Novato, CA, 94998

and

Amec Foster Wheeler
Environmental & Infrastructure, Inc.
4021 Stirrup Creek Dr., Suite 100
Durham, NC 27703

October 2015

The Region 10 Project Officer for the Interagency Agreement No. M12PGT00033R and EPA contract number EP-W-09-028 was Herman Wong with technical support provided by Robert Kotchenruther, PhD and Robert Elleman, PhD. From BOEM, the Project Officer was Eric J. Wolvovsky and the Technical Coordinator was Ronald Lai, PhD. The Project Lead for the prime contractor Amec Foster Wheeler was James Paumier while Project Lead for subcontractor RAMBOLL ENVIRON was Ken Richmond. Peer review of draft Volume 2 and/or draft Volume 3 was provided by Steven Hanna, PhD of Hanna Consultants, Robert Paine, CCM of AECOM and Christopher Lindsey, Shell Exploration and Production. Their reviews and comments are greatly appreciated by R10 and BOEM.

The collaboration study was funded in part by the U.S. Department of the Interior, Bureau of Ocean Energy Management, Environmental Studies Program, Washington DC, and the U.S. Environmental Protection Agency, Region 10, Seattle, WA.

DISCLAIMER

The opinions, findings, conclusions, or recommendations expressed in this report are those of the authors and do not necessarily reflect the view of the U.S. Environmental Protection Agency or the U.S. Department of the Interior, Bureau of Ocean Energy Management, nor does the mention of trade names or commercial products constitute endorsement or recommendation for use by the Federal Government.

PREFACE

The recommended American Meteorological Society/Environmental Protection Agency Regulatory Model (AERMOD) dispersion program continues to be studied for assessing air quality concentration impacts from emission sources located at overwater locations under an Interagency Agreement (IA) Number M12PGT00033R dated 9 August 2012 between the U.S. Environmental Protection Agency (EPA), Region 10 and the U.S. Department of the Interior (DOI), Bureau of Safety and Environmental Enforcement (BSEE) on behalf of the Bureau of Ocean Energy Management (BOEM). Specifically, the work scope under the IA calls for Region 10 and BOEM to (1) assess the use of AERMOD as a replacement for the Offshore and Coast Dispersion (OCD) model in a near-source (< 1,000 meters source-receptor distance) ambient air quality impact analysis for sea surface based emission sources and (2) evaluate the use of Weather Research and Forecasting (WRF) model predicted meteorology with AERMOD in lieu of overwater meteorological measurements from platforms and buoys.

Results of the Region 10/BOEM collaboration study are described in a three volume report. Volume 1 describes all six tasks completed under the IA. However, only a summary of the work completed under Task 2 and Task 3 appears in Volume 1. Volume 2 and Volume 3 provides a detailed description of the work in Task 2 and Task 3, respectively. The six tasks are:

Task 1. Evaluation of two Outer Continental Shelf Weather Research and Forecasting Model Simulations

Task 2. Evaluation of Weather Research and Forecasting Model Simulations for Five Tracer Gas Studies with AERMOD

Task 3. Analysis of AERMOD Performance Using Weather Research and Forecasting Model Predicted Meteorology and Measured Meteorology in the Arctic

Task 4. Comparison of Predicted and Measured Mixing Heights

Task 5. Development of AERSCREEN for Arctic Outer Continental Shelf Application

Task 6. Collaboration Study Seminar

Prior to the collaboration study, Region 10 on 1 April 2011 approved the use of the Coupled Ocean-Atmosphere Response Experiment (COARE) air-sea flux algorithm with AERMOD to preprocess overwater measured meteorological data from platforms and buoys. Initially, the preprocessing of the overwater measurements was done manually with COARE. Subsequently, Region 10 funded a study that was completed in September 2012 that coded the COARE air-sea flux procedure into a meteorological data preprocessor program called AERMOD-COARE (AERCOARE). The AERCOARE program was uploaded to the EPA Support Center for Regulatory Atmospheric Modeling (SCRAM) website on 23 May 2013 as a beta option for case-by-case approval by EPA regional offices.

[Blank]

TABLE OF CONTENTS

LIST OF FIGURES

LIST OF TABLES

[Blank]

LIST OF ABBREVIATIONS AND ACRONYMS

AERC ..... WRF meteorology extraction cases processed by AERCOARE
AERMIC ..... American Meteorological Society/Environmental Protection Agency Regulatory Model Improvement Committee
AERMOD ..... American Meteorological Society/Environmental Protection Agency Regulatory Model
AERCOARE ..... AERMOD-COARE
ASTD ..... Air-Sea Temperature Difference
AIDJEX ..... Arctic Ice Dynamics Joint Experiment

B ..... Bowen ratio
BOEM ..... Bureau of Ocean Energy Management
BSSE ..... Bureau of Safety and Environmental Enforcement

c ..... Model constant
c_o ..... Observed concentration value
c_p ..... Predicted concentration value
$\bar{c}$ ..... Average concentration value
c_n ..... nth highest concentration
°C ..... Degrees Centigrade
COARE ..... Coupled Ocean Atmospheric Response Experiment

DOI ..... Department of the Interior

ECMWF ..... European Center for Medium-Range Weather Forecasting
EPA ..... Environmental Protection Agency
ERA ..... ECMWF Reanalysis Project
ERA-40 ..... ERA 45-year global atmospheric reanalysis
ERA-I ..... ECMWF Re-Analysis project global atmospheric reanalysis
eta ..... Vertical pressure coordinate in WRF

f ..... Coriolis parameter
FF2 ..... Fraction-factor-of-two
FNMOC ..... Fleet Numerical Meteorology and Oceanography Center

g ..... Grams

H ..... Sensible heat flux

ISC3 ..... Industrial Source Complex 3

K ..... Degrees kelvin
kg ..... Kilograms
km ..... Kilometers

L ..... Monin-Obukhov length
LCC ..... Lambert Conformal Conic

m..... Meters
METSTAT ..... Meteorological Statistics
MG..... Geometric mean bias
MIXH..... PBL height or “mixing height”
MMIF ..... Mesoscale Model Interface Program
MYJ ..... Mellor-Yamada-Janjic PBL parameterization scheme used in WRF

NAAQS ..... National Ambient Air Quality Standards
NARR ..... North-American Regional Reanalysis
NBDC ..... National Buoy Data Center
NCAR ..... National Center for Atmospheric Research
NCEP..... National Center for Environmental Prediction
NOAA ..... National Oceanic and Atmospheric Administration
NSR ..... New Source Review

O..... Observed value
OBS, obs ..... Label for observation-based AERMOD simulations
OCD..... Offshore and Coastal Dispersion
OCS..... Outer Continental Shelf
OLM..... Ozone Limited Method

P ..... Sea level atmospheric pressure (also used to indicate “predicted” value in statistical calculations)
p ..... Predicted value
PBL..... Planetary boundary layer
PFL..... Profile file input to AERMOD
PRIME ..... Plume Rise Model Enhancements
PVMRM ..... Plume Volume Molar Ratio Method

Q-Q..... Quantile-Quantile (statistical plot)

r ..... Albedo
RCALF..... Label for WRF-MMIF AERMOD simulations where PBL height was not recalculated by MMIF
RCALT..... Label for WRF-MMIF AERMOD simulations where PBL height was recalculated MMIF
r_g ..... Geometric correlation coefficient
RH ..... Relative humidity
RHC..... Robust High Concentration

RMSE ..... Root Mean Square Error
RPO..... Regional Planning Organization
RTG..... Real Time Global sea-surface temperature analysis (from NCEP)

s..... Seconds
SFC ..... AERMOD surface meteorology input file
SST..... Sea Surface Temperature

T ..... Temperature
TKE..... Turbulent Kinetic Energy, Thermal Kinetic Energy
TMS..... Total Model Score statistical measure

U..... Zonal wind component
UW-PBL ..... University of Washington Shallow Convection PBL
u_*..... Friction velocity

V..... Meridional wind component
VG ..... Geometric variance
VPTLR..... Virtual Potential Temperature Lapse Rate

w_*..... Convective scaling velocity

W..... Watts
WD..... Wind direction
WRF ..... Weather Research and Forecasting
WS..... Wind Speed

YSU ..... Yonsei University

z..... Height above the surface
z_o ..... Surface roughness length
z_{ic} ..... Convective PBL height
z_{im} ..... Mechanical PBL height

°..... Degrees angular
μ_g ..... Geometric mean
σ_Θ..... Standard deviation of wind direction
σ_w..... Standard deviation of vertical wind speed
ψ..... Stability correction parameter

[Blank]

1 INTRODUCTION

This study aims to evaluate alternative methods for supplying meteorological variables to the American Meteorological Society/Environmental Protection Agency Regulatory Model (AERMOD) for regulatory air quality modeling of sources located over the ocean. It is hypothesized, given an appropriate overwater meteorological dataset, AERMOD can be used for New Source Review (NSR) following the same procedures as used for sources over land. A summary of all the elements of the study is contained within Volume I. Volume II summarizes Task 2 of the study which focused on evaluation of AERMOD against historical tracer study measurements using meteorology inputs derived from Weather Research and Forecasting (WRF) model datasets. Similarly, Volume 3 summarizes Task 3 of this study and focuses on evaluation of AERMOD using WRF and observational meteorology datasets over the Chukchi and Beaufort Seas along the Arctic coasts of Alaska. Like the Task 2 methodology, Task 3 evaluates a combined modeling approach where the meteorological variables are provided by WRF, processed by a combination of the Mesoscale Model Interface Program (MMIF)[1] and optionally, the AERMOD-Coupled Ocean-Atmosphere Response Experiment (COARE) or AERMOD-COARE (AERCOARE)[2]. WRF meteorology is used to drive AERMOD for several test cases. The results are compared to results of AERMOD driven by meteorological observations.

The purpose of this study is to provide evidence to help answer some of the following questions:

- How well does WRF predict overwater surface meteorology in the Arctic?
- Are pollutant concentrations predicted by AERMOD driven by WRF meteorology as conservative as those predicted by AERMOD driven by meteorological measurements?
- What WRF modeling configurations and meteorology extraction methods provide the best AERMOD inputs?
- How sensitive is AERMOD to differences between the WRF meteorology and observations for simulations of typical OCS sources?

A WRF meteorological dataset suitable for dispersion modeling in the Arctic was developed for this study. WRF meteorology is extracted from the WRF output files and used to drive AERMOD simulations for ice-free periods of 2009-2012, where overwater-based observational datasets were available. Results from the observation-based and WRF-based AERMOD simulations are compared and contrasted in an attempt to answer these questions.

Meteorological observation datasets from four overwater locations were obtained for this study. Two of the locations were in the Beaufort Sea and two were in the Chukchi Sea. Data were

[1] MMIF-Beta provided as a “related” alternative software for regulatory dispersion modeling by the U.S. EPA at the website: http://www.epa.gov/scram001/dispersion_related.htm

[2] AERCOARE is made publically available by the U.S. EPA at the website: http://www.epa.gov/ttn/scram/dispersion_related.htm

available at these locations for various time-spans during the ice-free summer and autumn periods of 2010, 2011, and 2012. The 2010-2012 periods were selected to overlap previous modeling efforts and to take advantage of the vertical temperature profiler data collected at Endeavor Island during this period. The profiler was a passive microwave radiometer operating from 2010 to 2012 at the offshore Endeavor Island facility near Prudhoe Bay, Alaska. The profiler data were used to assist in the estimates of atmospheric planetary boundary layer (PBL) height at each of the sites. The term “PBL height” is used to indicate the height or depth of the mixing layer and is synonymous with “mixing height.”

This report summarizes the methodology and results for each element of the Task 3 investigation, including:

i) The methodology used for the WRF simulations
ii) Evaluation of the WRF performance
iii) The methodologies used to prepare AERMOD meteorology from both the observational datasets and the WRF simulations.
iv) The AERMOD modeling approach and methodology.
v) Evaluation of the AERMOD results and comparisons of observation-based and WRF-based AERMOD results.
vi) Examination of the influence of the meteorological data on AERMOD performance.

2 ARCTIC WRF SIMULATIONS

Mesoscale atmospheric modeling of the Arctic is challenging in many regards. The region is characterized by a climate prone to extremes. Very cold winter temperatures, powerful cyclones, and extreme overwater surface inversions are typical features of the weather and climate in the region. Modeling of the surface energy balance is challenging considering unique features such as seasonal ice cover, frozen tundra ground surfaces, and solar insolation extremes. These extremes may result in conditions beyond the capabilities or bounds of the parameterization schemes used in WRF.

2.1 Polar WRF

The Ohio State University Polar Meteorology Group has developed a polar-optimized version of WRF, “Polar WRF.” This version of the model was developed to improve WRF Arctic modeling capabilities (Hines & Bromwich, 2008)(Bromwich, et al., 2009). Their modifications have focused on optimizing the surface energy budget and parameterization of sea-ice and permanent ice surfaces within the Noah land surface model (Chen, et al., 1997). The modifications have included implementation of a variable sea-ice and snow thickness and seasonally-variable sea-ice albedo. Polar WRF was used for this study.

The WRF simulations were run using the Mellor-Yamada-Janjic (MYJ) (Mellor & Yamada, 1982)(Janjic, 1994) PBL parameterization scheme. MYJ is a robust one-dimensional local-closure turbulent kinetic energy (TKE) scheme widely used in the modeling community. The MYJ PBL scheme was selected over its alternatives because it was the preferred PBL scheme for Polar WRF after the original Polar WRF benchmark study by Hines and Bromwich (2008). Bromwich et al. (2013) also confirmed MYJ performance was satisfactory for Arctic simulation.

An evaluation of Polar WRF performance under different sets of options and settings was not conducted and beyond the scope of this study. Significant effort has been made to optimize Polar WRF performance by the developers of the model, as documented in Hines and Bromwich (2008), Wilson et al. (2009), Bromwich et al. (2009), Bromwich et al.(2013), and Hines et al. (2015).

2.2 WRF Simulation Methodology

WRF modeling was conducted generally according to a modeling protocol reviewed and accepted by EPA and BOEM representatives prior to the study and is included in Appendix A. The WRF simulations were conducted using the National Center for Atmospheric Research (NCAR) community-developed WRF model dynamical core version 3.4.1 in conjunction with the Ohio State University Polar WRF version 3.4.1 modules (Hines & Bromwich, 2008). WRF is a limited-area non-hydrostatic, terrain-following eta-coordinate mesoscale model (NCAR, 2014). WRF is the state-of-the-art mesoscale model used today to forecast regional weather, diagnose historical weather events, and provide meteorological datasets for regional air quality dispersion modeling.

The simulations were conducted on a polar-stereographic map projection. The outer-most 36 kilometer (km) domain encompassed all of Alaska and parts of Northern Canada and Russia, as shown in Figure 1. A 12 km nested domain included most of interior Alaska and the Bering, Chukchi, and Beaufort Seas. A 4 km nested domain focused on the regions of the Chukchi Sea, Beaufort Sea, and the North Slope of Alaska. The 4 km domain was sized to contain all of the OCS Lease Blocks and was built with a 70 km buffer, as shown in Figure 2 to account for a 50 km buffer around sources and receptors. The additional 20 km buffer was used to account for WRF "edge-effect" contamination, an artifact of numerical downscaling. The additional 20 km buffer encompasses five grid points on the edge of the nested domain – the five grid point buffer is typically used to account for edge-effects (NCAR, 2014). The CALPUFF 50 km buffer is required by EPA long-range transport modeling guidance to account for possible recirculation of pollutants (EPA, 1998).

The 36 km domain was comprised of 110 by 120 grid points, south to north and west to east, respectively. The 12 km domain was 130 by 157 grid points and the 4 km domain was 151 by 271 grid points. The WRF vertical grid structure was built using 37 levels, disproportionately stacked towards the surface. The boundary layer resolution used finer vertical spacing than typically used for most simulations over land to help the meteorological fields respond more explicitly to dynamical influences. The vertical grid structure is described in Table 1, including layer average height and thickness estimates based on the hypsometric equation, Eq. **(1)**:

$$Z = \frac{T_o}{\frac{g}{ln\left(\frac{1000\ mb}{P(z)}\right)} - \frac{dT}{dz}} \qquad \textbf{(1)}$$

The ERA-Interim (ERA-I) global atmospheric reanalysis (Simmons, et al., 2006) was used as the driving reanalysis dataset for the 4-year WRF Arctic dataset. The ERA-I is a global atmospheric reanalysis produced by the European Centre for Medium Range Weather Forecasts (ECMWF). ERA-I includes 6-hourly output, 37 pressure levels, and 0.75^o x 0.75^o spatial resolution. It is a widely-used dataset with the appropriate coverage for simulations of the Arctic. The North American Regional Reanalysis (NARR) dataset could not be used for the study because the outer WRF domain exceeds the boundaries of the NARR domain.

WRF can use temporal and spatial data assimilation methods to "nudge" gridded wind, temperature, and water vapor towards observations or analysis data. When nudging is applied, meteorological variables at adjacent grid points are relaxed towards the observed or analysis value, weighted by distance. Observation nudging was not used for the WRF simulations in this study. Analysis nudging was used for the WRF simulations on the 36 and 12 km domains. PBL nudging of wind, moisture, and temperature was not used to comply with advice given in (Stauffer, Seaman, & Binkowski, 1991).

Observational nudging can also be used in a preliminary step using the WRF preprocessor "obsgrid" in an attempt to improve the analysis dataset. Observation nudging was used on the analysis dataset in this study.

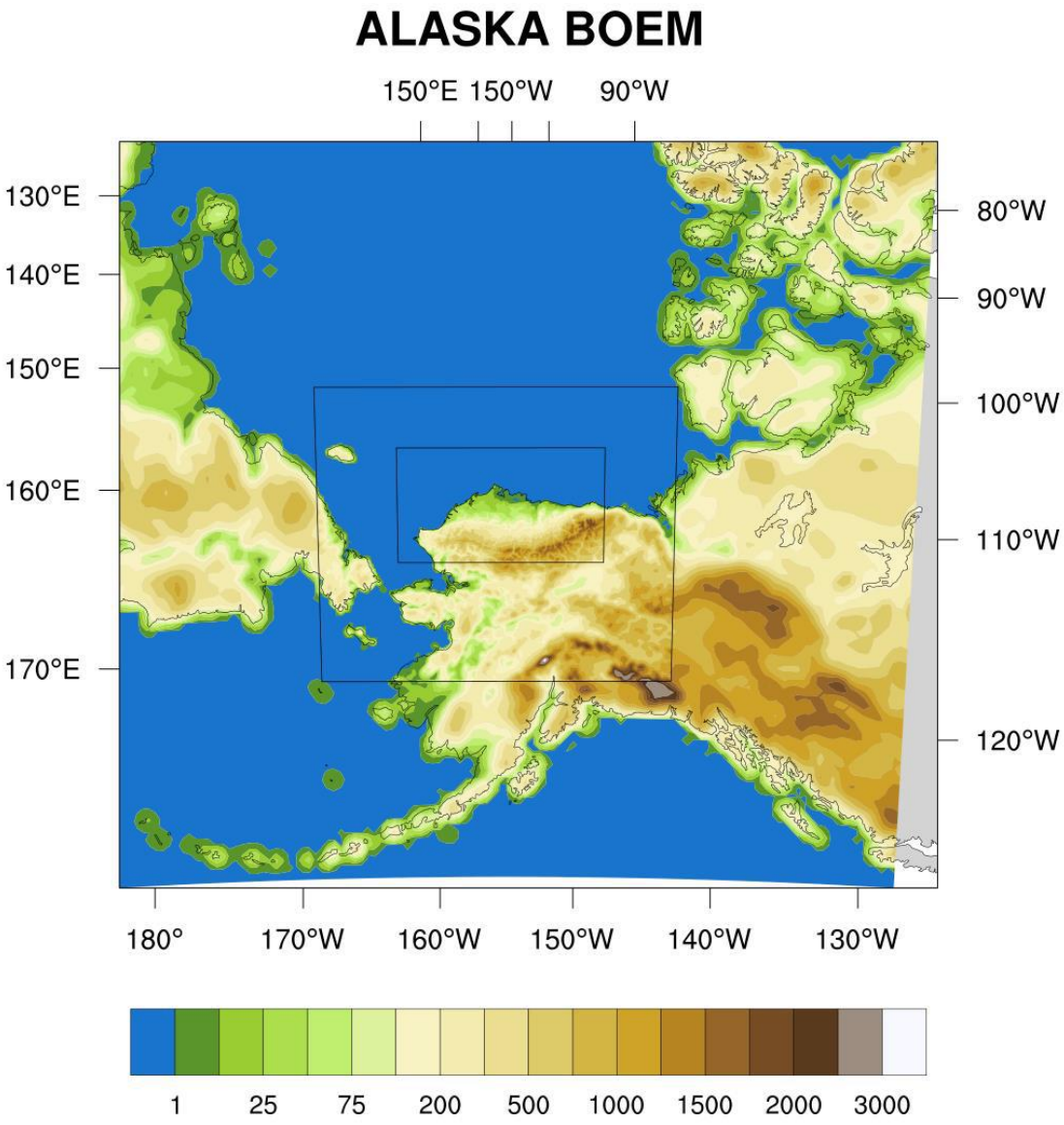

Figure 1. WRF four-year Arctic dataset nested modeling domains: 36km, 12km, and 4km.

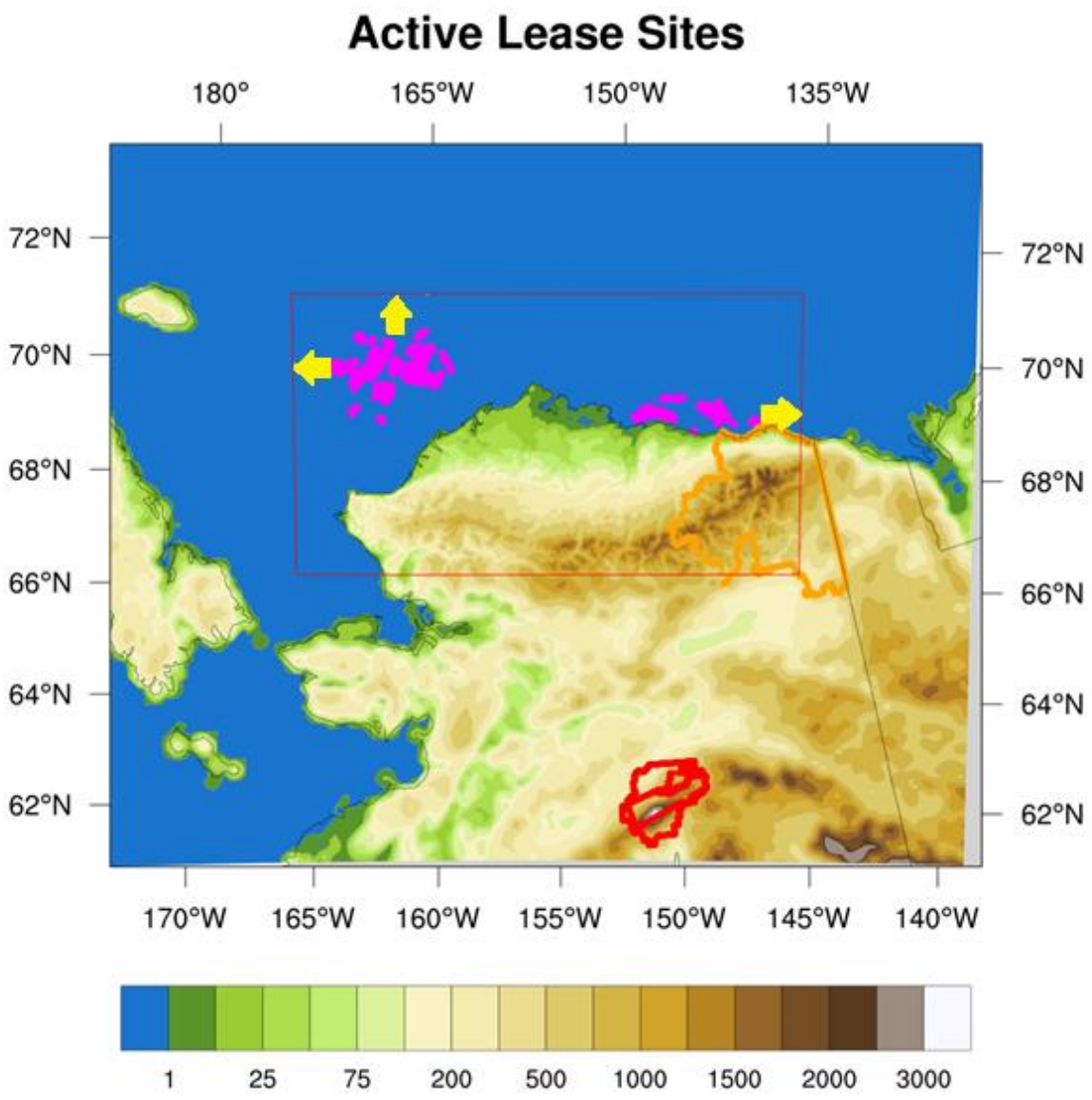

- **Lease site (magenta)**
- **Arctic National Wildlife Refuge (orange)**
- **Denali Wilderness, National Preserve, and National Park (red)**
- **70 km buffer from active lease sites (yellow arrows)**

Figure 2. 12 km and 4 km WRF domains.

Table 1. WRF vertical grid structure.

Level	"eta" level	Pressure (mb)	Height (m)*	Mid Height (m)*	Layer Thickness (m)*
1	1	1000	0.0	--	--
2	0.9985	999	12.2	6.1	12.2
3	0.997	997	24.5	18.4	12.2
4	0.995	995	40.8	32.7	16.4
5	0.993	993	57.2	49.0	16.4
6	0.991	991	73.6	65.4	16.4
7	0.988	989	98.3	85.9	24.7
8	0.985	986	123.0	110.6	24.7
9	0.98	981	164.3	143.6	41.3
10	0.97	972	247.4	205.9	83.1
11	0.96	962	331.2	289.3	83.8
12	0.95	953	415.7	373.4	84.5
13	0.94	943	500.8	458.2	85.1
14	0.93	934	586.6	543.7	85.8
15	0.91	915	760.5	673.5	173.8
16	0.89	896	937.2	848.8	176.8
17	0.87	877	1117.1	1027.1	179.8
18	0.84	848	1392.8	1254.9	275.8
19	0.8	810	1772.4	1582.6	379.6
20	0.76	772	2166.7	1969.6	394.3
21	0.72	734	2577.0	2371.9	410.3
22	0.68	696	3005.0	2791.0	427.9
23	0.64	658	3452.2	3228.6	447.3
24	0.6	620	3921.0	3686.6	468.7
25	0.55	573	4540.7	4230.8	619.8
26	0.5	525	5203.7	4872.2	662.9
27	0.45	478	5917.1	5560.4	713.4
28	0.4	430	6690.5	6303.8	773.4
29	0.35	383	7536.4	7113.5	846.0
30	0.3	335	8472.3	8004.4	935.8
31	0.25	288	9522.5	8997.4	1050.2
32	0.2	240	10724.1	10123.3	1201.6
33	0.15	193	12136.7	11430.4	1412.6
34	0.1	145	13866.9	13001.8	1730.1
35	0.06	107	15621.6	14744.2	1754.7
36	0.027	76	17503.4	16562.5	1881.8
37	0	50	19594.2	18548.8	2090.8

* Standard height and thickness estimated using P_o=1000mb, Ptop=50mb, T_o=20.15 °C, and dT/dz=-6.5 °C/km.

The 4-year WRF simulation (2009-2012) was conducted in 5.5-day simulation blocks with 12 hours of overlapping time to account for model "spin-up." The spin-up time allows for the model to develop sub-grid scale processes, including mature vorticity, convection, and moisture fields. The list of physics parameterization schemes used in the WRF modeling is included in Table 2. The same schemes and settings used for the Task 2 study WRF modeling were used except only the MYJ PBL scheme was used for this study.

Table 2. WRF physics parameterization schemes used for the four-year Arctic simulation.

Parameterization	Option selected	WRF option #	Description	Source
Micro-physics (mp_physics)*	Thompson	8	Moisture physics parameterization. Thompson scheme: 6-class hydrometeors	Thompson et al. (2008)
PBL physics (bl_pbl_physics)*	MYJ	2	MYJ: local TKE scheme	(Mellor and Yamada, 1982 and Janjic, 1994)
Cumulus / convection (cu_physics)*	Kain-Fritsch	1	Sub-grid convection scheme using mass-flux approach. Used on 36 and 12 km domains only: resolved explicitly on high resolution domains. Also used Kain-Fritsch "Eta" moisture advection trigger	Kain (2004)
Radiation (ra_sw_physics)* (ra_lw_physics)*	RRTMG	4	Rapid radiative transfer model using cloud overlap schemes	Iacono et al. (2008)
Land surface (sf_surface_physics)*	Unified Noah LSM	2	4-layer soil model with fractional snow cover, frozen soil physics, and ice sheet cover physics	Tewari et al. (2004)
Surface layer (sf_sfclay_physics)*	ETA M-O similarity	2	Monin-Obukhov similarity theory based scheme	Janjic (1994)

*WRF model keywords and options names.

2.3 Sea Surface Temperature Datasets

The simulation originally used the National Center for Environmental Prediction (NCEP) Real Time Global (RTG) SST analysis dataset. The RTG dataset contains satellite-derived SST at 0.5°C resolution. Arctic WRF simulations may be quite sensitive to the accuracy of the sea-ice or sea-surface temperature (SST) dataset used. Preliminary investigation revealed deficiencies within the NCEP RTG SST analysis dataset over a span of the open water periods of interest. Warm water surface plumes from Mackenzie River outflow resulted in overpredictions of SST across the Beaufort Sea in the RTG dataset. The overprediction of SST was attributed to smoothing techniques used in RTG data analysis.

The U.S. Naval Fleet Numerical Meteorology and Oceanography Center (FNMOC) Global SST analysis dataset (USN, 2014) was identified as a sufficient alternative to correct for the biases observed in the RTG dataset. Preliminary investigation of the FNMOC dataset revealed superior accuracy and depiction of the Mackenzie River plume when compared to the RTG dataset.

The FNMOC dataset is created using satellite-derived SST data at 0.25°C resolution and in situ SST data from ships and buoys and updated every 6 hours. Remotely-sensed SST data using passive infra-red sensors may be prone to error due to difficulties estimating temperature when low cloud cover or partial sea-ice cover is present (Xu & Ignatov, 2010). As a result, the time series of SST data may be discontinuous, marked by sudden shifts in SST magnitude during weather regime changes or in the case where in-situ data becomes available as ships or buoys enter the grid cell. The dataset is also temporally coarse with an update frequency of every six hours that also contributes to the discontinuous nature of the dataset. Despite these deficiencies, the FNMOC dataset represents one of the highest quality SST datasets available.

[Blank]

3 EVALUATION OF WRF PERFORMANCE OVER OPEN-WATER PERIODS

FNMOC-SST-based WRF performance was assessed in two ways: quantitatively with statistics relating WRF meteorology to measurements and qualitatively by graphical comparison of WRF meteorology to measurements. A portion of the quantitative analysis was conducted using the publically-available METSTAT software (ENVIRON Int. Corp., 2014). METSTAT calculates a suite of model performance statistics using wind speed and direction, temperature, and moisture observations. WRF predictions are extracted from the nearest grid cell for comparison to the observed values. METSTAT computes metrics for bias, error, and correlation and compares them to a set of performance benchmarks set for ideal model performance (Emery, et al., 2001).

3.1 METSTAT Statistics

Statistical measures calculated by METSTAT include observation and prediction means, prediction bias, and prediction error. The METSTAT analyses are valuable for evaluating the performance of the WRF simulations on a domain-wide level.

Mean observation (M_o) is calculated using values from all sites for a given time period by Eq. **(2)**:

$$M_o = \frac{1}{IJ}\sum_{j=1}^{J}\sum_{i=1}^{I} O_j^i \qquad \textbf{(2)}$$

where O^i_j is the individual observed quantity at site i and time j, and the summations are over all sites (I) and over time periods (J).

Mean Prediction (M_p) is calculated from simulation results that are interpolated to each observation used to calculate the mean observation for a given time period by Eq. **(3)**:

$$M_p = \frac{1}{IJ}\sum_{j=1}^{J}\sum_{i=1}^{I} P_j^i \qquad \textbf{(3)}$$

where P^i_j is the individual predicted quantity at site i and time j. Note the predicted mean wind speed and mean resultant direction are derived from the vector-average (for east-west component u and north-south component v).

Bias (B) is calculated as the mean difference in prediction-observation pairings with valid data within a given analysis region and for a given time period by Eq. **(4)**:

$$B = \frac{1}{IJ}\sum_{j=1}^{J}\sum_{i=1}^{I}\left(P_j^i - O_j^i\right) \qquad \textbf{(4)}$$

Gross Error (E) is calculated as the mean absolute difference in prediction-observation pairings with valid data within a given analysis region and for a given time period by Eq. **(5)**:

$$E = \frac{1}{IJ}\sum_{j=1}^{J}\sum_{i=1}^{I}\left|P_j^i - O_j^i\right| \quad \textbf{(5)}$$

Note the bias and gross error for winds are calculated from the predicted-observed residuals in speed and direction (not from vector components u and v). The direction error for a given prediction-observation pairing is limited to range from 0 to ±180°.

Root Mean Square Error (RMSE) is calculated as the square root of the mean squared difference in prediction-observation pairings with valid data within a given analysis region and for a given time period by Eq. **(6)**:

$$RMSE = \left[\frac{1}{IJ}\sum_{j=1}^{J}\sum_{i=1}^{I}\left(P_j^i - O_j^i\right)^2\right]^{\frac{1}{2}} \quad \textbf{(6)}$$

The RMSE, as with the gross error, is a good overall measure of model performance. However, since large errors are weighted heavily (due to squaring), large errors in a small sub-region may produce a large RMSE even though the errors may be small and quite acceptable elsewhere.

Additional WRF performance analyses were conducted using the time series of meteorological variables extracted at the buoy measurement sites. The approach and analysis is discussed in Section 4.0. The time series comparisons are a valuable tool for understanding the influence of meteorology on AERMOD prediction performance because the meteorology at the extracted point is used to drive AERMOD.

3.2 METSTAT Benchmarks

The METSTAT benchmarks were developed using the results of about 30 meteorological model performance simulations performed to support air quality studies of urban areas (Emery, et al., 2001). Another set of model performance benchmarks were developed for complex conditions as part of the Western Regional Air Partnership (WRAP) meteorological modeling of the western United States, including the Rocky Mountain Region as well as the complex conditions in Alaska (Kemball-Cook, et al., 2005).

Table 3 lists the meteorological model performance benchmarks for simple and complex (Kemball-Cook, et al., 2005) terrain. The benchmarks provide a measure of WRF model performance with regards to other modeling cases in the U.S. However, given the wide variety of landforms, weather, and climatic regions in the U.S. it is likely these benchmarks are applicable to most regions of the world. Less stringent criteria have been developed for complex

terrain conditions based on the higher degree of variance found in regions of heterogeneous terrain and microclimate. Point measurements along the coast can be influenced by marine or land-based boundary layers, depending on the conditions at any given moment. Strong gradients of temperature, relative humidity (RH), and cloud can exist at the interface between the marine and land PBLs. Large differences in meteorology between WRF and measurement data may occur if WRF grid resolution is not dense enough to resolve these tight gradients, or if the WRF grid cell location is not located within the same PBL (marine or land-based) as the measurement location. Given the complexity of meteorological conditions in the Arctic, it may be assumed the complex criteria provide a more suitable set of performance goals.

Table 3. Performance benchmarks for simple and complex conditions.

Parameter	Simple	Complex
Temperature Bias	≤ ±0.5 K	≤ ±2.0 K
Temperature Error	≤ 2.0 K	≤ 3.5 K
Humidity Bias	≤ ±0.8 g/kg	≤ ±1.0 g/kg
Humidity Error	≤ 2.0 g/kg	≤ 2.0 g/kg
Wind Speed Bias	≤ ±0.5 m/s	≤ ±1.5 m/s
Wind Speed RMSE	≤ 2.0 m/s	≤ 2.5 m/s
Wind Direction Bias	≤ ±10 degrees	≤ ±10 degrees
Wind Direction Error	≤ 30 degrees	≤ 55 degrees

Although METSTAT analysis can be applied to individual meteorological station datasets, it is typically used to evaluate performance against a group of stations within the WRF domain. This approach is advantageous because it evaluates performance across the entire domain and dampens bias that can occur at any individual site (advantageous if the climate at the site is heavily influenced by small-scale local terrain or roughness features not resolved in the WRF domain). However, if too many stations are used in the analysis the statistics may be unduly smoothed and not truly representative of WRF performance.

METSTAT statistical results are typically displayed in a “soccerplot.” This type of plot contains the statistical results for selected periods plotted with respect to the simple and complex “goals” listed in Table 3. If a point is located within the goals, it indicates the METSTAT results from the given period satisfy the criteria benchmarks for the meteorological variable in question. If the point is outside the goals it does not satisfy the criteria, indicating WRF performance was poor for the particular period and region evaluated, if the observational data used is sufficiently representative of the regional meteorology. If the point is within the complex terrain criteria goals but outside the simple criteria goals, WRF performance is satisfactory for complex terrain and meteorological conditions, but not necessarily for simple terrain and meteorological conditions. If the point is inside both the simple and complex criteria goals, WRF performance is considered satisfactory if the observational datasets used are accurate and representative. This result indicates good agreement between observations and simulated surface meteorology.

METSTAT was used to evaluate the performance of each WRF simulation using surface meteorological data from the U.S. National Climatic Data Center DS-3505 database (NOAA-NCDC, 2014). The database contains records of most official surface meteorological stations from airports, military bases, reservoirs/dams, agricultural sites, and other sources dating from 1901 to the present.

4 EVALUATION OF WRF SIMULATION RESULTS

This section evaluates WRF performance with respect to observed meteorology using the methods described in Section 3. The evaluation includes both time series comparisons and METSTAT analyses. Time series of observed and extracted meteorology were plotted for each site for the open-water periods used in this study, together for qualitative comparison. The qualitative analysis provided insight into the capabilities of WRF for each scenario at each measurement site. A full description of the four measurement sites used in this study is provided in Section 5.2.

The data plotted are from the direct MMIF extractions (without AERCOARE processing). AERCOARE and MMIF PBL height recalculation does not change wind speed and direction, RH, or sea-surface temperature. PBL height time series plots contain both direct WRF PBL height heights (referred to hereafter as “RCALF” values) and MMIF-calculated PBL heights (referred to hereafter as “RCALT” values). Both WRF and MMIF can produce unphysically low PBL heights during highly stable conditions. A minimum PBL height limit of 25 m was enforced for all the datasets used in this study. The minimum PBL height value of 25 m was set after deliberations with EPA Region 10. It was noted that the 25 m value is a reasonable minimum mixing height for the most extreme stable periods, based on measurements reported in (Hsu, 1988) (Garratt, 1992). A minimum absolute value of 5 m was established for the Monin-Obukhov length (*L*), synonymous with the *L* limits used in the OCD model (DiCristofaro & Hanna, 1989). AERCOARE reprocessing of WRF meteorology did not substantially change PBL height.

4.1 Overland METSTAT Results

METSTAT was used to evaluate WRF performance using observations from land-based measurement stored in the NOAA DS-3505 database (NOAA-NCDC, 2014). The inner-domain (Domain 3) METSTAT results were selected for evaluation in this study. A total of 19 surface station datasets were obtained and used for the METSTAT analysis for all periods analyzed. The periods included the open-water seasons (Aug. – Oct.) of 2010, 2011, and 2012. These results were useful for evaluating WRF performance on a domain-wide level.

The land-based METSTAT soccer plot results for temperature performance are plotted in Figure 3. Results were favorable, exhibiting low bias and error falling within the criteria for simple conditions. Temperature simulation performance was favorable for each month and year simulated.

Results for humidity performance are plotted in Figure 4. WRF humidity was slightly positively biased, but the statistical scores were also within the simple conditions criteria. Results were favorable for all periods simulated.

Results for wind speed and wind direction performance are plotted in Figure 5 and Figure 6, respectively. Wind speed was biased slightly low, but generally within the simple conditions criteria. Wind speed RMSE exceeded the criteria for simple terrain conditions for 2010 and 2011

October simulation periods. The RMSE for these periods were within the complex conditions criteria, however. Wind direction bias and error were favorable, falling within the simple conditions criteria for all periods simulated.

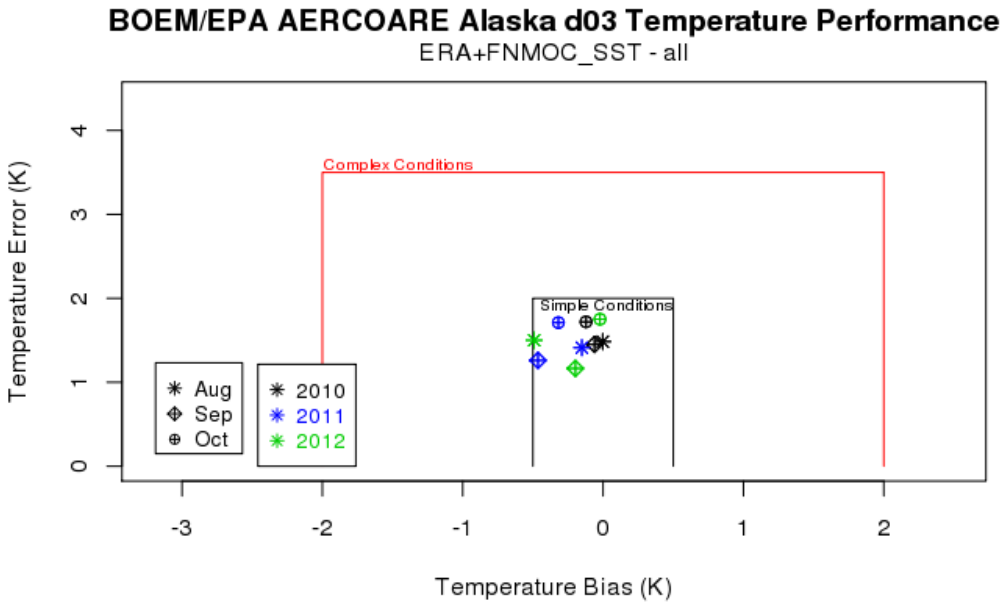

Figure 3. Land-based temperature METSTAT results.

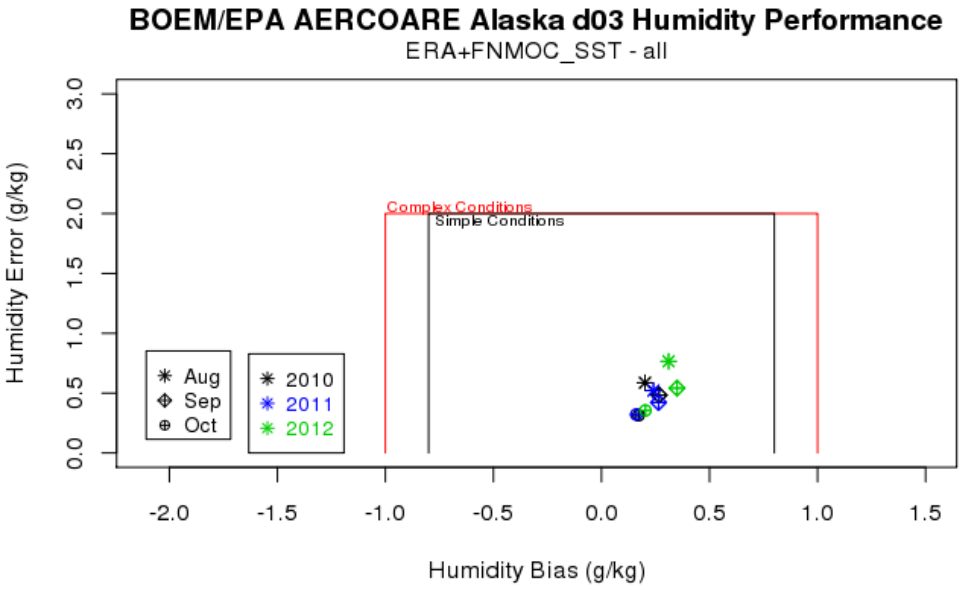

Figure 4. Land-based humidity METSTAT results.

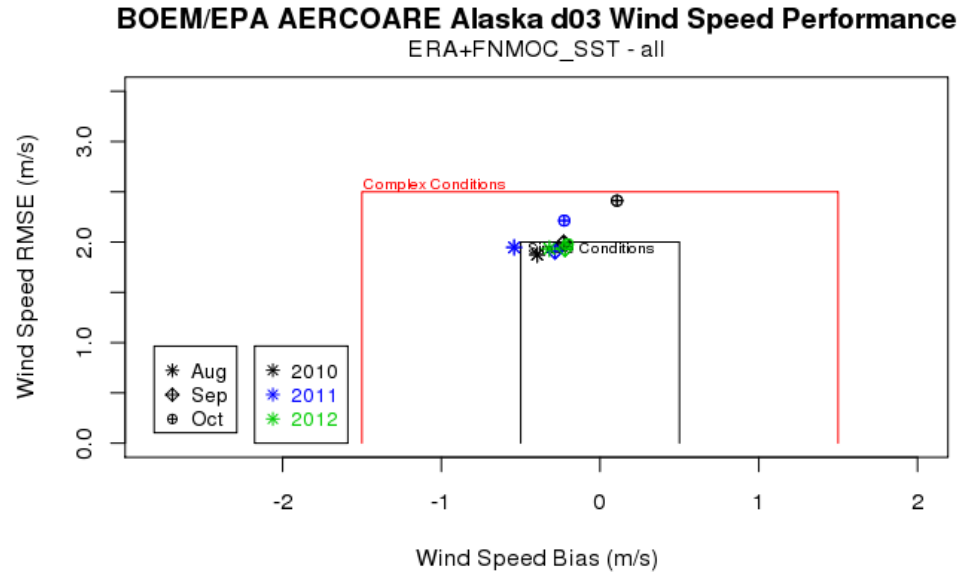

Figure 5. Land-based wind speed METSTAT results.

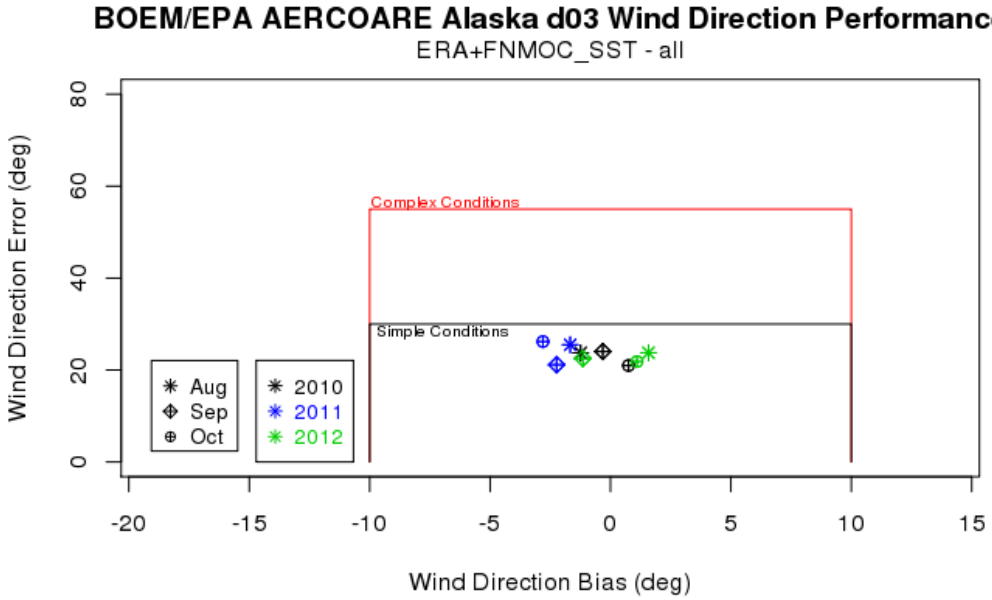

Figure 6. Land-based wind direction METSTAT results.

4.2 Overwater METSTAT Results

METSTAT was used to evaluate WRF performance using observations from ships and meteorological buoys stored in the NOAA DS-3505 database. The observation datasets used for the METSTAT analysis included those from several of the meteorological buoys used in this study to drive AERMOD simulations. The observation datasets used for each period are listed in Table 4. Note that buoy MOB2 is located at the site of the Chukchi-Klondike position in 2011. Therefore, some of the datasets included in the METSTAT analysis are also used for AERMOD modeling in this study. Data are lacking for 2012 in the database: only temperature data are available at one buoy site in the DS-3505 database.

Table 4. Overwater datasets used in METSTAT evaluation.

Year	Month	Datasets (listed by buoy/station identifiers)[a]	Total Stations
2010	Aug.	101, CK	2
	Sep.	101, CB, CK	3
	Oct.	102, CB, CK	3
2011	Aug.	CB, MOB3, MOB1, MOB2	4
	Sep.	48536, MOB1, MOB2, CB, HB, MOB3	6
	Oct.	CB, HB, MOB1, MOB2, MOB3	5
2012	Aug.	48536	1

	Sep.	48536	1
	Oct.	48536	1

[a] 101: ConocoPhillips Klondike buoy 1 located at 70.9N, 165.2W
CK: Shell Chukchi-Klondike buoy located at 71.5N, 164.1W (corresponds to Site C2 dataset)
CB: Shell Camden Bay buoy located at 70.4N, 146.0W (corresponds to Site B3 dataset)
102: ConocoPhillips Klondike buoy 2 located at 70.99N, 164.99W
MOB1: Joint (ConocoPhillips, Shell) Hanna Shoal buoy located at 72.2N, 161.5W
MOB2: Joint Chukchi-Klondike buoy (2011 only) located at 70.9N, 165.2W (corresponds to Site C1 dataset)
MOB3: Joint Chukchi-Burger buoy (2011 only) located at 71.5N, 164.1W
48536: ICEX-AIR free arctic ice buoy; position varied
HB: Shell Harrison Bay buoy located at 70.9N, 150.3W

The METSTAT results for temperature are plotted in Figure 7. The results suggested WRF was able to accurately predict temperature given the error and bias were within the more stringent simple conditions criteria for 2010 and 2011. The 2012 results, from a single buoy, fell within the complex conditions criteria for 2012.

Figure 8 shows the METSTAT results for humidity. Humidity bias and error were very low for 2010 and 2011, resulting in statistics that fell within the criteria. Note these criteria were developed for land-based datasets that typically exhibit a larger variance in humidity. Sea-based humidity in the Arctic tended to be near water vapor saturation most of the time.

The wind speed METSTAT results are shown on Figure 9. Although August and September statistics were within the simple conditions criteria, WRF tended to underpredict wind speeds by exhibiting a degree of negative bias. The October simulations were more scattered, with scores exceeding the RMSE criteria, but falling within the complex conditions criteria for bias.

Figure 10 shows the METSTAT results for wind direction. The wind direction error and bias is misrepresented because the Arctic buoy datasets contained in the National Buoy Data Center (NBDC) database are aligned to magnetic north. The correction of measurements to true north in this region is about a +14° adjustment. This adjustment would result in WRF bias falling within the “simple conditions” criteria and would likely reduce error into the “simple conditions” criteria also.

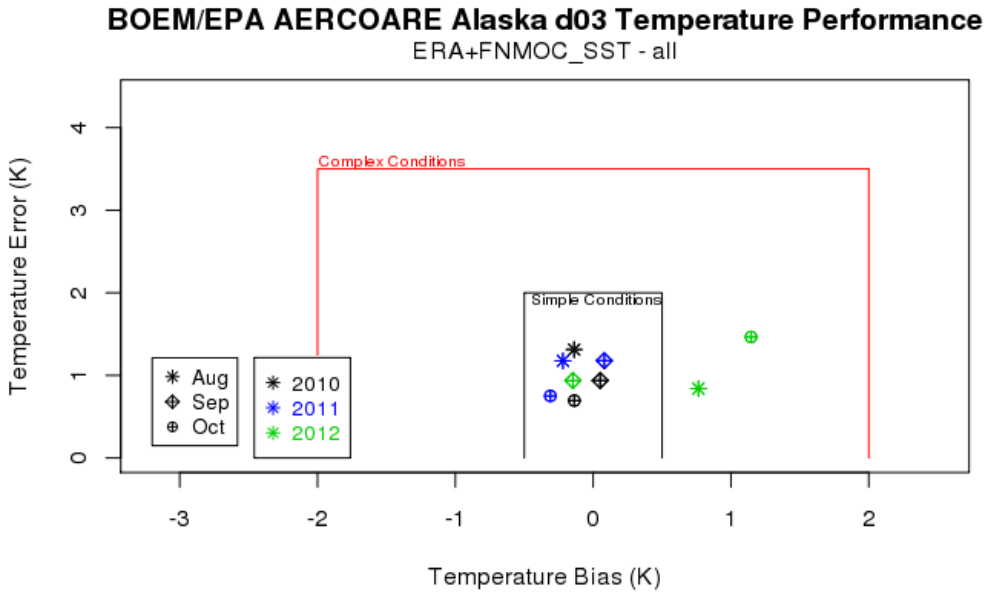

Figure 7. Overwater temperature METSTAT results.

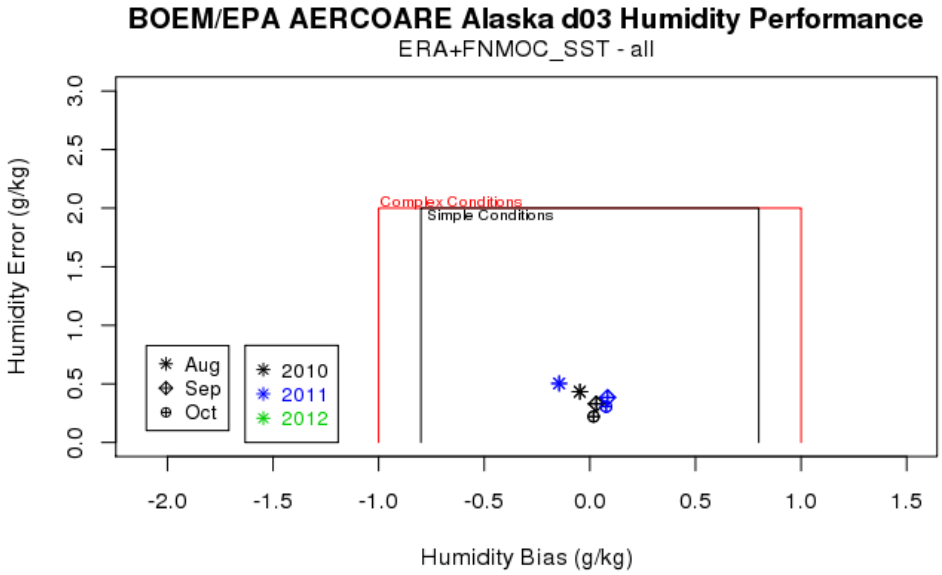

Figure 8. Overwater humidity METSTAT results.

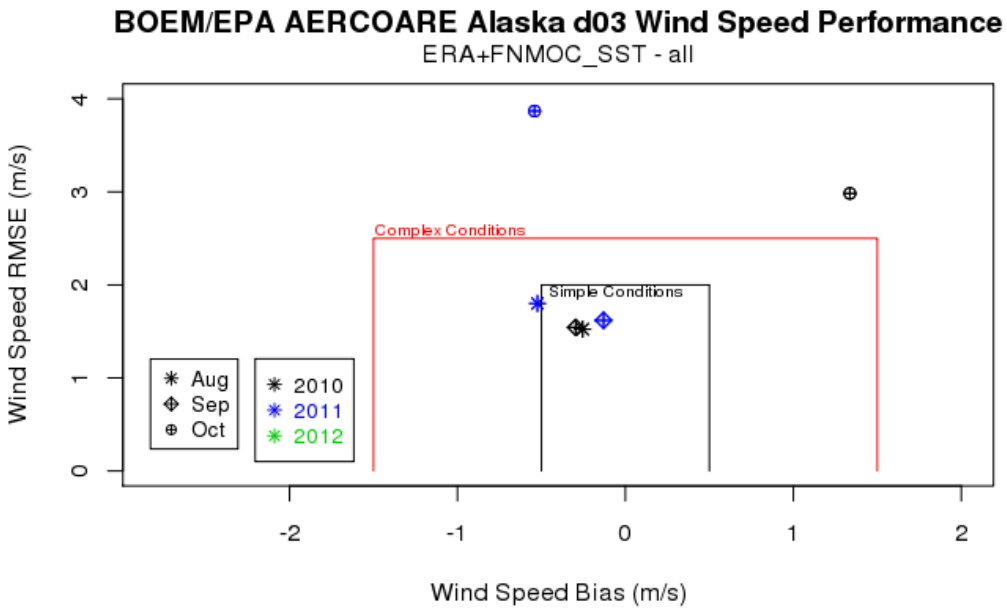

Figure 9. Overwater wind speed METSTAT results.

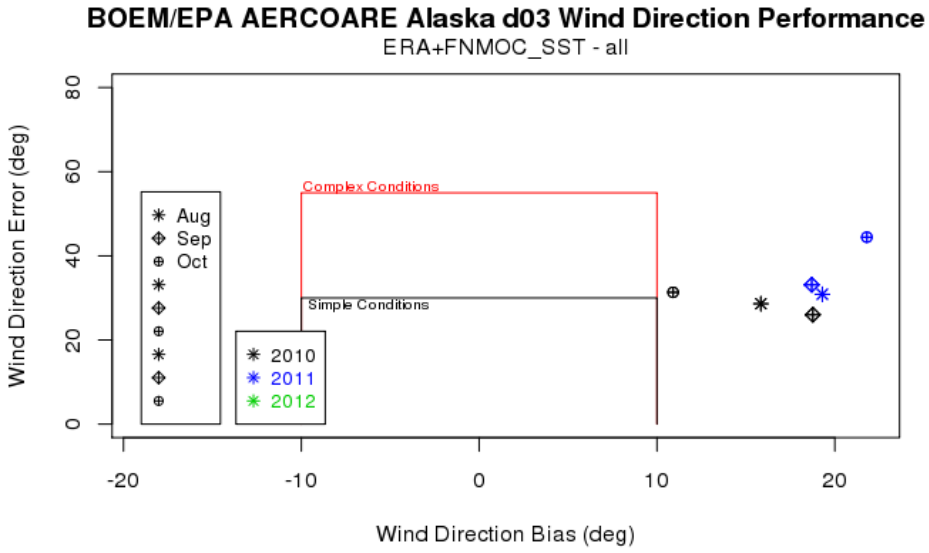

Figure 10. Overwater wind direction METSTAT results.

4.3 Meteorological Time Series at Site C1: Chukchi-Burger

4.3.1 Wind speed

Time series plots of site C1 2011 and 2012 wind speed are shown in Figure 11 and Figure 12, respectively. Note WRF wind speed is at 10 m while the observed wind speed was measured at 3.5 m. In general, the WRF simulations results followed the 2011 and 2012 trends in observed wind speed. However, it might be expected that the observed wind speeds would be slightly less on average given the lower measurement height. On the contrary, there was a tendency for WRF to underpredict wind speed on average, by 0.5 m/s and 0.4 m/s over the 2011 and 2012 periods, respectively. The standard deviation of wind speed was 1.2 and 1.0 m/s for these periods, respectively. The WRF negative wind speed bias corresponded to the same bias indicated by the METSTAT analysis. For most near surface sources, lower wind speeds would tend to result in overprediction of concentration by AERMOD.

4.3.2 Wind direction

Time series plots of site C1 2011 and 2012 wind direction are shown in Figure 13 and Figure 14, respectively. WRF wind directions compared very well to the measurements, as can be seen in the figures. The average wind direction deviation for both periods was 5.1° and -3.6°, respectively.

4.3.3 Air temperature

Time series plots of site C1 2011 and 2012 air temperature are shown in Figure 15 and Figure 16, respectively. Air temperature WRF extractions were at a height of 2.0 m above the surface and the buoy probe measured temperature at 3.0 m, so some slight deviation in temperature could be expected. WRF underpredicted temperatures for most of the 2011 season. The average hourly temperature error was -0.85°C for 2011. The 2012 WRF average temperature error was -0.36°C. In 2012, a period of significant deviation was evident from Sept. 19th to Sept. 22nd with WRF overpredicting temperature by 2-3°C.

4.3.4 Sea surface temperature

Time series plots of site C1 2011 and 2012 SST are shown in Figure 17 and Figure 18, respectively. The FNMOC SST analyses underpredicted SSTs for all of 2011, substantially so for most of August. The 2012 SST analysis matched closely with measurements from mid-September through October except for a short period in late September where the SST was underpredicted. The SST analysis underpredicted SST from August to early September 2012, by almost 6 °C at some points. The deviations may be due to errors within the FNMOC dataset possibly due to cloud contamination or partial sea-ice cover. The period of August 13th – August 28th 2011 was the longest period of underpredicted SST and corresponded to a period of

northeasterly winds (correctly simulated by WRF). The period of high SST error abruptly begins with the shift from east to northeasterly winds and abruptly ends after a shift to more southerly winds. Given the relatively high winds and constant RH before, during, and after this period, it is less likely low cloud cover was the cause of the error. The northerly wind component and the fact that the period was relatively early in the ice-free period suggests partial ice-cover may have been to blame for the error.

Abrupt shifts to erroneously low FNMOC SST also occur for shorter periods throughout 2011 and 2012, not necessarily corresponding to any wind direction or shift in wind direction. Average WRF deviations were -0.88°C and -0.97°C for 2011 and 2012, respectively.

4.3.5 Air-sea temperature difference

Time series plots of site C1 2011 and 2012 air-sea temperature difference (ASTD) are shown in Figure 19 and Figure 20. In general, the “sign” of the WRF ASTD matched the observations for most of 2011 and 2012. Only for a few short periods did WRF support a negative ASTD while the observations supported a significant positive ASTD. The magnitude of the ASTD did vary quite substantially over some periods, with an average root mean square error of about 1.0°C for both periods. Hours with significant difference between WRF and measurement ASTD (significant considered as an absolute value of 0.5°C or more difference) and opposite ASTD sign occurred 13% and 6% of the time for 2011 and 2012, respectively.

4.3.6 Relative humidity

Time series plots of site C1 2011 and 2012 RH are shown in Figure 21 and Figure 22, respectively. The 2011 WRF predictions tended to overpredict RH on average (+4% on average), significantly so over periods of September where observed RH dropped into the 70-80% range. It is unknown why WRF produces a mode of 94% RH values.

For 2012, the buoy consistently measured RH of 100% for extended periods. It is unknown why similar periods were not evident in the 2011 dataset. Although WRF RH did peak at 100% for a few hours in 2012, WRF did not favor the mode of 100% values evident in the measurement dataset. Again, as in 2011, a mode of 94% humidity occurred in the WRF results.

In 2011, two periods were identified where measured RH was relatively low and WRF RH was high. From Sep. 2 – 9 and Sep. 16 – 24, measured RH ranged generally from 70 – 90 % while WRF maintained RH around 94%. WRF ASTD predictions were favorable during this period and both WRF and measurements supported unstable conditions.

4.3.7 PBL height

Time series plots of site C1 2011 and 2012 PBL heights are shown in Figure 23 and Figure 24, respectively. Note no measurements of PBL were available at this site. The MMIF recalculated PBL heights (RCALT) were of similar magnitude to the WRF RCALF PBL heights most of the

time except for several periods when WRF PBL heights (RCALF) were at the minimum 25 m height. The MMIF recalculation produced much higher PBL heights during many of these periods. Notable cases included Oct. 1-7, 2011 where WRF PBL heights were sustained at 25 m through the period and MMIF recalculated heights ranged generally from 400 to 600 m. Several notable cases in 2012 included Sept. 7-8 and Sept. 13-14, where WRF sustained the minimum 25 m height for long periods and MMIF resulted in PBL heights ranging from 200 – 1000 m during these periods.

4.3.8 Discussion

The C1 WRF meteorology featured lower average wind speed than measured 2011 and 2012. The underpredicted wind speed was a factor in conservative AERMOD predictions because higher wind speeds generally result in lower concentrations downwind of the source. Both WRF air temperature and SST values were biased cold on average. The sign and magnitude of ASTD predicted by WRF consistently agreed with measured values for much of the periods modeled. However, the magnitude of the predicted ASTD did vary substantially by up to 4 ºC for several short periods (about a day each instance) in late August and early September, 2012. Differences in ASTD may affect the PBL scaling and mixing parameters. The ASTD differences would likely result in PBL height differences also if measured PBL heights were available for this site.

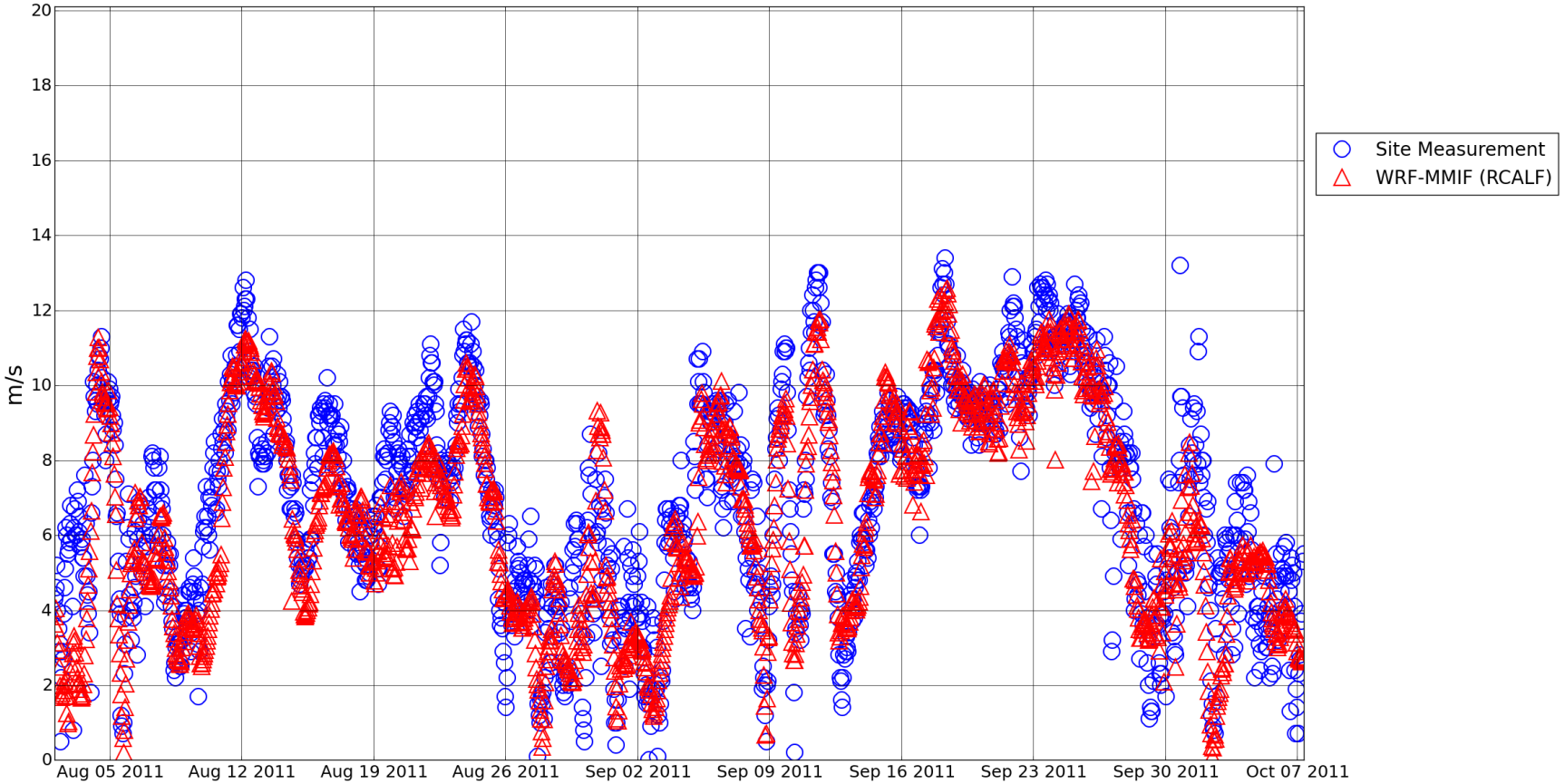

Figure 11. C1 2011 wind speed time series.

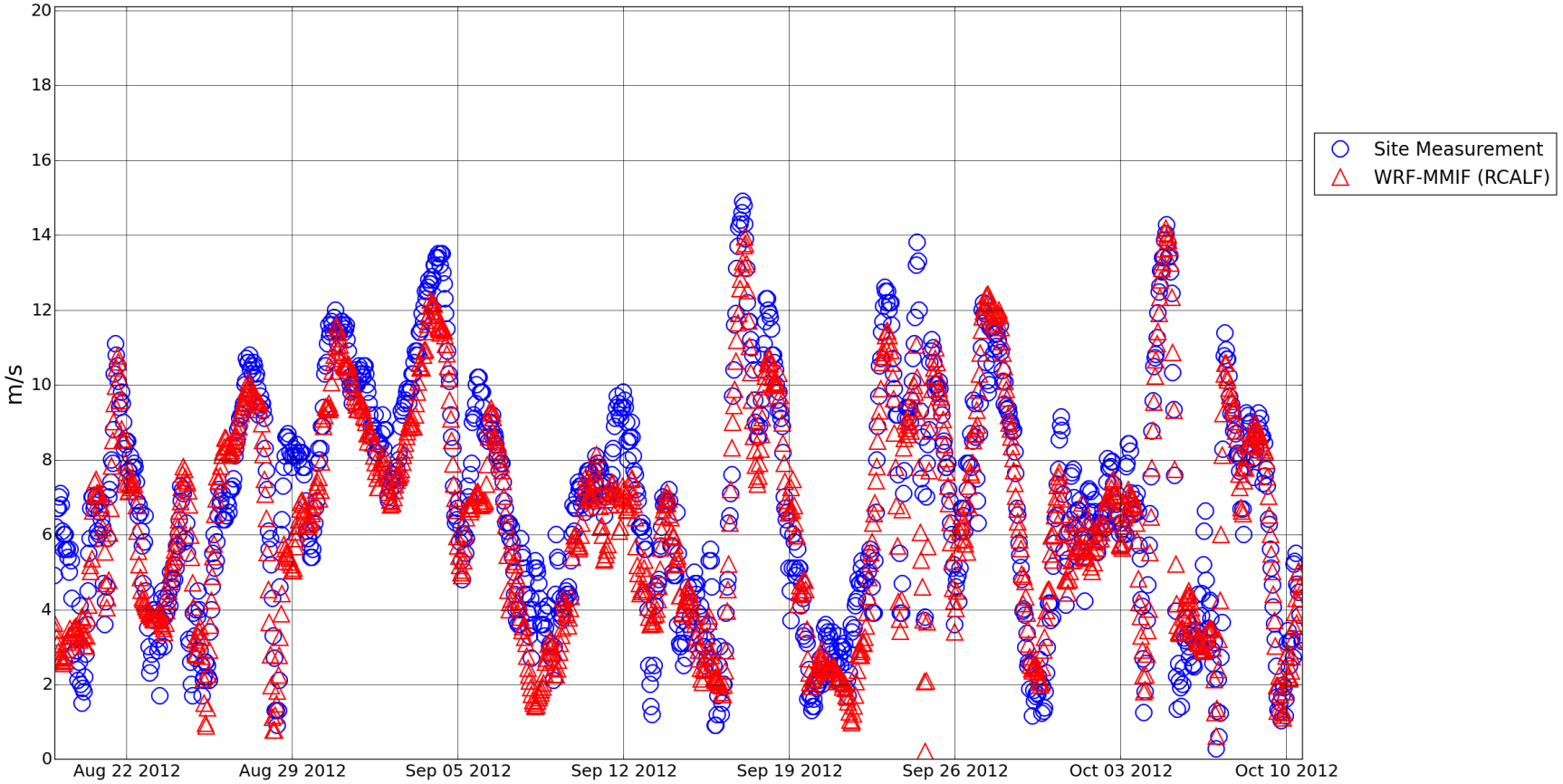

Figure 12. C1 2012 wind speed time series.

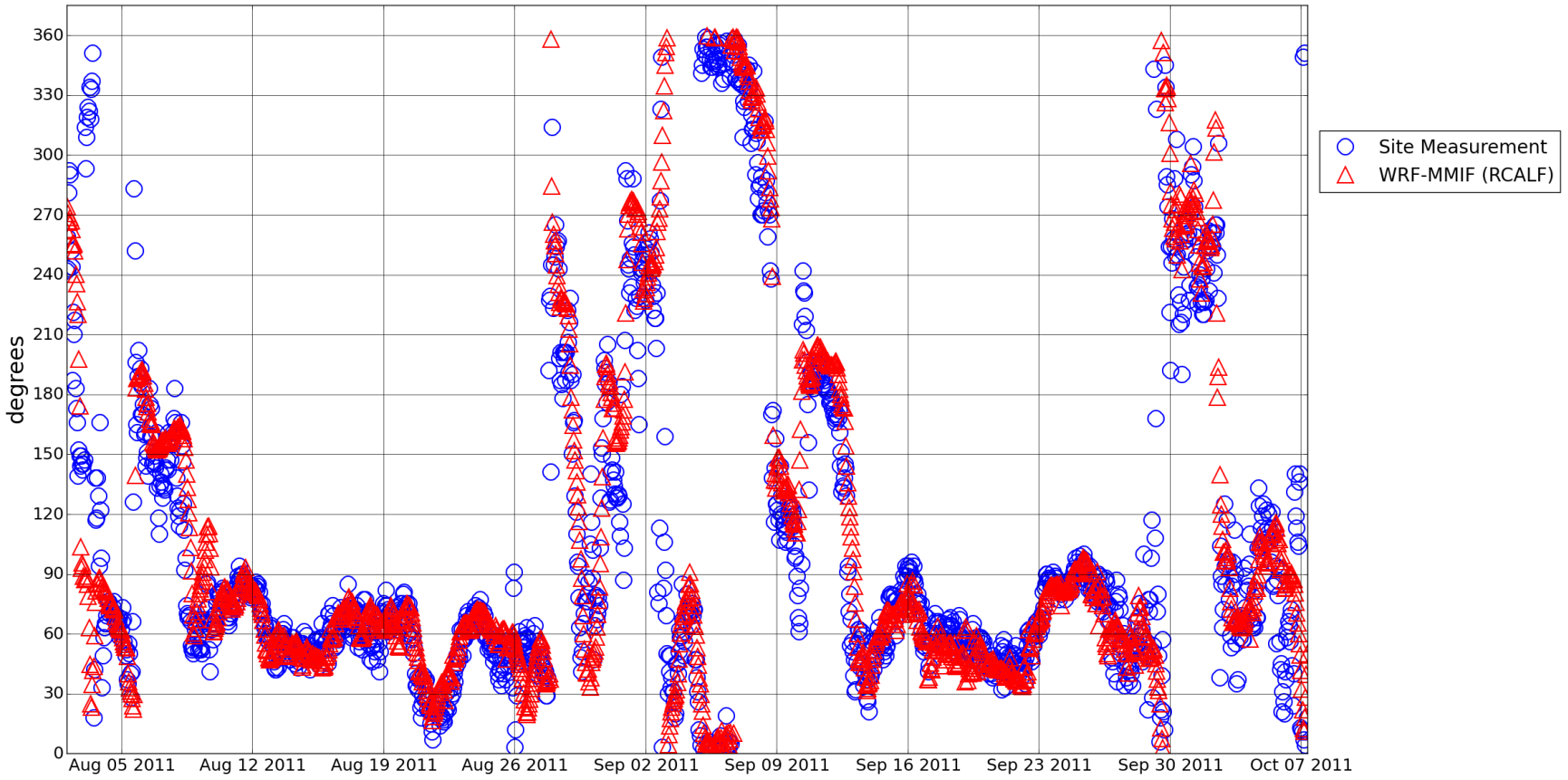

Figure 13. C1 2011 wind direction time series.

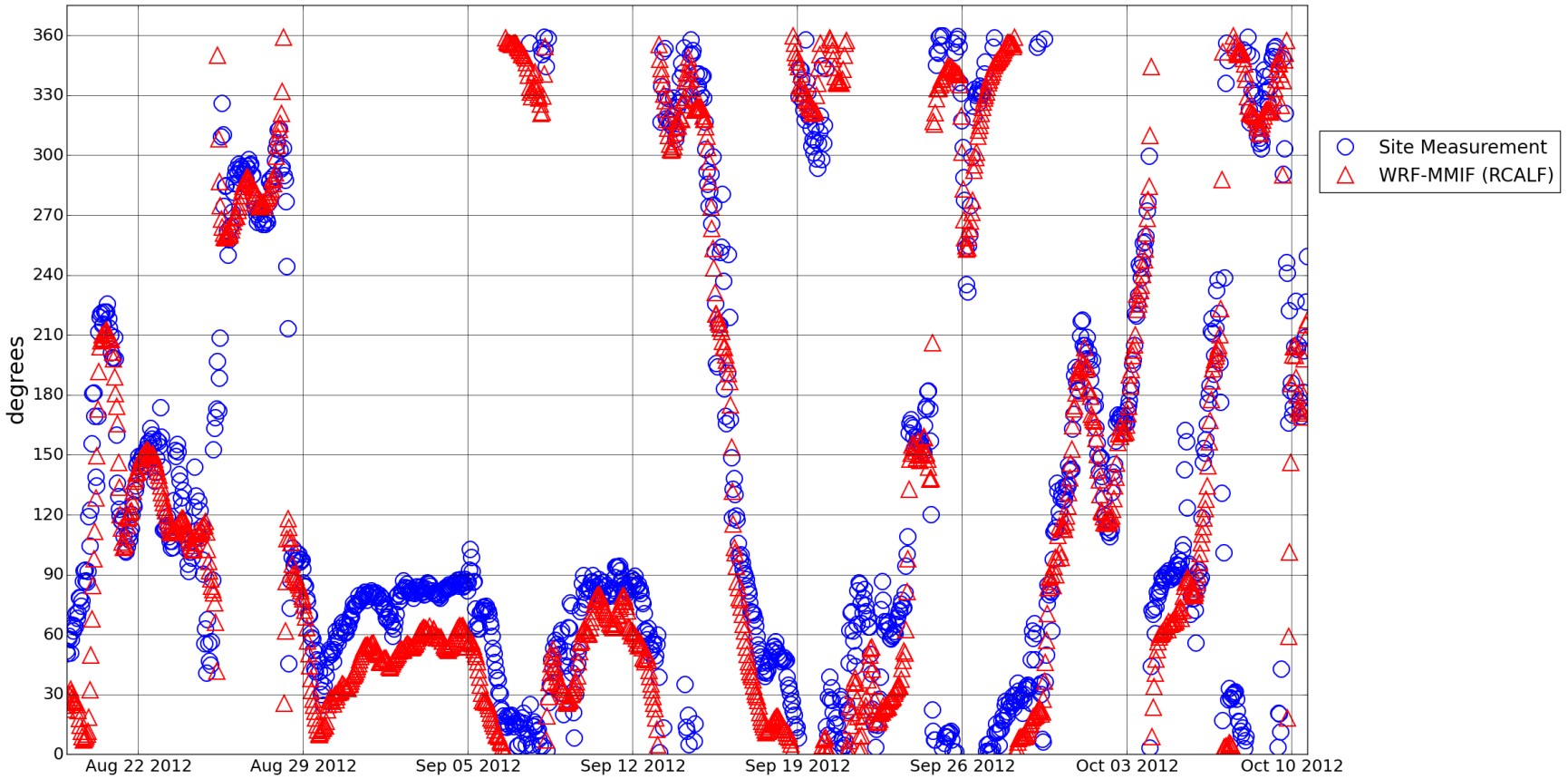

Figure 14. C1 2012 wind direction time series.

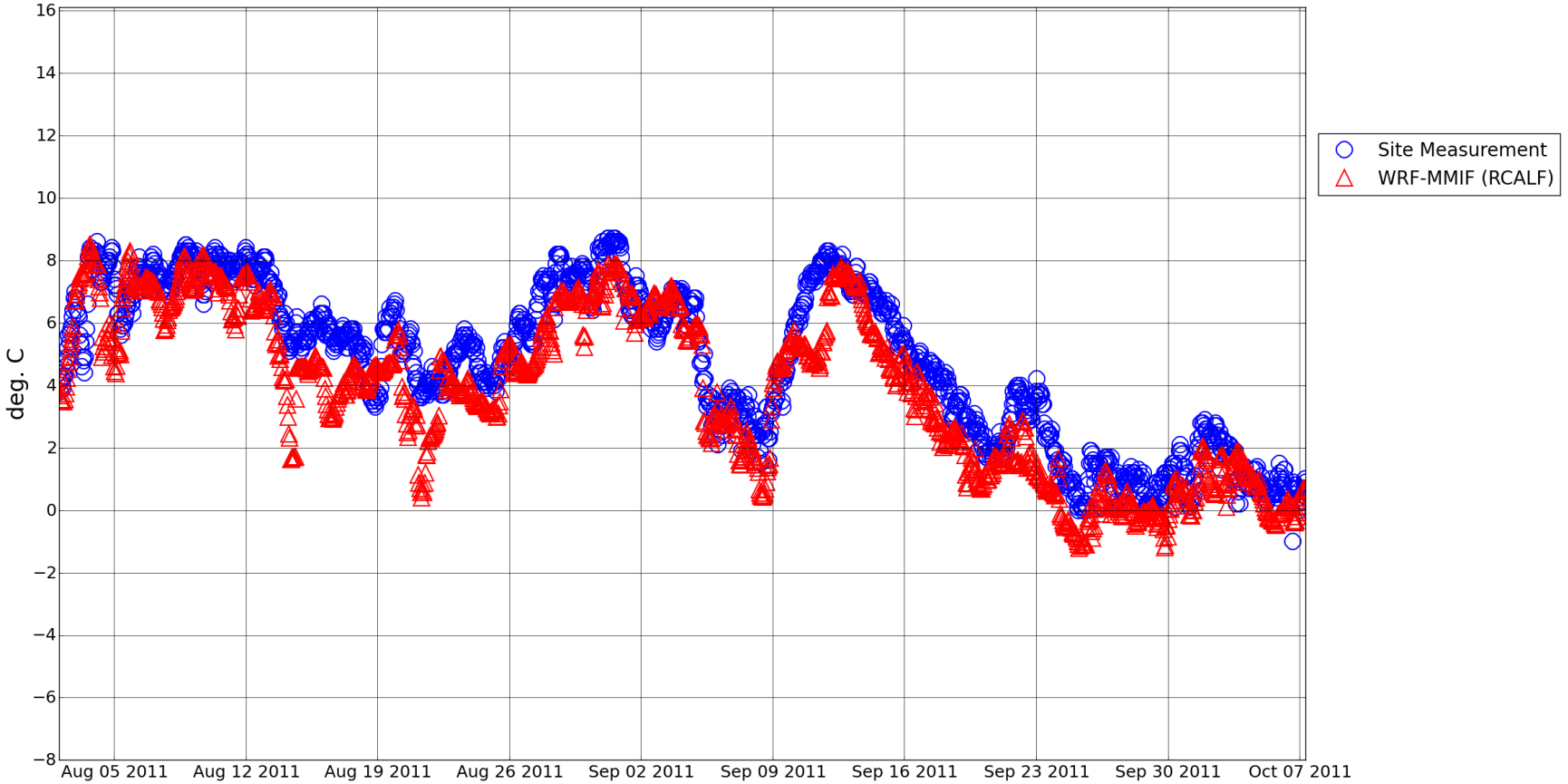

Figure 15. C1 2011 air temperature time series.

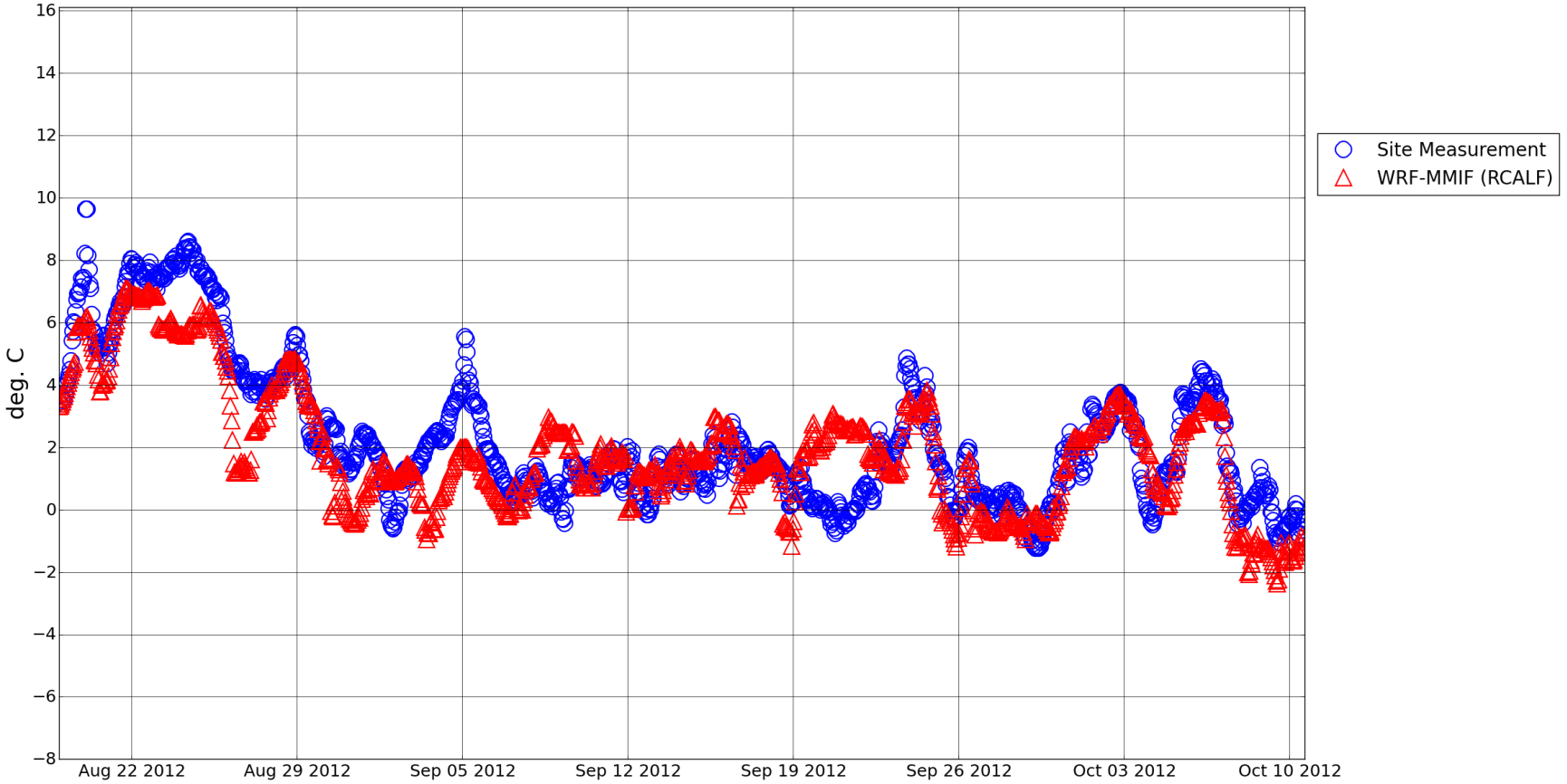

Figure 16. C1 2012 air temperature time series.

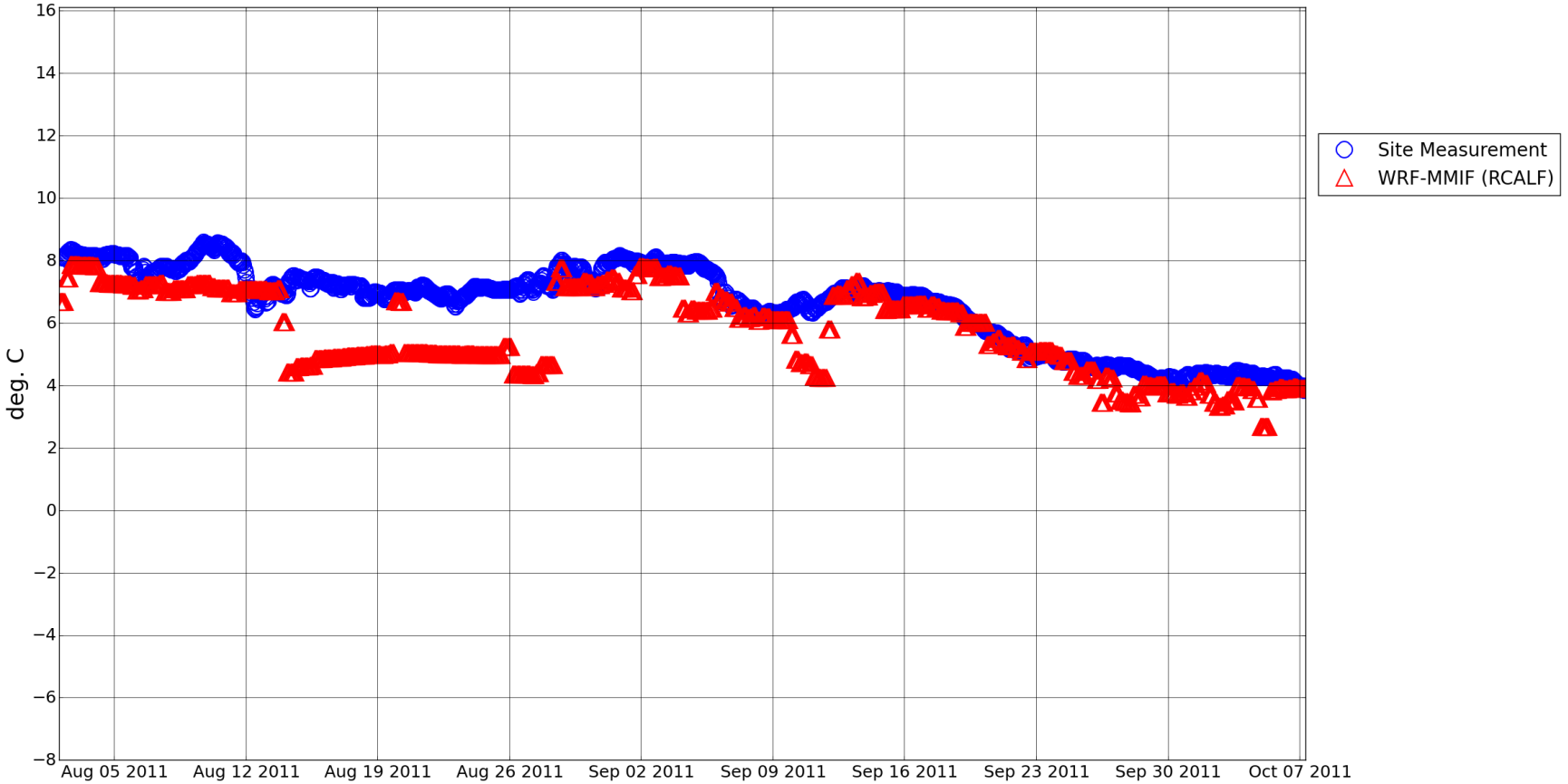

Figure 17. C1 2011 sea-surface temperature time series.

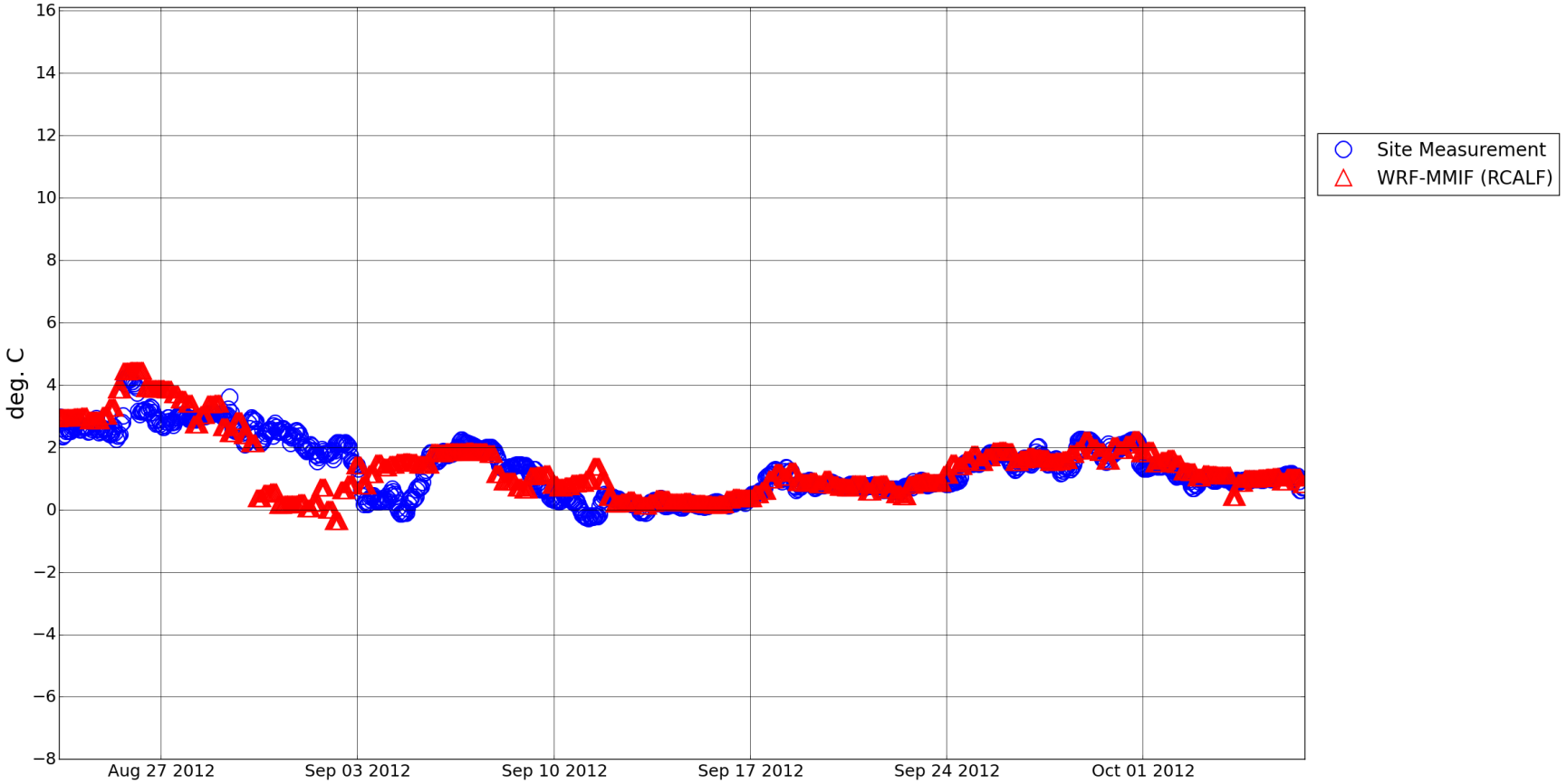

Figure 18. C1 2012 sea-surface temperature time series.

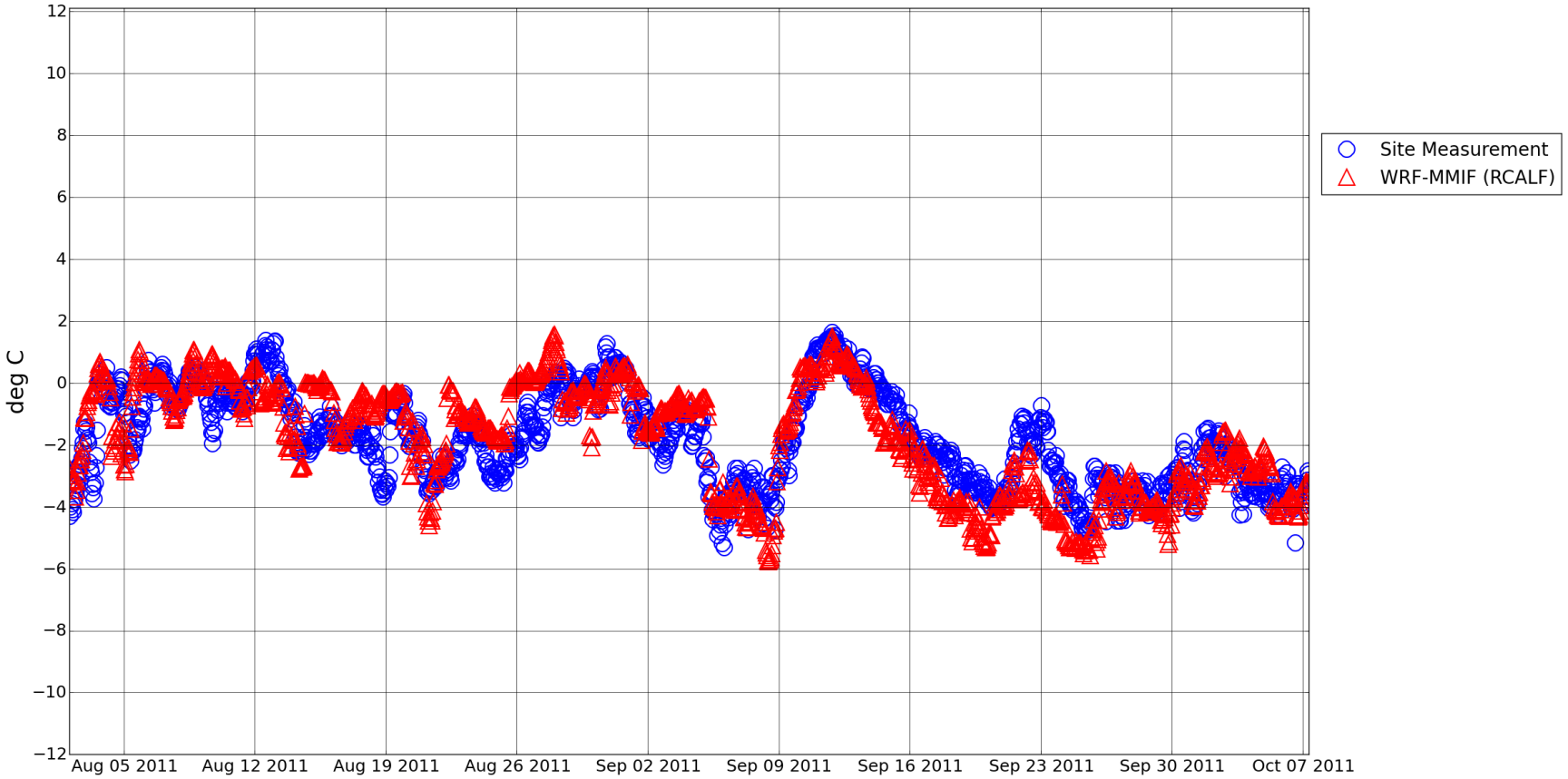

Figure 19. C1 2011 air-sea temperature difference time series.

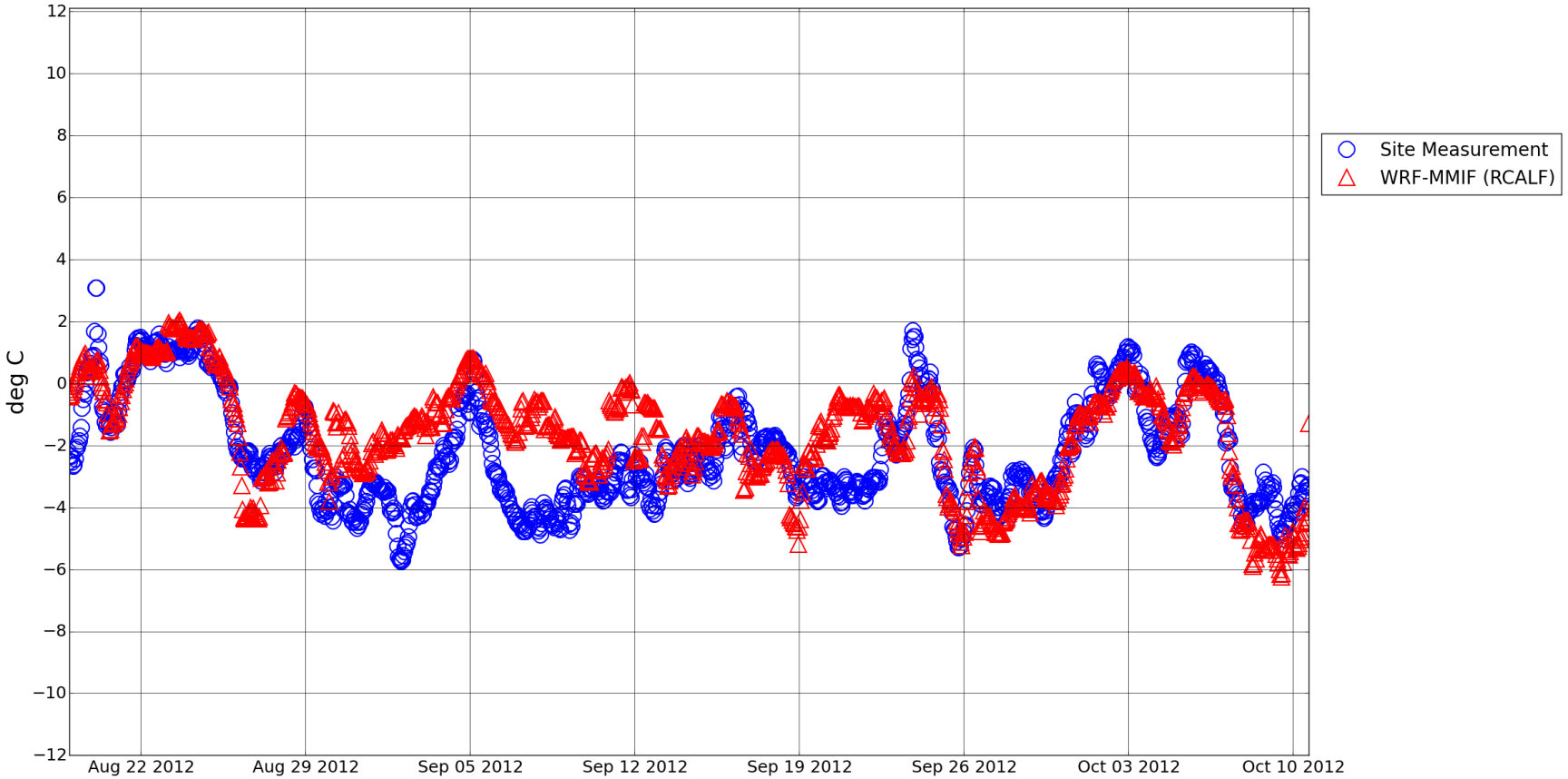

Figure 20. C1 2012 air-sea temperature difference time series.

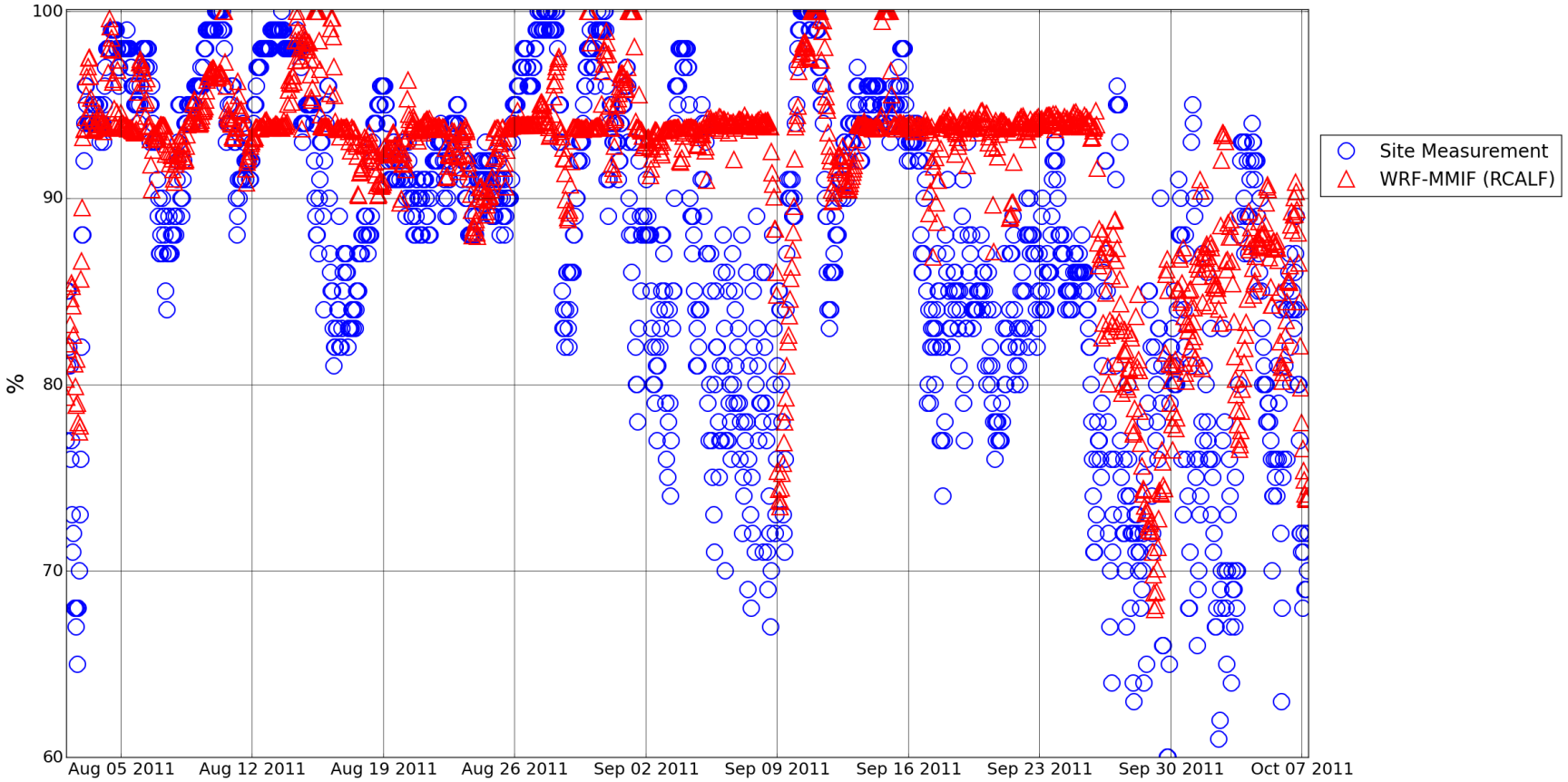

Figure 21. C1 2011 relative humidity time series.

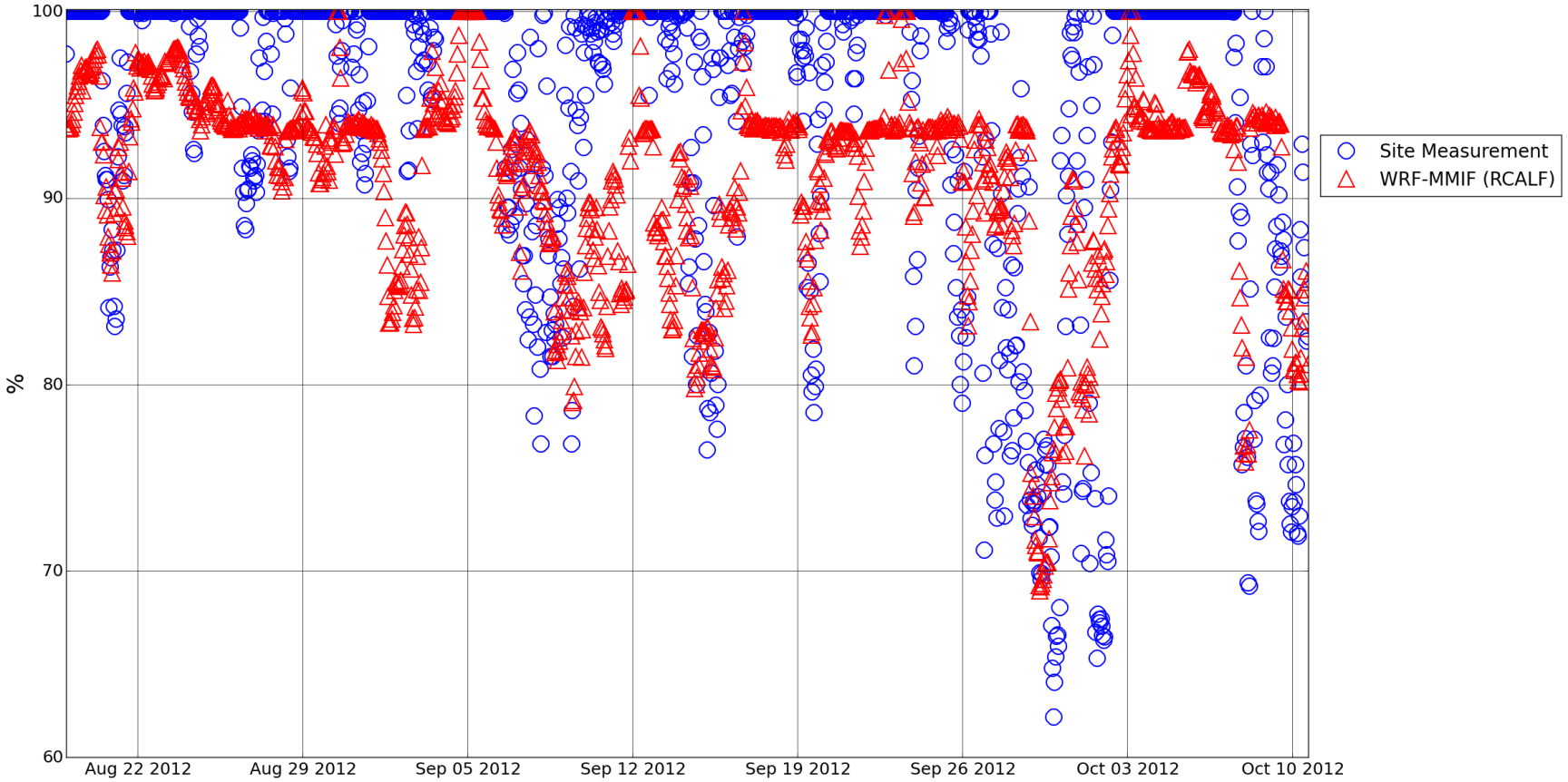

Figure 22. C1 2012 relative humidity time series.

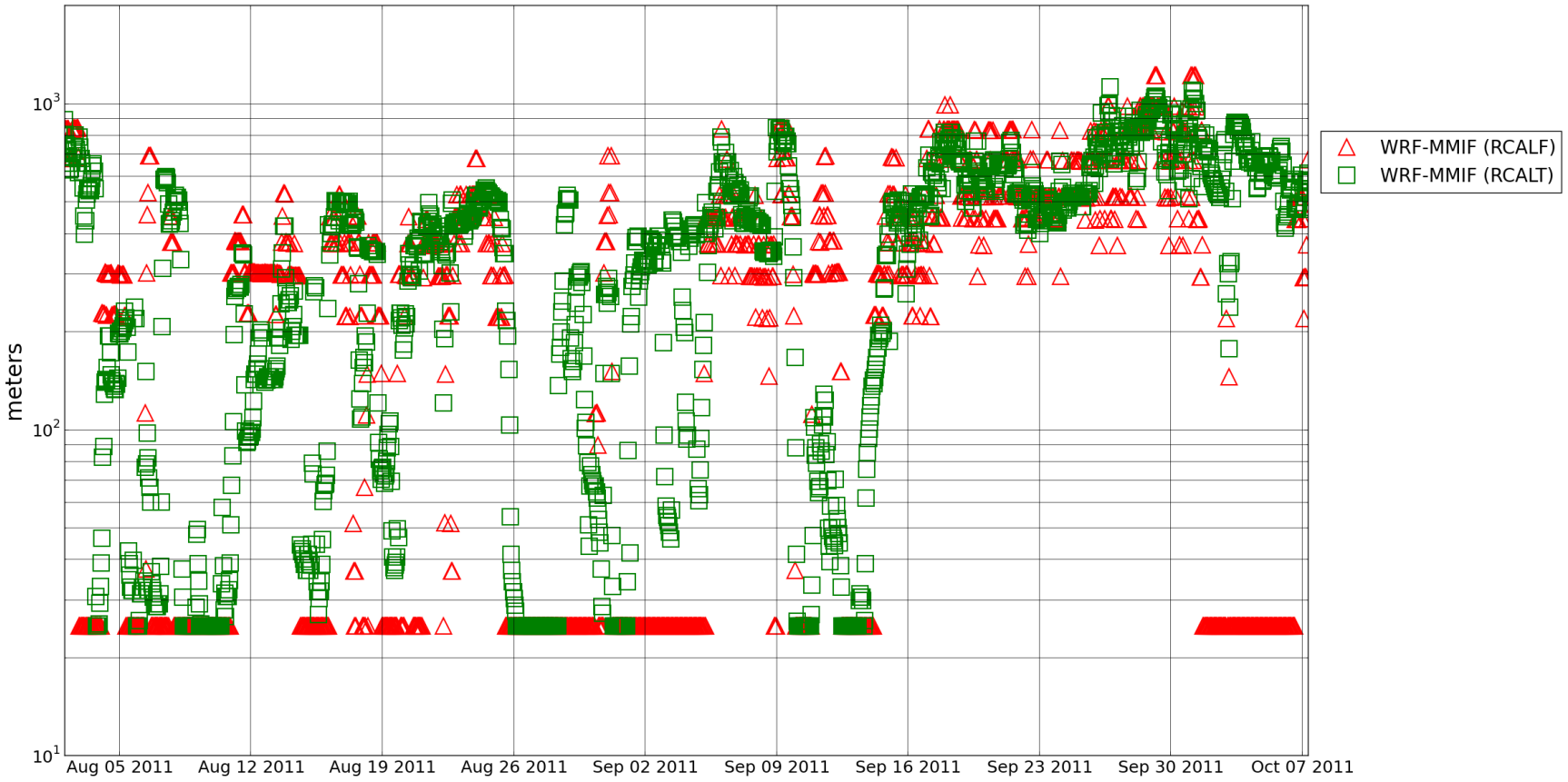

Figure 23. C1 2011 PBL height time series.

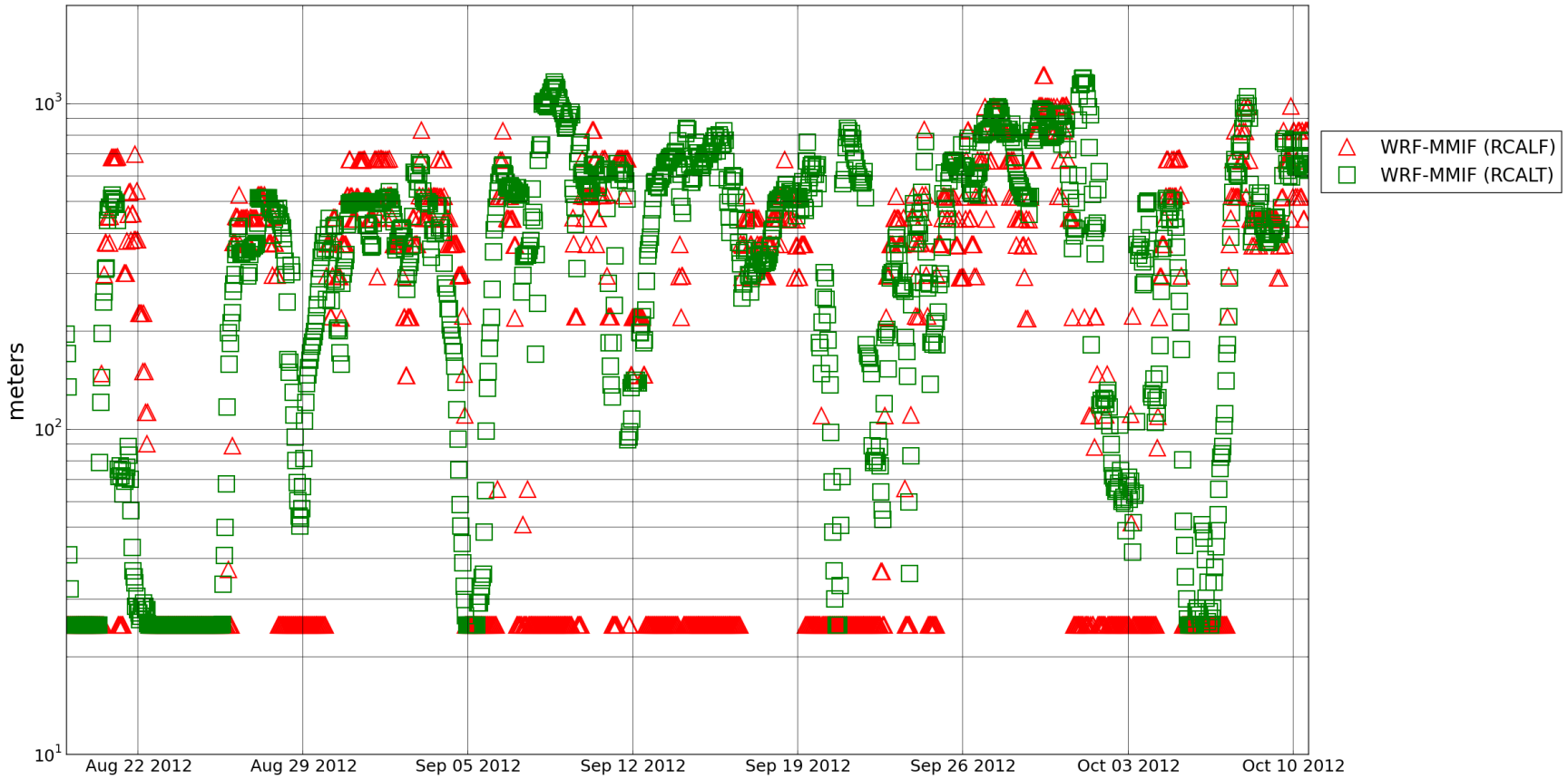

Figure 24. C1 2012 PBL height time series.

4.4 Site C2: Chukchi-Klondike

4.4.1 Wind speed

Time series plots of site C2 during 2010 and 2012 are shown in Figure 25 and Figure 26, respectively. WRF wind speed predictions resulted in average error of 0.1 m/s and -0.2 m/s and RMSE of 1.1 and 1.0 m/s for the two periods, respectively. Qualitatively, the figures show WRF predicted wind speed quite well. The negative bias of 2012 was caused mainly by short periods of underpredicted wind speed, generally -1 to -2 m/s, occurring Sep. 1st - 3rd, Sep. 9th – 11th, and Sep. 20th to 22nd. However, given WRF wind speed was calculated at 10 m height and the observed wind speed was at 3.5 m, the WRF wind speed should have been biased high in comparison to the measurements.

4.4.2 Wind direction

Time series plots of site C2 during 2010 and 2012 are shown in Figure 27 and Figure 28, respectively. Average wind direction error for 2010 was +0.7° and RMSE was 19.5°. Average 2012 wind direction error was +10° and RMSE was 16.2°.

4.4.3 Air temperature

Time series plots of site C2 during 2010 and 2012 are shown in Figure 29 and Figure 30, respectively. The WRF simulation results followed the temperature magnitude and trends closely, but periods of significant deviation were evident. WRF overpredicted temperature by 2-4°C early August 2010 and by 1 - 2 °C short periods in late September 2010 and 2012. WRF also underpredicted temperature in 2010 by 1 - 2 °C Aug 8 – 14 and Sep. 12-19. Overall, the WRF simulation average deviation was +0.1°C and +0.2 °C for 2010 and 2012, respectively. Given the high frequency of stable conditions, the temperature bias may have been an artifact of the differences in height: WRF temperature was extracted at 2.0 m and the measurement height was 3.0 m.

4.4.4 Sea surface temperature

Time series plots of site C2 for 2010 and 2012 are shown in Figure 31 and Figure 32, respectively. The early 2010 FNMOC SST analysis estimates were different than the observations. The SST estimates improved in September 2010, but were biased about +1°C for the rest of the season. The FNMOC analysis data matched the measurements closely with very little error all of 2012. Overall, the average 2010 bias was -0.06°C and 0.02°C for 2012.

4.4.5 Air-sea temperature difference

Time series plots of site C2 during 2010 and 2012 are shown in Figure 33 and Figure 34, respectively. WRF simulated the correct sign of the ASTD for most of the simulated time for both the 2010 and 2012 periods. Hours with significant difference between WRF and measurement ASTD (significant considered as an absolute value of 0.5°C or more difference) and opposite ASTD sign occurred 15% and 11% of the time for 2010 and 2012, respectively.

A significant deviation occurred August 21-22, 2010 when WRF predicted a positive +1°C ASTD while the measurements indicated a negative difference of about -2°C. In 2010, WRF tended to predict a lower magnitude of ASTD more often than the measurements until late September. In 2012, WRF ASTD error was low except for short periods Sep. 1st – 3rd and Sep. 21st, where WRF predicted ASTD near 0 ºC and measurements indicated an ASTD of -2 to -4 ºC. . WRF average ASTD bias was -0.13° in 2010 and +0.16° in 2012.

4.4.6 Relative humidity

Time series plots of site C2 during 2010 and 2012 are shown in Figure 35 and Figure 36, respectively. The 2010 WRF RH results were quite accurate overall, with an average error of +1.3%. WRF RH was biased high on average during the low-RH period occurs late September and early October. In 2012, WRF consistently produces an RH of 94% and rarely produces an RH above 94%, while measurements exceed 94% in these periods. WRF overpredicts RH during periods where measured RH dips into the 80 – 90 % range. Overall, the 2012 WRF bias is +0.43%.

4.4.7 PBL height

Time series plots of site C2 PBL height for 2010 and 2012 are shown in Figure 37 and Figure 38, respectively. There is no set of measurements to compare to WRF predictions, so the plots contain only WRF (RCALF) and MMIF PBL height (RCALT) predictions. In 2010, minimum PBL heights of 25 m occur most of the time, as predicted by WRF. The MMIF rediagnosis results in the same minimum 25 m PBL heights for most of these same hours. The maximum MMIF PBL heights agree well in time and relative magnitude. In 2012, WRF predicts minimum PBL heights most of the time also. The MMIF rediagnosis results in higher PBL heights of 30 -100 m for a majority of these periods. The timing and magnitude of the maximum PBL heights agree well between WRF and MMIF.

4.4.8 Discussion

Overall, WRF period bias was relatively small for all variables. Wind speed was consistently within 1 m/s of the measurements except for a few short periods. The sign and magnitude of ASTD predicted by WRF was the same as the measurements for the majority of the hours modeled. Given the relative accuracy of the WRF predictions at C2, it was assumed AERMOD predictions using WRF and measured meteorology would be similar. WRF-MMIF PBL heights are used for AERMOD modeling for both the WRF and measurement-based simulations.

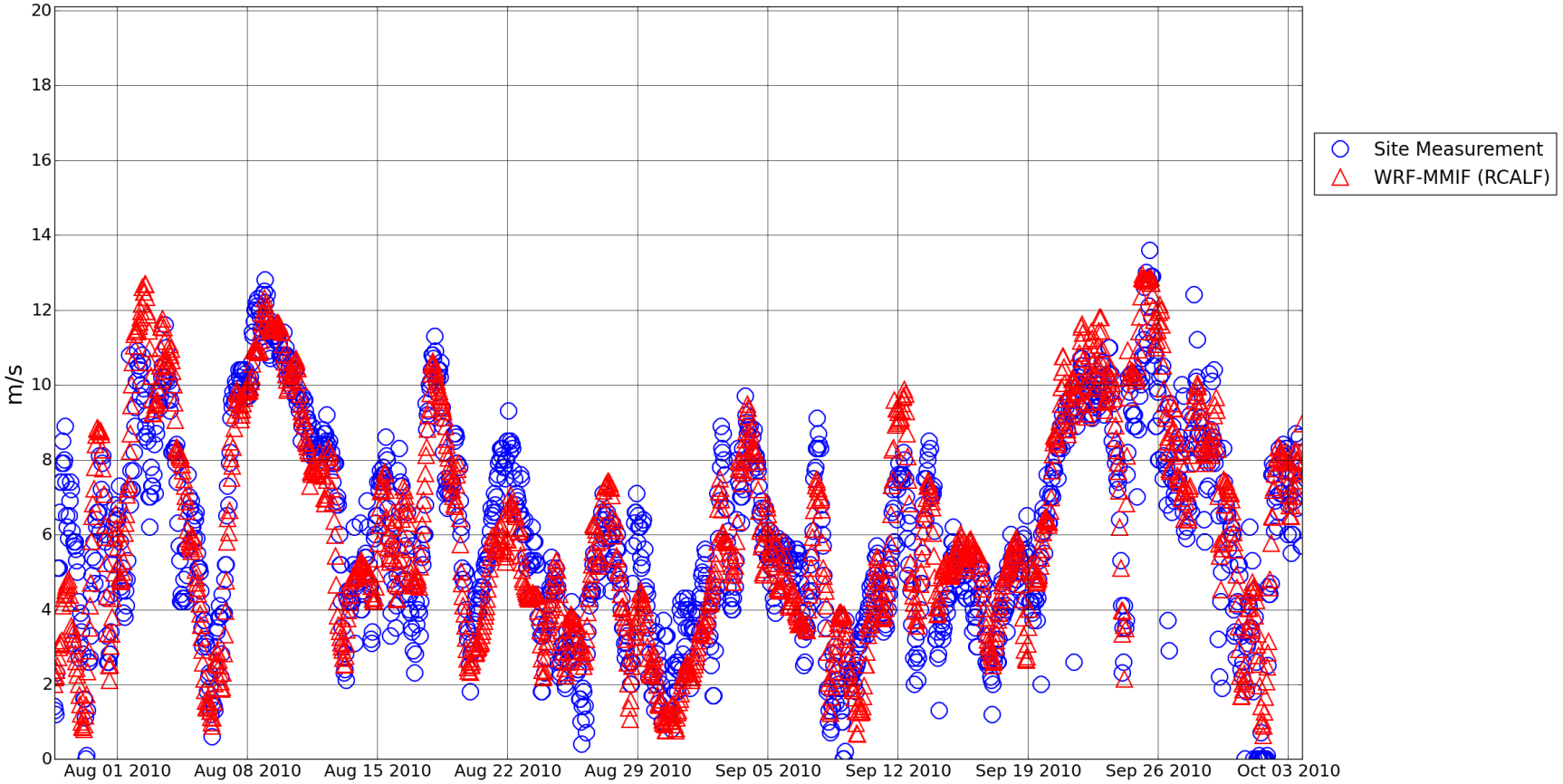

Figure 25. C2 2010 wind speed time series.

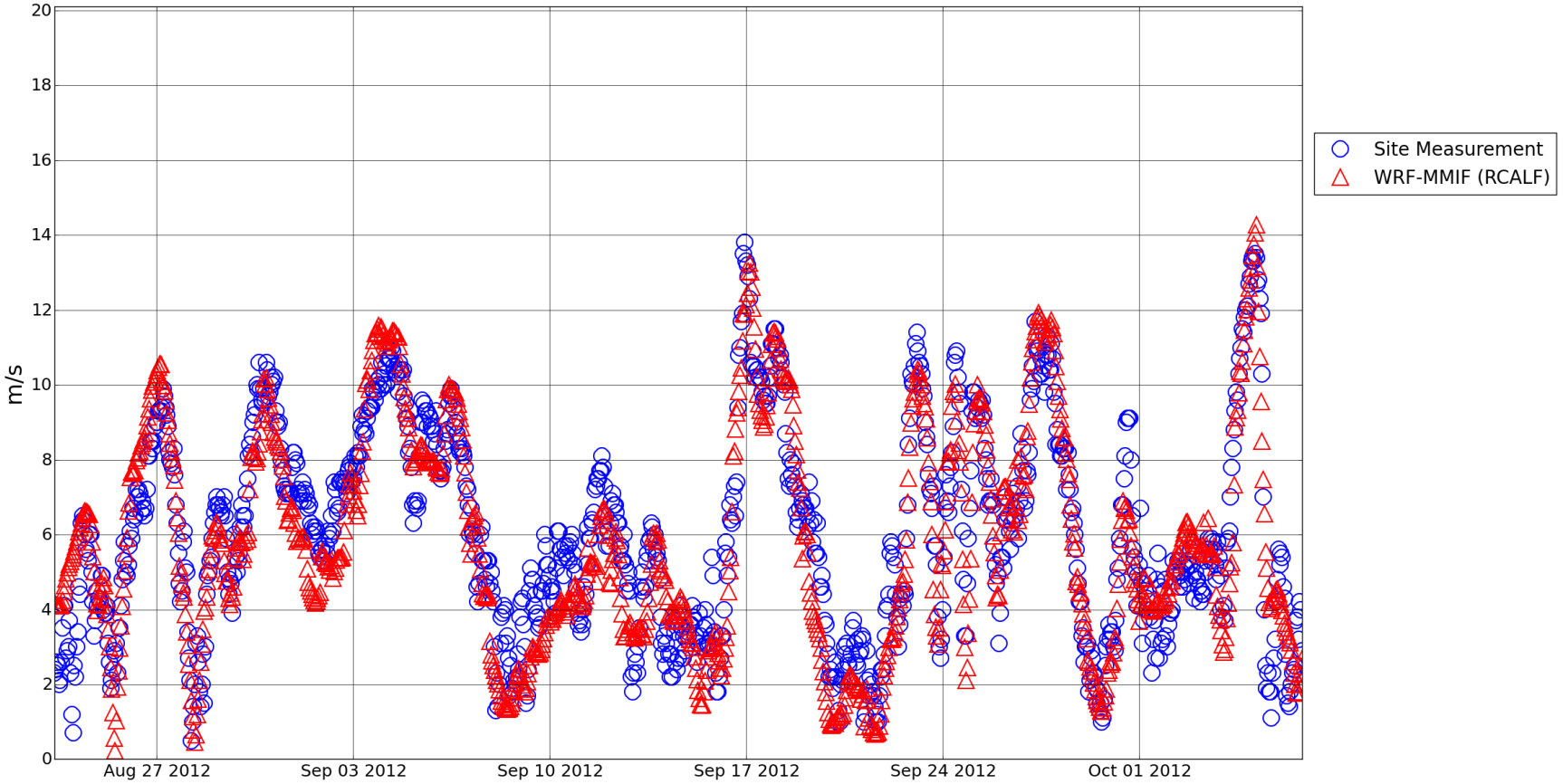

Figure 26. C2 2012 wind speed time series.

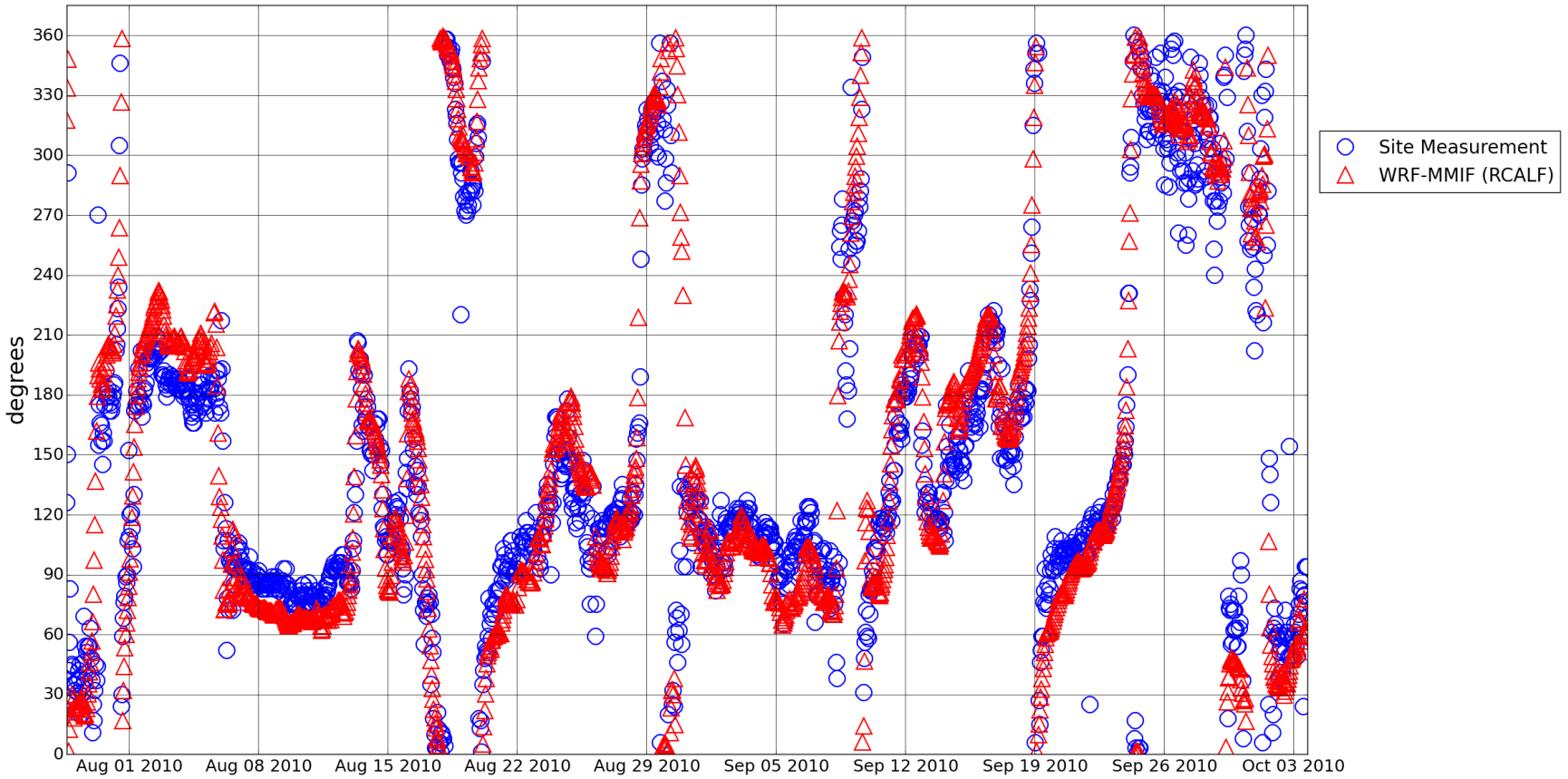

Figure 27. C2 2010 wind direction time series.

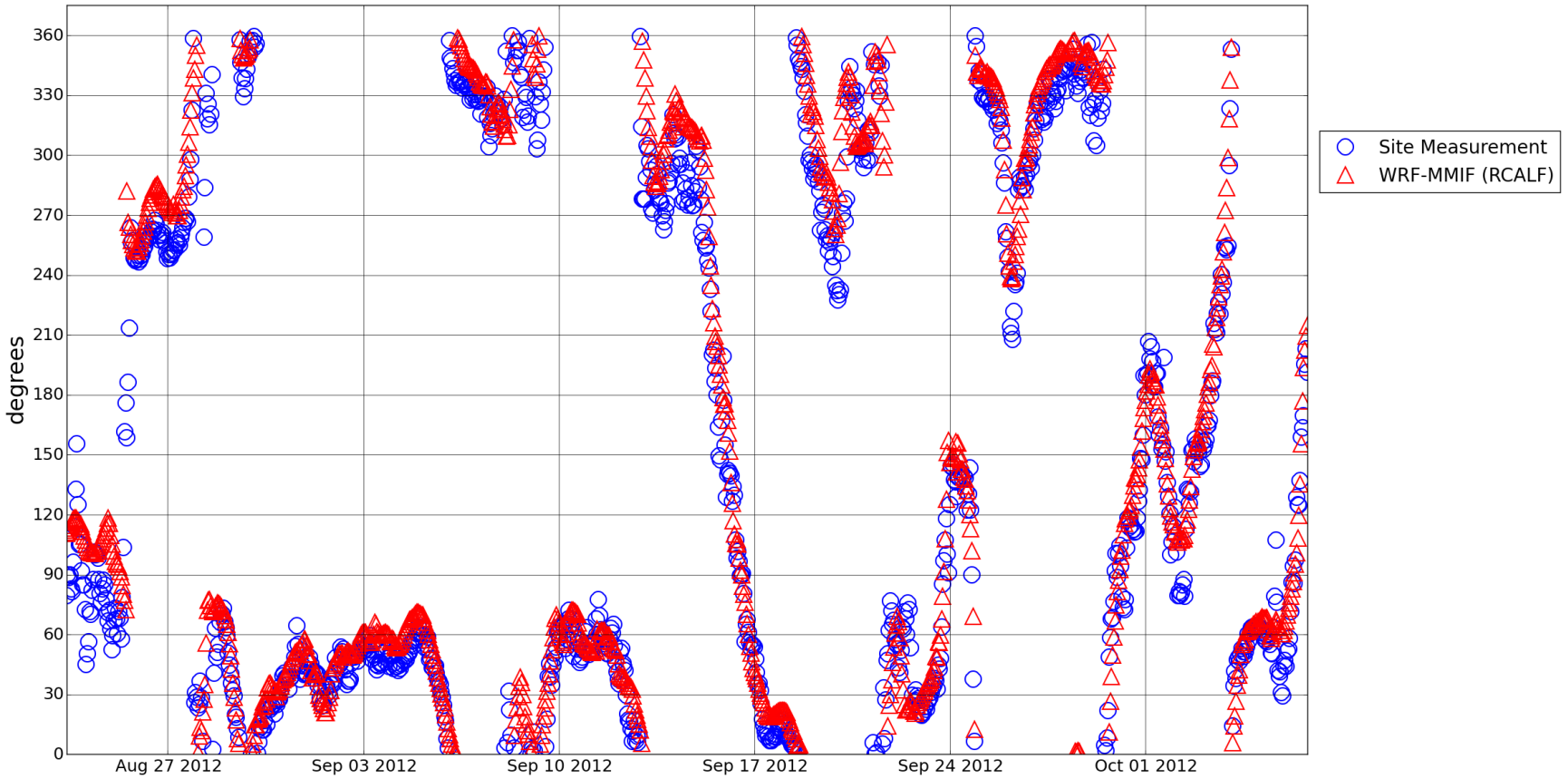

Figure 28. C2 2012 wind direction time series.

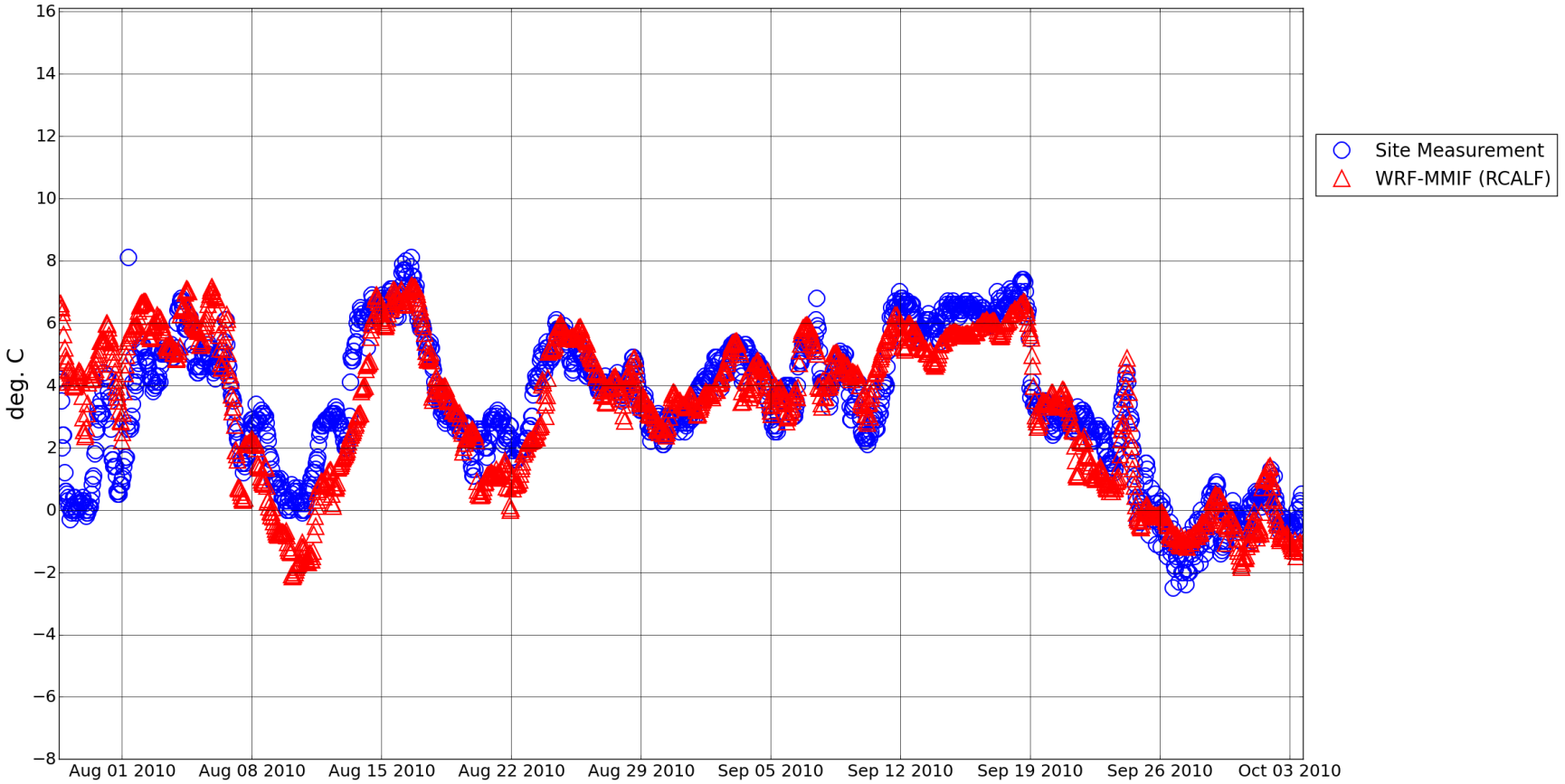

Figure 29. C2 2010 air temperature time series.

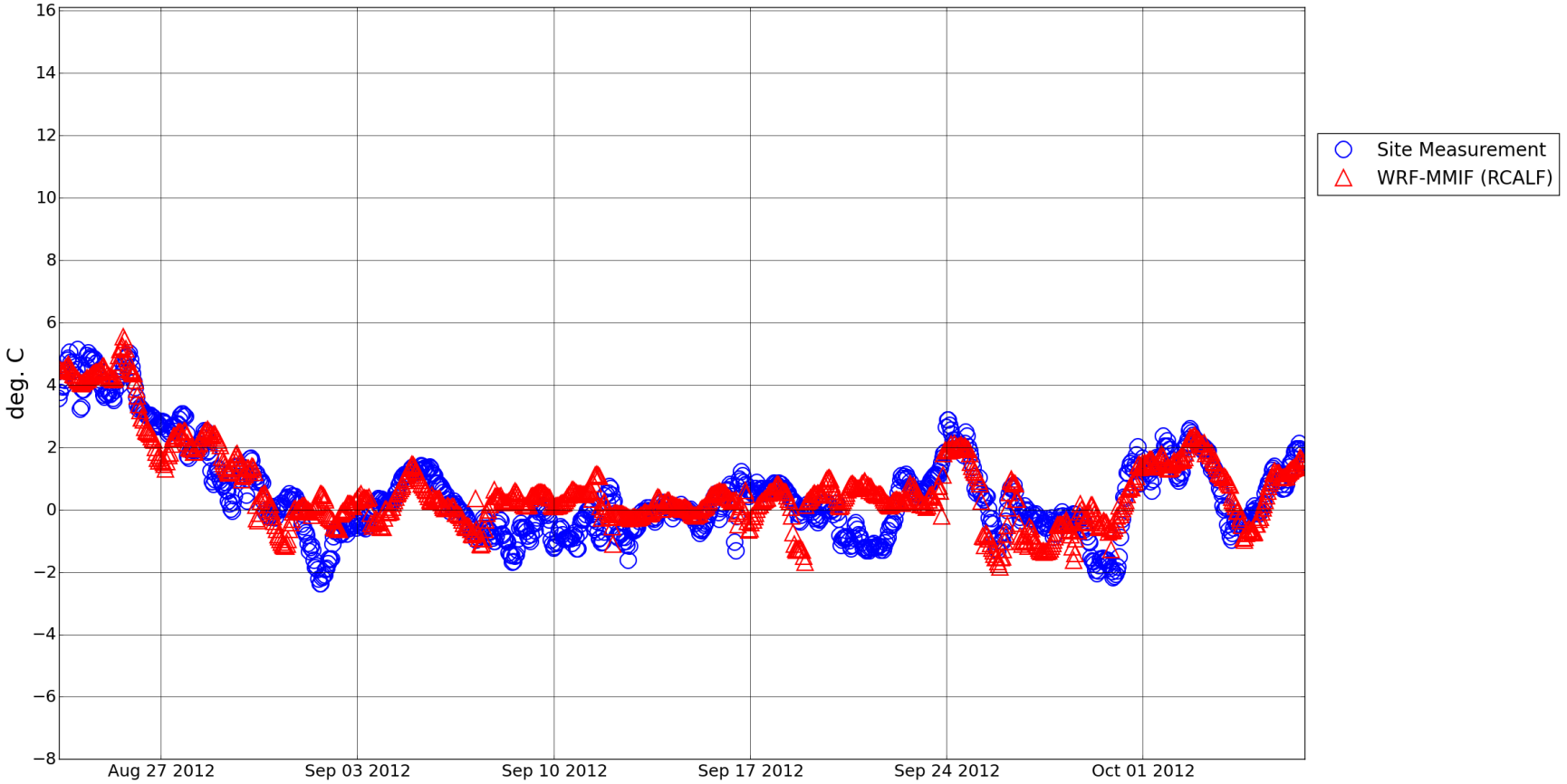

Figure 30. C2 2012 air temperature time series.

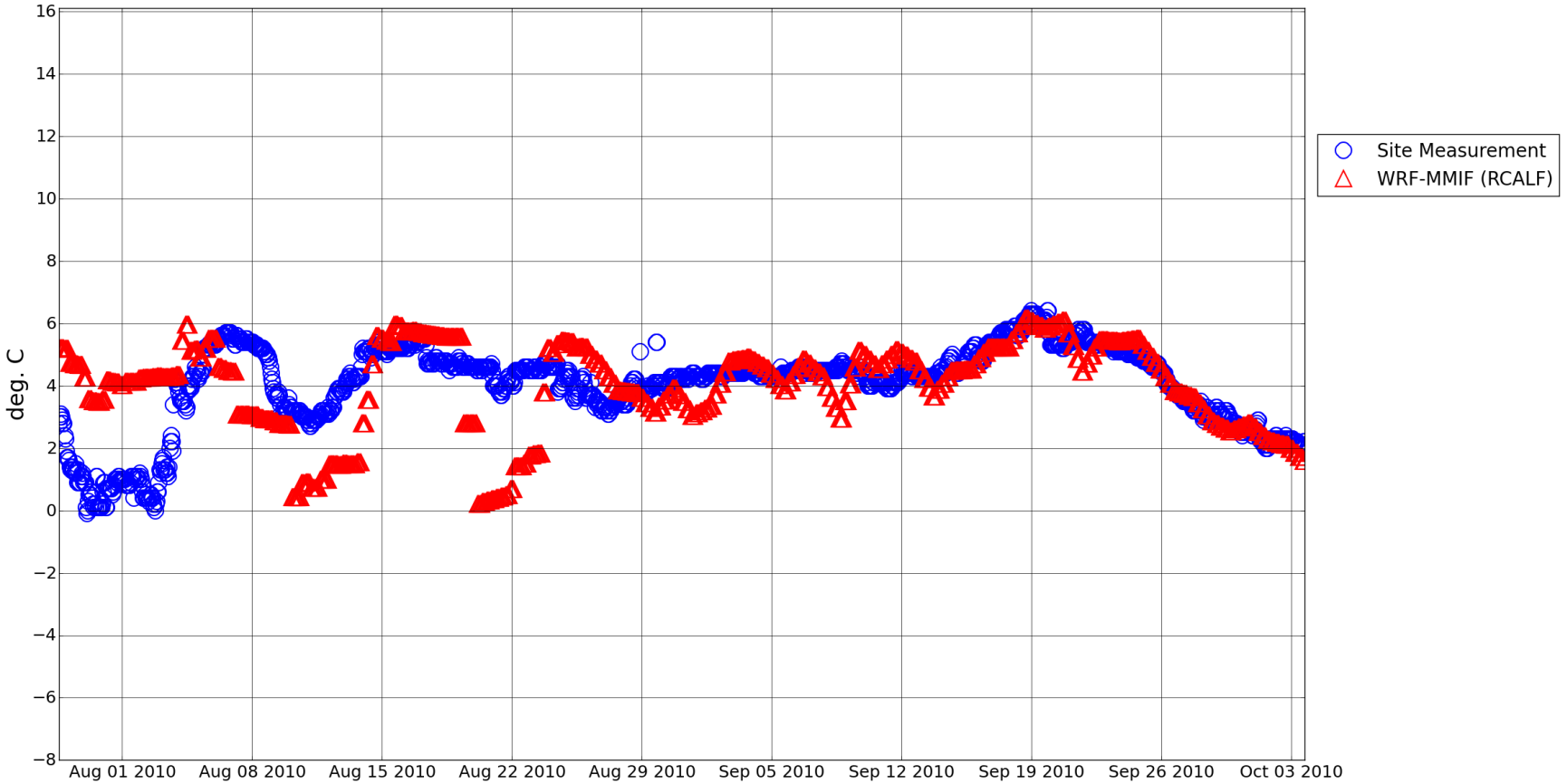

Figure 31. C2 2010 sea surface temperature time series.

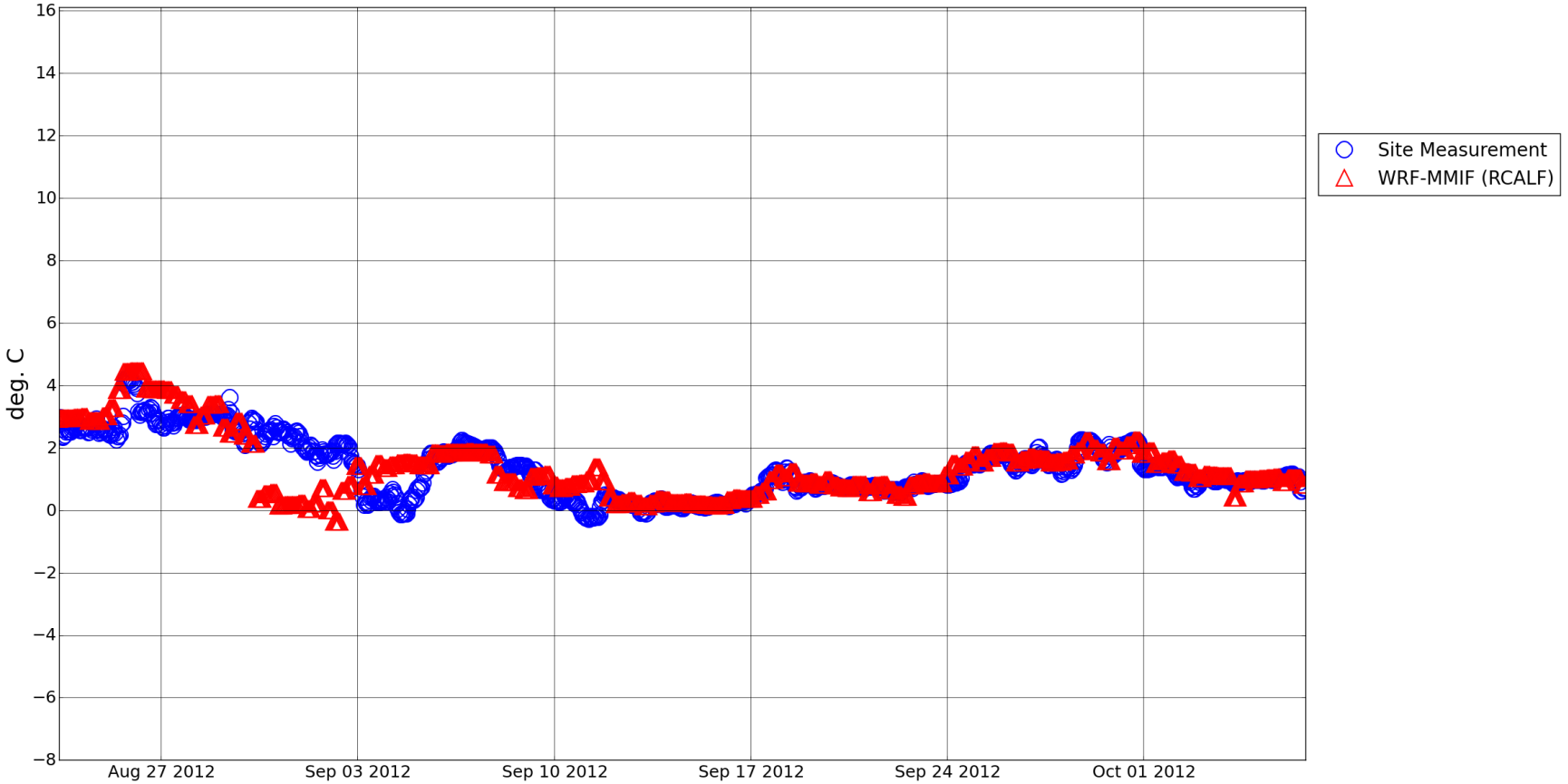

Figure 32. C2 2012 sea surface temperature time series.

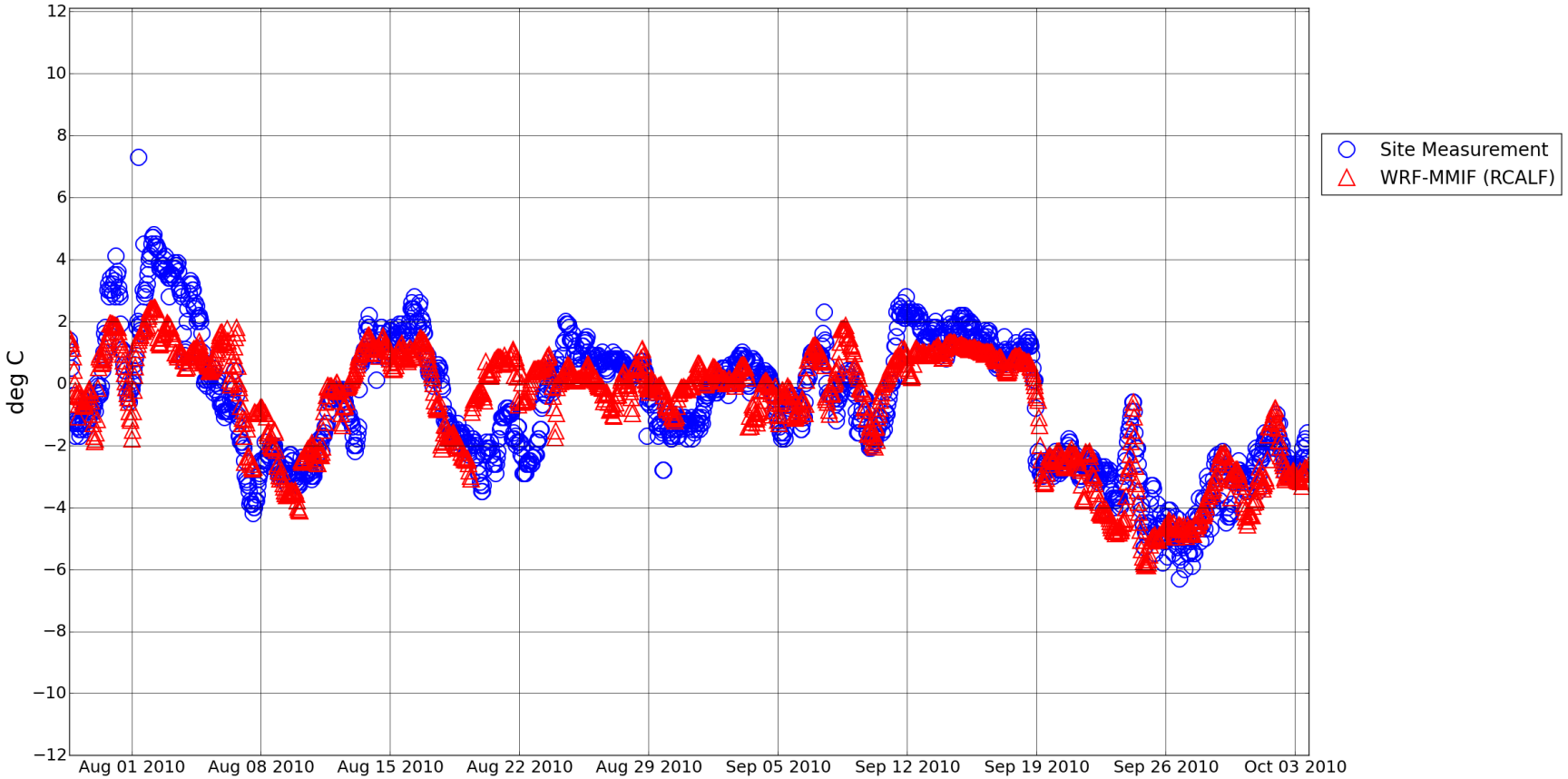

Figure 33. C2 2010 air-sea temperature difference time series.

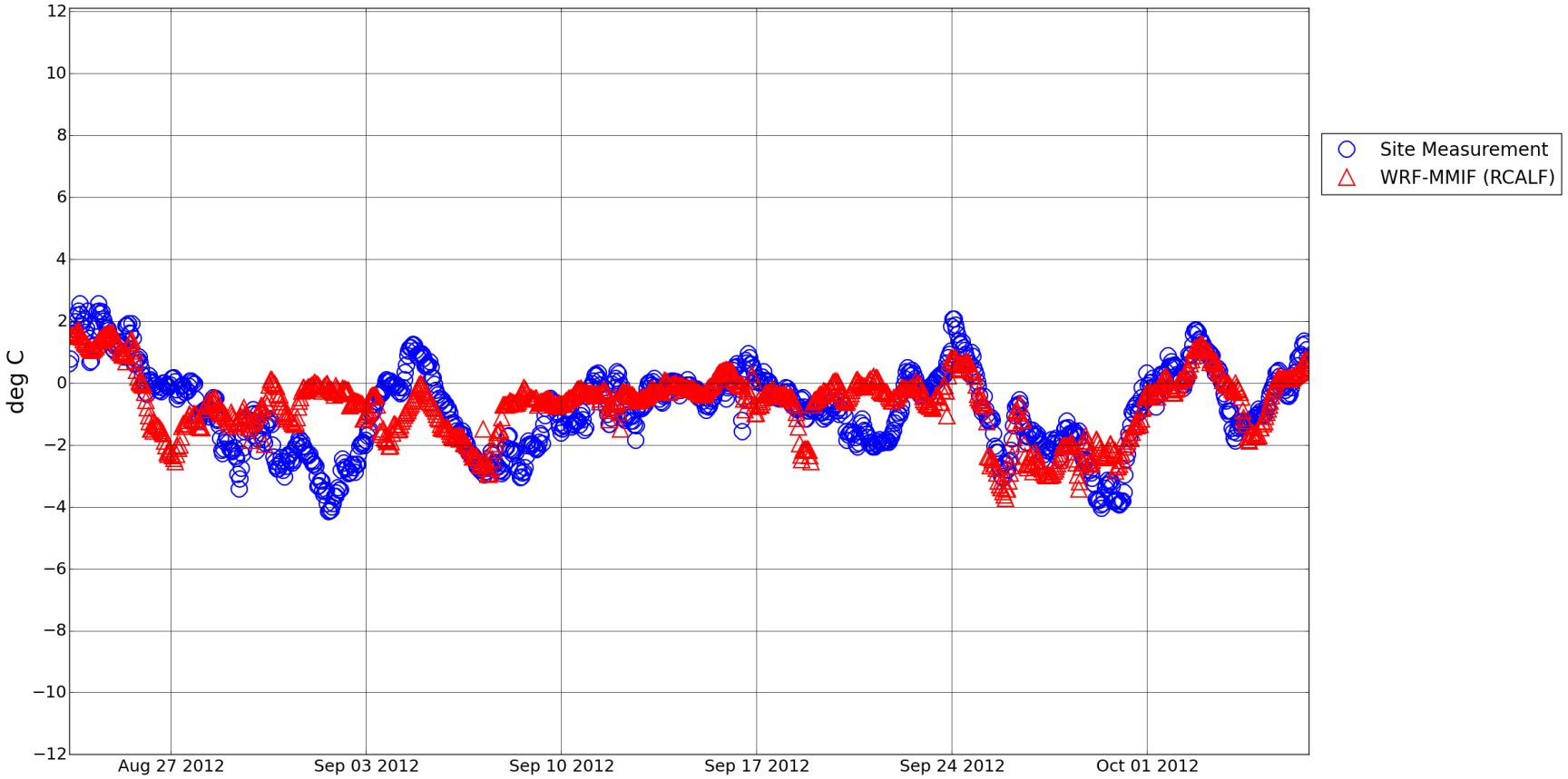

Figure 34. C2 2012 air-sea temperature difference time series.

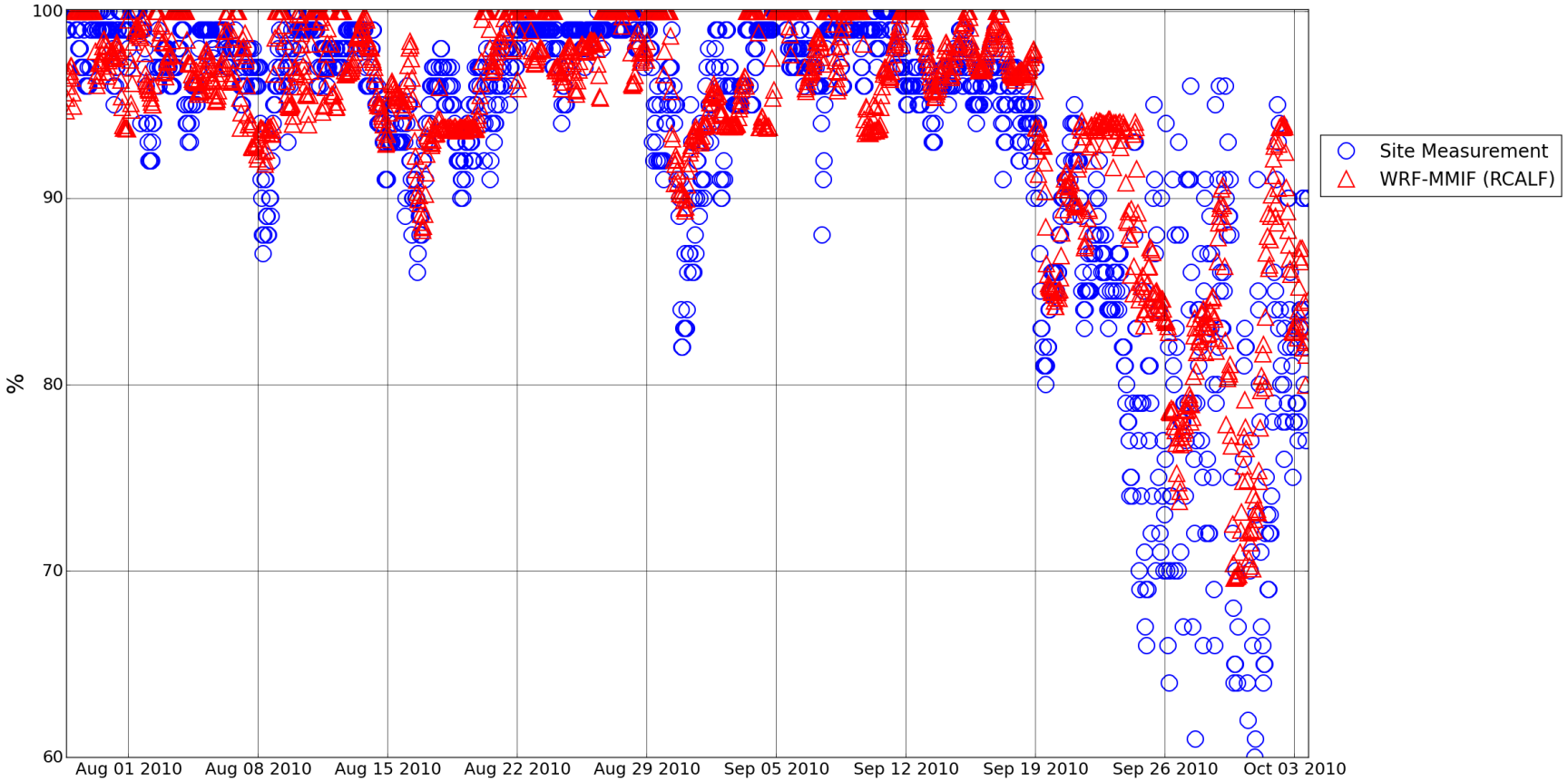

Figure 35. C2 2010 relative humidity time series.

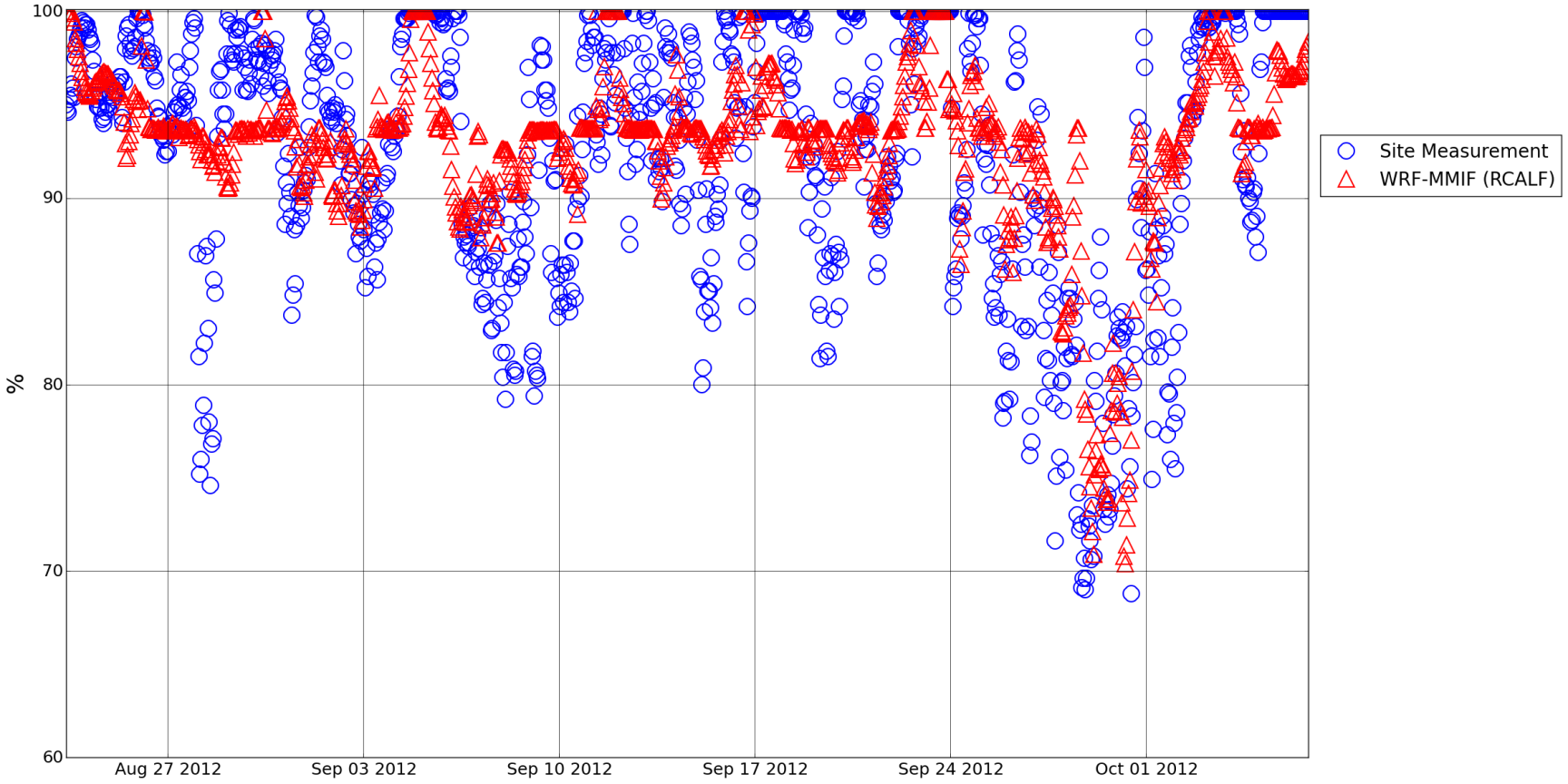

Figure 36. C2 2012 relative humidity time series.

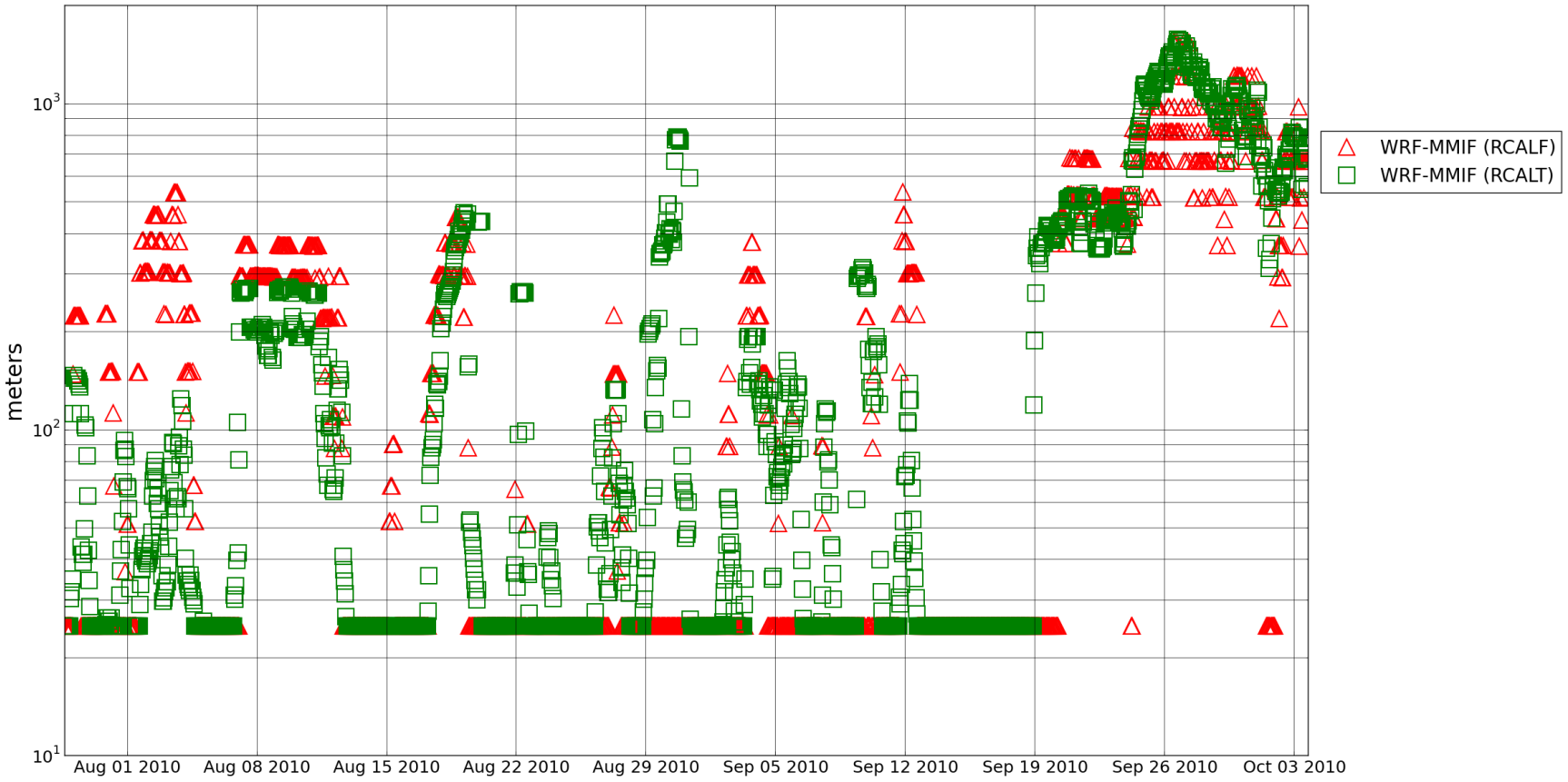

Figure 37. C2 2010 PBL height time series.

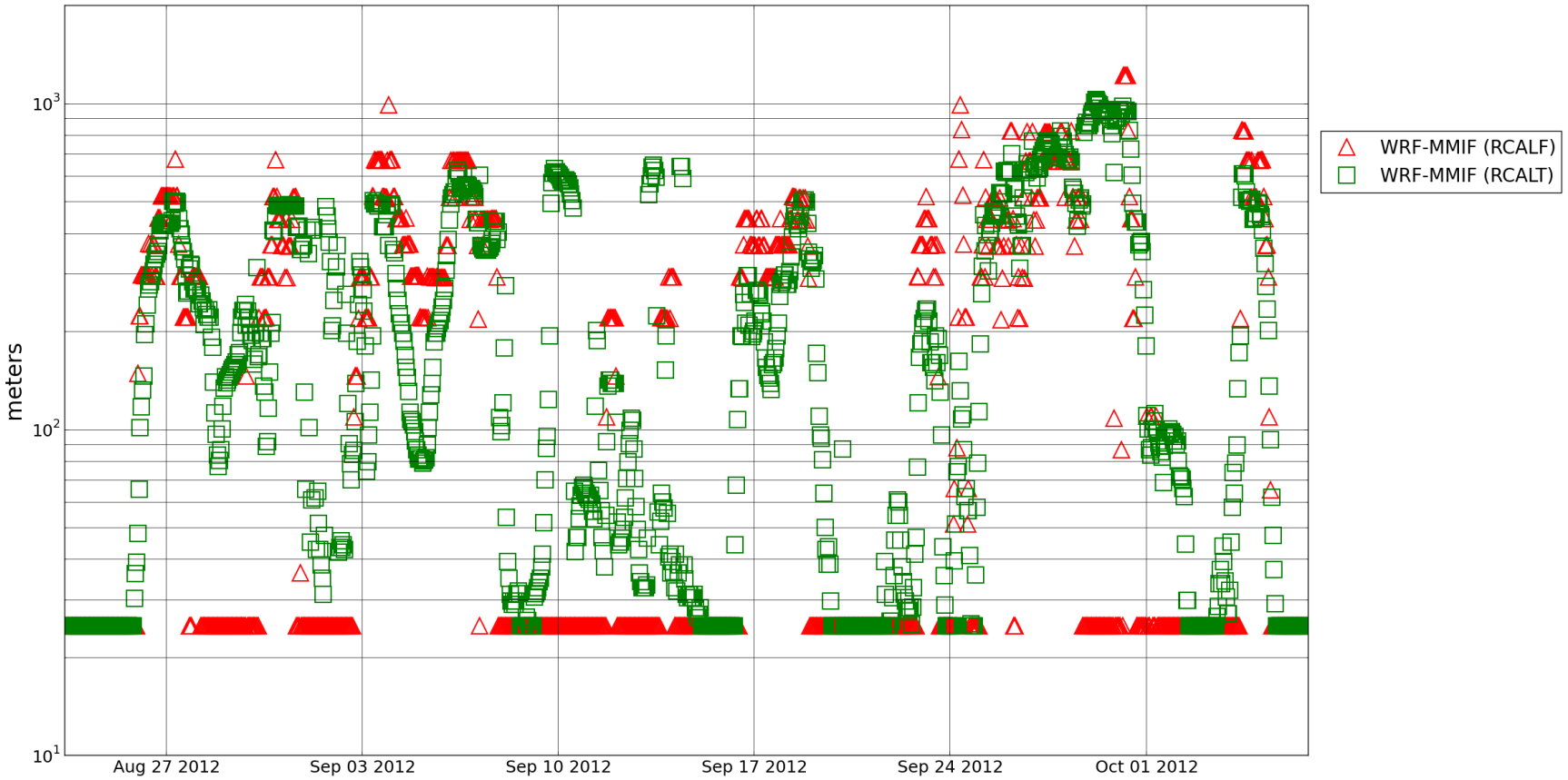

Figure 38. C2 2012 PBL height time series.

4.5 Site B2: Reindeer Island

4.5.1 Wind speed

Time series plots of site B2 during 2010 and 2011 are shown in Figure 39 and Figure 40, respectively. WRF underpredicted wind speed over portions of both seasons and rarely overpredicted wind speed. As a result, the average wind speed was biased low. The average wind speed deviation was -0.7 and -0.9 m/s for 2010 and 2011, respectively. The measurement height was 10.7 m and the WRF wind speed was calculated at 10.0 m. As a result, a small amount of negative bias would be expected. The negative bias at Site B2 correlated with the regional negative bias found by the METSTAT analysis (note Reindeer Island data were not included in the METSTAT database).

4.5.2 Wind direction

Time series plots of site B2 in 2010 and 2011 are shown in Figure 41 and Figure 42, respectively. During both seasons, WRF wind directions correlated well with the observations, based on qualitative comparison of the WRF data and site measurements. No extended period of significant wind direction deviation was evident.

4.5.3 Air temperature

Time series plots of site B2 for 2010 and 2011 are shown in Figure 43 and Figure 44 , respectively. WRF consistently overpredicted air temperature for 2010 with a peak overprediction of 5.2° occurring at the beginning of the record on August 18th. The average temperature was 0.9° warmer than the observed temperature. Temperature predictions for 2011 were more accurate overall, resulting in an average temperature deviation of only 0.25°C. However, significant deviations did occur for 2011. WRF overpredicted temperature by 2-5° on September 1st and underpredicted temperature by 2-3° on August 11th.

4.5.4 Sea surface temperature

Time series plots of site B2 during 2010 and 2011 were shown in Figure 45 and Figure 46, respectively. The FNMOC SST analysis data used by WRF were warmer than observed for most of 2010 with the exception of a period of significant underprediction in mid-August. The average 2010 deviation in SST was +0.28°C. For 2011, the SSTs provided to WRF were cooler than observed, resulting in an average SST deviation of -0.63°C.

4.5.5 Air-sea temperature difference

Time series plots of site B2 for 2010 and 2011 are shown in Figure 47 and Figure 48, respectively. For much of 2010 and 2011, the observed SST was near 0°C.This was disadvantageous for atmospheric stability prediction because small errors in ASTD could lead to an opposite sign of stability. However, ASTD magnitude is small and would likely tend to support near-neutral stability conditions, regardless of sign. Hours with significant difference

between WRF and measurement ASTD ('significant' considered as an absolute value of 0.5° or more difference) and opposite ASTD sign occurred 28% and 48% of the time for 2010 and 2011, respectively.

Overall, the WRF ASTD was warmer than observed due to overpredicted air temperatures in 2010 and underpredicted water temperatures in 2011. The average ASTD deviation from the observations was +0.62°C in 2010 and +0.88°C in 2011.

A significant period of opposite ASTD sign occurred from Aug. 22-25, 2010 as WRF predicted positive ASTD while the measurements indicated negative ASTD. In this case, WRF supported stable atmospheric conditions while the measurements supported unstable conditions. A significant period of opposite ASTD sign also occurred from Aug. 26 – Sep. 7, 2012, where WRF predicted an average ASTD of +0.5°C while the measurements indicated an average ASTD of -0.9°C.

Periods of reversed heat flux appeared frequently in August 2011, but mainly because the ASTD was near 0°C throughout the period. WRF consistently overpredicts ASTD by predicting ASTD values near 0°C while the measurements average near -1°C.

4.5.6 Relative humidity

Time series plots of site B2 in 2010 and 2011 are shown in Figure 49 and Figure 50, respectively. The observations revealed a nearly saturated surface layer for most of 2010 and 2011. The WRF predictions followed this trend closely and correctly simulated the drier periods that occur late in 2010 and early in 2011.

4.5.7 PBL height

Time series plots of site B2 during 2010 and 2011 are shown in Figure 51 and Figure 52, respectively. WRF tended to overpredict the frequency of highly stable conditions based on the high frequency of minimum PBL heights evident for both 2010 and 2011, resulting in underprediction of average PBL height. The average deviation of the WRF (RCALF) predictions was -94 m and -46 m, respectively. WRF tended to overpredict PBL height during a portion of the unstable periods, evident in late September 2010 and 2011. The MMIF recalculated PBL heights were more accurate on average, but still excessively low, resulting in an average bias of -62 m and -23 m for 2010 and 2011, respectively.

High PBL error did occur during the significant period of opposite sign ASTD identified in Section 5.5.5 from Aug. 22 – 25 and Aug. 30 – Sep. 1, 2010. Both WRF (RCALF) and MMIF (RCALT) underpredict PBL height during these periods. The primary cause of these differences is the incorrect sign of ASTD which resulted in the prediction of stable atmospheric conditions during an unstable period.

PBL height error was as prevalent in 2011 as 2010 as both WRF (RCALF) and MMIF (RCALT) predicted minimum PBL heights of 25 m during extended periods with measured PBL heights of 50 -200 m. Again, incorrect ASTD sign is to blame. WRF consistently predicts slightly positive

ASTD, supporting stable conditions and the measurements support unstable conditions given the negative ASTD.

4.5.8 Discussion

WRF temperatures support stable conditions through much of 2010 and 2011, while measurements support unstable conditions. This results in significant underprediction of PBL height for large portions of 2010 and 2011. Far-source (> 1,000 m from source to receptors) AERMOD results using WRF-derived PBL heights would likely be conservative overall due to the persistence of minimum 25 m heights during stable periods. The persistence of stable conditions predicted by WRF in 2011 due to ASTD error likely would result in more conservative long-term average concentrations in the mid- and far-source. It is unlikely the PBL height bias would affect short term near-source maximum concentrations since these will tend to occur during unstable conditions. WRF overpredicted PBL height during unstable conditions on average, suggesting maximum near-source concentrations could be conservative. The consistent underprediction of wind speed could also result in overprediction of concentrations by AERMOD at both the near-source and far-source receptors.

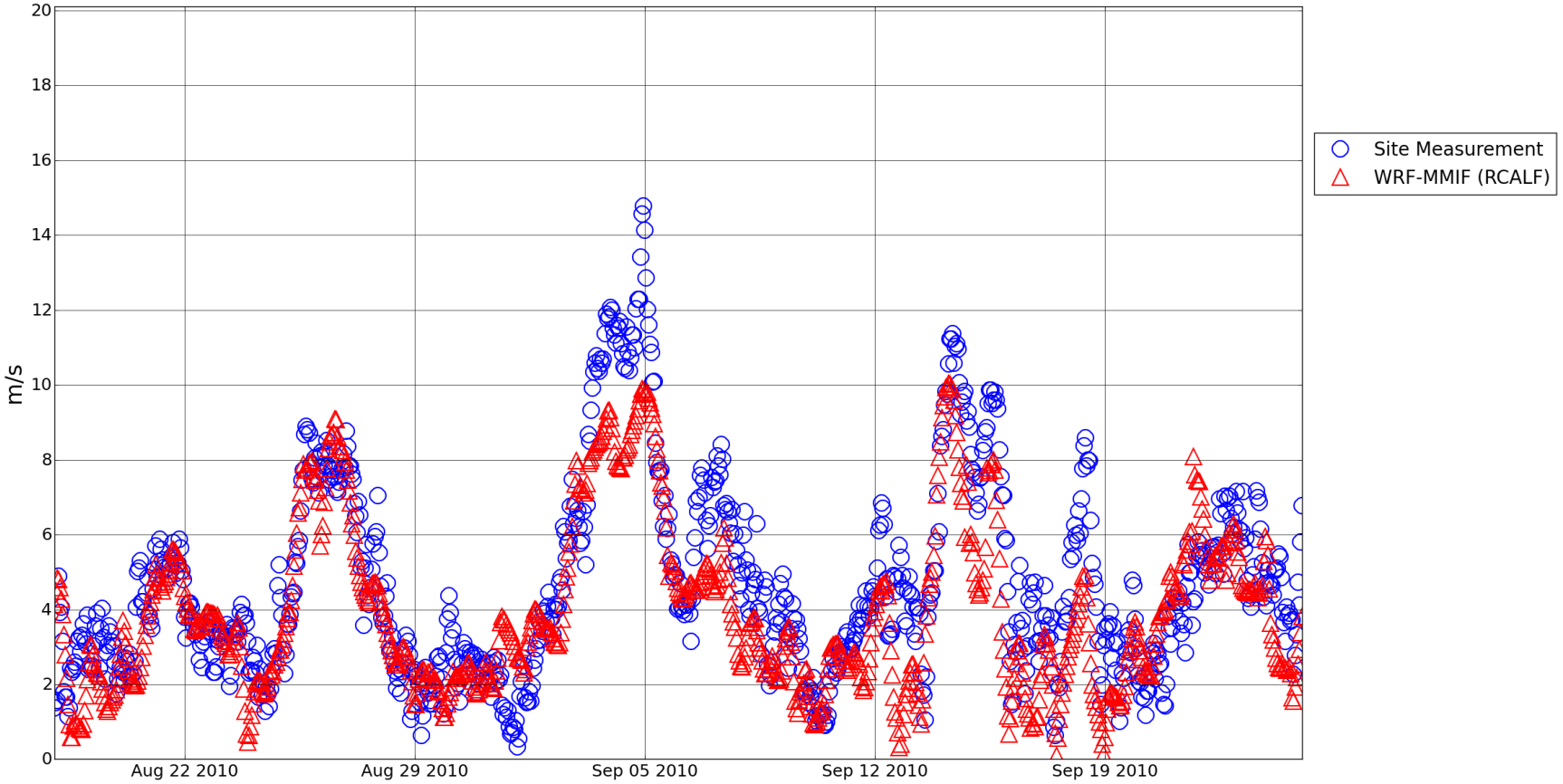

Figure 39. B2 2010 wind speed time series.

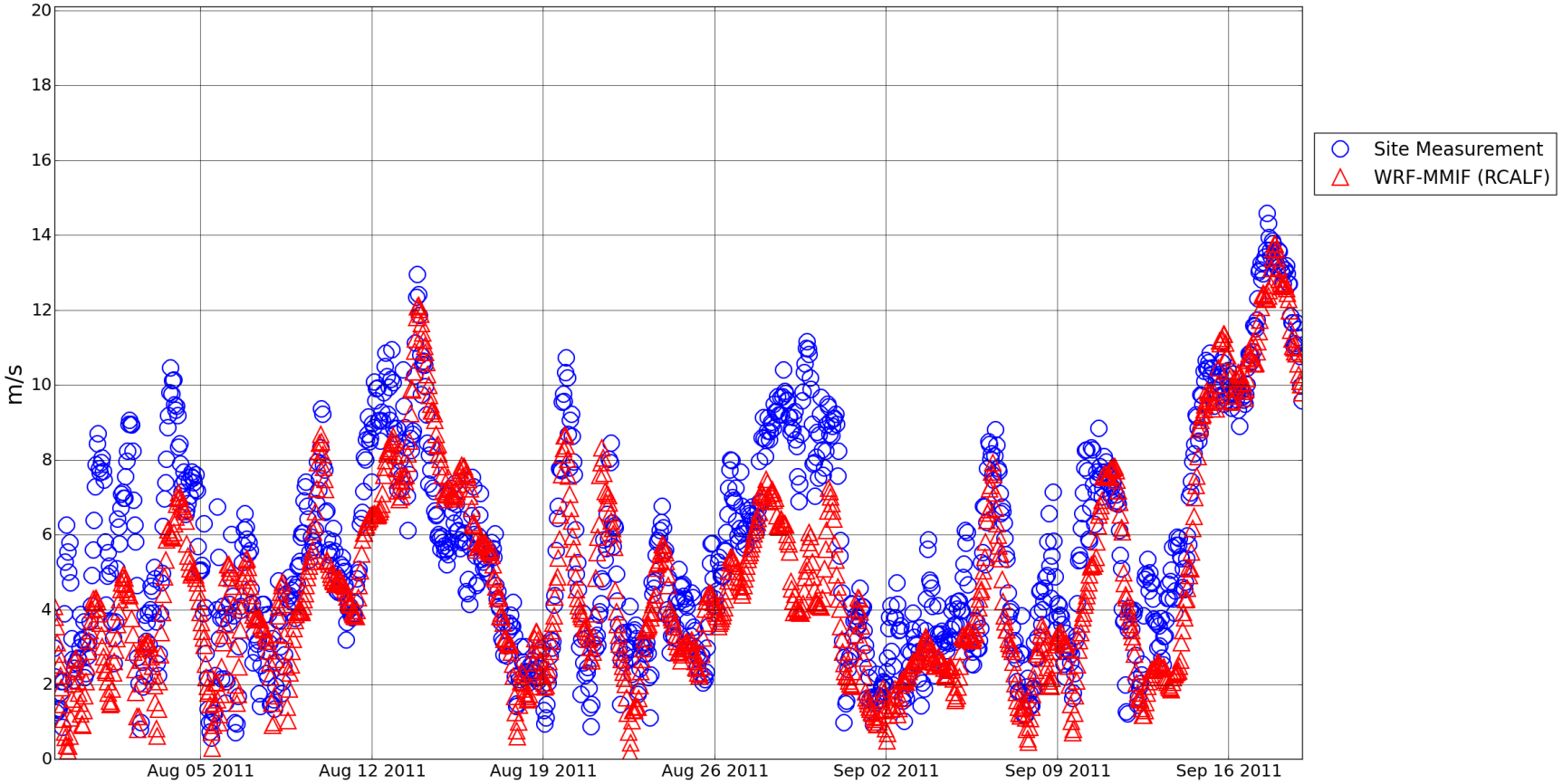

Figure 40. B2 2011 wind speed time series.

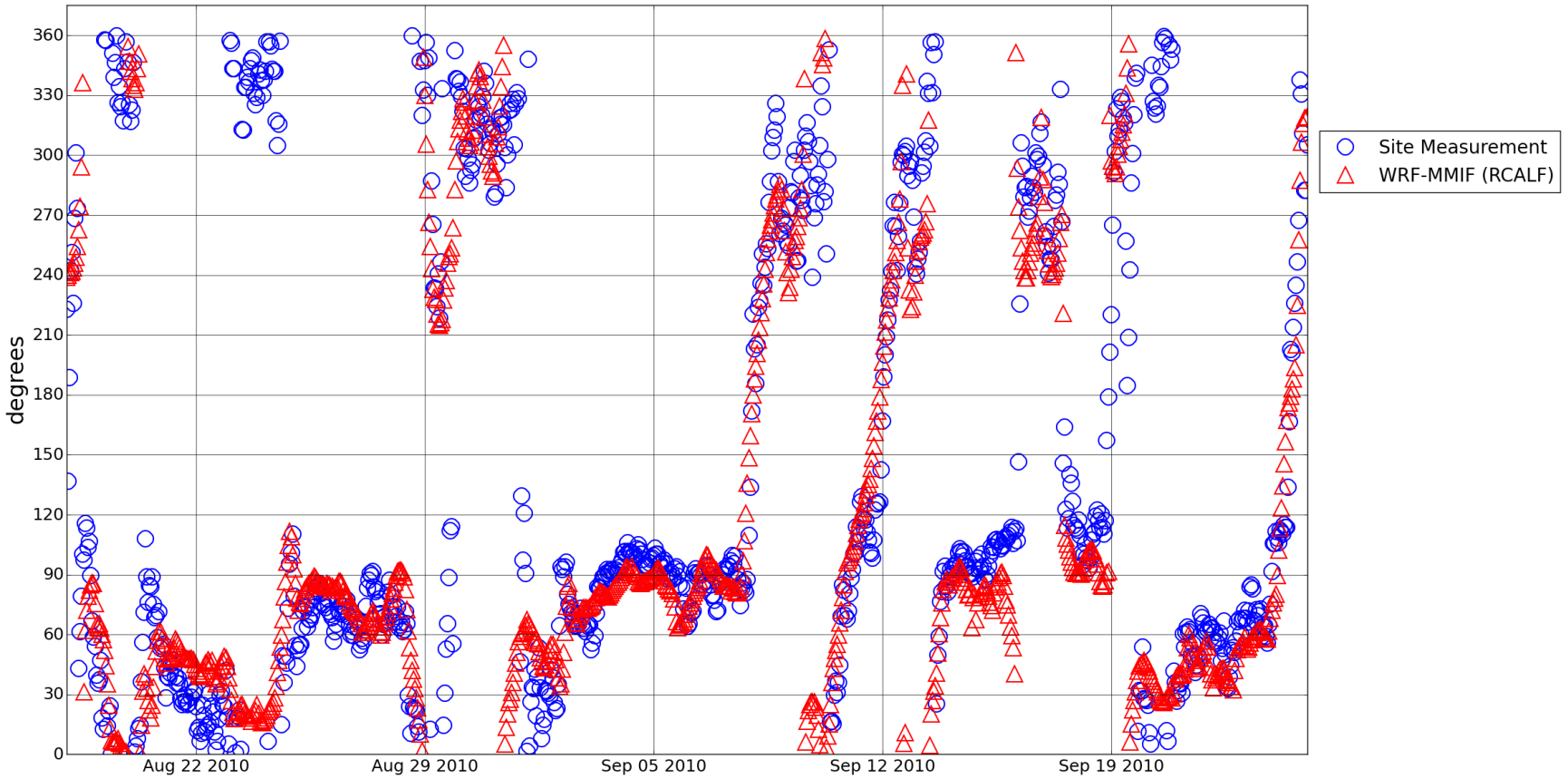

Figure 41. B2 2010 wind direction time series.

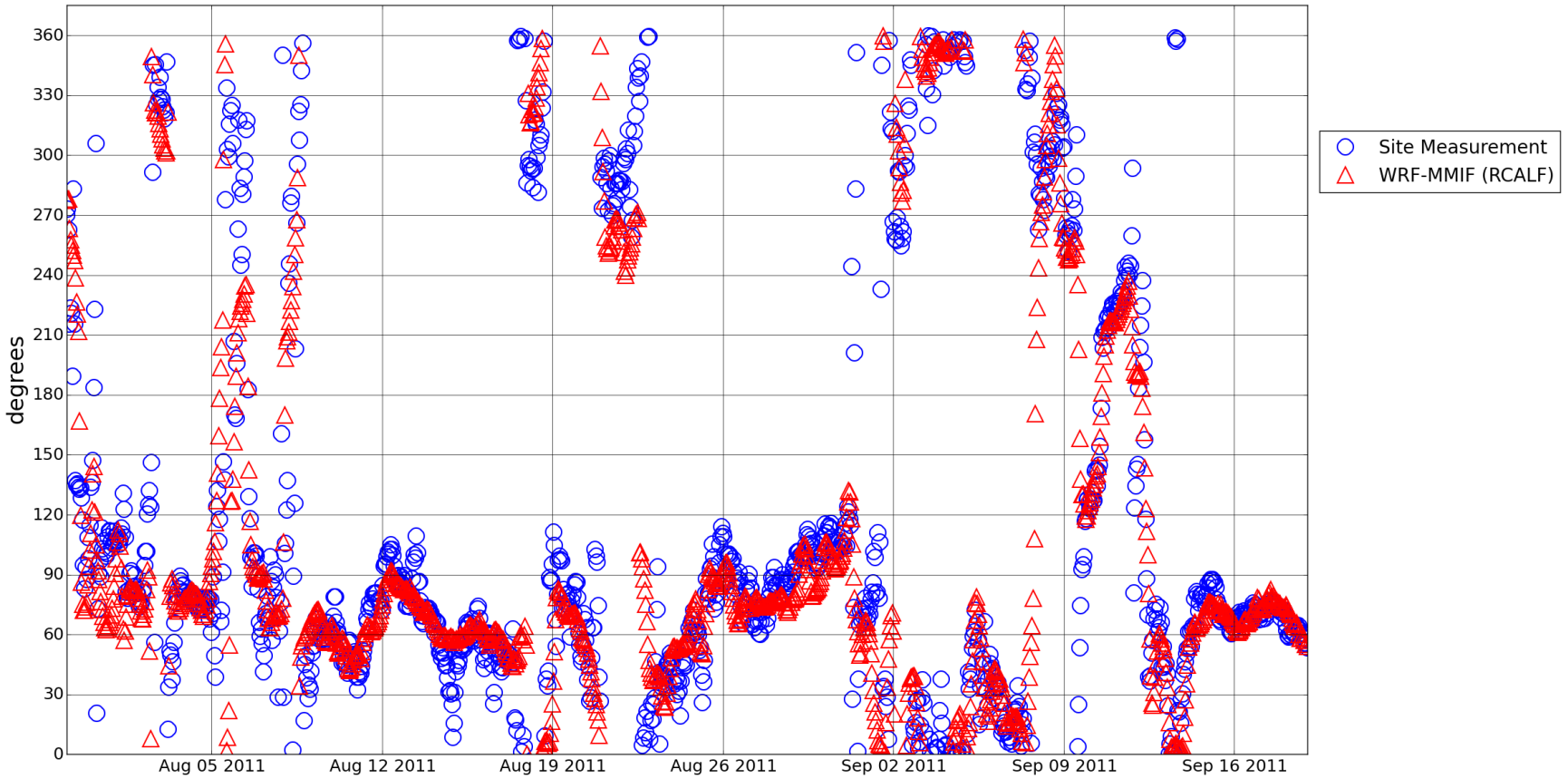

Figure 42. B2 2011 wind direction time series.

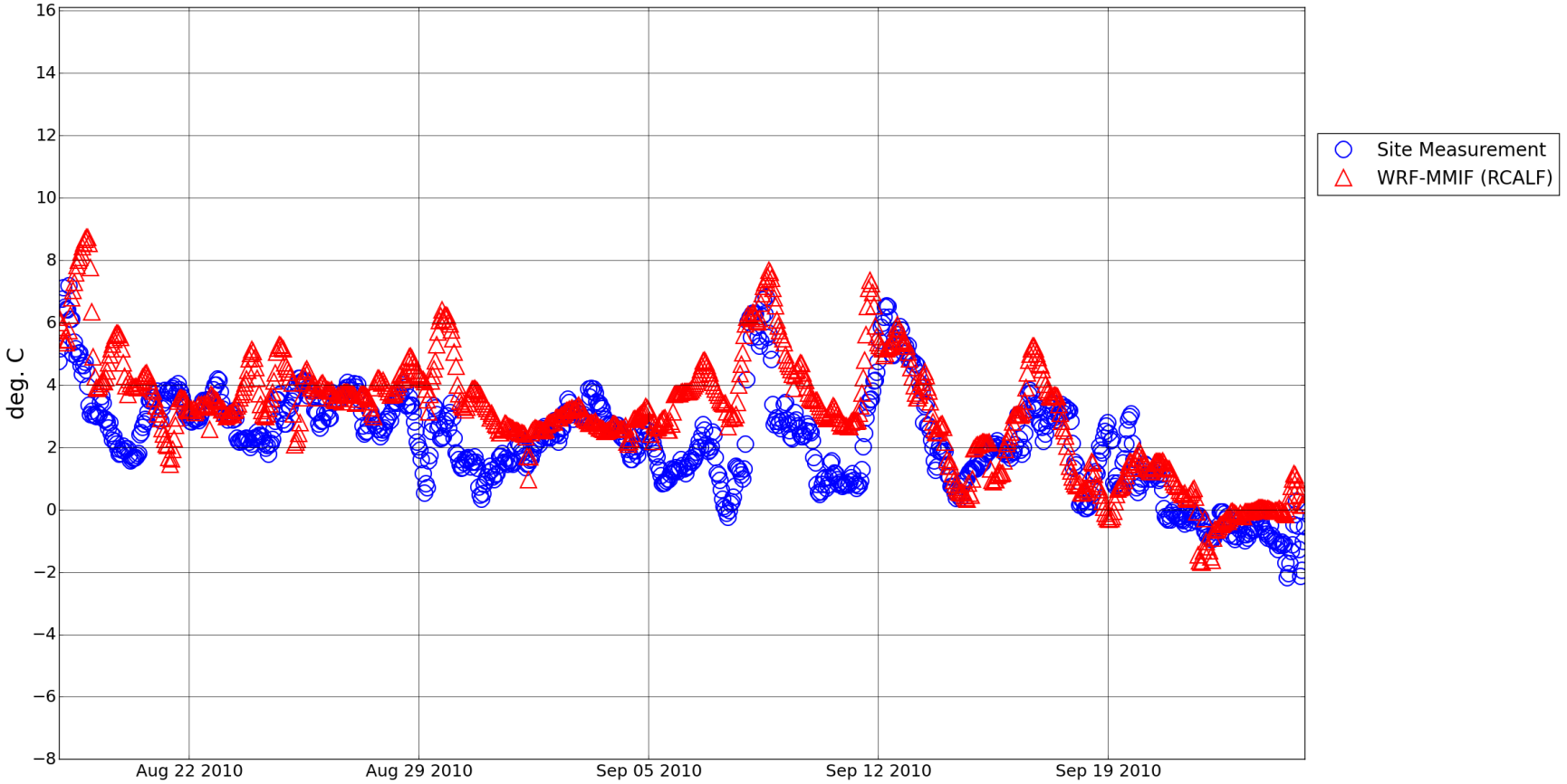

Figure 43. B2 2010 air temperature time series.

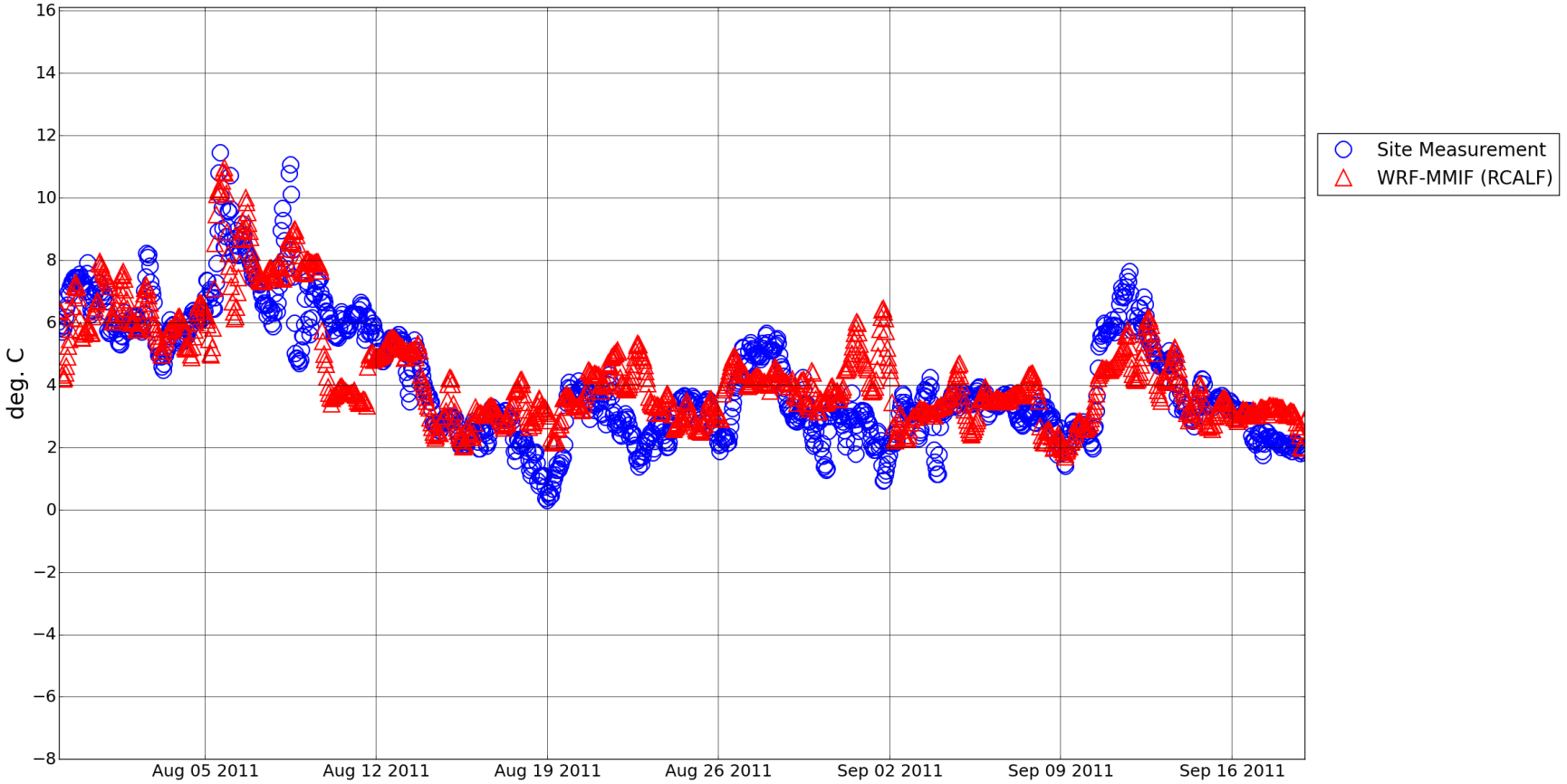

Figure 44. B2 2011 air temperature time series.

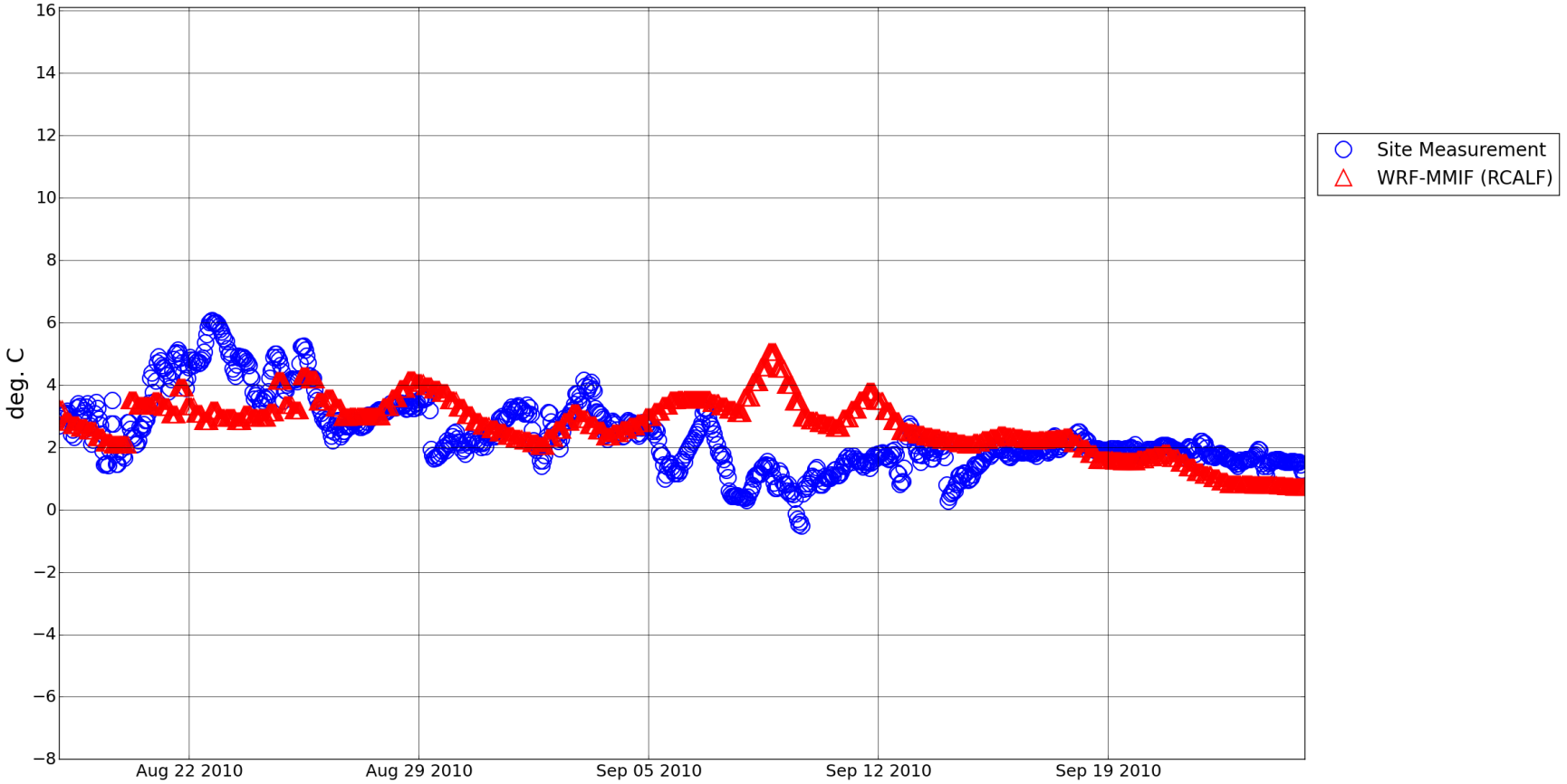

Figure 45. B2 2010 sea surface temperature time series.

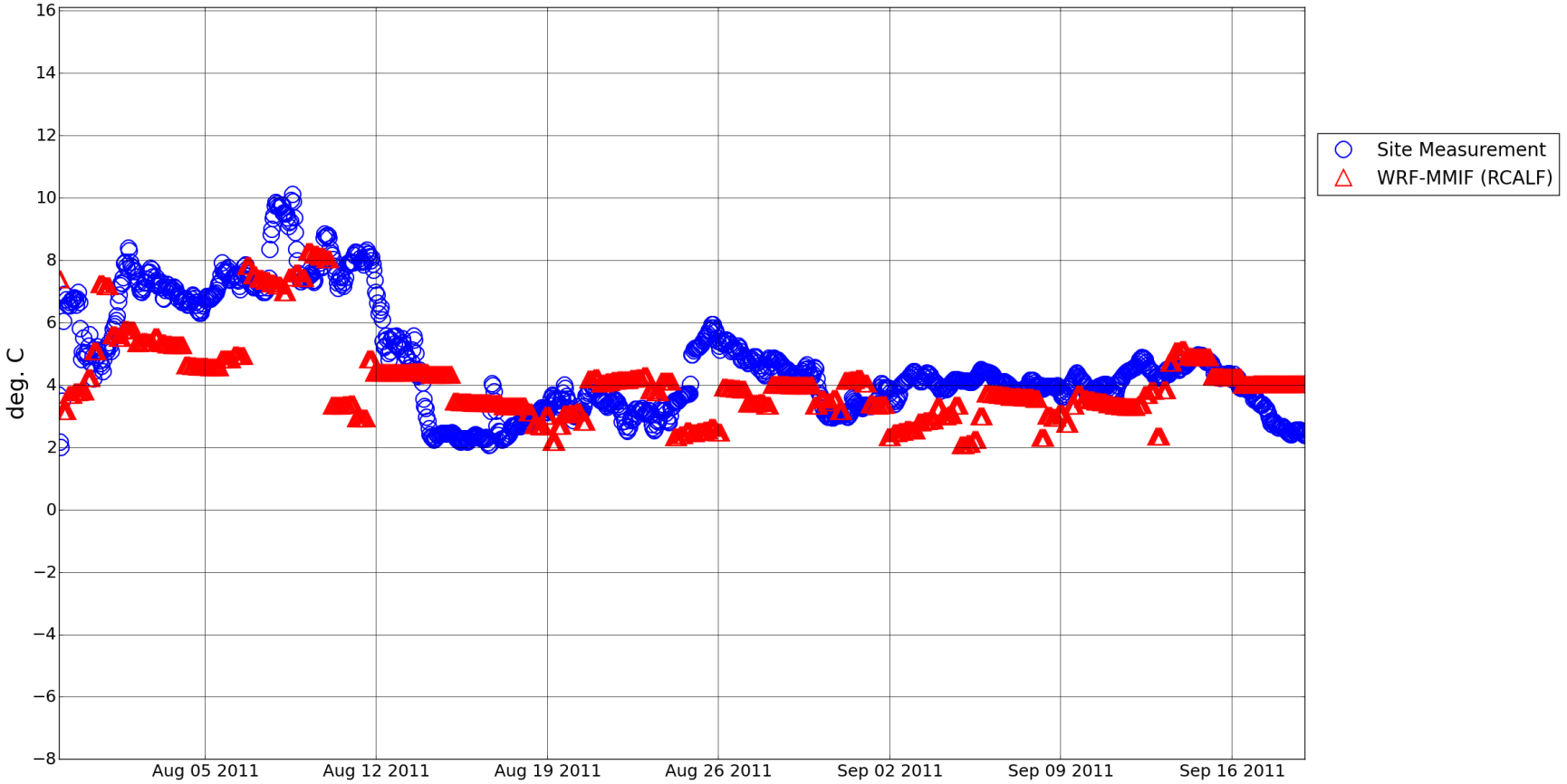

Figure 46. B2 2011 sea surface temperature time series.

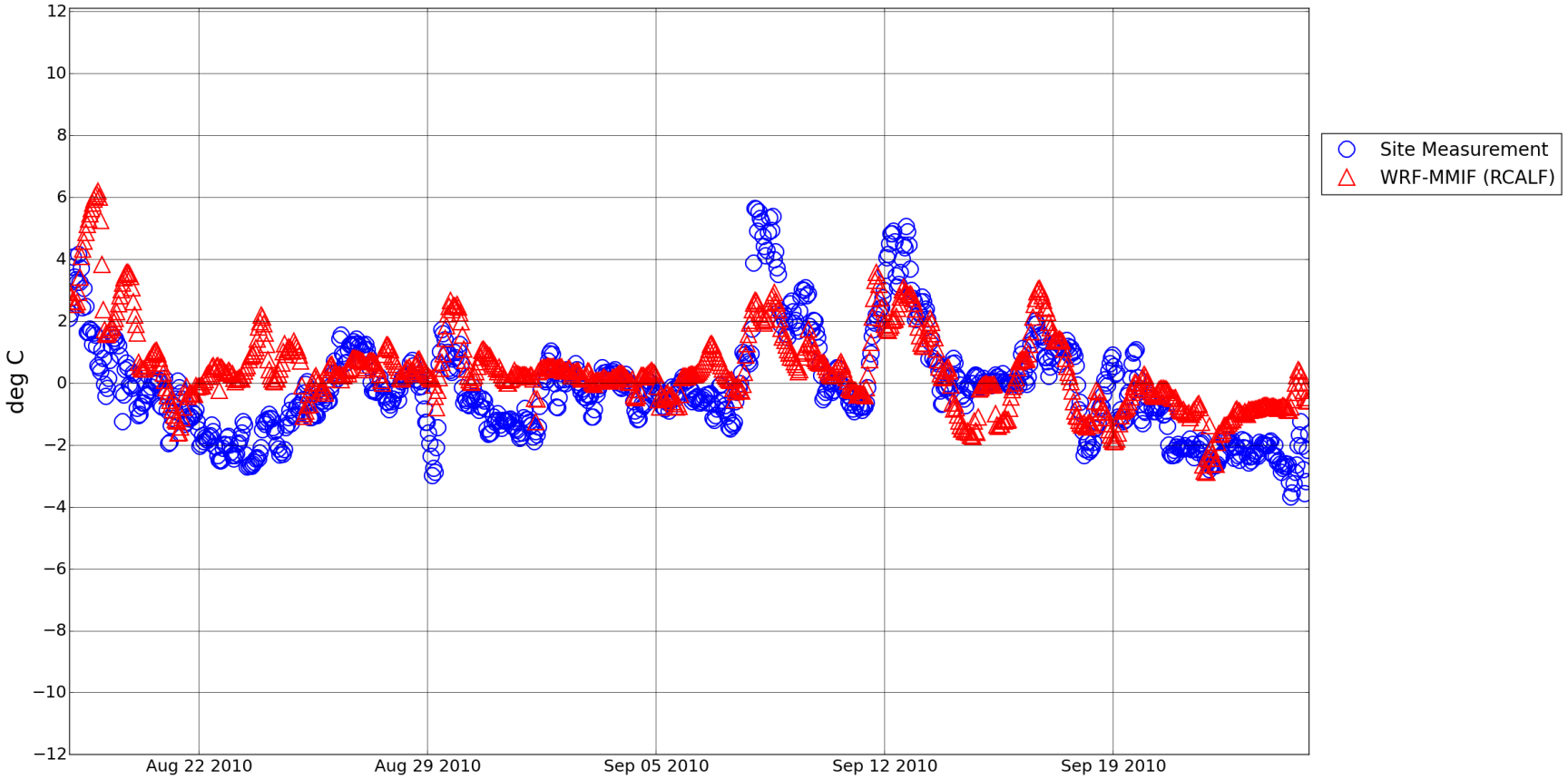

Figure 47. B2 2010 air-sea temperature difference time series.

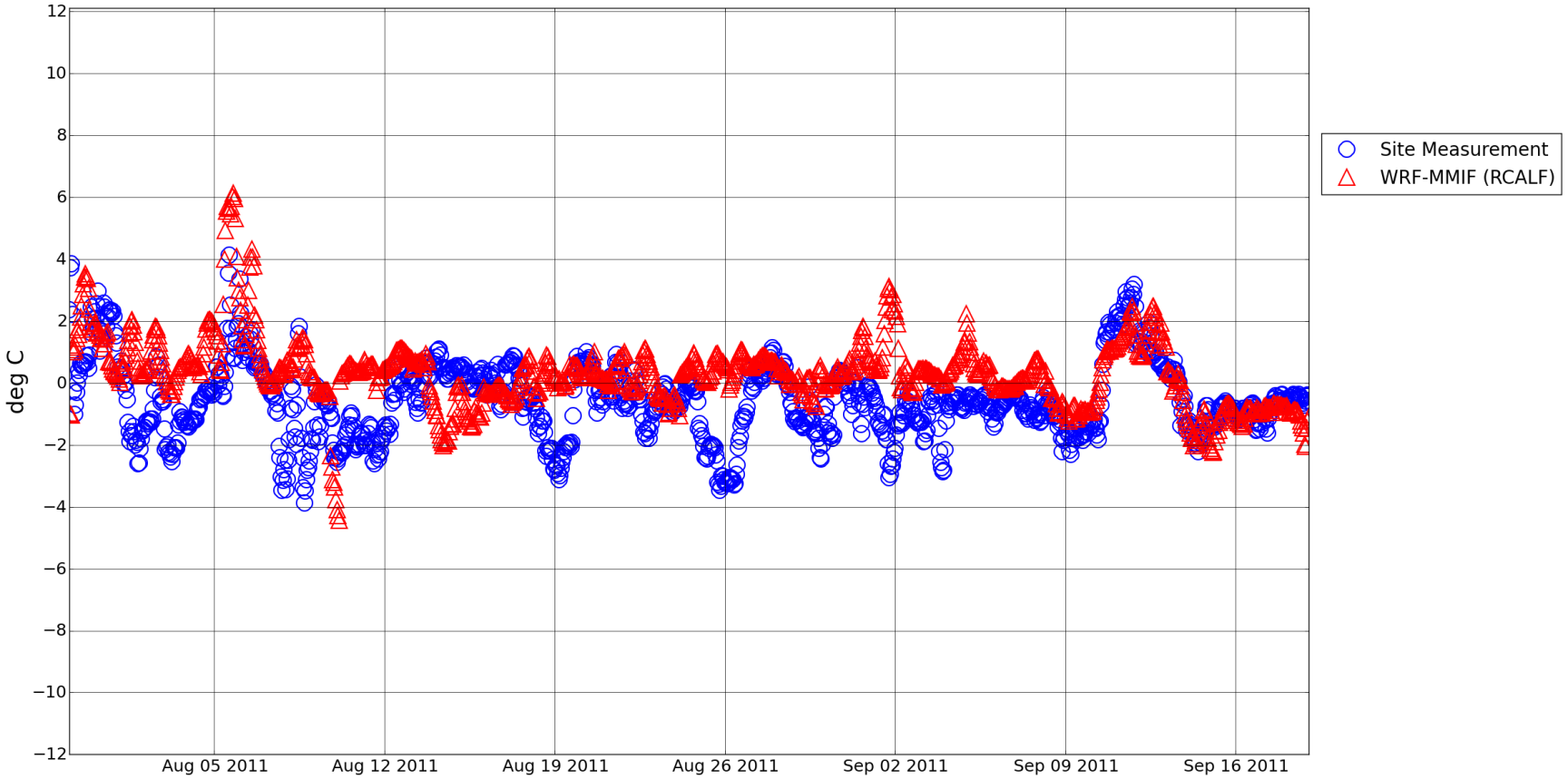

Figure 48. B2 2011 air-sea temperature difference time series.

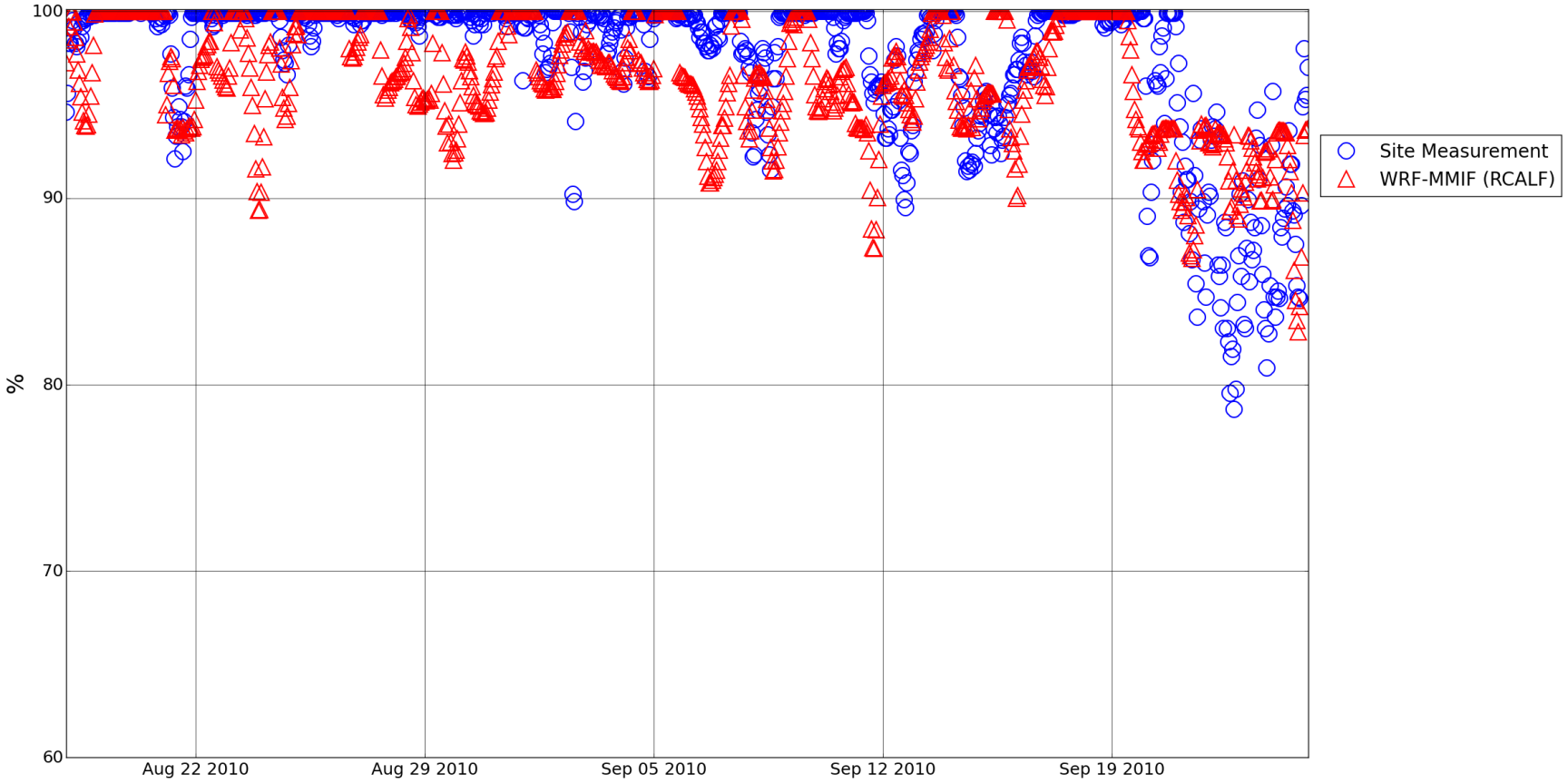

Figure 49. B2 2010 relative humidity time series.

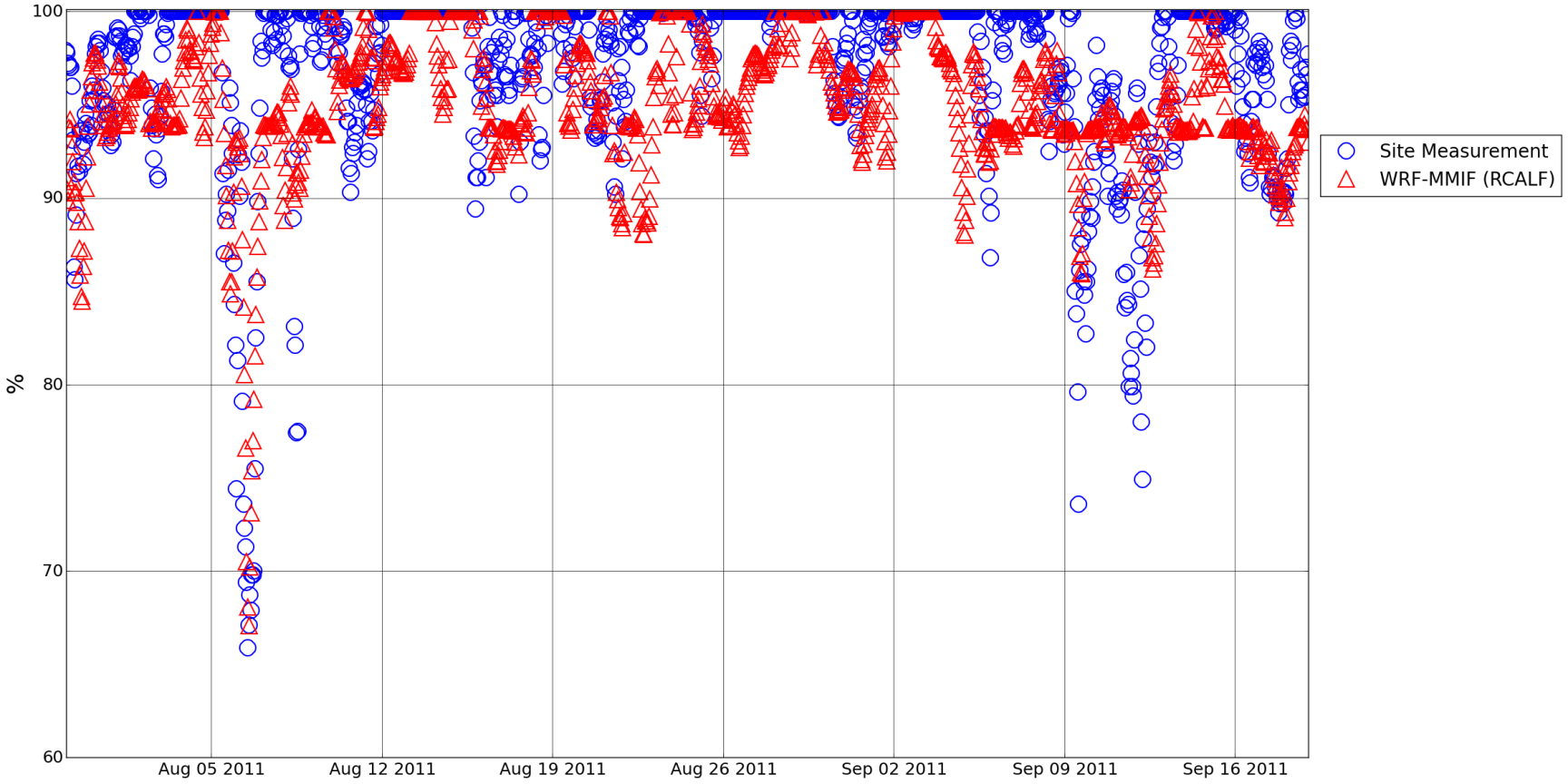

Figure 50. B2 2011 relative humidity time series.

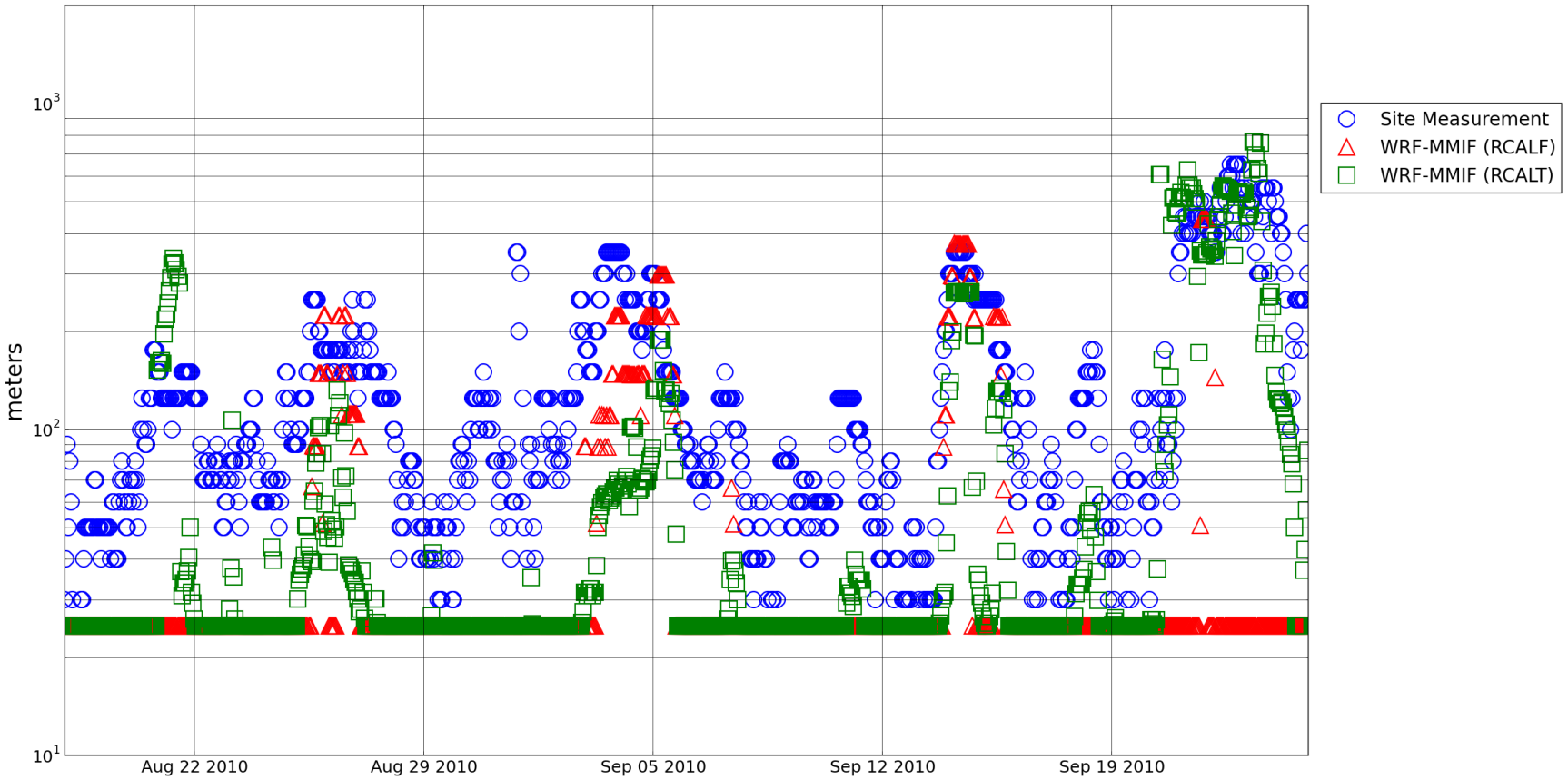

Figure 51. B2 2010 PBL height time series.

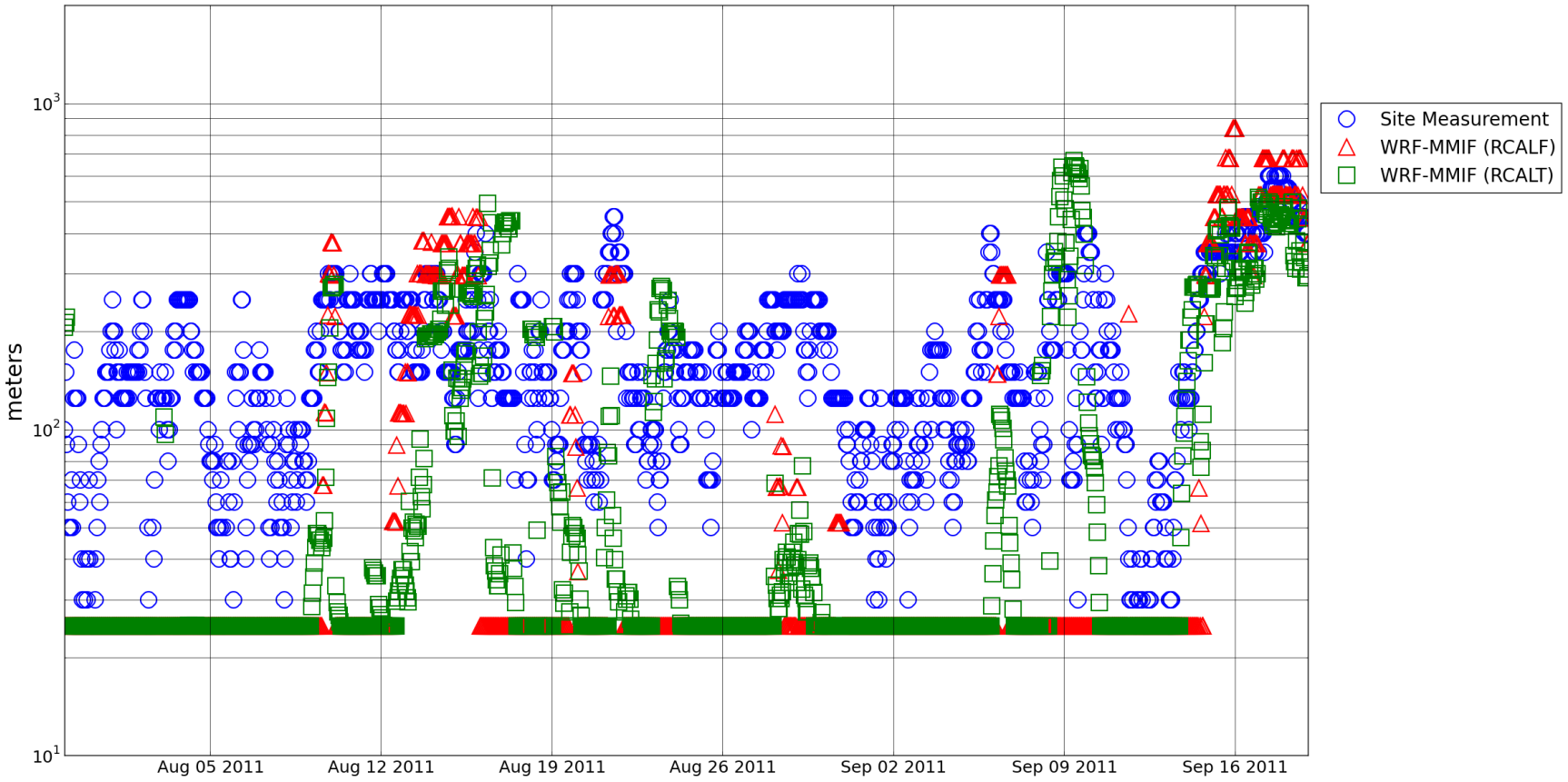

Figure 52. B2 2011 PBL height time series.

4.6 Site B3: Beaufort-Sivulliq

4.6.1 Wind speed

Time series plots of site B3 for 2010, 2011, and 2012 are shown in Figure 53, Figure 54, and Figure 55, respectively. WRF predicted the wind speed trend accurately through 2010, with the exception of periods of maximum wind speed where WRF slightly underpredicted wind speed. WRF consistently underpredicted wind speeds through most of 2011 and 2012. The average wind speed deviation was -0.42, -1.07, and -0.54 m/s for the three periods, respectively. The negative bias was likely magnified by the fact WRF wind speeds were calculated at the 10 m height and the buoy measurements were at 3.3 and 3.5 m height for 2010 and 2011/2012, respectively. The negative bias at the measurement location corresponded with the negative bias for wind speed found by the regional METSTAT analysis.

4.6.2 Wind direction

Time series plots of site B3 in 2010, 2011, and 2012 are shown in Figure 56, Figure 57, and Figure 58, respectively. WRF appears to have accurately predicted wind direction for most periods. The standard deviation was 24°, 19°, and 31° for the three periods, respectively. Again, the wind direction bias would likely not affect the AERMOD results because the methodology used in this study limits the influence of wind direction.

4.6.3 Air temperature

Time series plots of site B3 during 2010, 2011, and 2012 are shown in Figure 59, Figure 60, and Figure 61, respectively. WRF overpredicted air temperature through August and September 2010 on average. The 2011 WRF predictions appear to match the magnitude and trend of temperature well with the exception of a period of underprediction in early October. Periods of underprediction were also evident in mid-September and early October 2012. Average temperature deviations were +0.49°, -0.39°, and -0.57° for the three years, respectively.

4.6.4 Sea surface temperature

Time series plots of site B3 in 2010, 2011, and 2012 are shown in Figure 62, Figure 63, and Figure 64 , respectively. Each year SST predictions are more erroneous at the beginning of the open-water season and more accurate near the end of the season. The transition appears to occur around mid-September. The average WRF SST biases were +0.55°, +0.33°, and -0.67°, for 2010, 2011, and 2012, respectively.

4.6.5 Air-sea temperature difference

Time series plots of site B3 for 2010, 2011, and 2012 are shown in Figure 65, Figure 66, and Figure 67, respectively. The WRF air temperature and SST warm biases in 2010 coincide, resulting in relatively low error in ASTD. As seen in the figure, the magnitude, trend, and sign of

heat flux in 2010 tracked well with the observations. ASTD error was greater in 2011 and substantial periods of opposite ASTD sign were evident. In 2012, the ASTD trends and heat flux sign were predicted well, but the magnitude of ASTD was underpredicted during several notable periods.

Hours with significant difference between WRF and measurement ASTD (significant considered as an absolute value of 0.5°C or more difference) and opposite ASTD sign occurred 11%, 35%, and 11% of the time for 2010, 2011, and 2012, respectively. Significant periods of opposite ASTD sign occurred in 2011, notably Sep. 21 – 27 and Oct. 15 – 20. During these periods the site measurements predicted a positive ASTD while WRF predicted a negative ASTD. The measurements supported stable atmospheric conditions while WRF results supported unstable atmospheric conditions.

For 2012, WRF underpredicted ASTD from Sep. 17 – Sep. 21 and overpredicted ASTD from Sep. 25 – Sep. 28. However, the sign of ASTD was predicted favorably during these periods.

Overall, WRF predictions favored a negative bias (underprediction), resulting in average ASTD deviations of -0.06°C, -0.72°C, and +0.10°C, respectively. This bias was caused mainly by WRF predicting ASTD near 0°C during periods in all three years where ASTD measurements were +1-2°C.

4.6.6 Relative humidity

Time series plots of site B3 2010, 2011, and 2012 are shown in Figure 68, Figure 69, and Figure 70, respectively.

WRF appears to predict the magnitude and trend of RH for 2010 and 2011 well. Average RH error was +0.9% and +2.3% for 2010 and 2011, respectively. The 2011 time series plot reveals WRF RH trends and magnitude followed the measurements quite well. However, WRF did overpredict RH by 10 - 20% periodically during low-RH episodes in late October 2011, corresponding to short periods of northeasterly winds (therefore, not associated with offshore flows).

For 2012, the measurement dataset maintained an almost constant RH near 99% the entire open water season. It is possible these data were erroneous either due to faulty equipment or a problem with data transfer. Though WRF RH trends did correspond with the measurements, RH remained high, greater than 90% for most of the season except for a few short periods where RH dipped down to near 80%. These events corresponded to periods of offshore flow, with south to southwesterly winds (180-210°). Southwesterly wind events were very rare in 2010 and 2011 and quite common in 2012. The average 2012 RH bias is -6.4%.

4.6.7 PBL height

Time series plots of site B3 in 2010, 2011, and 2012 are shown in Figure 71, Figure 72, and Figure 73, respectively. Again, WRF PBL height estimates are low, favoring the minimum 25 m height through most of the three years. The MMIF RCALT rediagnosis results in a lower

frequency of minimum 25 m PBL heights. However, the average PBL height is still lower than measured. Average PBL height deviations were -46, -113, and -31 m for the three years, respectively. Average MMIF-recalculated PBL height deviations were -23, -27, and -14 m, respectively.

In Section 4.6.5 several periods of significant differences in ASTD sign and magnitude were identified for 2011, notably the Sep. 21 – 27, and Oct. 15 – 20 episodes where WRF supported unstable atmospheric conditions while the measurements supported stable conditions. Despite a positive ASTD, measured PBL heights are relatively high from 200 – 600 m during this period. The unstable conditions in WRF result in PBL heights of similar magnitude, resulting in good agreement with measurements.

For the Sep. 21 - 27, 2011 period the average measured PBL height was 350 m. WRF RCALF and MMIF RCALT average PBL heights were 140 m and 250 m, respectively. Measured PBL height was relatively high despite the positive ASTD of +1 to +2 ºC that would tend to support stable atmospheric conditions. It is possible PBL structure in the region was influenced more by synoptic conditions than local forcing during this period.

For the Oct. 15 - 20, 2011 period the average measured PBL height was 330 m while average WRF RCALF and RCALT PBL heights were 320 and 350 m, respectively. Again, relatively high PBL heights were measured despite ASTD values that supported stable conditions. The relatively high WRF PBL heights corresponded to the unstable conditions supported by negative ASTD.

4.6.8 Discussion

The tendency for WRF to underpredict wind speed at this site should contribute to higher AERMOD concentrations. However, the wind speeds were biased low most often during peak winds, so it is unknown whether the bias would have an influence on the maximum short term average concentrations. Both the WRF and MMIF (RCALT and RCALF) PBL height predictions were consistently underpredicted during stable periods. Measured PBL heights were less than 50 m on brief occasions, while WRF and MMIF supported extensive periods of minimum 25 m PBL height. The tendency of WRF to underpredict PBL height may lead to concentration overpredictions by AERMOD. Near-source short term maximum concentrations predicted using WRF meteorology may be more accurate (in terms of comparison to predictions using measured meteorology) because PBL heights were more accurate during unstable periods. The influence of these biases on AERMOD concentration predictions are reviewed in Section 6.0.

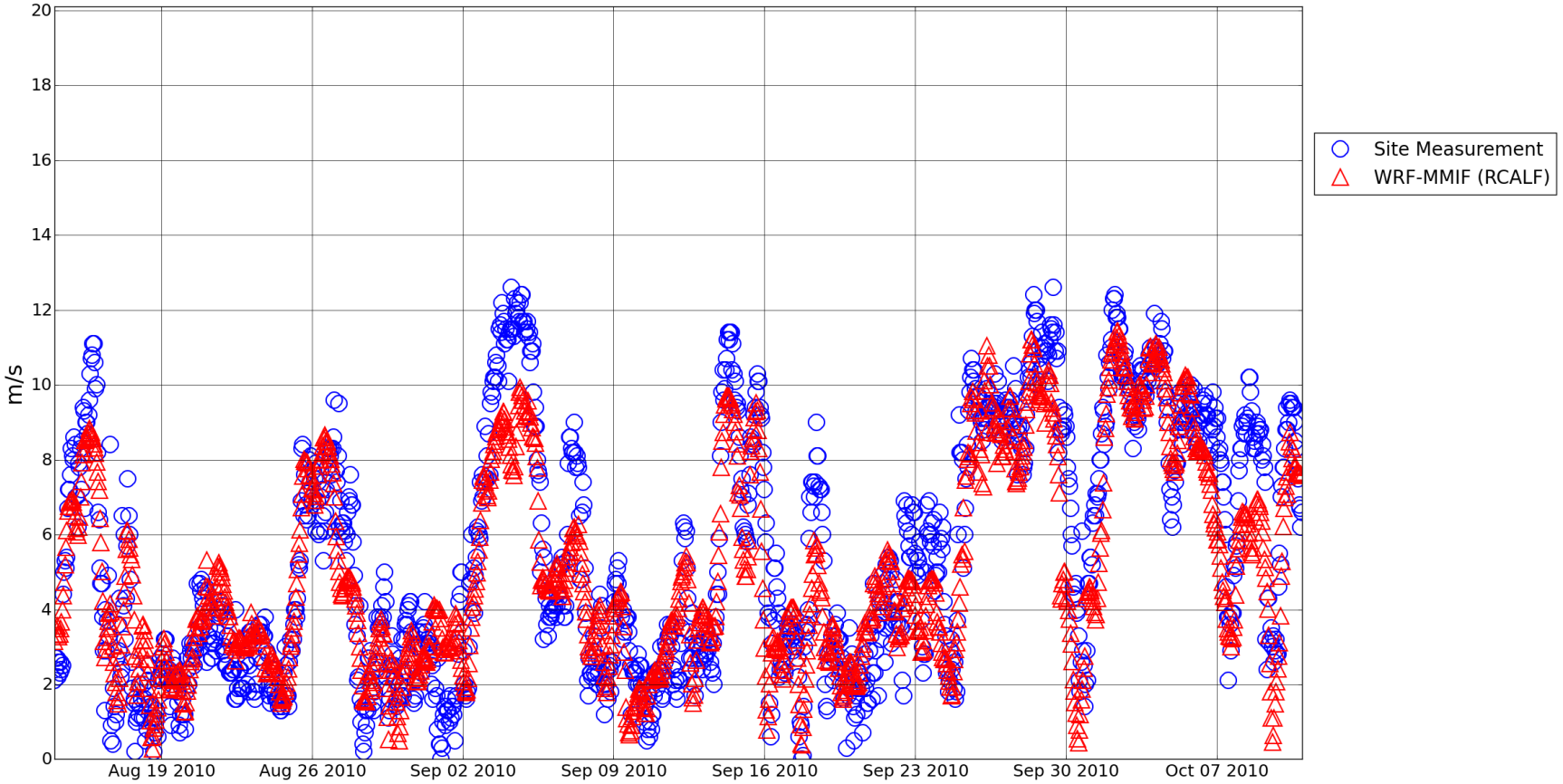

Figure 53. B3 2010 wind speed time series.

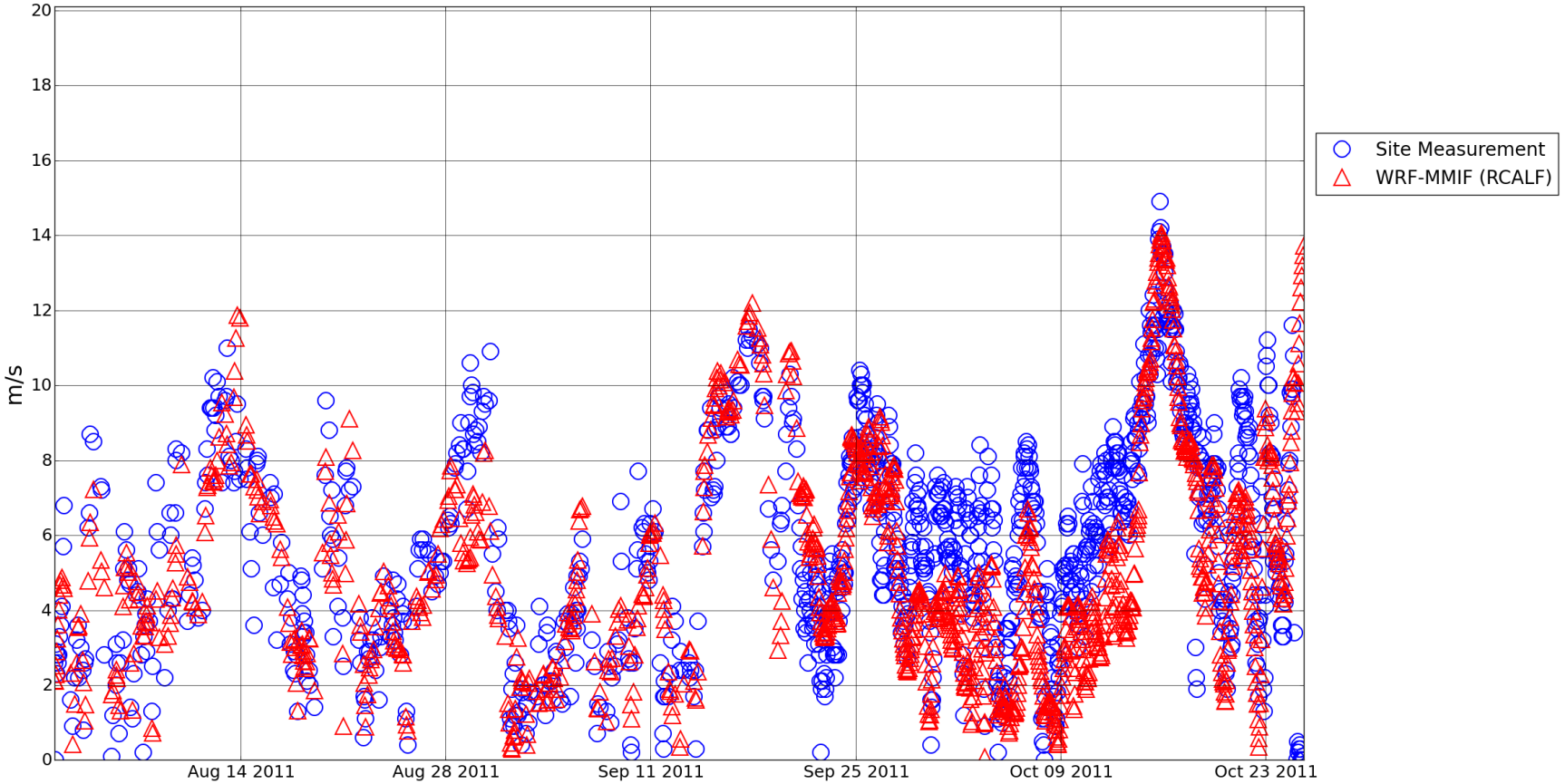

Figure 54. B3 2011 wind speed time series.

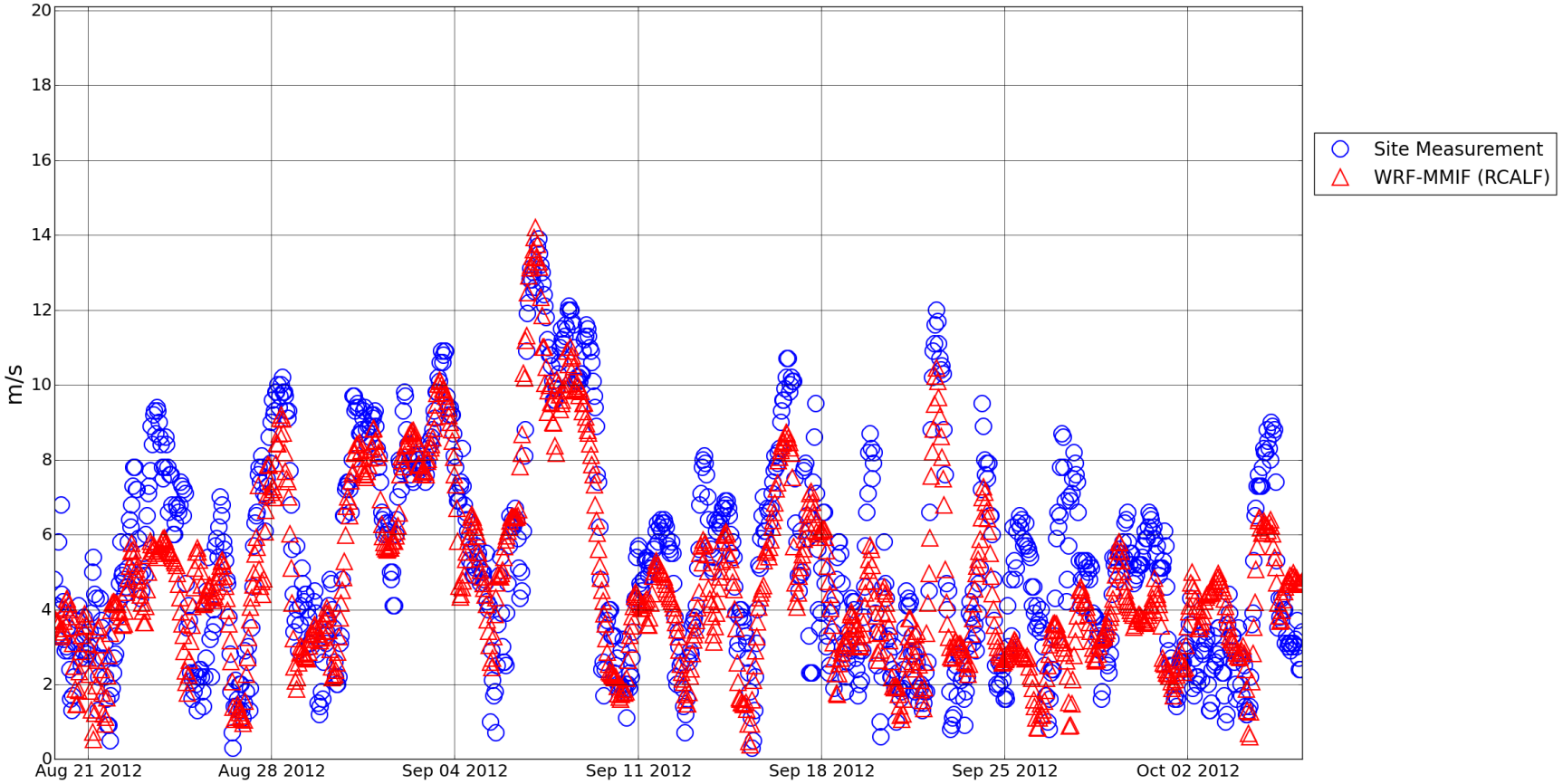

Figure 55. B3 2012 wind speed time series.

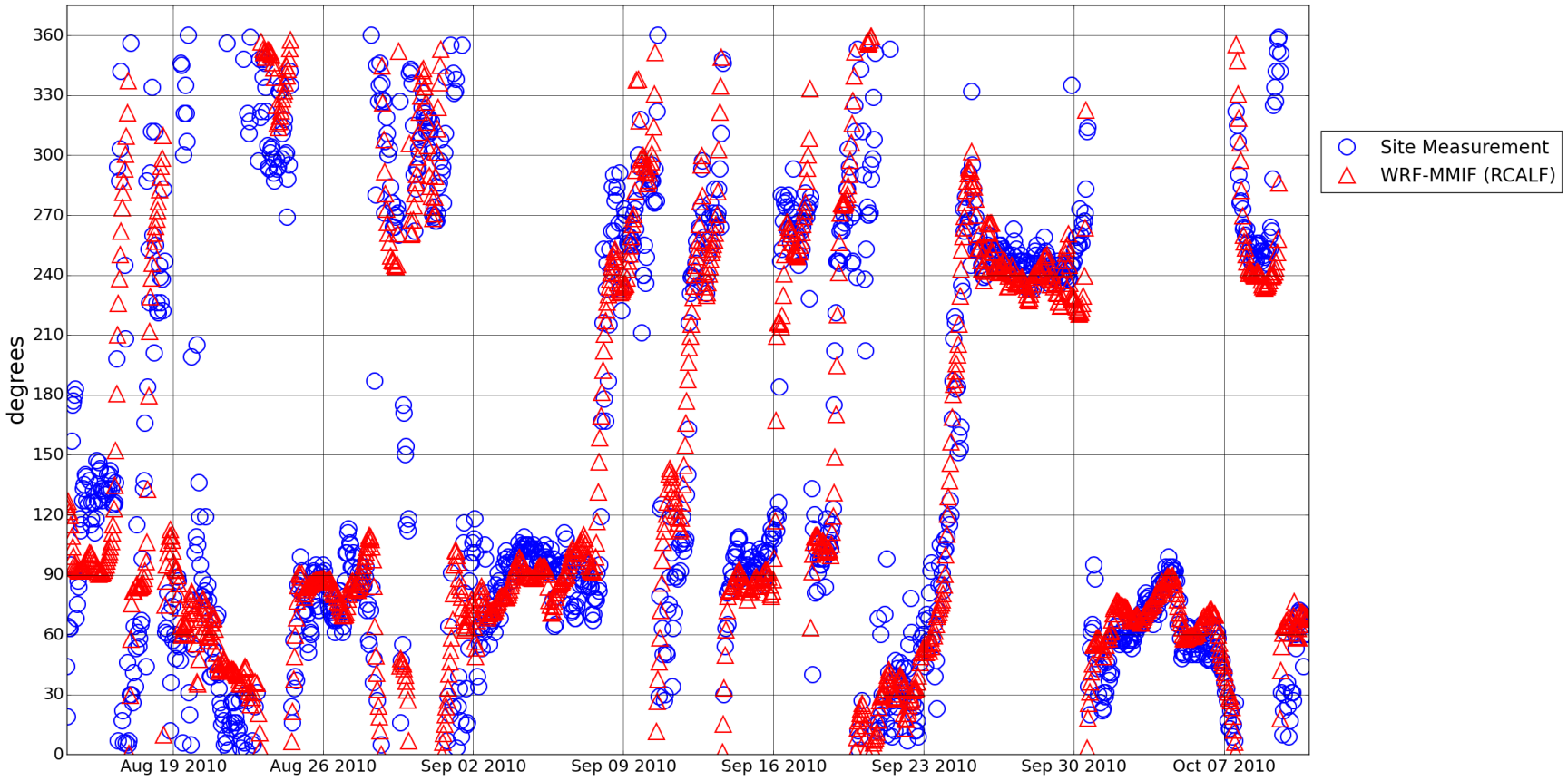

Figure 56. B3 2010 wind direction time series.

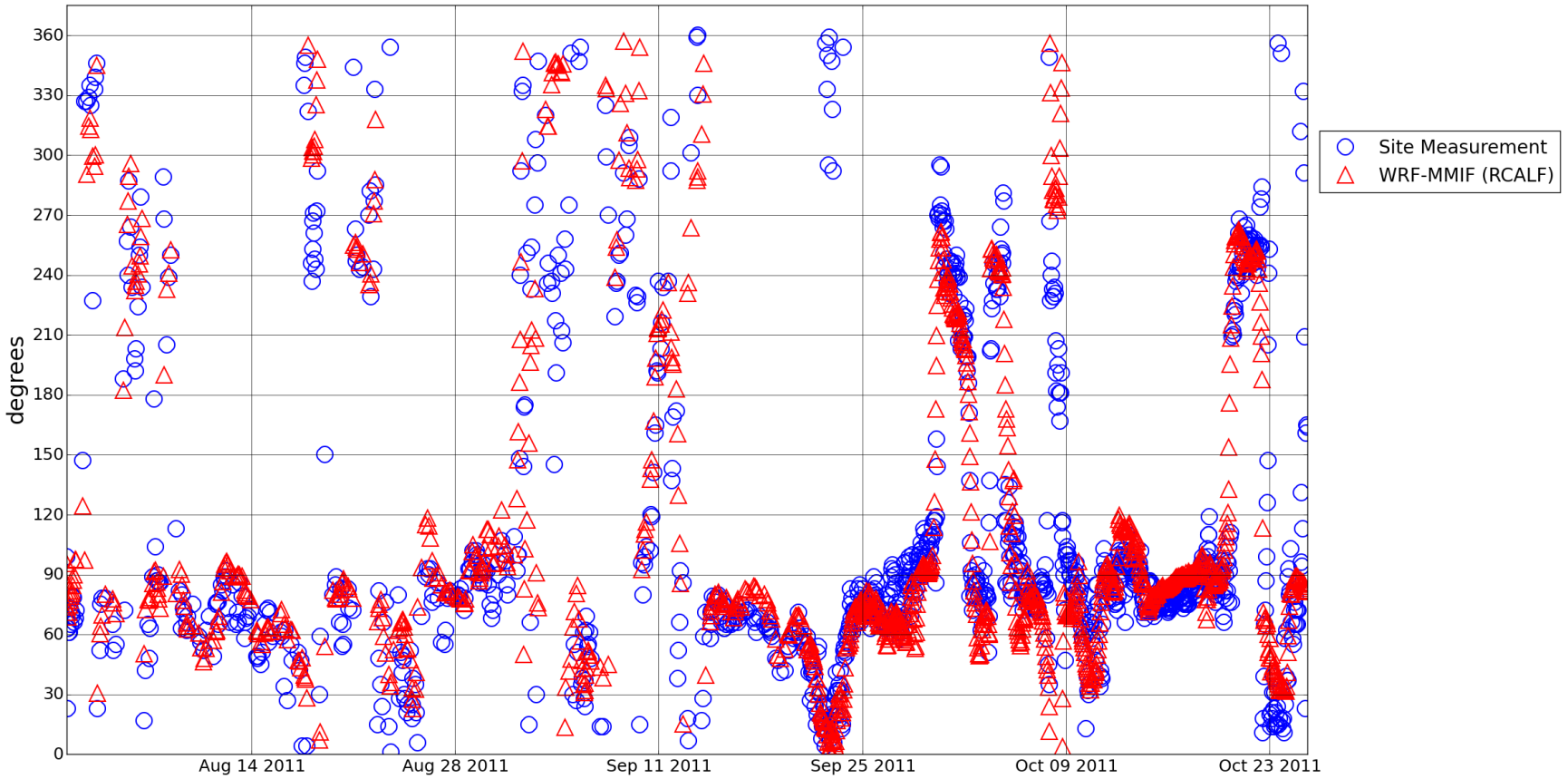

Figure 57. B3 2011 wind direction time series.

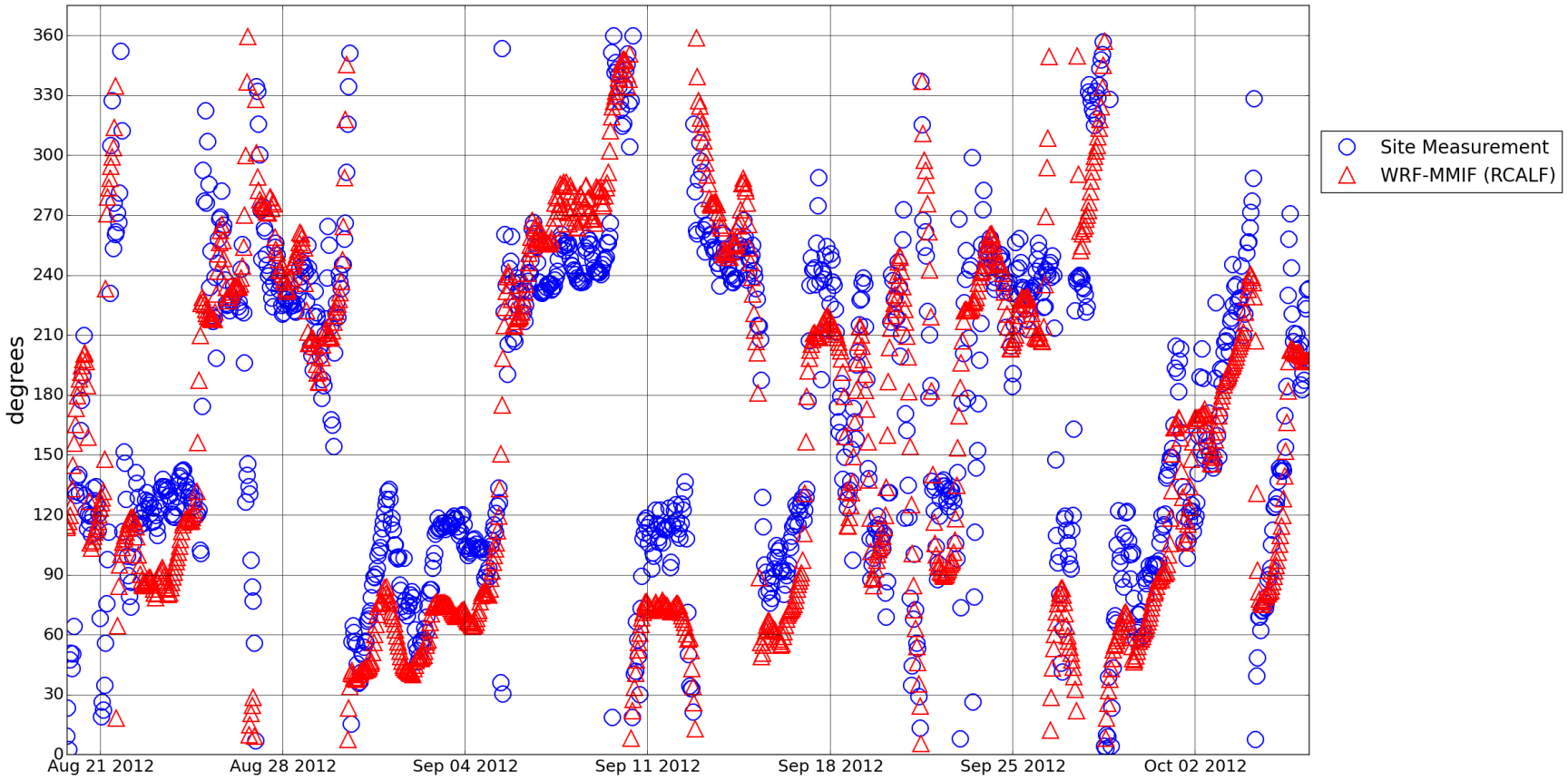

Figure 58. B3 2012 wind direction time series.

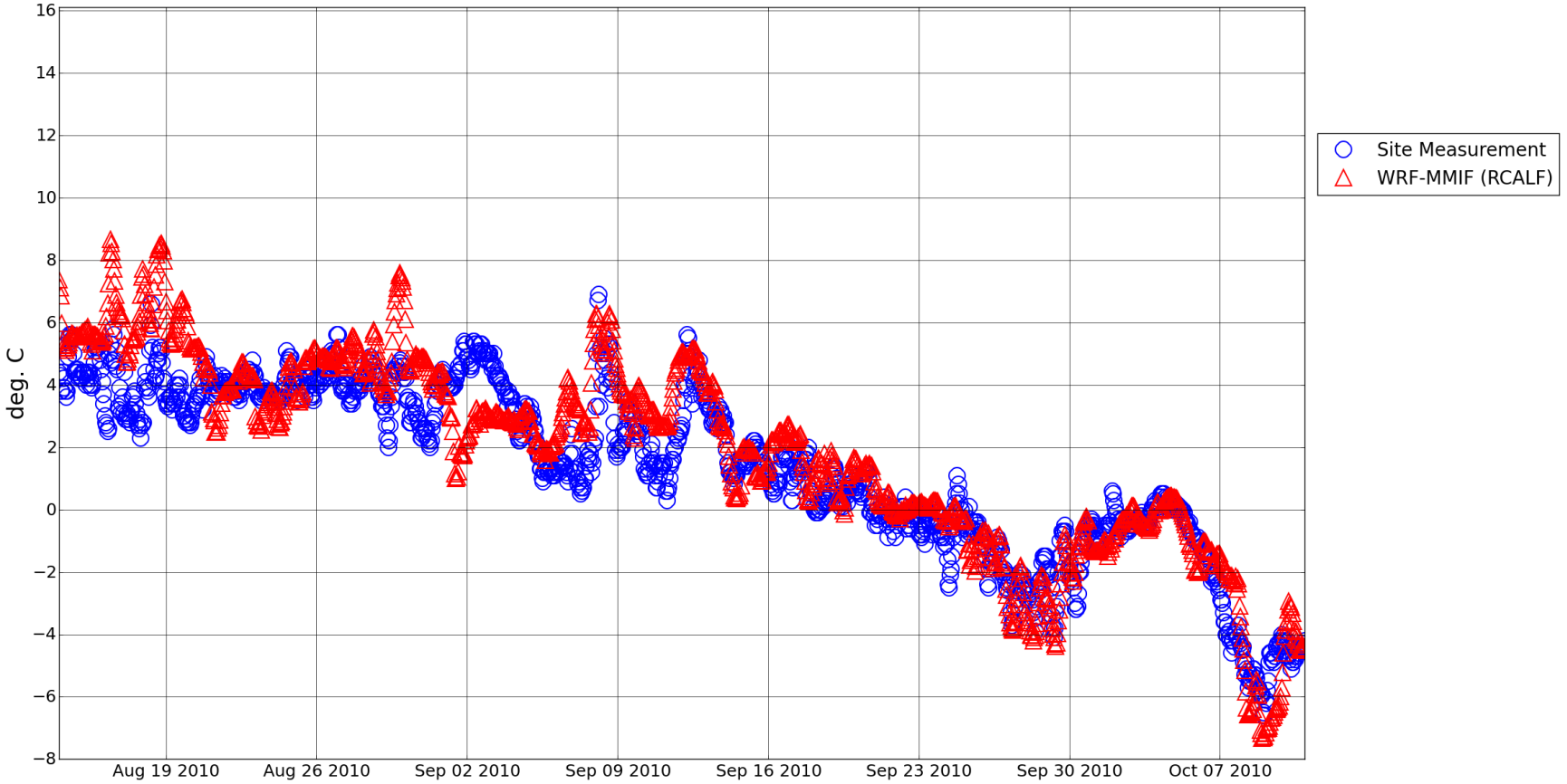

Figure 59. B3 2010 air temperature time series.

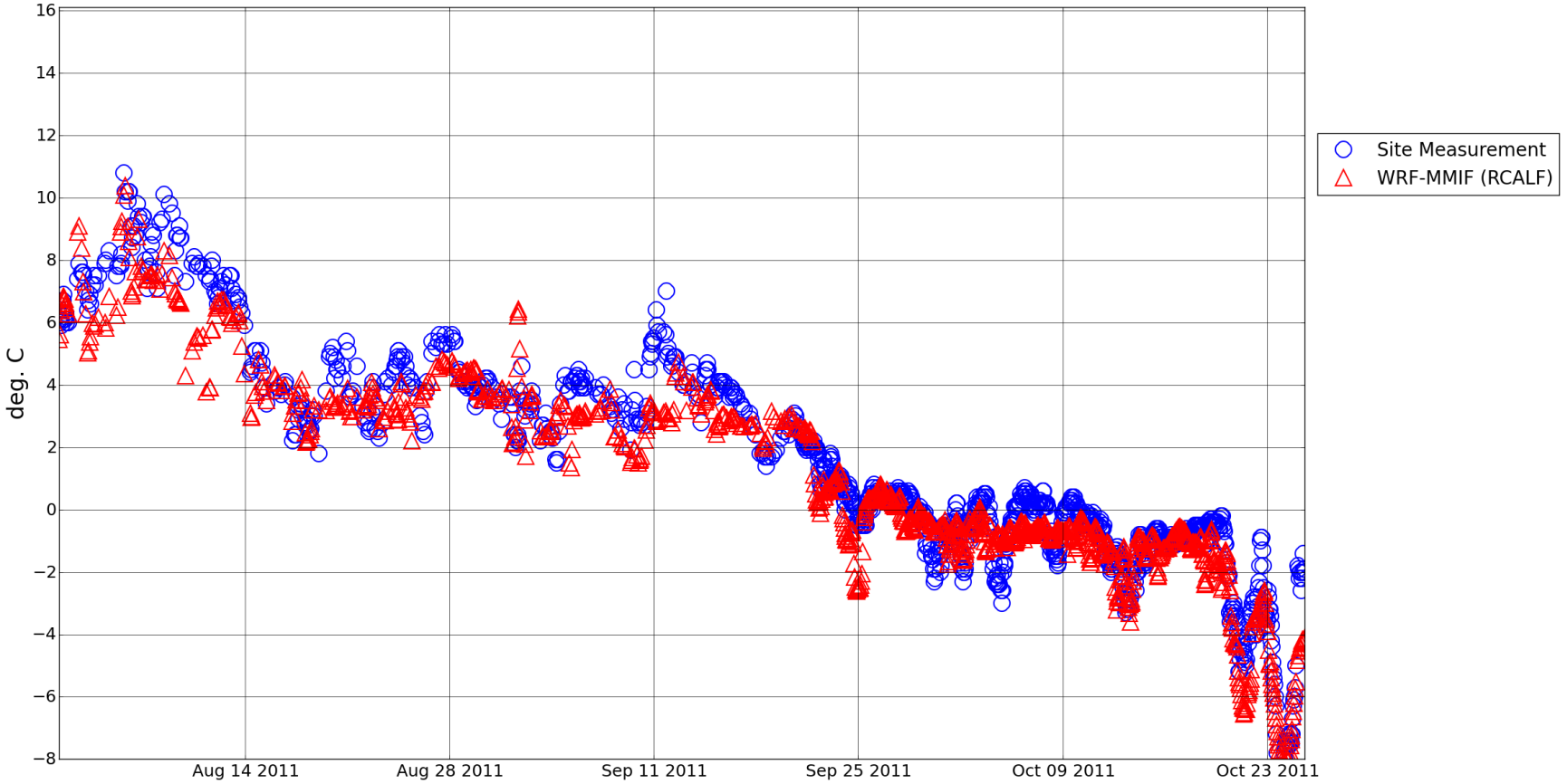

Figure 60. B3 2011 air temperature time series.

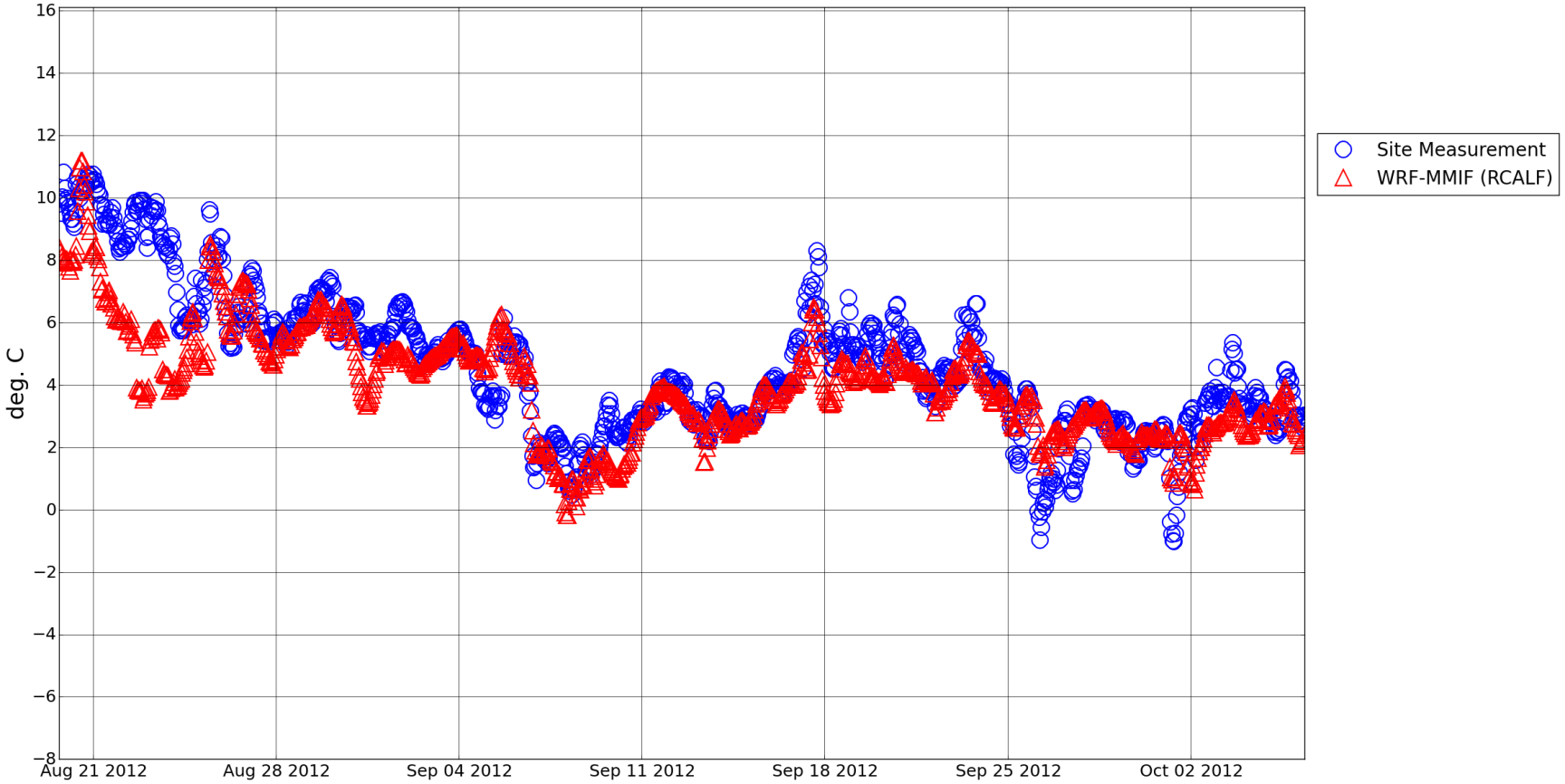

Figure 61. B3 2012 air temperature time series.

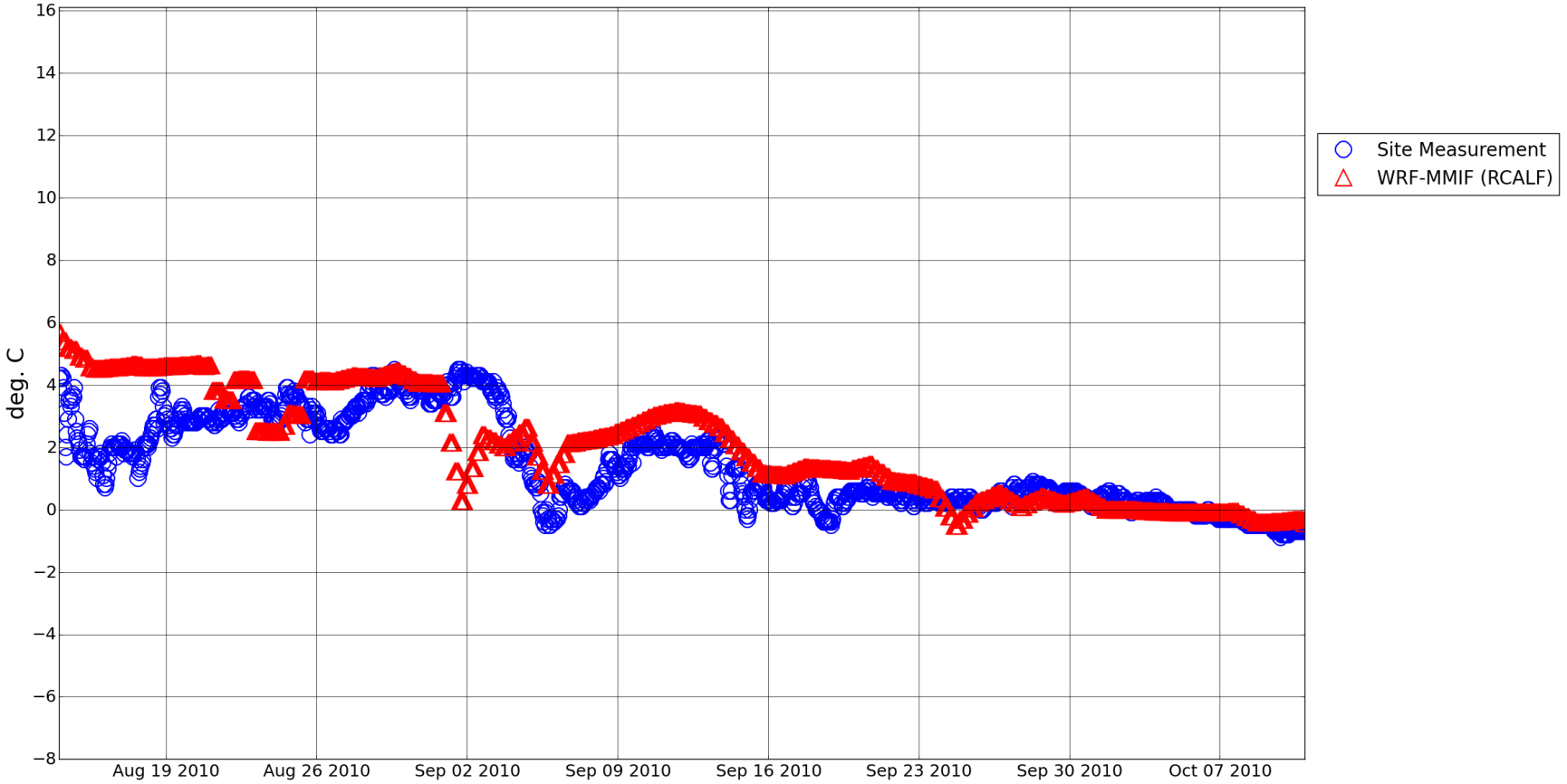

Figure 62. B3 2010 sea surface temperature time series.

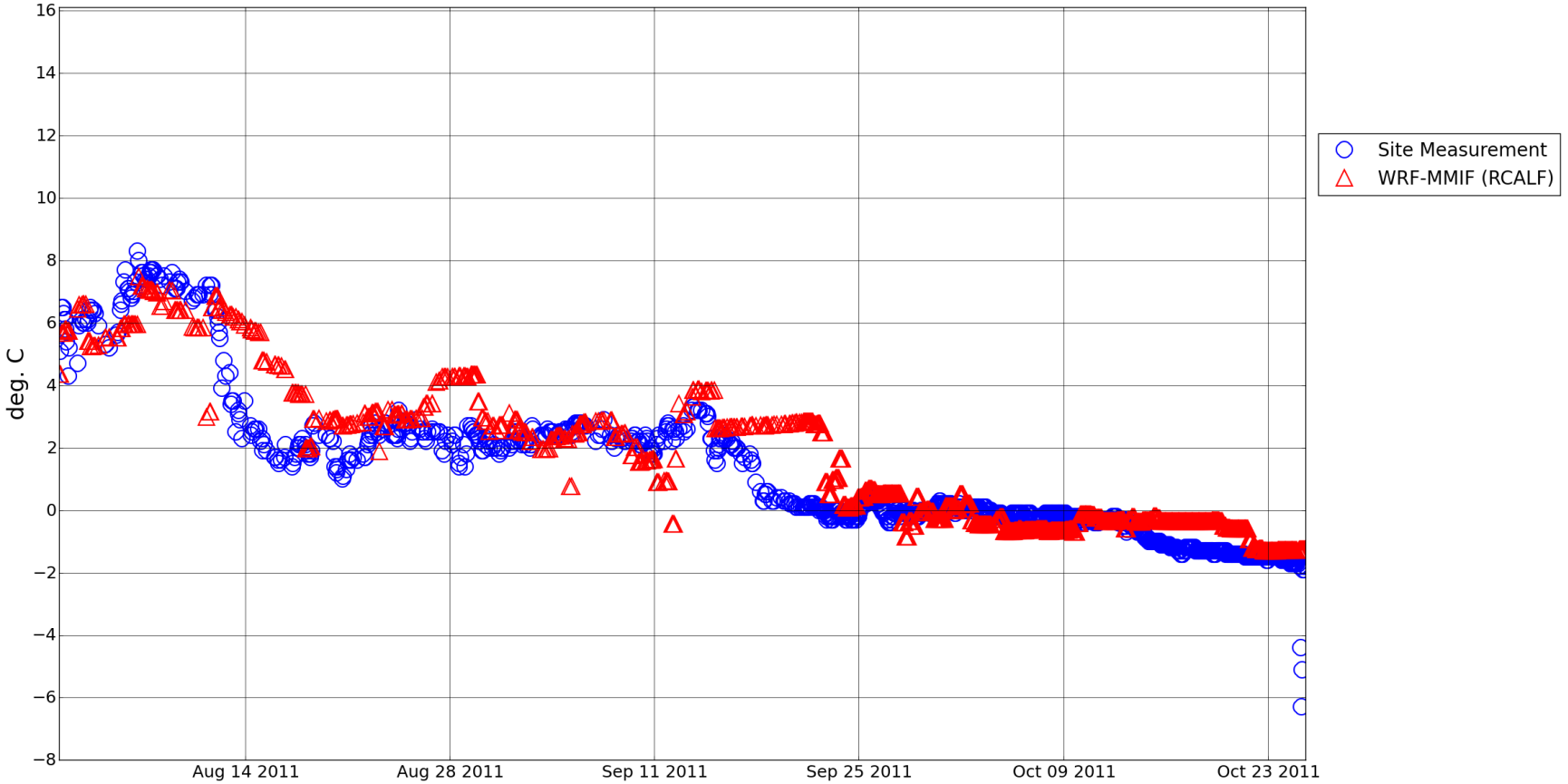

Figure 63. B3 2011 sea surface temperature time series.

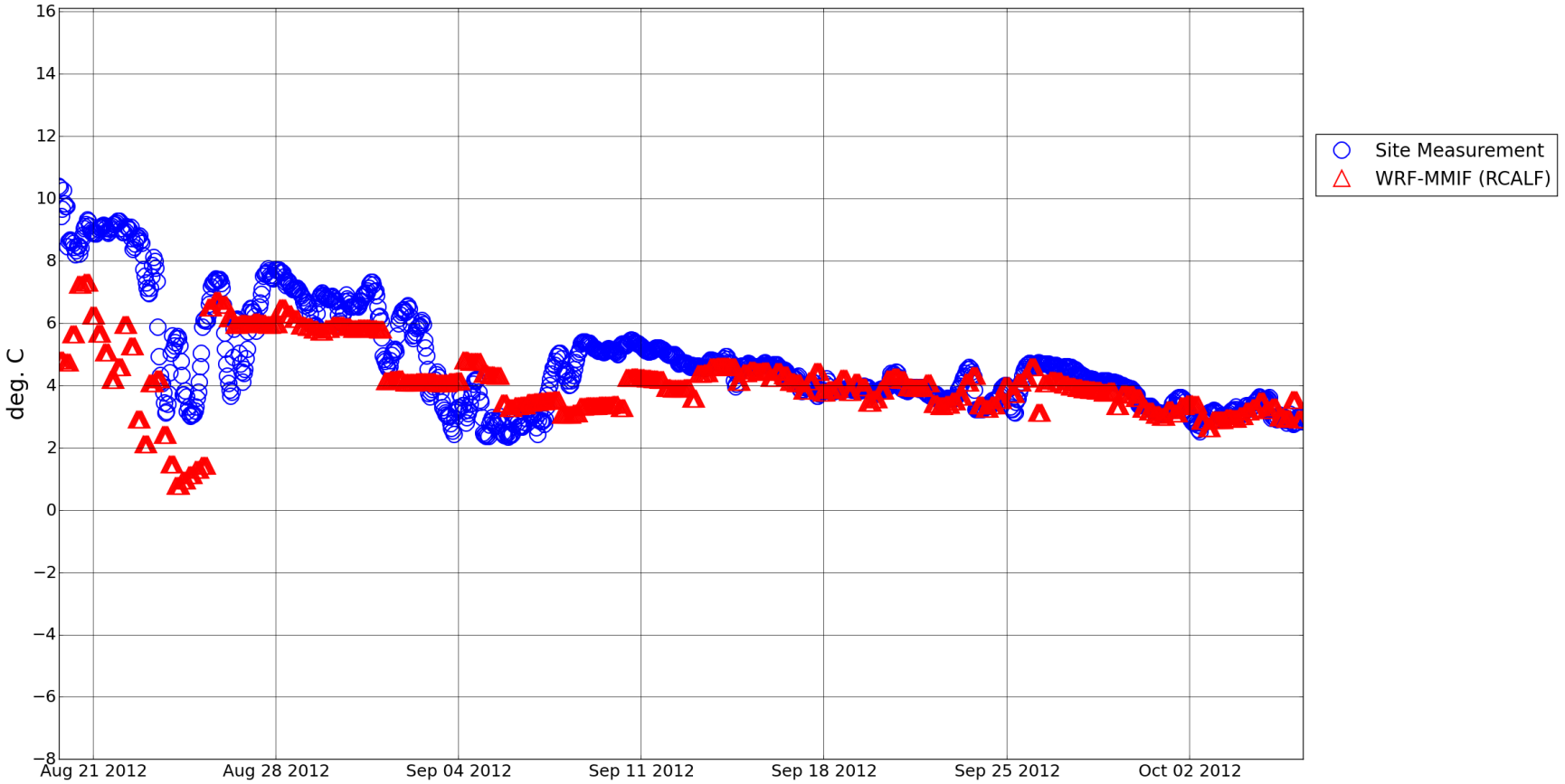

Figure 64. B3 2012 sea surface temperature time series.

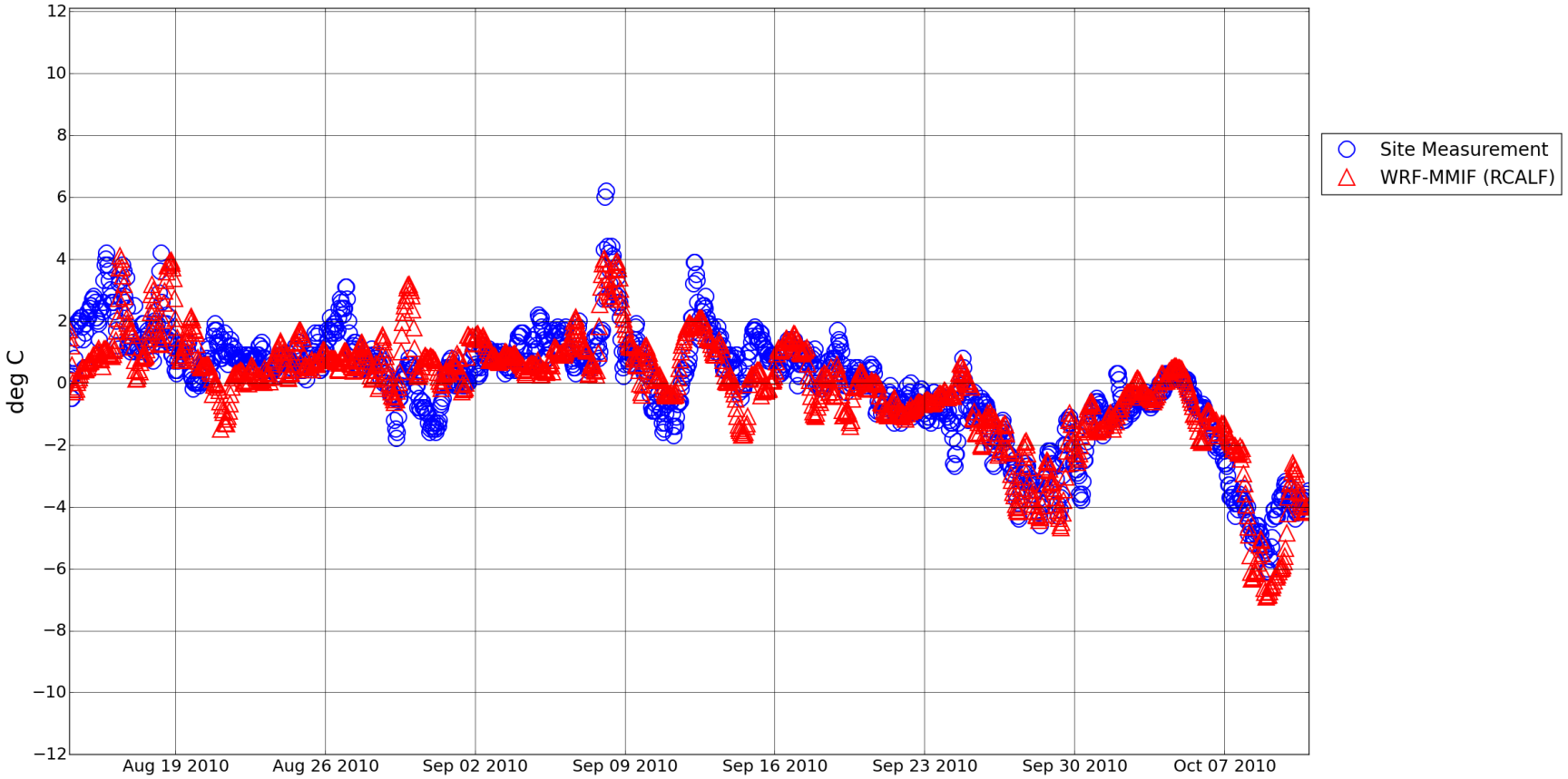

Figure 65. B3 2010 air-sea temperature difference time series.

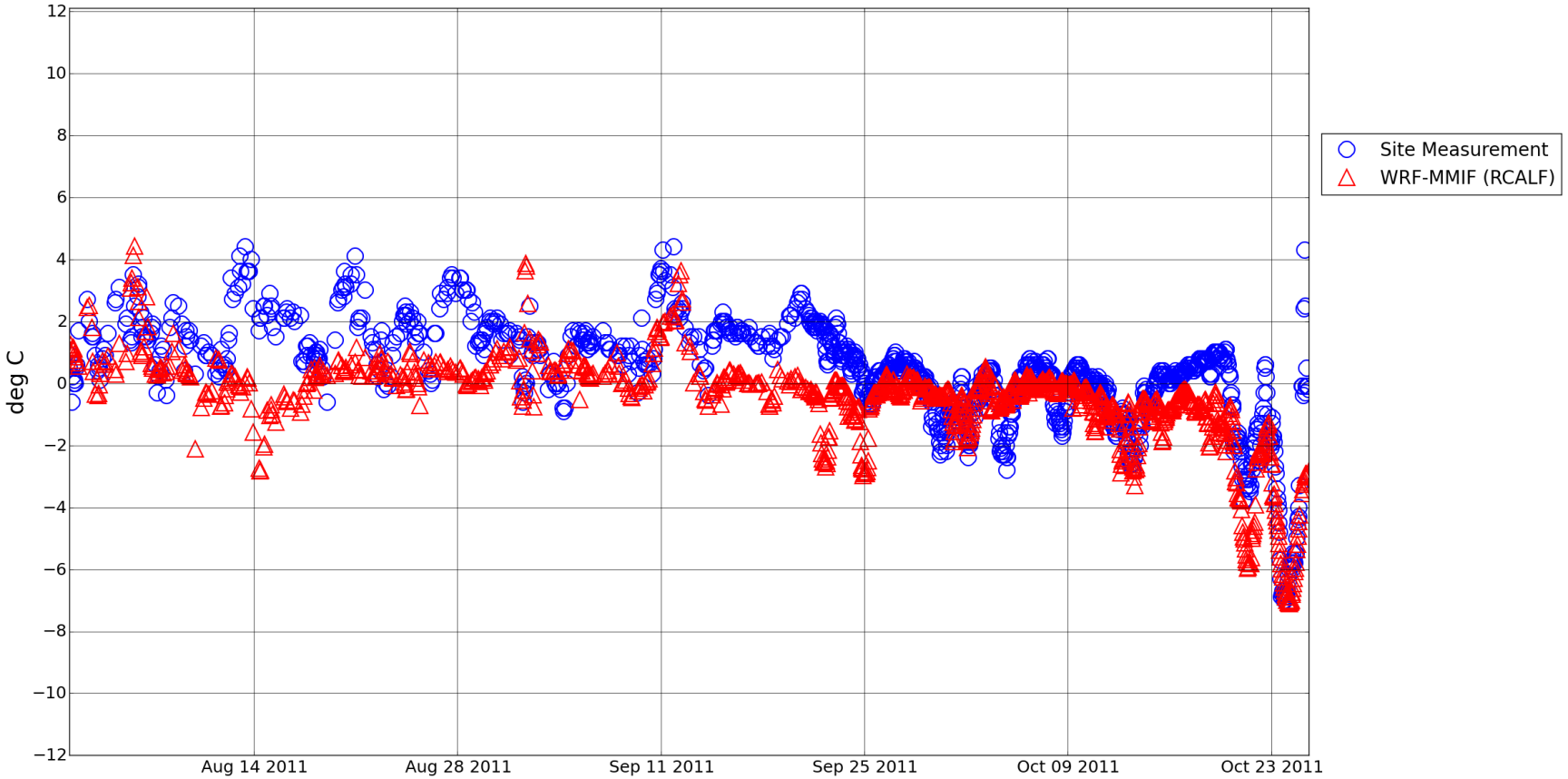

Figure 66. B3 2011 air-sea temperature difference time series.

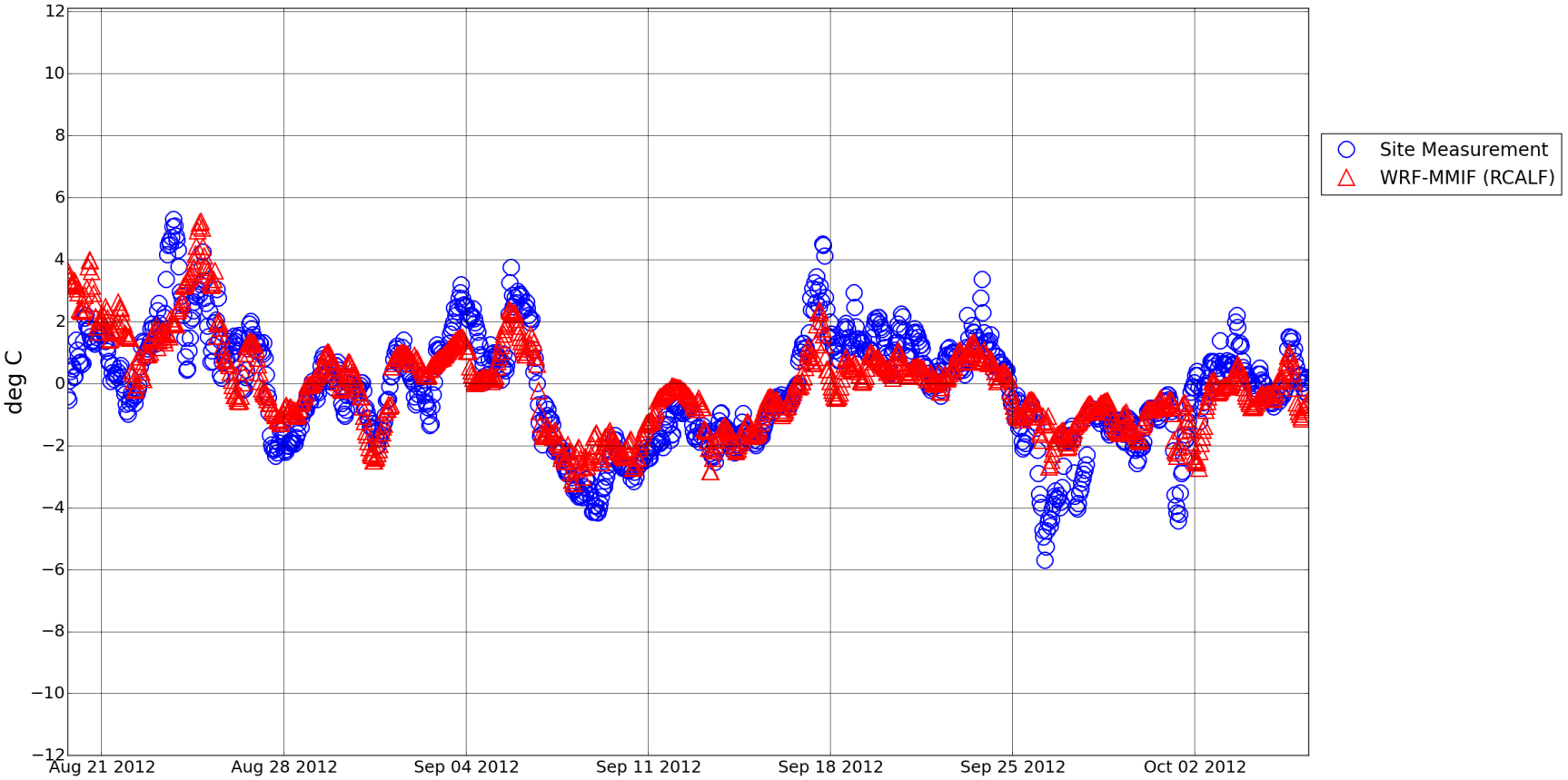

Figure 67. B3 2012 air-sea temperature difference time series.

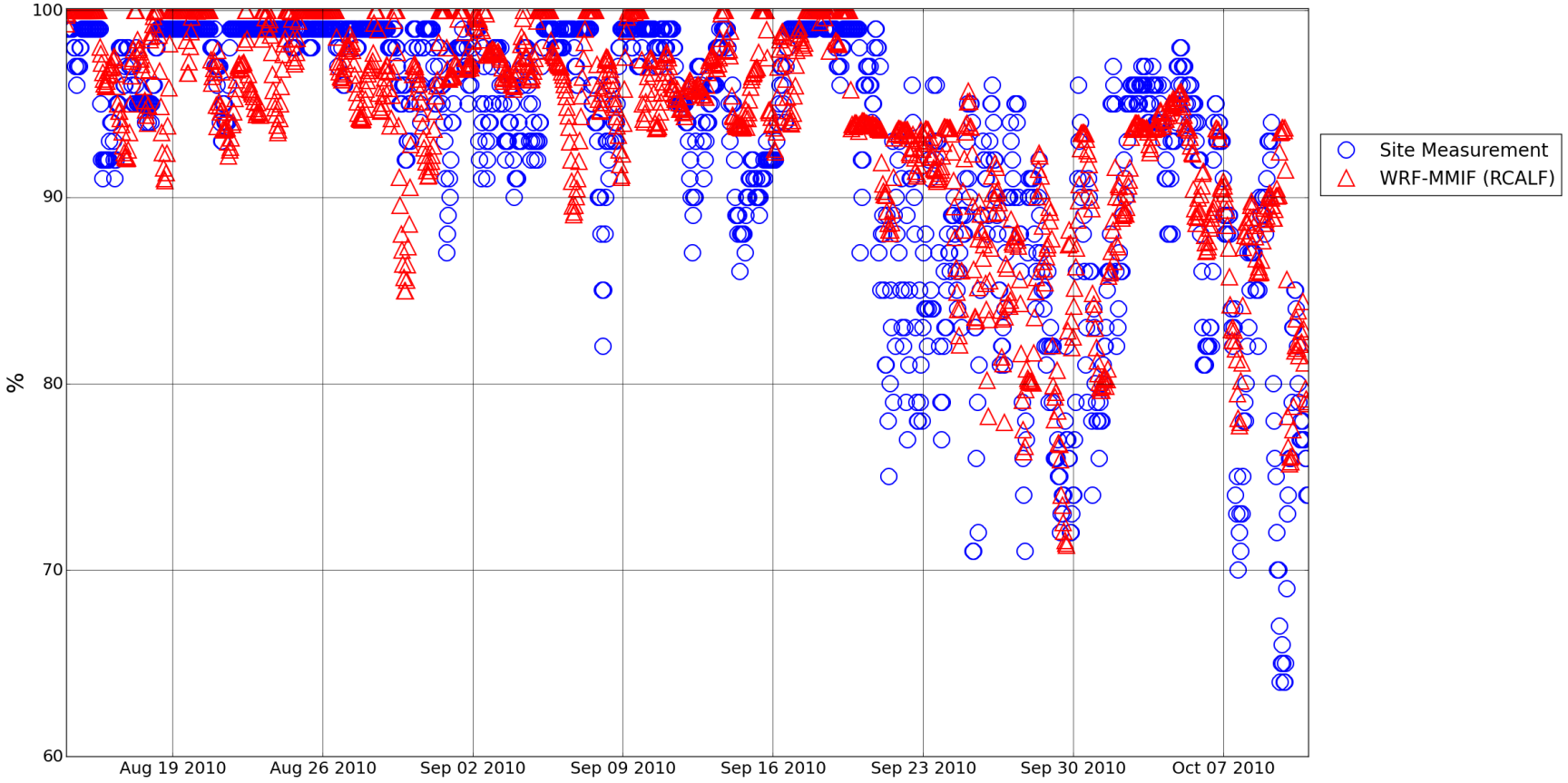

Figure 68. B3 2010 relative humidity time series.

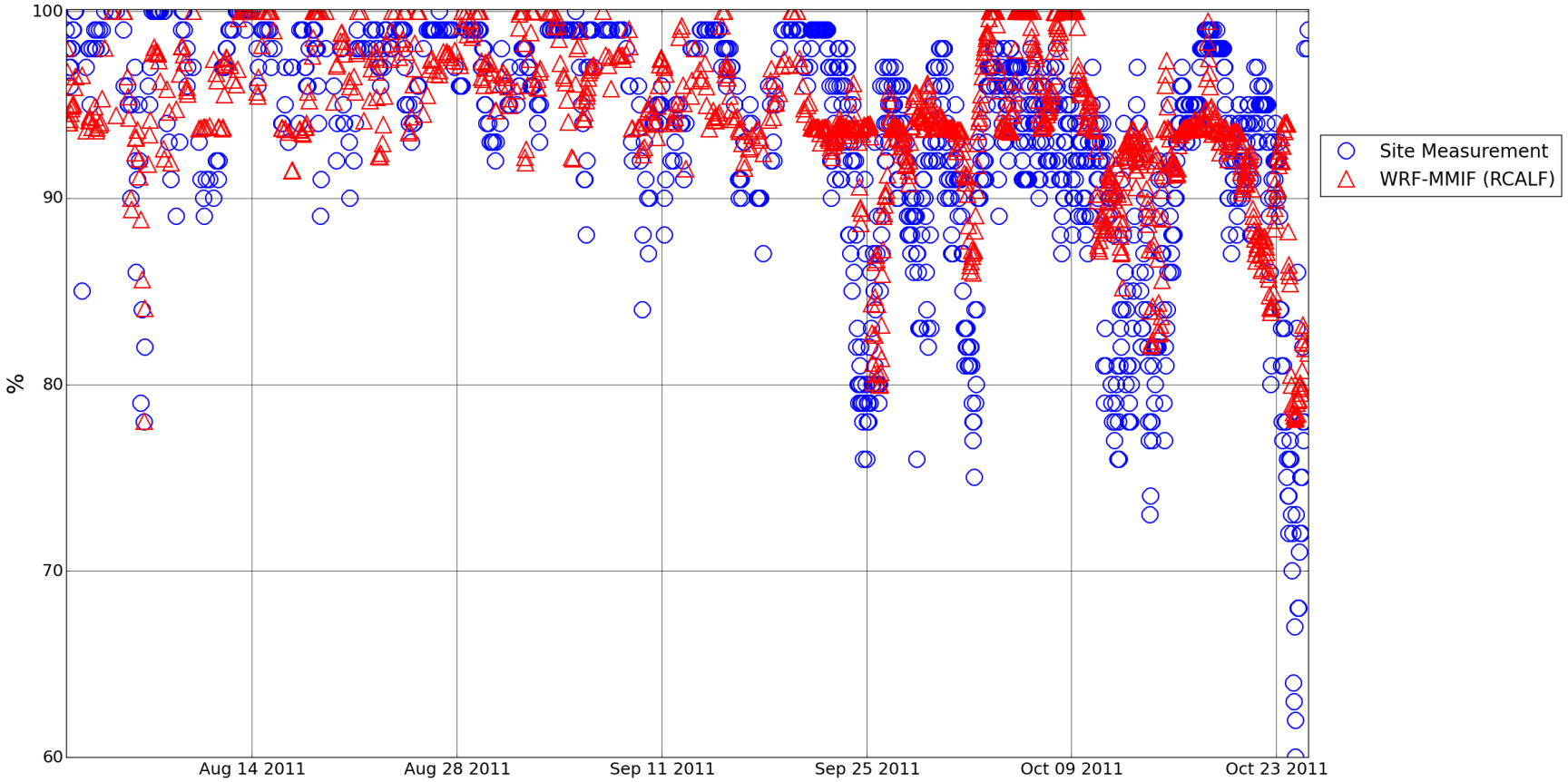

Figure 69. B3 2011 relative humidity time series.

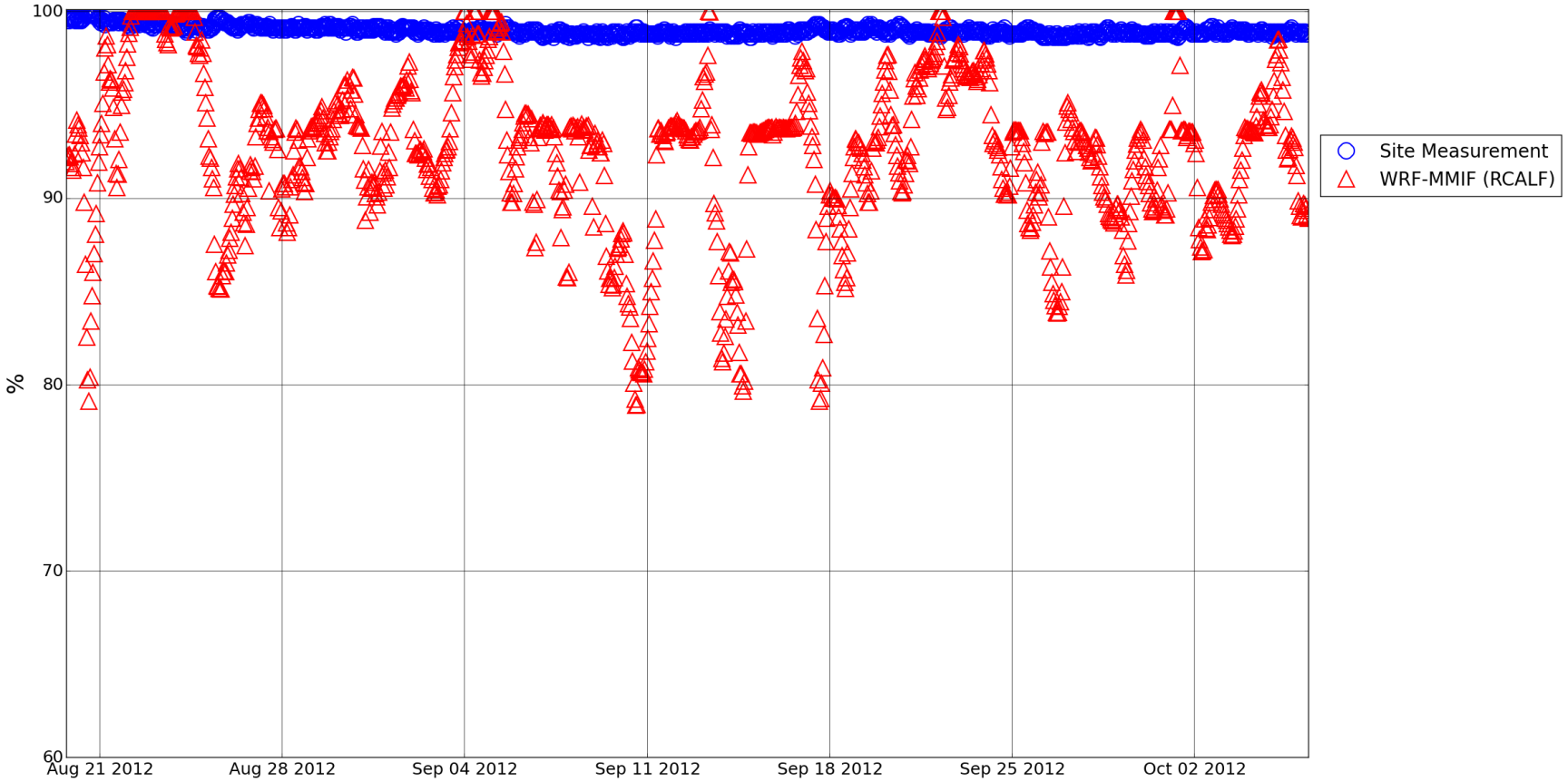

Figure 70. B3 2012 relative humidity time series.

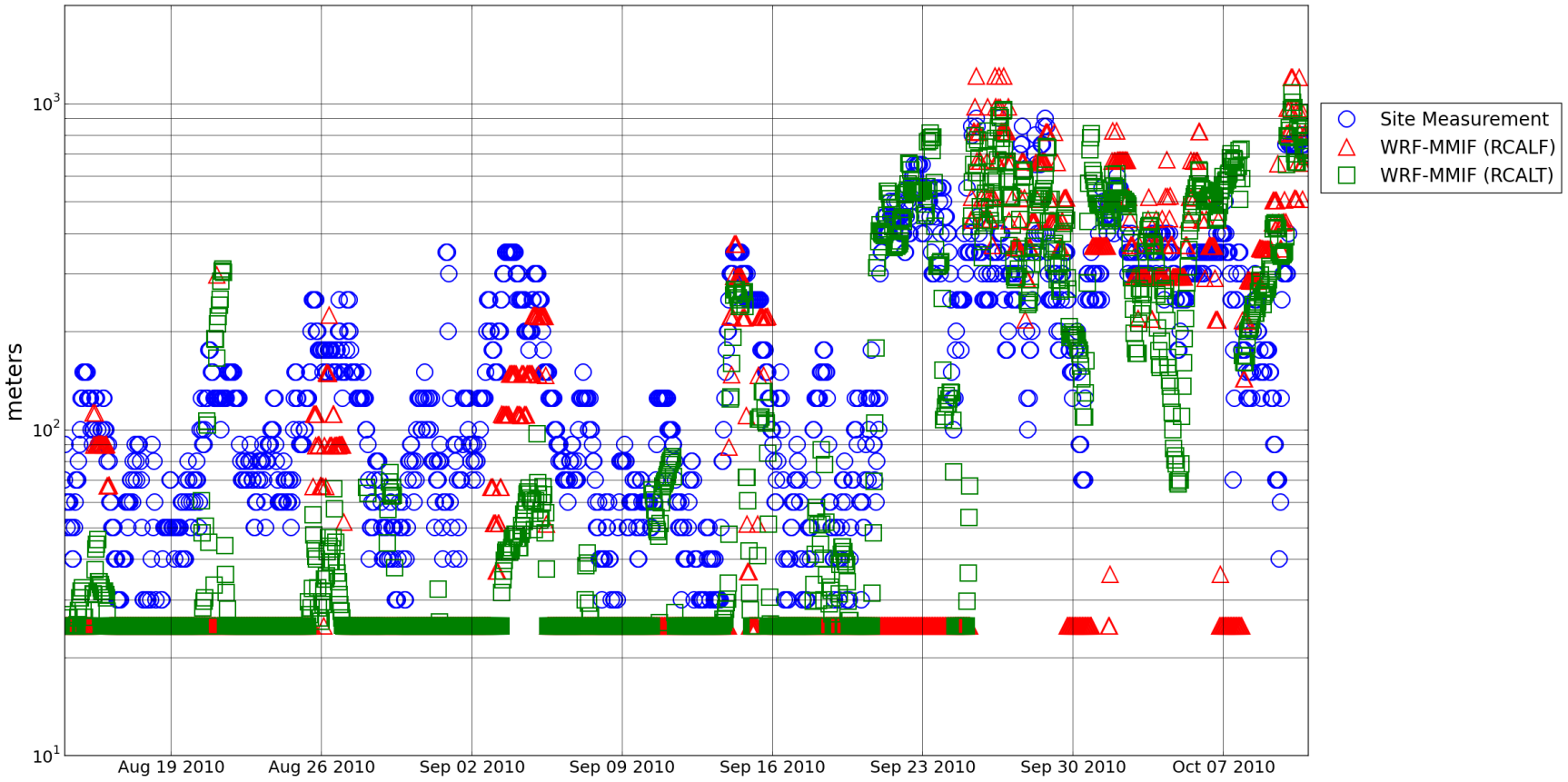

Figure 71. B3 2010 PBL height time series.

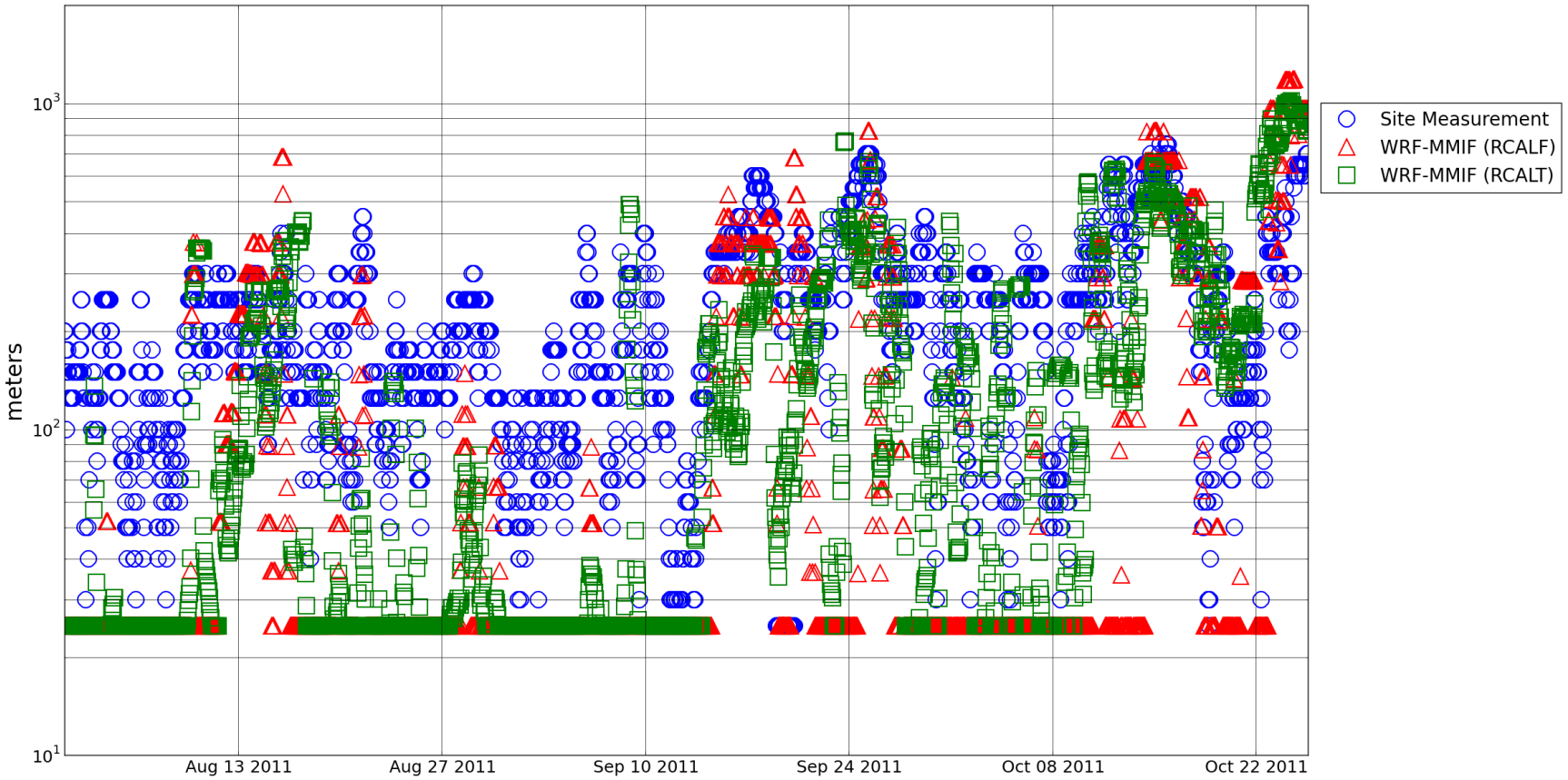

Figure 72. B3 2011 PBL height time series.

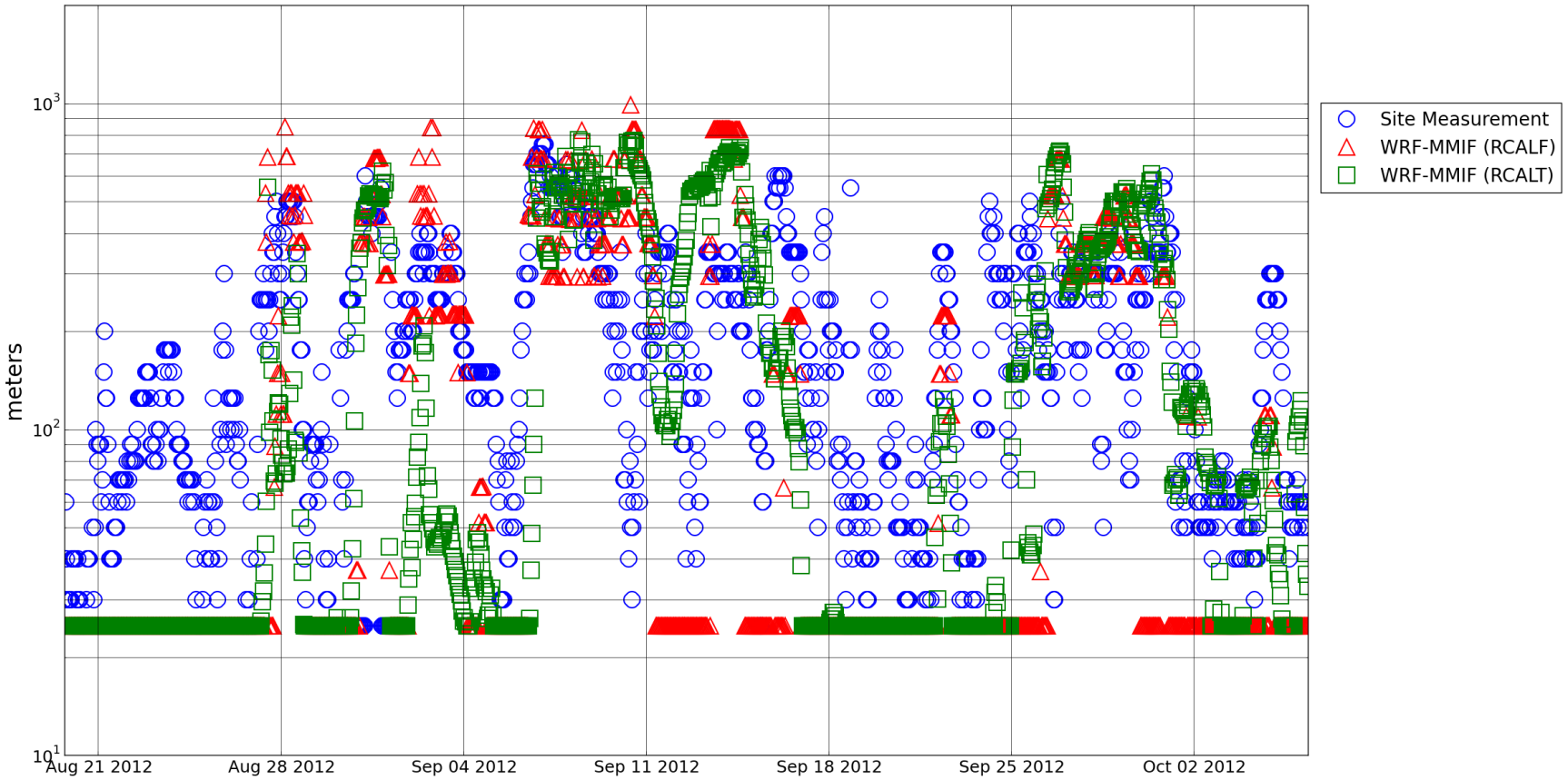

Figure 73. B3 2012 PBL height time series.

4.7 Summary

The statistics for all meteorological values analyzed in this section are listed in Table 5. Overall, it is evident WRF tends to underpredict wind speed, especially at site B3 given B3 winds were measured at 3.5 m and WRF winds were extracted at 10 m. SST was consistently overpredicted at site B2. WRF simulations resulted in less ASTD sign error for the Chukchi Sea locations than the Beaufort Sea locations, primarily because ASTD at the Beaufort Sea locations was near 0°C for a majority of the open-water seasons.

PBL Heights were overpredicted overall at site B3. Predictions of PBL height at site B2 were the most favorable, resulting in relatively low error and bias.

Table 5. Summary statistics for WRF meteorology extractions.

Parameter	Site	Year	Hours	Obs. Mean	WRF Mean	Bias	Std. Error
Wind speed	C1	2011	1591	6.97	6.46	-0.51	1.17
	C1	2012	1266	6.82	6.37	-0.44	1.00
	C2	2010	1612	6.04	6.11	0.07	1.06
	C2	2012	1067	6.08	5.89	-0.19	0.97
	B2	2010	912	4.69	3.98	-0.70	1.24
	B2	2011	1224	5.65	4.78	-0.87	1.38
	B3	2010	1391	5.51	5.10	-0.41	1.14
	B3	2011	811	6.29	5.19	-1.10	1.75
	B3	2012	1145	5.33	4.79	-0.54	1.32
Wind Direction	C1	2011	1591	108	106	5.2	17.7
	C1	2012	1266	131	149	-16.5	23.6
	C2	2010	1612	148	151	0.7	19.5
	C2	2012	1067	157	159	10.0	16.2
	B2	2010	912	146	116	3.6	25.4
	B2	2011	1224	118	110	0.8	21.3
	B3	2010	1391	150	141	4.5	24.5
	B3	2011	811	110	105	1.7	19.2
	B3	2012	1145	172	164	-4.2	31.1
Air Temp.	C1	2011	1591	4.76	3.91	-0.85	1.04
	C1	2012	1266	2.28	1.92	-0.36	1.01
	C2	2010	1612	3.37	3.30	-0.08	0.92
	C2	2012	1067	0.52	0.70	0.18	0.63
	B2	2010	912	2.21	3.11	0.90	1.22
	B2	2011	1224	4.12	4.37	0.25	0.95

Table 5, continued. Summary statistics for WRF meteorology extractions.

Parameter	Site	Year	Hours	Obs. Mean	WRF Mean	Bias	Std. Error
Air Temp.	B3	2010	1391	1.40	1.89	0.49	1.04
	B3	2011	811	-1.02	-1.40	-0.39	0.70
	B3	2012	1145	4.61	4.03	-0.57	0.93
SST	C1	2011	1591	6.60	5.70	-0.88	0.90
	C1	2012	1266	4.50	3.53	-0.97	1.12
	C2	2010	1612	4.04	3.98	-0.06	3.98
	C2	2012	1067	1.36	1.38	0.02	1.38
	B2	2010	912	2.39	2.67	0.28	0.96
	B2	2011	1224	4.7	4.07	-0.63	1.21
	B3	2010	1391	1.47	2.02	0.55	0.93
	B3	2011	811	-0.53	-0.20	0.33	0.58
	B3	2012	1145	4.77	4.10	-0.67	0.96
ASTD	C1	2011	1591	-1.83	-1.80	0.03	0.86
	C1	2012	1266	-2.22	-1.60	0.62	1.14
	C2	2010	1612	-0.67	-0.68	-0.01	0.86
	C2	2012	1067	-0.84	-0.68	0.16	0.82
	B2	2010	912	-0.18	0.44	0.62	1.16
	B2	2011	1224	-0.57	0.31	0.88	1.25
	B3	2010	1391	-0.06	-0.13	-0.06	0.77
	B3	2011	811	-0.49	-1.20	-0.71	1.01
	B3	2012	1145	-0.16	-0.06	0.1	0.82
RH	C1	2011	1591	88	92	3.8	6.1
	C1	2012	1266	95	91	-3.7	6.4
	C2	2010	1612	93	95	1.3	3.3
	C2	2012	1067	93	93	0.4	4.1
	B2	2010	912	98	97	-1.1	2.5
	B2	2011	1224	97	95	-1.9	3.3
	B3	2010	1391	93	94	0.9	3.5
	B3	2011	811	90	93	2.34	5.0
	B3	2012	1145	99	93	-6.4	6.5
PBL Height (WRF RCALF comparison)	C1	2011	1591	NA	293	NA	NA
	C1	2012	1266	NA	270	NA	NA
	C2	2010	1612	NA	213	NA	NA
	C2	2012	1067	NA	195	NA	NA
	B2	2010	912	143	49	-94	98
	B2	2011	1224	176	94	-82	115
	B3	2010	1391	194	147	-46	124
	B3	2011	811	305	193	-113	216

Table 5, continued. Summary statistics for WRF meteorology extractions.

Parameter	Site	Year	Hours	Obs. Mean	WRF Mean	Bias	Std. Error
	B3	2012	1145	194	163	-31	143
PBL Height (WRF-MMIF RCALT comparison)	C1	2011	1591	NA	397	NA	NA
	C1	2012	1266	NA	401	NA	NA
	C2	2010	1612	NA	239	NA	NA
	C2	2012	1067	NA	239	NA	NA
	B2	2010	912	143	81	-62	84
	B2	2011	1224	176	94	-82	115
	B3	2010	1391	194	171	-22	103
	B3	2011	811	305	278	-27	177
	B3	2012	1145	194	181	-14	151

5 AERMOD SIMULATION METHODOLOGY

The AERMOD modeling system was developed as the next generation regulatory air quality dispersion model, designed to incorporate state-of-the-art PBL parameterizations based on Monin-Obukhov Similarity theory. Monin-Obukhov theory uses scaling factors based on the rate of heat and momentum flux to describe the structure and evolution of the PBL. AERMOD replaced the ISC modeling system that used Pasquill-Gifford stability classes and corresponding lookup tables to estimate dispersion scaling parameters. AERMOD requires a complex set of meteorological input to characterize the PBL structure and the turbulence parameters used to estimate rates of dispersion. A full description of the formulas and parameterization schemes used in AERMOD and its meteorological pre-processor AERMET can be found in USEPA (2004a).

5.1 AERMOD Meteorological Input Files

AERMOD requires two meteorological files as input: a surface meteorological file (SFC file) and a near-surface profile of temperature and wind profile file (PFL file). Each file contains a time series of hourly-averaged meteorological variables. The PFL file need only include wind and temperature information at a single height, but turbulence measurements and information at additional heights may improve the accuracy of the simulation by providing a more complete description of the atmospheric structure for AERMOD. The meteorological variables contained in the SFC and PFL files relevant to this study are listed and described in Table 6.

Table 6. AERMOD meteorology fields.

Meteorological variable	Units[a]	Abbreviation	Description
Sensible heat flux	W/m^2	H	The rate of heat transfer to the atmosphere from the ground, positive H the ground is heating the PBL, negative H the ground is cooling the PBL.
(Surface) Friction velocity	m/s	u_*	Characteristic velocity scaling factor used to describe the rate of transfer of energy from atmospheric momentum to the surface through turbulent motions. Mechanical turbulence and the rate of pollutant dispersion in the PBL is a function of u_*.
Convective scaling velocity	m/s	w_*	Characteristic vertical velocity scaling factor used to describe the transfer of momentum due to convective processes in the PBL. It is used to estimate turbulence and corresponding rates of dispersion in the convective PBL.
Vertical potential temperature gradient above the mixed layer	K/m	$d\Theta / dz$	Used in convective conditions only: describes the gradient of potential temperature (temperature a parcel of air would have at sea-level pressure) at the interfacial layer above the well-mixed layer. This value specifies the "strength" of the top of the well-mixed layer for describing the fraction of plume penetration into and above the interfacial layer.

Table 6, continued. AERMOD meteorology fields.

Meteorological variable	Units[a]	Abbreviation	Description
PBL height potential under convective processes	m	z_{ic}	Depth of the mixed layer possible under convective forcing. AERMOD uses the maximum of z_{ic} or z_{im} for the PBL height.
PBL height potential under mechanical processes	m	z_{im}	Depth of the mixed layer possible under mechanical forcing. AERMOD uses the maximum of z_{ic} or z_{im} for the PBL height.
Monin-Obukhov length	m	L	The fundamental scaling parameter of Monin-Obukhov similarity theory that is used to define the influence of buoyancy-induced and mechanical turbulence on the structure of the surface layer of the atmosphere. In stable conditions it can be considered as the relative height at which buoyant production of turbulent energy is equal to that produced by mechanical/wind-shear processes. A negative L indicates unstable, convective conditions while a positive L indicates stable conditions. Large absolute value of L is indicative of neutral conditions while small absolute values of L are indicative of strongly stable or unstable conditions.
Surface roughness length	m	z_o	A scaling parameter used to describe the influence of ground surface friction on the structure of the PBL. Values of z_o over the ocean are very low (10^{-5} – 10^{-3} m) and are a function of wave height (Arya, 1988).
Bowen ratio	--	B	The ratio of sensible heat flux to latent heat flux from the ground. Values > 1 occur in drier conditions when most heat flux is in the form of sensible heat. Values < 1 occur in moist conditions, when sufficient surface moisture is available for evaporation. In marine environments, the Bowen ratio is always small. It is used by AERMET to estimate sensible and latent heat fluxes during unstable conditions and passed thru to AERMOD to estimate the deposition of gases.
Albedo	--	r	The fraction of total incident solar radiation reflected by the earth's surface. It is used by AERMET to estimate the surface radiation balance but only used by AERMOD for the deposition of gases.
Wind speed	m/s	WS	The average scalar wind speed at a specified measurement height. Typical measurement height is 10 m (the meteorological file provides a column to specify measurement height), but may be as low as a few meters on meteorological buoys.
Wind direction	degrees	WD	The average wind direction at a specified measurement height.
Temperature	K	T or Θ (absolute temp.)	The average atmospheric temperature at a specified measurement height, typically 2 m (the meteorological file provides a column to specify measurement height).
Standard deviation of wind direction	degrees	σ_Θ	(Provided in the PFL file only). Standard deviation of the wind direction during the period.
Standard deviation of vertical wind speed	m/s	σ_w	(Provided in the PFL file only). Standard deviation of the vertical wind speed during the period.

[a] meters (m), seconds (s), watts (W), kelvin (K).

The meteorology files used by AERMOD are typically built by a preprocessor program. AERMET is the accepted preprocessor for regulatory modeling of land-based air pollutant sources. MMIF and AERCOARE are the alternative pre-processors examined in this study. The MMIF program provides a method to extract WRF data directly from the WRF output files and create SFC and PFL meteorology files for AERMOD. It uses the fields available in WRF to estimate the meteorological variables listed in Table 6 or to create input files for AERCOARE.

Meteorological preprocessors produce the AERMOD meteorological parameters from a set of raw meteorological measurements or model data: wind speed, wind direction, temperature, solar radiation, differential temperature, humidity, cloud cover, and atmospheric pressure are typical inputs to the pre-processor. The quality of the AERMOD meteorological input is therefore highly dependent on the representativeness of the raw meteorology fed to the preprocessor.

AERCOARE requires overwater ASTD, RH, and WS to characterize the surface layer energy fluxes. The resulting static stability of the overwater atmospheric PBL is highly dependent on the "sign" of the ASTD, especially during light to moderate winds speeds. RH is important because it is used to determine the rate of sensible heat flux from the sea to the PBL. Lower RH promotes greater latent heat flux from the sea to the PBL and less sensible heat flux. Therefore, the rate of PBL heating is reduced with lower RH as more energy is invested into sea-surface evaporation.

5.2 Overwater Measurement Datasets and AERCOARE Processing

Meteorological datasets collected at four overwater sites from 2010-2012 were selected for this study (Air Sciences Inc., 2010) (AECOM Environment, 2009). Meteorological data collected at these sites were sufficient to provide inputs for AERCOARE. Two of the sites, "Burger" and "Klondike," are the locations of meteorological buoys that collected data during open-water periods on the Chukchi Sea. The other two sites, "Sivulliq" and "Reindeer Island," are the locations of a meteorological buoy and an island-based meteorological station that collected measurements during open-water periods on the Beaufort Sea. The temperature profiler dataset collected on Endeavor Island was used in conjunction with the buoy data to estimate PBL heights at the Beaufort sites. The temperature profiler was operated as part of a PSD-quality meteorological monitoring campaign conducted at Endeavor Island for Shell Offshore, Inc. (SLR, Inc., 2011). The sites are shown in Figure 74 and described in detail in Table 7.

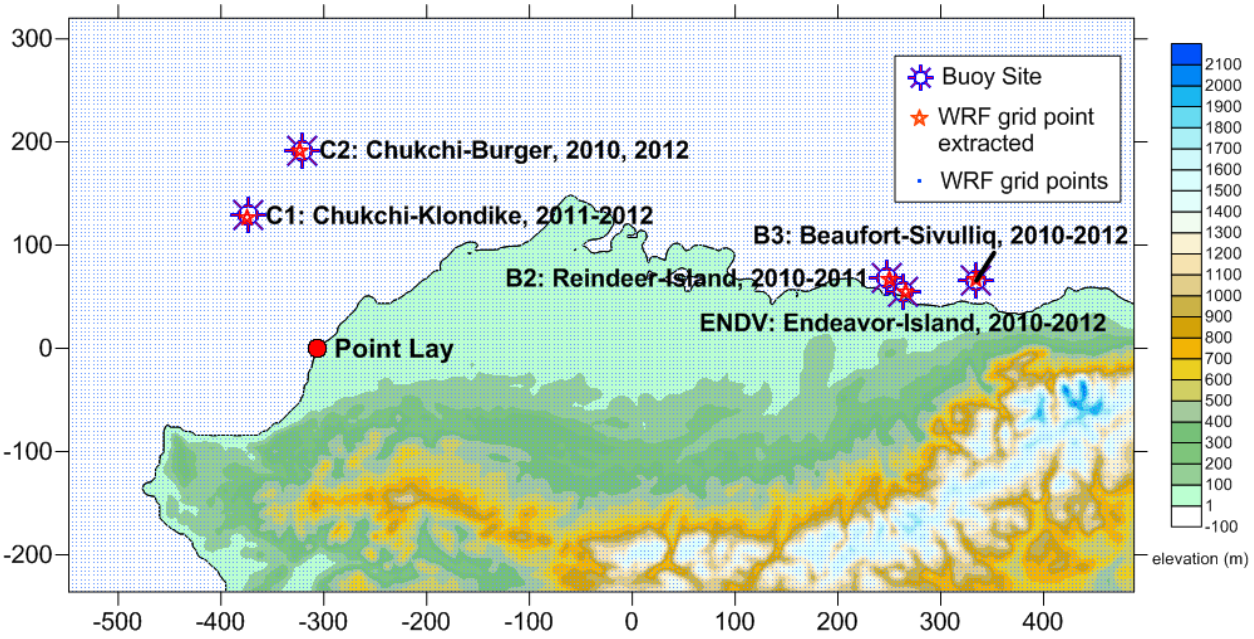

Figure 74. Overwater meteorological measurement sites and corresponding WRF inner-domain extraction points.

Table 7. Overwater measurement site details.

Site Identifier [a]	Location		Year	PBL height method	Measurement height (m)		
	Site	Lat/Lon			Air Temp.	Sea Temp.	Wind
C1	Chukchi-Burger	70.9 N, 165.3 W	2011, 2012	from WRF	3.0	-1.2 [b]	3.5
C2	Chukchi-Klondike	71.5 N, 164.1 W	2010, 2012	from WRF	3.0	-1.2	3.5
B2	Beaufort-Reindeer Island	70.5 N, 148.3 W	2010, 2011	critical bulk-Richardson layer method	1.4	-1.2	10.7
B3	Beaufort-Sivulliq	70.4 N, 146.0 W	2010, 2011, 2012	critical bulk-Richardson layer method	1.4 (2010) 3.0	-1.2	3.3 (2010) 3.5

[a] The site identifiers used in Task 1 and the Task 3 protocol of this study were retained. Note that B1 was a buoy site in the Beaufort Sea that collected data in 2009 but not the 2010-2012 period of Task 3.

[b] Negative value indicates temperature measurement is below the sea surface.

AERCOARE requires hourly WS, WS, T, SST, RH, air pressure, σ_Θ (optionally), and PBL height to create the overwater input meteorology for AERMOD.

For the Reindeer Island 2011 dataset, the Endeavor Island RH measurements were used for substitution because the RH sensor had missing or invalid data for most of the period. Although the Endeavor Island measurement site was technically land-based, the RH was near saturation (>90%) for most of the 2011 period and therefore would not have likely varied much from the true RH at the buoy locations. The Endeavor Island monitoring program Quality Assurance Project Plan (QAPP) (SLR, Inc., 2011) states the RH sensor height was selected to monitor RH within the marine layer.

PBL height is a parameter used by AERMOD. It was estimated in this study using a method described in Section 5.3 for the Beaufort Sea sites. No measurements were available for the Chukchi Sea sites to estimate PBL height directly. Although simplistic parameterizations such as the Venkatram (1980) method could be used to estimate PBL height at the Chukchi buoy locations, it was deemed inappropriate for this study. The WRF-MMIF (RCALT) PBL heights were used at the Chukchi locations in the AERMOD meteorology files. Therefore, PBL height was only a factor in the comparison of AERMOD performance at the Beaufort Sea sites.

The temperature profiler dataset was collected using a Kipp & Zonen MTP-5 passive microwave radiometer. The device was operated from 2010 to 2012 at the Endeavor Island facility near Prudhoe Bay, Alaska. The profiler was oriented to collect estimates of temperature at 31 levels from 0 to 1000 m above instrument height over the Beaufort Sea. Although the Endeavor Island meteorological station was technically a land-based station, it was located on a small man-made island located at the end of a thin peninsula that extends out about 6 kilometers (km) into the Beaufort Sea.. The profiler site was located, with approval by EPA Region 10, in the most practical site for measuring the marine boundary layer on the Beaufort Sea (SLR, Inc., 2011). The profiler data and accompanying Endeavor Island meteorological tower dataset were collected under an EPA-approved QAPP (SLR, Inc., 2011) satisfying PSD-quality data collection requirements.

The Endeavor Island meteorological tower was deployed on a small man-made island that was surrounded by the sea. Despite this, the wind, temperature, and humidity data measured at the site may be influenced by nearby industrial structures and operations or the landscape of the island depending on the meteorological conditions.

The Reindeer Island station was operated under an EPA-approved QAPP (AECOM Environment, 2009) to provide PSD-quality meteorological data for air emissions permitting. Reindeer Island is essentially a sandbar (about 250 m wide at its widest point and 3 km long) located about 16 km north of Prudhoe Bay in the Beaufort Sea. The station was deployed at this location to collect marine meteorological measurements during both ice and ice-free conditions. The monitoring project specifically included a marine buoy located about 2 km south of the Island to collect the data necessary for overwater dispersion modeling during the ice-free periods.

AERCOARE processing was conducted using a PBL height of 600 m for the COARE “gustiness” calculation (USEPA, 2012). Minimum PBL height and absolute value of *L* limits were set to 25 m and 5 m, respectively, as described in Section 4.

5.3 PBL Height Diagnosis Methods

Ideally, direct measurements of PBL height should be used for validation of WRF data and for use in the observation-driven AERMOD simulations. However, direct PBL height measurements were not available at the sites. The Endeavor Island temperature profiler data provided the means for estimating PBL height at the Beaufort Sea sites. There was no equivalent dataset for estimating PBL heights for the Chukchi Sea sites.

The 2010-2012 temperature profiler dataset provided the best means for diagnosing PBL height at the Beaufort Sea sites. The temperature profile data can be used to estimate PBL height using a method based on Richardson number theory. The Richardson number (Ri) is a measure of the ratio of potential to kinetic energy in an atmospheric layer, represented by the vertical stability and vertical wind shear, respectively. Small values of Ri indicate weak static stability or strong wind shear, indicative of conditions where vertical mixing is prevalent. Large values of Ri are indicative of a layer where the strength of the static stability is greater than the energy provided by vertical wind shear. Vertical mixing is restrained in such conditions.

The bulk-Richardson number, Ri_b, is a form of Richardson number that provides an estimate of the energy ratio over a layer between heights z_1 and z_2. The Ri_b is calculated using Equation **(7)** (Vogelezang & Holtslag, 1996):

$$Ri_b = \frac{g(z_2 - z_1)}{\theta(z_1)} \frac{\left(\theta(z_2) - \theta(z_1)\right)}{\left(u(z_2) - u(z_1)\right)^2 + b{u_*}^2} \quad \textbf{(7)}$$

where b is a parameterization constant, recommended by Vogelezang and Holtslag (1996) to be 100. The profiler does not measure wind speed so not all of the information needed to estimate the Ri_b at each layer is provided. Using Monin-Obukhov similarity theory, profile of wind speed can be estimated using values of u_*, z_o, and L provided by AERCOARE:

$$u(z) = \frac{u_*}{k} \sin\Theta \left(ln\left[\frac{z}{z_o}\right] + \Psi\left(\frac{z}{L}\right)\right) \quad \textbf{(8)}$$

where k is the von Karman constant (0.4) and ψ is the stability correction function. Equation (8) provides a means for estimating the wind shear between the two layers.

The height of the PBL can be assumed to be the height where $\mathrm{Ri_b}$ exceeds a critical value, referred to as the critical Richardson number (Ri_{crit}). A Ri_{crit} of 0.03 was used to diagnose the PBL height, based on the recommendations of Gryning and Batchvarova (2003). It must be emphasized this method relies on assumptions and parameterizations that may not result in accurate PBL height estimates in all cases. WRF PBL heights that do not compare well to the

“observed” PBL heights estimated using this method and may not necessarily indicate WRF performance is poor.

It is unlikely the hourly profiler data were representative of conditions at the Chukchi Sea buoy sites, given the sites were over 500 km away from the profiler location. Since there were no alternative datasets in the immediate region, PBL height estimates for sites C1 and C2 could only be made using an empirical parameterization scheme. However, a decision was made not to use a parameterization scheme to estimate PBL heights at these locations. Initial investigation of applicable parameterization schemes found no reliable method to produce consistently accurate PBL height estimates. Instead, the WRF-MMIF PBL heights at the Chukchi buoy locations were provided to AERMOD for modeling. Therefore, PBL height was only a factor in the comparison of AERMOD performance at the Beaufort Sea sites.

5.4 Hypothetical Sources

EPA provided five unique source group configurations for this study (Wong, 2012). Each group represented a hypothetical OCS source with stack characteristics typical of drill ship sources that have operated on the OCS in the recent past or have been proposed in recent permit applications for the Arctic as shown in Table 8. Each source contained multiple vertical stacks with warm, buoyant plumes. Emissions from Source Group #1 and #2 are lowest to the ground, with stacks averaging about 15 m in height. Emissions from Source Group #3 are concentrated at a height of 23 m. Emissions from Source Group #4 are concentrated at a height of 27 m. Given these values, Sources #1 and #2 can be considered representative of “short” stacks. Source #4 can be considered representative of “tall stacks.” Source #3 average stack height falls within the average heights of the tall and short stack groups.

AERMOD can account for the influence of the wakes of structures on downwind concentrations using the Prime Rise Model Enhancements (PRIME) algorithm (Schulman, et al., 2002). Building/structure downwash effects were not considered for Source Groups #1-4. Source Group #5 was comprised of the same stacks and parameters as Source Group #2, but with structure downwash applied. A hypothetical set of structures based on typical OCS source structure dimensions were provided for Source Group #5. The structure layout is shown in Figure 75. All sources were located at the same central location with respect to the receptors and structures (indicated as position 0 m, 0 m in the x- and y- coordinate system shown on Figure 75).

.

Table 8. Hypothetical source and stack parameters.

Source Group	Unit	Stack height (m)	Stack temp. (K)	Stack exit velocity (m/s)	Stack diameter (m)	Downwash effects
1	Diesel engine	16	700	30	0.50	No
	Incinerator	14	550	20	0.40	No
2	Diesel engine	18	680	28	0.40	No
	Boiler	17	500	10	0.45	No
	Incinerator	10	525	17	0.40	No
3	Propulsion engine	25	570	30	0.60	No
	Generator	20	610	22	0.25	No
	Boiler	15	420	2	0.30	No
4	Diesel engine	39	580	21	0.70	No
	Winch	25	580	14	0.20	No
	Heater	23	510	42	0.15	No
5	Diesel engine	18	680	28	0.40	Yes
	Boiler	17	500	10	0.45	Yes
	Incinerator	10	525	17	0.40	Yes

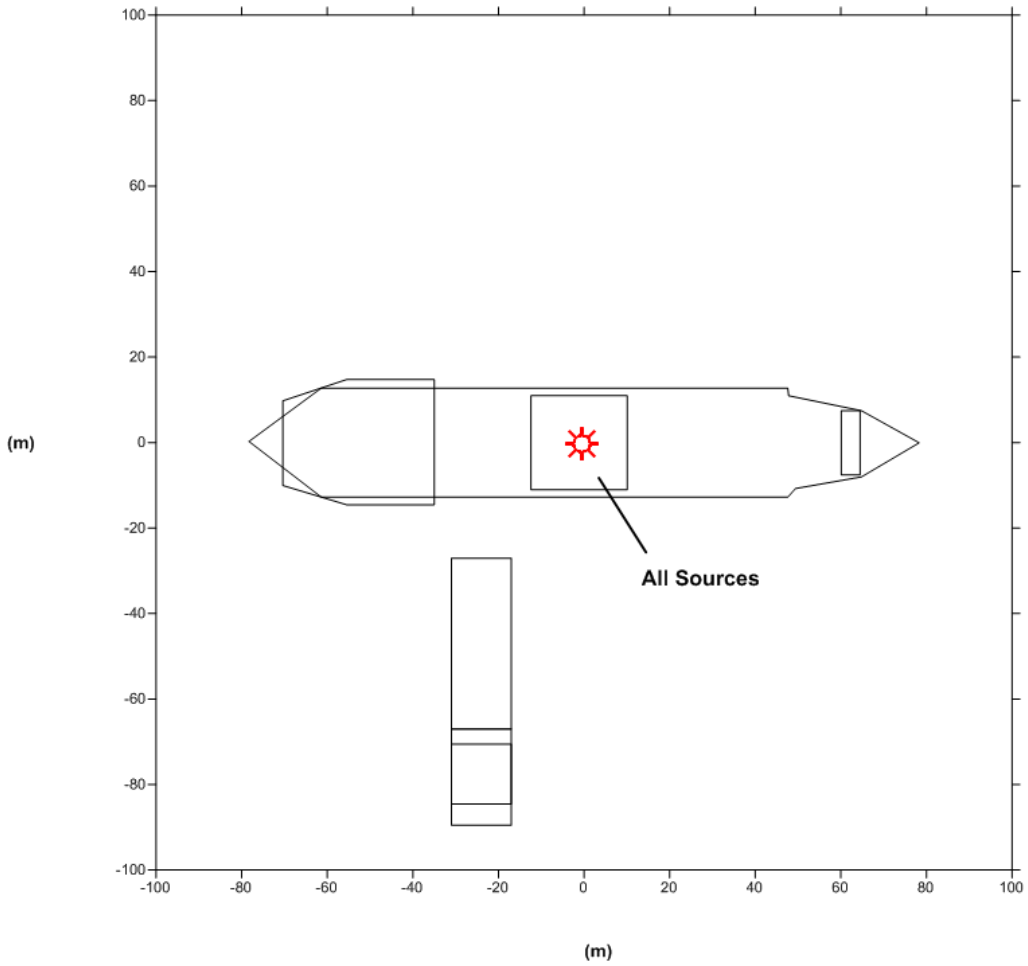

Figure 75. Source locations and structures.

5.5 Receptor Grid

AERMOD predicts pollutant concentration at assigned receptors based on their distance from sources and proximity to terrain features. For this study, a network of 50 receptor rings was used. Each ring contained 360 receptors at 1° spacing. The rings were centered at the same origin (origin of 0, 0 in the x- and y- directions, respectively, as shown in Figure 75) with incremental radial spacing of downwind distance based on a geometric series from 30 m to 10 km. The geometric series equation was formulated using Equation **(9)**:

$$Distance\ of\ ring\ N\ (m) = 30(m) * 1.1259^{(N-1)} \quad \textbf{(9)}$$

where *N* is the number of the receptor ring. The value of 1.1259 was determined iteratively to fit a geometric series of 50 rings spaced between 30 m and 10 km.

Receptors were placed at a height of 0.0 m (no flagpole receptors). The inner-most rings are shown with respect to the structures and sources in Figure 76. The vessel to the south had no

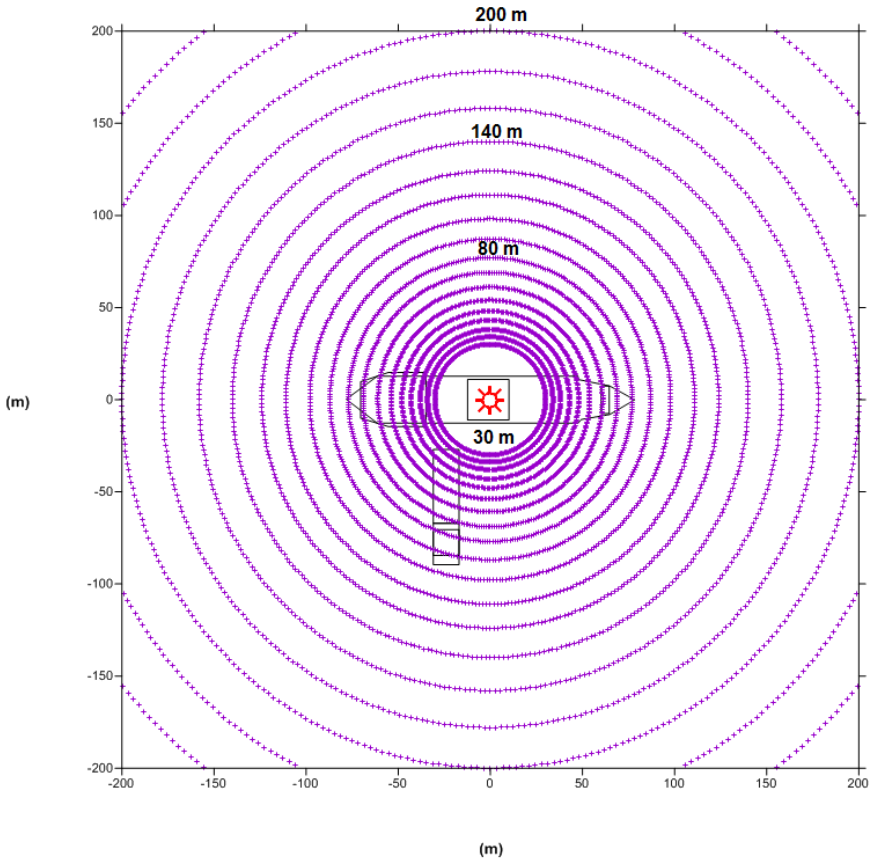

Figure 76. Visual of inner-most receptor rings

source nor downwash influence on the drill rig sources. The vessel was considered part of the ambient air.

5.6 WRF Meteorology Extraction and Processing

The variables listed in the SFC and PFL files can be calculated directly or indirectly by MMIF using the fields available in the WRF output files. The three ways MMIF can create meteorological files for AERMOD are:

a) Create onsite, upper air, and land use data and run AERMET
b) Create AERCOARE input files and run AERCOARE: AERCOARE produces SFC and PFL files for input into AERMOD.
c) Create AERMET-like SFC and PFL files directly.

Method *a* would be inappropriate for overwater dispersion studies because AERMET is only configured for overland meteorology. Methods *b* and *c* are both tested in this study. For Method *b*, the WRF simulations provide the variables that might be measured by a buoy, ship, or offshore platform. The meteorological fields from WRF were ported to AERCOARE. AERCOARE produces the AERMOD SFC and PFL files using its specialized overwater

algorithms. For Method *c*, MMIF passes through or calculates all variables directly from the WRF output files. If not available from WRF output, MMIF estimates the similarity scaling variables *L* and w_* from Richardson-number methodology defined in Louis (1979). In the current study, *L* is calculated and supplied directly by WRF under all scenarios simulated. The variable w_* is not calculated by WRF but calculated by MMIF.

Limits were placed on values of *L* and PBL height to prevent the occurrence of unphysical extreme values in both the observation-based and WRF-based meteorological datasets, as mentioned in Section 4. A minimum absolute value of 5.0 m was set as the limit for L in both MMIF and AERCOARE. A minimum PBL height of 25 m was established for all datasets. The PBL height and *L* limits used for both WRF- and observation- based simulations ensure the most stable atmospheric conditions result in similar parameters. The limits on *L* are the same limits used in the OCD model (Hanna, et al., 1985) (DiCristofaro & Hanna, 1989).

WRF estimates PBL height through the PBL parameterization scheme and each scheme uses a different method to formulate PBL height. The WRF PBL heights are also fixed to the nearest vertical grid cell center and can vary abruptly over small distances. MMIF can also rediagnose the PBL height using the bulk-Richardson approach of Vogelezang and Holtslag (1996) as described in Section 5.3. AERMOD simulations can be very sensitive to the PBL height (Richmond & Morris, 2012). Therefore, MMIF-predicted PBL heights may provide significantly different predicted concentrations than the PBL height used internally by WRF.

Given the options described above, four different MMIF extraction methods were tested:

1. MMIF was applied to extract and prepare data sets for direct use by AERMOD (MMIF produces the AERMOD SFC and PFL input files directly). The PBL height predicted by WRF is used in the SFC file.
2. As in Option 1), but the PBL height was rediagnosed from the wind speed and potential temperature profiles using the Bulk-Richardson algorithm within MMIF.
3. MMIF was applied to extract the key meteorological variables of overwater wind speed, wind direction, temperature, humidity, and PBL height from WRF results. The MMIF extracted data were used to build an AERCOARE input file. AERCOARE used these variables to predict the surface energy fluxes, surface roughness length and other variables needed for the AERMOD simulations. For the current study, AERCOARE was applied using the defaults recommended in the AERCOARE model evaluations study (Richmond & Morris, 2012).
4. As in Option 3), but the PBL height was rediagnosed using the bulk-Richardson algorithm within MMIF.

The naming convention and description of the four extraction methods are listed in Table 9. Note “RCALT” refers to extractions with MMIF rediagnosis of PBL height and “RCALF” refers to direct use of WRF PBL height (with the minimum 25 m PBL height applied). Also, note “AERC”

refers to simulations with additional AERCOARE processing after MMIF extraction, and “MMIF” refers to simulations using the WRF meteorology directly without further processing by AERCOARE.

Table 9. WRF AERMOD meteorology extraction methods.

WRF Extraction Method	Process Path
1) MMIF.RCALF	WRF ➔ MMIF ➔ AERMOD
2) MMIF.RCALT	WRF ➔ MMIF (with PBL diagnosis) ➔ AERMOD
3) AERC.RCALF	WRF ➔ MMIF ➔ AERCOARE ➔ AERMOD
4) AERC.RCALT	WRF ➔ MMIF (with PBL diagnosis) ➔ AERCOARE ➔ AERMOD

MMIF identifies the nearest WRF grid point to the coordinates of the overwater measurement site and extracts the data time series from this point (no interpolation between points). The extraction points used in Task 3 were selected to correspond with the meteorological measurement sites as closely as possible. The extraction points are shown in Figure 74.

5.7 AERMOD Evaluation Methodology

In this study, AERMOD concentrations were calculated using meteorology from overwater observations and meteorology extracted from WRF simulations. The maximum predicted concentrations at each receptor ring were extracted and the observation-driven AERMOD results were compared directly to the WRF-driven AERMOD results. This approach simplifies the investigation of the bias of the WRF simulations and removes the influence of wind direction differences.

AERMOD version 14134 was used for this study, using all regulatory defaults except the “VECTORWS” flag was used for WRF wind speed. The regulatory default for AERMOD version 14134 assumes scalar wind speed. AERMOD retains a non-regulatory algorithm that corrects for the use of vector wind speeds, initiated using the “VECTORWS” flag. The algorithm, described in USEPA (2004a) estimates the scalar wind from a vector wind using turbulent fluctuations as an estimate or measurement of σ_θ. This correction is most useful for low wind speed conditions where the scalar and vector wind speeds are most likely to diverge. It was also necessary to specify the “Beta” option in AERMOD to use the MMIF extracted data.

5.7.1 Simulation scenarios

The periods of available measurement data varied depending on the length of the open-water season and buoy deployments. The open-water season is the period during the summer and early autumn when the polar ice has melted and retreated northward enough to allow exposure of the sea surface to the open air. A transitional period occurs between the ice- and ice-free periods when a substantial portion of the sea surface is covered by broken ice. The buoys were

typically deployed at the end of the transitional period to prevent damage to the buoys from floating ice. Table 10 lists the periods of continuous overwater data extracted for this study. The seasonal length varied from 811 hours at site B3 in 2011, to 1612 hours at site C2 in 2010. As shown in Table 10, very few hours of calm wind occurred in the measurement- and extracted-WRF datasets. The site B3 2011 observational dataset had the most hours of calm wind or missing data, but such hours were still less than 3% of the dataset.

Five different averaging periods were simulated for each combination of site, year, and source type: 1-hour, 3-hour, 8-hour, 24-hour, and period-long averaging periods. These averaging times were selected because they correspond to the averaging periods applicable to the NAAQS. To ensure tracer emission rate independence, AERMOD simulations were conducted using a stack unit emission rate of 1 g/s. The resulting AERMOD concentrations were divided by the tracer release rates to provide normalized concentration with units of $\mu s/m^3$.

This study involved a large number of AERMOD simulations. A total of 1,125 AERMOD simulations were conducted to satisfy all of the possible scenarios:

- 3 site datasets per year (two years of data at sites C1, C2, and B2 and three years of data at site B3) ,
- 3 years (2010-2012),
- 5 sources,
- 5 averaging periods,
- 5 meteorological datasets:
    - i) Observations
    - ii) MMIF.RCALF WRF extractions
    - iii) MMIF.RCALT WRF extractions
    - iv) AERC.RCALF WRF extractions
    - v) AERC.RCALT WRF extractions

The definitions the WRF extractions in ii) through v) are explained in Table 9.

A set of summary statistics were calculated for each simulation to evaluate the performance of WRF-based simulations compared to the observation-based simulations, included in Appendix B. All AERMOD input and output files and analysis plots are included in electronic form on a data disk attached as Appendix C.

Table 10. AERMOD simulation periods.

Site Identifier	Date range	Total Possible Hours	Scenario	Total Hours Modeled [a]
1	Aug. 2, 2011, Hour 2 – Oct. 7, 2011, Hour 8	1591	Observations	1584
			MMIF.RCALF	1591
			MMIF.RCALT	1591
			AERC.RCALF	1586
			AERC.RCALT	1586
	Aug. 18, 2012, Hour 23 – Oct. 10, 2012, Hour 16	1266	Observations	1266
			MMIF.RCALF	1266
			MMIF.RCALT	1266
			AERC.RCALF	1266
			AERC.RCALT	1266
C2	Jul. 25, 2010, Hour 15 – Oct. 3, 2010, Hour 17	1612	Observations	1591
			MMIF.RCALF	1612
			MMIF.RCALT	1612
			AERC.RCALF	1612
			AERC.RCALT	1612
	Aug. 23, 2012, Hour 9 – Oct. 6, 2012, Hour 19	1067	Observations	1067
			MMIF.RCALF	1067
			MMIF.RCALT	1067
			AERC.RCALF	1067
			AERC.RCALT	1067
B2	Aug. 18, 2010, Hour 1 – Sep. 24, 2010, Hour 24	912	Observations	911
			MMIF.RCALF	912
			MMIF.RCALT	912
			AERC.RCALF	907
			AERC.RCALT	907
	Jul. 30, 2011, Hour 1 – Sep. 18, 2011, Hour 24	1224	Observations	1219
			MMIF.RCALF	1224
			MMIF.RCALT	1224
			AERC.RCALF	1216
			AERC.RCALT	1216
B3	Aug. 14, 2010, Hour 1 – Oct. 10, 2010, Hour 23	1391	Observations	1379
			MMIF.RCALF	1391
			MMIF.RCALT	1391
			AERC.RCALF	1384
			AERC.RCALT	1384
	Sep. 21, 2011, Hour 5 – Oct. 25, 2011, Hour 14	811	Observations	795
			MMIF.RCALF	811
			MMIF.RCALT	811
			AERC.RCALF	811
			AERC.RCALT	811
	Aug. 19, 2012, Hour 17 – Oct. 6, Hour 9	1145	Observations	1145
			MMIF.RCALF	1145
			MMIF.RCALT	1145
			AERC.RCALF	1145
			AERC.RCALT	1145

[a] Total hours modeled – hours without calms or missing data.

5.7.2 Statistical measures and methods

The statistical measures and methods are similar to the techniques applied in the EPA evaluation of AERMOD (USEPA, 2003). The statistical scores were calculated using the maximum concentration results from each receptor ring. The maximum concentration at each receptor ring for each AERMOD scenario was extracted resulting in a set of 50 values (one value for each ring) for each scenario. The results from the WRF meteorology based AERMOD simulations were compared to the results from the meteorological measurement based AERMOD simulations. The primary purpose of the investigation was to judge whether the WRF-based method provided results similar to maximum predictions from observation-based methods, and not biased towards underprediction. The tools used for the evaluation are described below:

- Quantile-quantile (Q-Q) plots. Q-Q plots were prepared to test the ability of the WRF-based concentration predictions to represent the frequency distribution of the observation-based AERMOD concentration predictions. Q-Q plots are simple ranked pairings of predicted and observed concentration, such that any rank of the predicted concentration is plotted against the same ranking of the observed concentration. The Q-Q plots can be inspected to examine whether the predictions are biased towards underestimates at the important upper-end of the frequency distribution.

- Log-log scatter diagrams. Log-log diagrams were prepared in which each plot contains a plot of the WRF-extraction AERMOD predictions versus the observation-based AERMOD predictions paired in time.

- Robust Highest Concentration (RHC). RHC has been used in most EPA model evaluation studies to measure the model's ability to characterize the upper end of the frequency distribution. Note this can also be accomplished by visual inspection of the Q-Q plots.

$$RHC = c_n + (\bar{c} - c_n) ln\left(\frac{3n-1}{2}\right) \quad \textbf{(10)}$$

  where c_n is the nth highest concentration and $\bar{c}$ is the average of the (n-1) highest concentrations. For the small sample size data sets in the current analysis, n was taken to be 5.

- Fraction-factor-of-two (FF2). FF2 is the ratio of the number of WRF-based concentration predictions within a factor-of-two from the observation-based predictions to the total number of predictions.

- Geometric correlation coefficient (r_g). r_g is a standard correlation coefficient computed using the natural log of the predictions and measurements and is calculated as follows:

$$r_g = \frac{\sum\left(\ln(x) - \overline{\ln(x)}\right)\left(\ln(y) - \overline{\ln(y)}\right)}{\sqrt{\sum\left(\ln(x) - \overline{\ln(x)}\right)^2}\sqrt{\sum\left(\ln(y) - \overline{\ln(y)}\right)^2}} \quad \textbf{(11)}$$

- Geometric mean (μ_g). μ_g is the nth root of the product of n numbers. The geometric mean provides a method to evaluate a general expected value with dampened outlier influence. Geometric mean is calculated as follows:

$$\mu_g = \left(\prod_{i=1}^{n} c_i\right)^{1/n} \quad \textbf{(12)}$$

- Bias of the geometric mean (*MG*). MG is a symmetric measure independent of the magnitude of the concentration. A perfect model would result in *MG* = 1. *MG* is calculated as follows:

$$MG = e^{\left(\overline{ln\left(\frac{c_o}{c_p}\right)}\right)} \quad \textbf{(13)}$$

  where c_o and c_p are the observed and predicted concentrations, respectively.

- Geometric variance (*VG*). *VG* is a measure of the precision of the dataset. A perfect model would result in *VG* = 1. *VG* is calculated as follows:

$$VG = e^{\left(\sqrt{\left(ln\left(\frac{c_o}{c_p}\right)\right)^2}\right)} \quad \textbf{(14)}$$

- Total modeling score (TMS). To summarize the modeling results with one composite score, a "model score" was calculated for each AERMOD case. The formula for this score is basically an average of five statistics: the FF2, geometric correlation coefficient, geometric mean, RHC, and VG with equal weighting. MG is not included in the model score because μ_g is an equivalent measure. The value ranges from 0 to 1, with 1 being a "perfect" model:

$$\frac{\left\{FF2 + r_g + \frac{\min(\mu_{g,p}, \mu_{g,obs})}{\max(\mu_{g,p}, \mu_{g,obs})} + \frac{\min(RHC_p, RHC_{obs})}{\max(RHC_p, RHC_{obs})} + \frac{1.0}{VG_p}\right\}}{5} \quad \textbf{(15)}$$

6 AERMOD SIMULATION RESULTS

Given the large number of AERMOD simulations conducted for this study, it would be tedious to review each set of simulation results individually in this report. Instead, summary statistics are used to compare AERMOD performance. Several individual AERMOD simulations with interesting results are investigated further in this report. For each of the 1,125 AERMOD simulations, a set of plots were produced to evaluate and compare concentration results and corresponding meteorological conditions. The scenarios simulated were described in Section 5.7.1, using the source groups described in Table 8 over the periods outlined in Table 10. Meteorology for each AERMOD simulation was produced using the methods described in Table 9. All results plots were included on a data disk in Appendix C

The summary statistics for each simulation, defined in 5.7.2, provide an effective set of tools for evaluating the simulations. The summary statistics were calculated for each of the source groups identified in Table 8. As described in Section 5.4, Source Groups #1 and #2 can be considered representative of "short" stacks. Source Group #4 can be considered representative of "tall stacks." Source Group #3 average stack height falls within the average heights of the tall and short stack groups. Some interesting cases were selected for further investigation using the concentration and meteorology plots developed for each simulation.

For each simulation, the maximum concentration at each receptor ring was extracted. The statistics are computed for the data pairs comprised of the maximums values from each ring from the WRF-based and measurement-based AERMOD simulations. Each statistic is computed using the 50 data pairs representing the maximum values from each receptor ring. Therefore, each data pair is not necessarily extracted from the same receptor but is extracted from receptors with the same downwind distance from the sources. Q-Q plots and scatter plots of the results from each scenario are included in Appendix C.

The RHC may be the most relevant statistic for this study. The capability of WRF-driven AERMOD simulations to produce conservative concentration estimates (as conservative as the measurement-based AERMOD simulations) is inferred by the RHC. RHC provides a tool to investigate the accuracy of results on the high end of the concentration spectrum for each simulation. The FF2 statistic provides a means to evaluate the accuracy of the entire distribution of concentration for each WRF-driven AERMOD simulation. All other statistics are implied through its value. Plots were prepared for direct comparison of the RHC and FF2 statistic values.

In the figures of the statistical score, different features were used to identify each separate simulation. A color scheme was used to identify the results by site (B2: green, B3: black, C1: red, and C2: blue). An outline symbol was used to identify each simulation by year (circle for 2010 simulations, triangle for 2011 simulations, and square for 2012 simulations). The results for each source group were identified by the symbol inner number. This symbol/color scheme was used to compare the results of all simulations together in a single plot for each WRF meteorology extraction method.

The statistical scores were examined for each averaging period followed by summaries for each measurement site. A few interesting cases were selected for deeper analysis. The full set of statistical scores at each site is reported in Sections 6.6, 6.7, 6.8, and 6.9 for Sites B2, B3, C1, and C2, respectively for the 1-hour averaging periods only. Tables of the statistical scores for the 3-hour, 8-hour, 24-hour, and period averaging periods are included in Appendix B.

6.1 1-hour Averages

The 1-hour averaging period is the shortest averaging period used in this study. The 1-hour averaging period is important because it is the shortest averaging period used in the NAAQS used for peak SO_2, NO_2, O_3, and CO concentrations.

6.1.1 Robust high concentration

RHC values were calculated using the AERMOD results from all four WRF-meteorology extraction methods as shown in Table 7 and for each of the emission sources listed in Table 6. The values from all scenarios are shown in Figure 77 - Figure 80 for the 1-hour averaging period simulations for each WRF extraction method (MMIF.RCALF, MMIF.RCALT, AERC.RCALF, and AERC.RCALT, respectively). Figure 77 - Figure 80 demonstrate RHC values were greatest for Source Group #5 and lowest for Source Group #1. Since emission rate was not normalized between the groups, magnitude of the concentrations was irrelevant except for when comparing between Source Groups #2 and #5 (same stack groups, no-downwash vs. downwash). The downwash cases resulted in the highest RHC due to early transport of the plume to the surface that resulted in high concentrations at the near-source receptors.

Most of the WRF-based RHC values were similar in magnitude to the observation-based RHC predictions: all WRF RHC values were within a factor of two of the measurement RHCs. The overall WRF-based average RHC value was slightly underpredicted in comparison to the observation-based runs. WRF-based RHCs at site B2 were consistently lower than observation-based RHCs, although still within a factor of two. Site C1 RHCs compared the most favorably.

Source Group #4, representative of emissions from “tall” stacks as described in Section 4.4, appeared the most sensitive to differences in extracted meteorology. The RHC was underpredicted in the AERC and MMIF.RCALF cases. The 2010 and 2011 site B2 simulations for Source Group #4 produced the WRF RHC values that differed most from the observation-based RHC values.

From the results of the meteorological analysis, it was hypothesized underpredicted wind speeds at sites C1, B2, and B3 could result in overprediction of concentration. The hypothesized trends were not evident in the 1-hour average RHC results. However, the bias over the entire period would not likely relate to the short term concentration bias (which is inferred through RHC) since worst case concentrations would occur during short term periods of extreme weather: generally low wind speed, highly stable or unstable conditions.

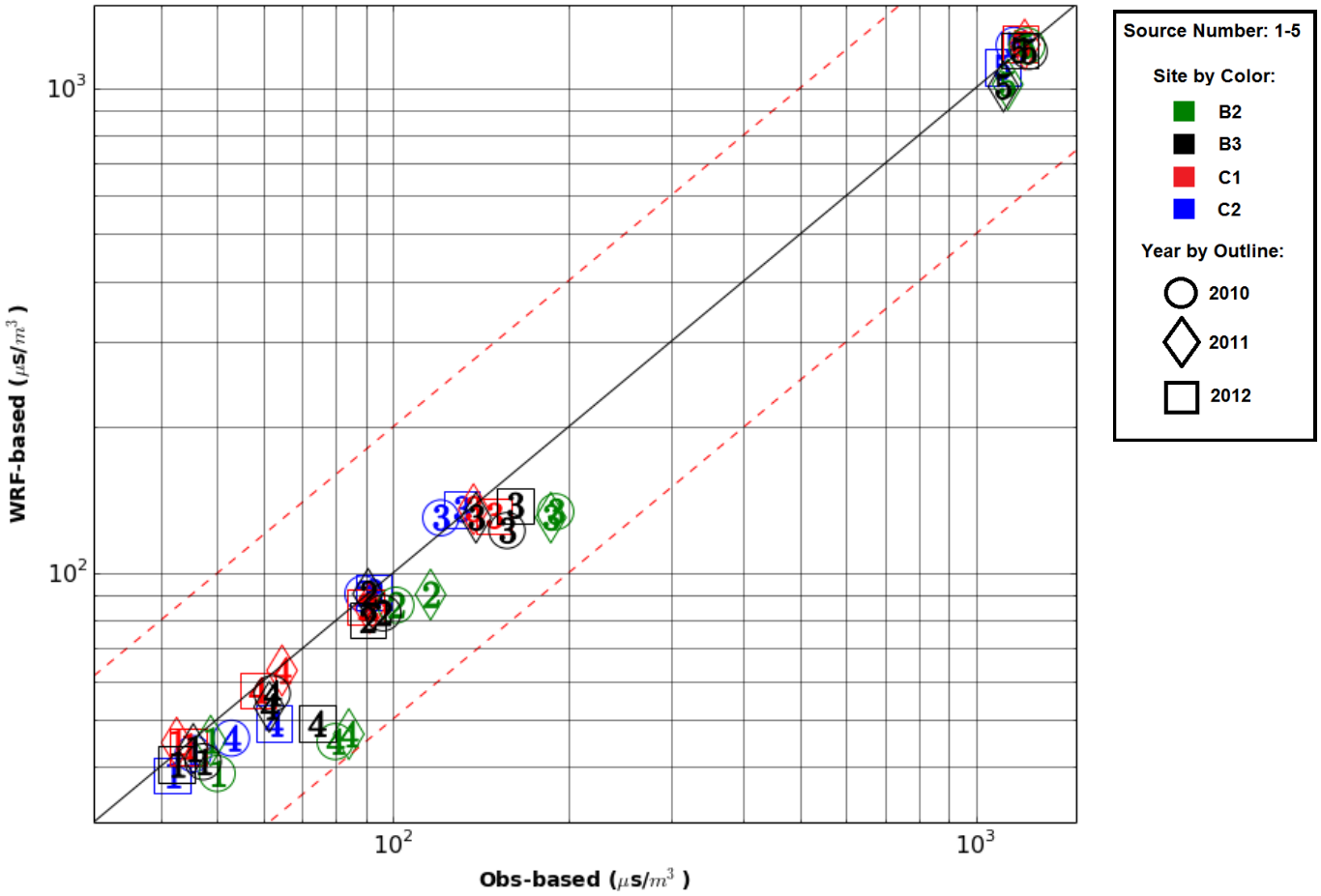

Figure 77. Robust high concentration results for MMIF.RCALF AERMOD 1-hour averaging times.

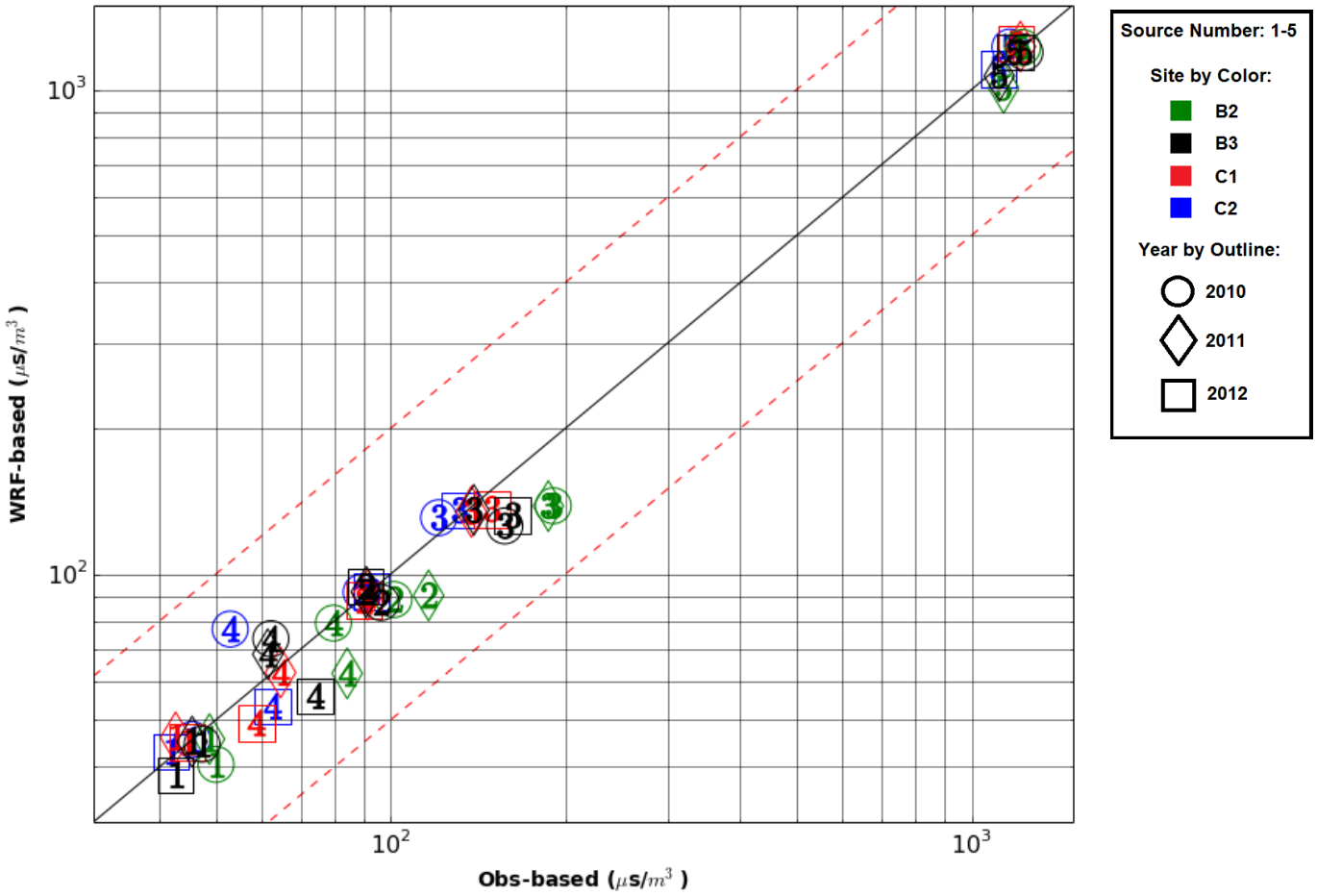

Figure 78. Robust high concentration results for MMIF.RCALT AERMOD 1-hour averaging times.

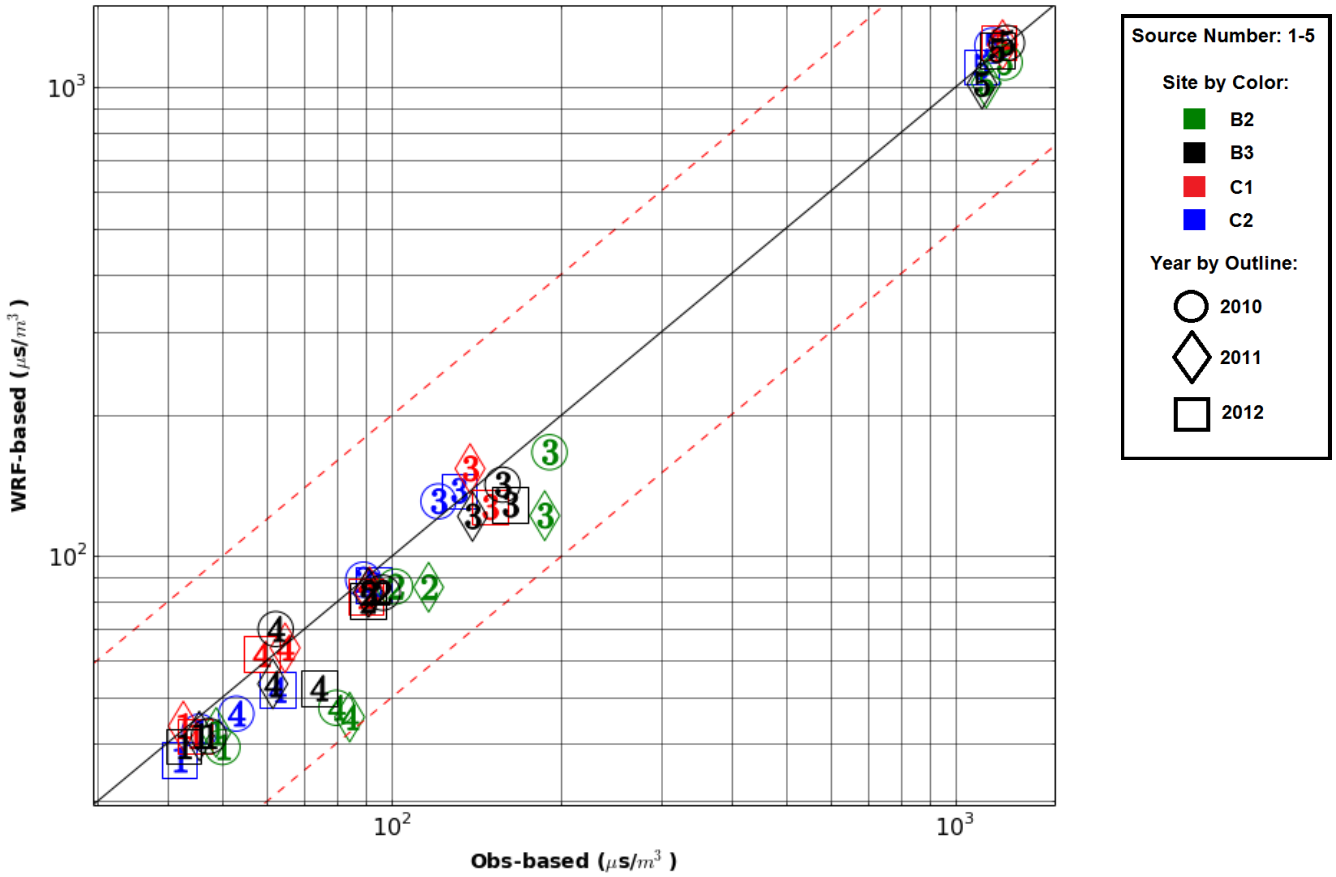

Figure 79. Robust high concentration results for AERC.RCALF AERMOD 1-hour averaging times.

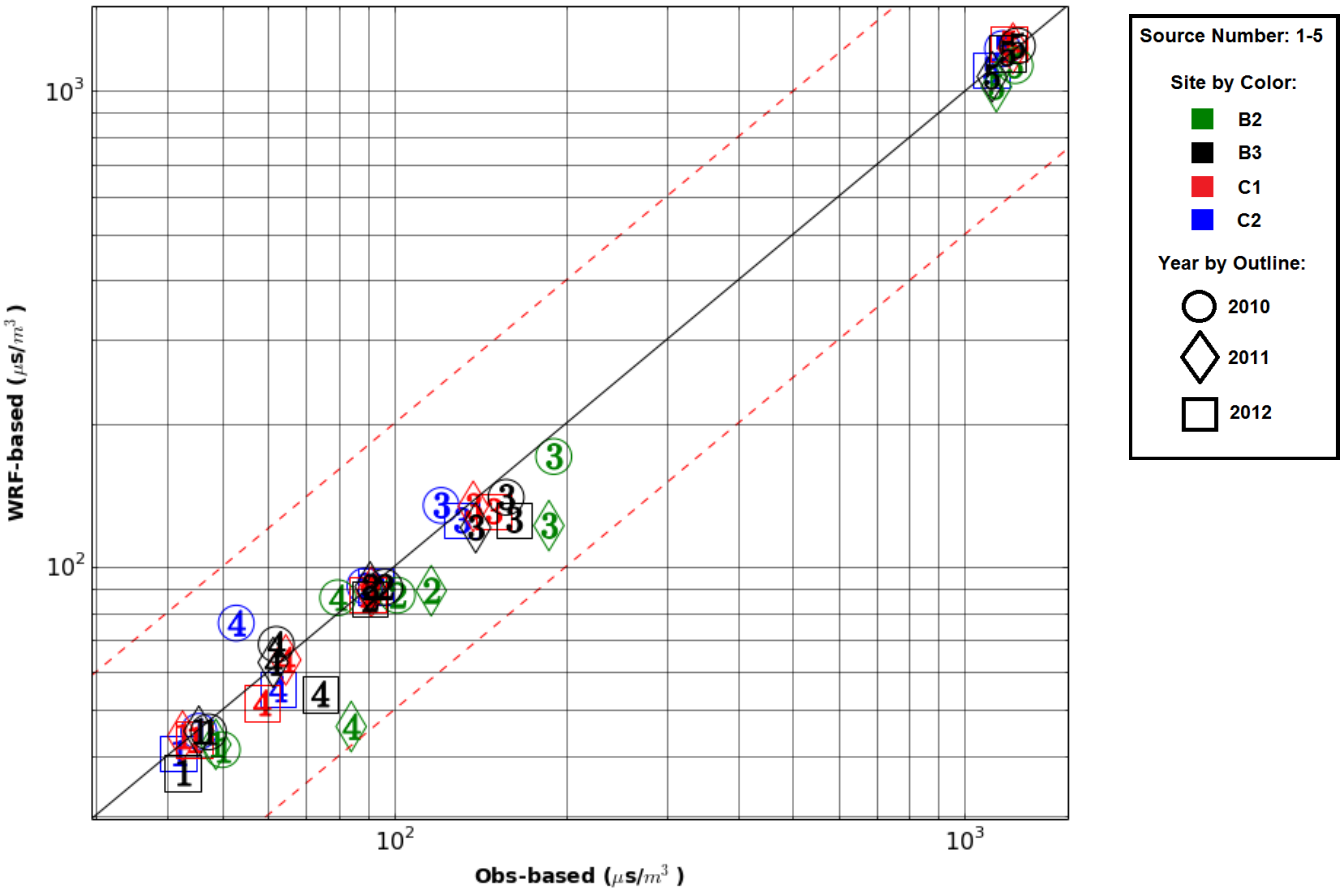

Figure 80. Robust high concentration results for AERC.RCALT AERMOD 1-hour averaging times.

6.1.2 Fraction-factor-of-two

The FF2 results for 1-hour averaging times are plotted in Figure 81 - Figure 84 for the four WRF extraction simulation sets, respectively. Most of the AERMOD simulations using WRF meteorology performed similarly to the observation-based AERMOD simulations. The FF2 scores tended to be between 0.7 and 1.0. Site B2 simulations fare the worst under all cases, particularly the tall stack source group (#3 and #4) B3 simulations. Overall, there is no significant difference in FF2 between the WRF extraction methods.

The lowest FF2 scores occurred for simulations involving Source #4. The average FF2 for all Source Group #4 simulations was 0.77 compared to 0.85, 0.87, 0.80, and 0.99 for Source Groups #1, 2, 3, and 5, respectively. Again as with the RHC results, concentration results from units with greater stack height resulted in the lowest scores.

Chukchi Sea sites average FF2 results are higher on average compared to the Beaufort Sea sites, which is not surprising given the WRF-MMIF PBL heights are used for C1 and C2.

6.1.3 Discussion

Source Group #4 2011 simulations were selected for further investigation, based on the low RHC and FF2 scores. The concentration maxima are shown in Figure 85, plotted with respect to distance from the origin. The maximum observation-based concentrations occurred about 500 m downwind of the source. The RCALF maximum concentrations occurred at the same distance, but were almost a factor of two lower in magnitude. The MMIF.RCALT simulation resulted in a more accurate maximum concentration, but it occurred farther downwind at about 1000 m from the source.

The PBL height and wind speed for this case are shown in Figure 86 and Figure 87, respectively. In Figure 86 and Figure 87, the meteorological parameter values shown are the values from the hour that results in the maximum concentration at each receptor ring. Therefore, the meteorological variables at each point do not necessarily occur at the same time as those at the other points. At the 500 m distance (distance of the maximum observation-based concentrations) RCALF simulations have a high wind speed of about 7 m/s compared to the observed and RCALT wind speeds of 4 m/s. The RCALT wind speeds, PBL heights, L, and u_* (Appendix C is the data disk for plots of L and u_* for this case) are all similar in magnitude to the observation-based values around the 500 m downwind distance. It is therefore surprising concentrations do not agree more favorably at this point.

The Source Group #5 simulations resulted in the best FF2 scores and most favorable RHC scores. Examination of the meteorology reveals large differences in PBL height, wind speed, and other factors despite good agreement in concentration. It is evident that when downwash is used, the influence of differences in meteorology is minimal.

The Source Group #2 simulations were the second best performing set of simulations in terms of FF2 and RHC score. For the B2 2011 case, the WRF-based runs resulted in RHC values

ranging from 86 – 93 μs/m^3 compared to the observation-based RHC value of 116. FF2 values ranged from 0.8 to 1.0. The Source Group #2 maximum concentrations occurred at roughly 350 m downwind for the observation-based and WRF cases. The PBL height and wind speed for this case are shown in Figure 88 and Figure 89, respectively. The observed wind speed is about 5.7 m/s and the WRF-based wind speeds are around 8 m/s for the concentration maxima cases at 350 m distance. Observed PBL height is about 180 m compared to the RCALT WRF heights at about 150 m and RCALF cases at 210 m.

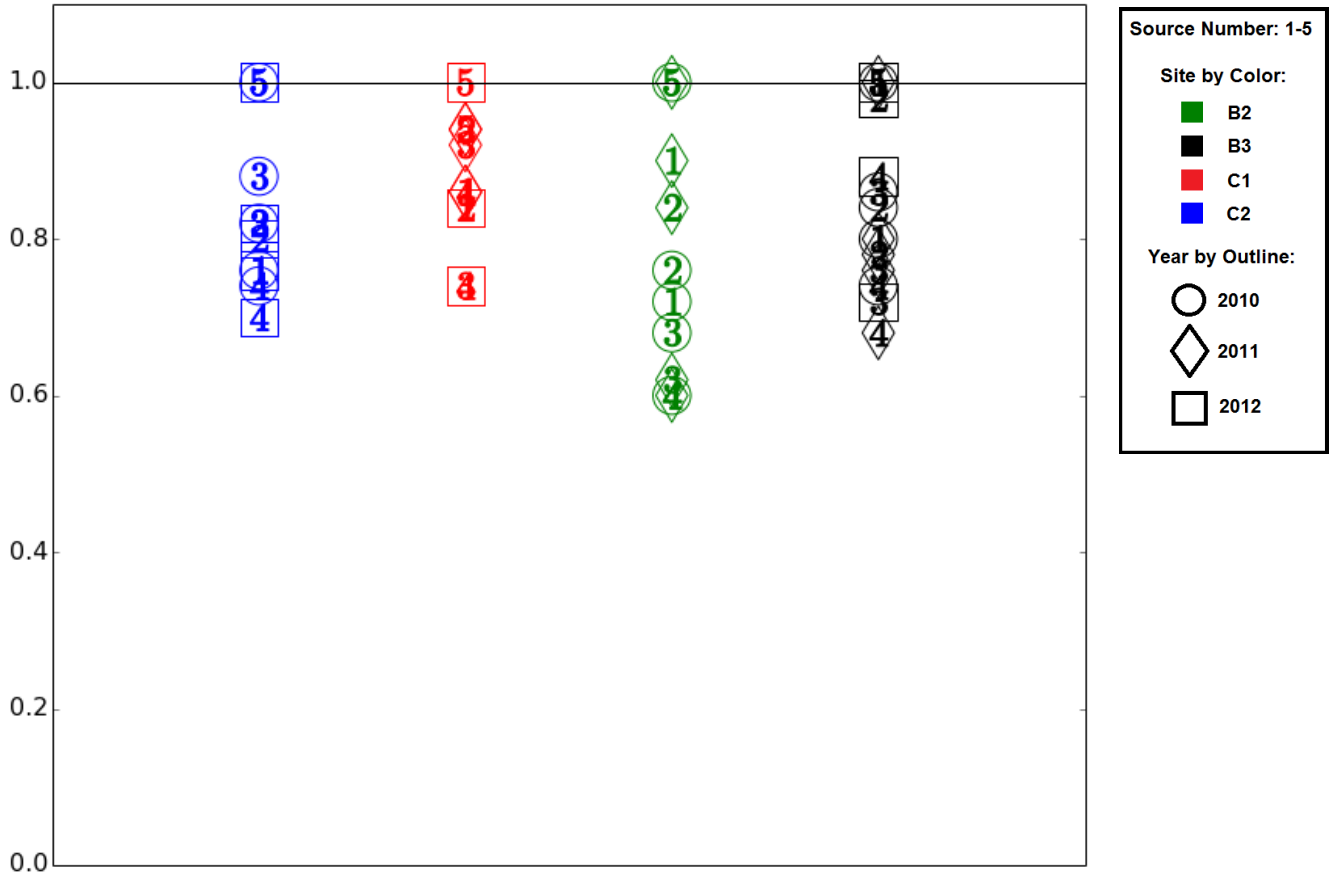

Figure 81. Fraction-factor-of-two MMIF.RCALF AERMOD results for 1-hour averaging time.

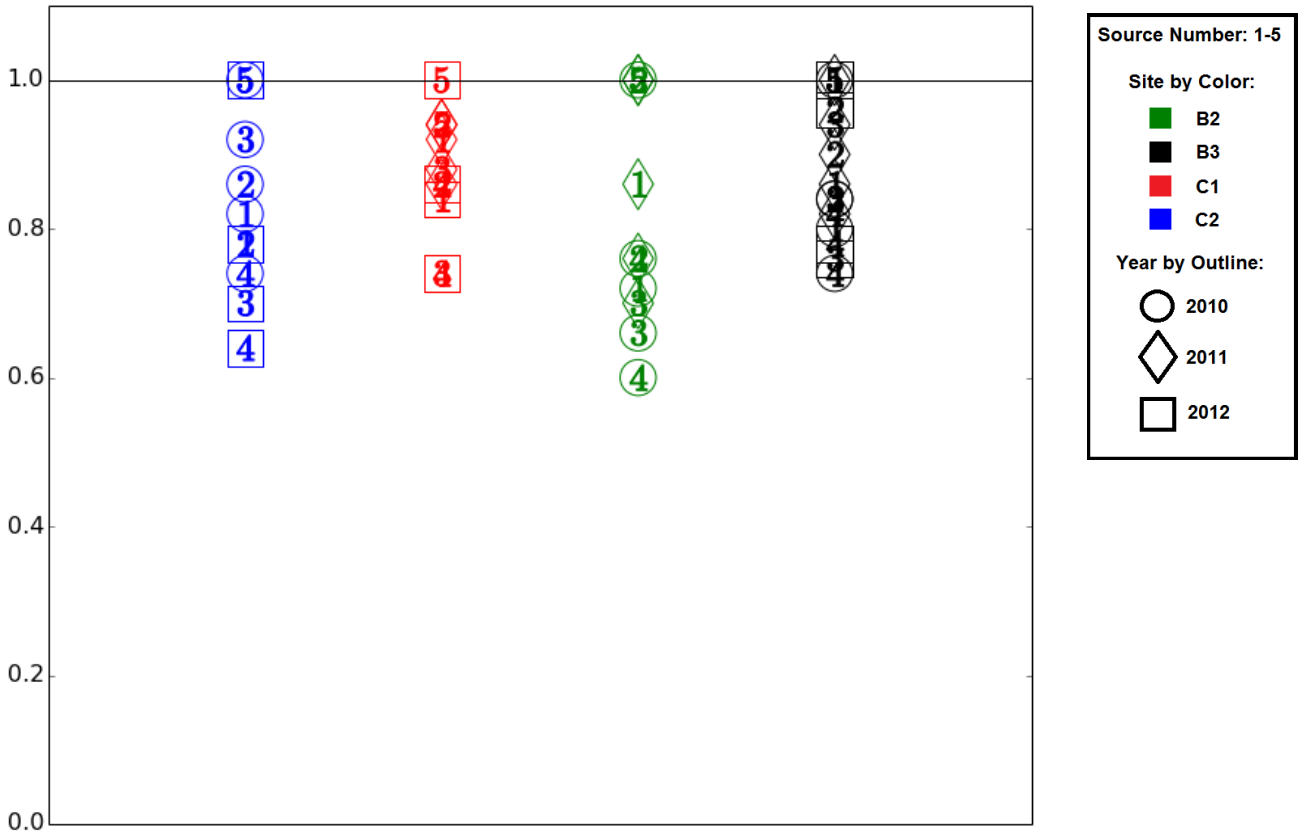

Figure 82. Fraction-factor-of-two MMIF.RCALT AERMOD results for 1-hour averaging time.

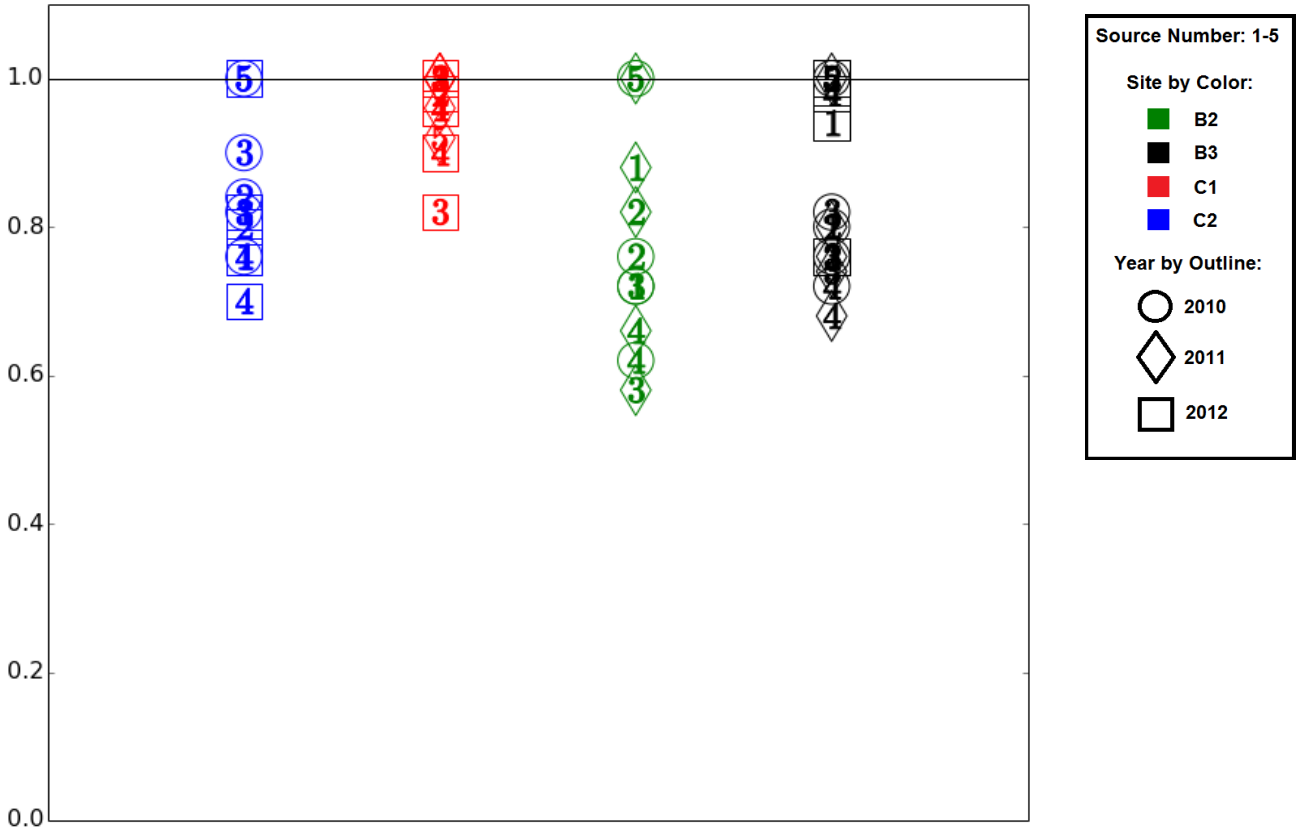

Figure 83. Fraction-factor-of-two AERC.RCALF AERMOD results for 1-hour averaging time.

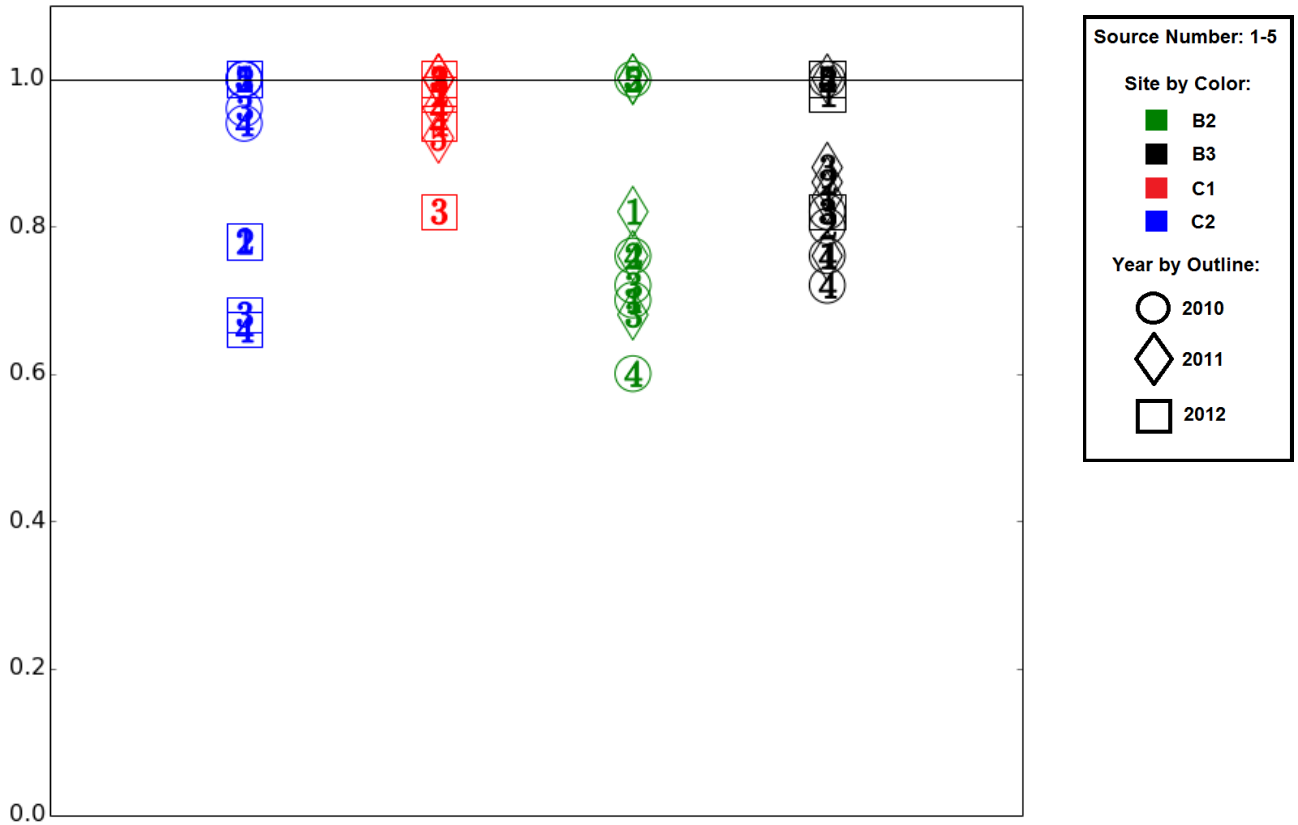

Figure 84. Fraction-factor-of-two AERC.RCALT AERMOD results for 1-hour averaging time.

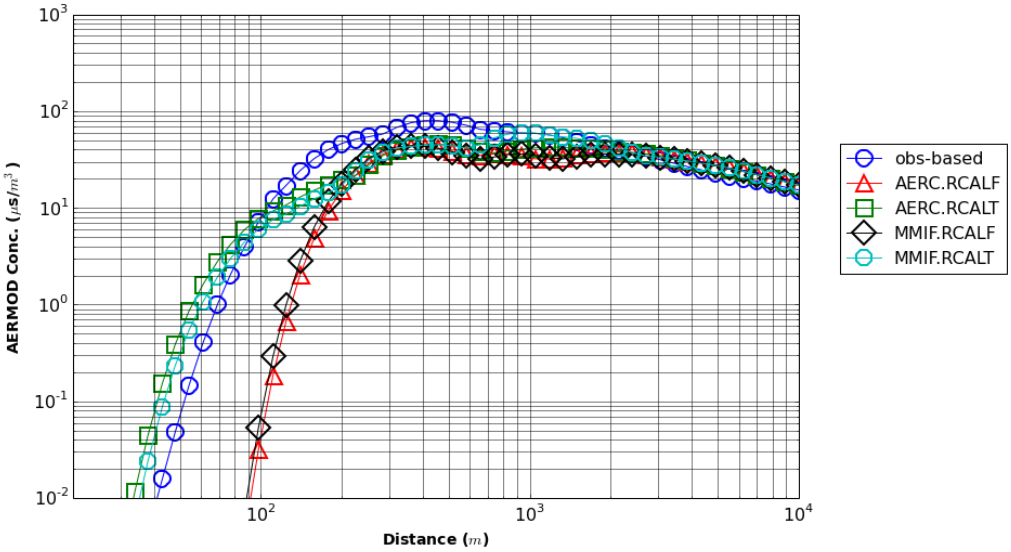

Figure 85. Concentration maxima vs. distance, Site B2, 2011, Source Group #4, 1-hr avg.

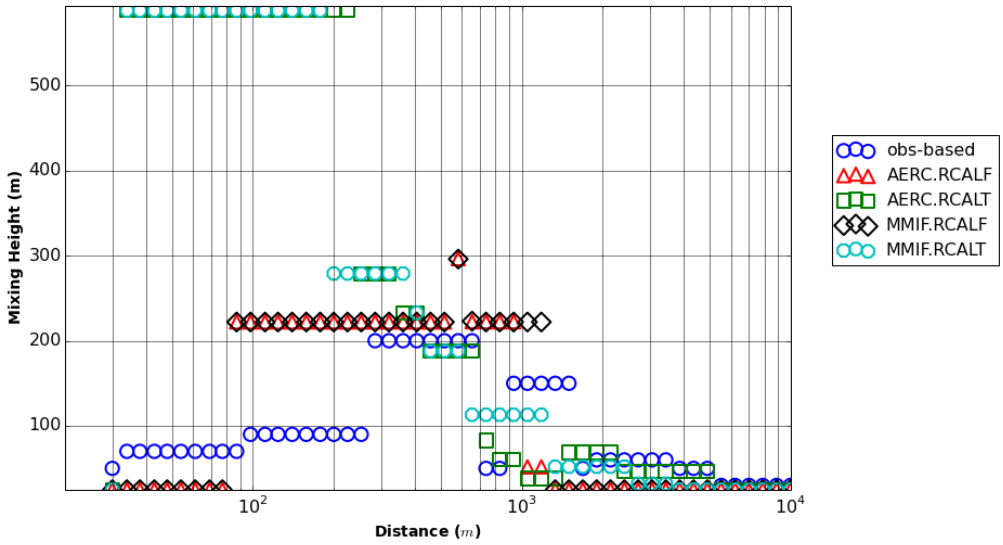

Figure 86. PBL height corresponding to concentration maxima, Site B2, 2011, Source Group #4, 1-hr avg.

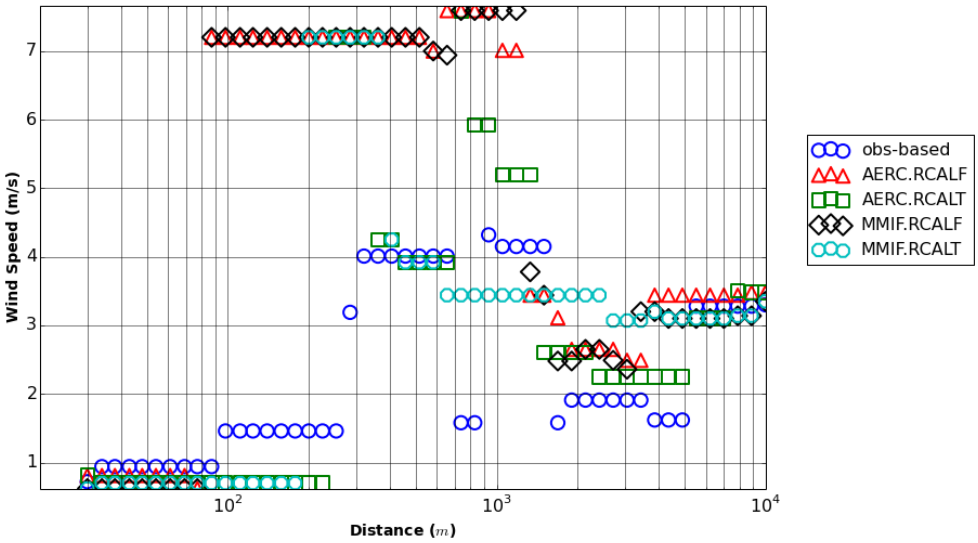

Figure 87. Wind speeds corresponding to concentration maxima, Site B2, 2011, Source Group #4, 1-hr avg.

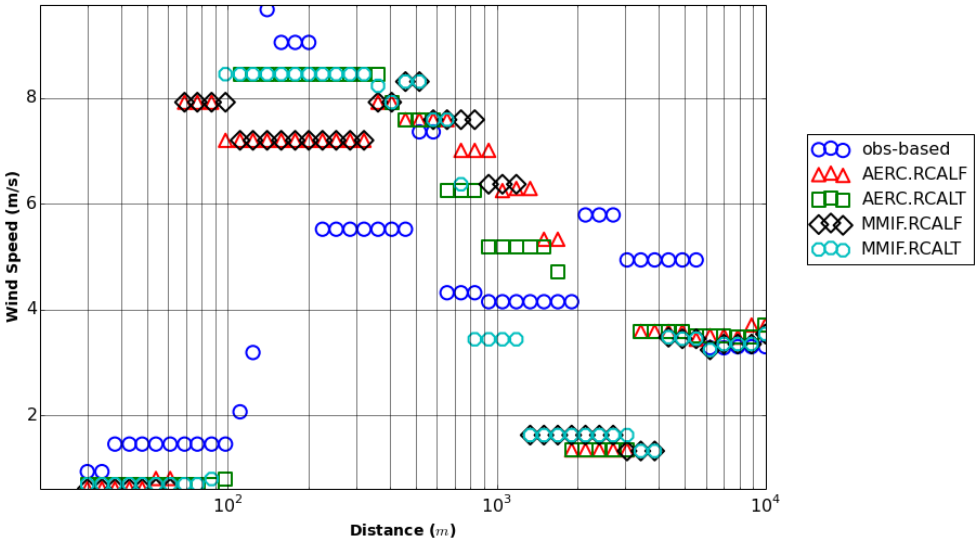

Figure 88. Wind speed corresponding to concentration maxima, Site B2, 2011, Source Group #2, 1-hr avg.

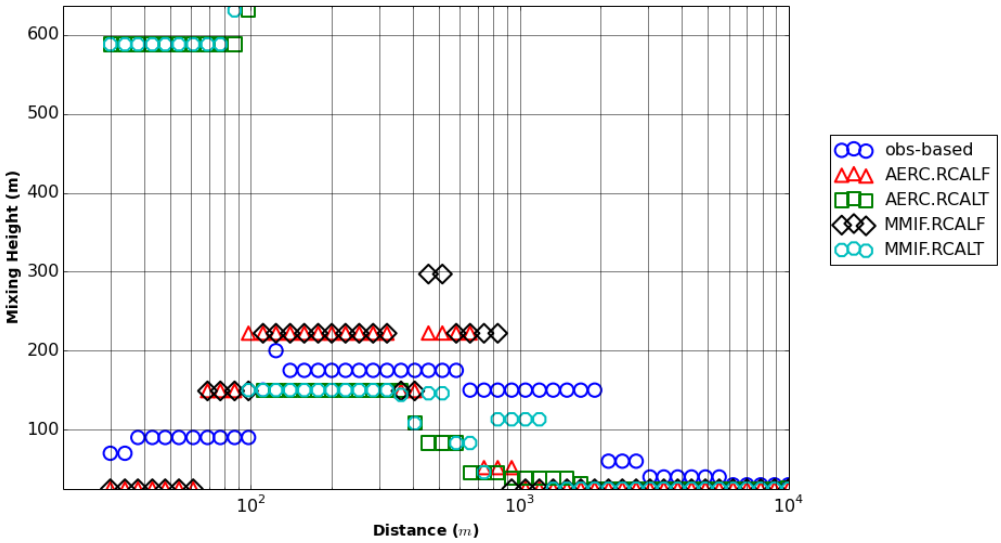

Figure 89. PBL height corresponding to concentration maxima, Site B2, 2011, Source Group #2, 1-hr avg.

6.2 3-hour Averages

6.2.1 Robust high concentration

The RHC results for all 3-hour average simulations are plotted in Figure 90 - Figure 93 for the four WRF extraction methods, respectively. All of the RHC results were within a factor of two of the observation-based RHC results. Again, the downwash simulations (Source Group #5) resulted in the highest normalized concentrations and best agreement with the observation-based simulations. The Source Groups #4 and #3 simulations at site B2 consistently underpredicted RHC values, similar to the 1-hour averages, but were still within a factor of two.

Overall the WRF meteorology rediagnosed PBL heights (MMIF.RCALT) provided the most accurate and conservative results, when compared to the observation driven AERMOD predictions. The AERC.RCALF simulations resulted in the least conservative results, based on the number of cases where WRF-based RHC was lower than observation-based RHC.

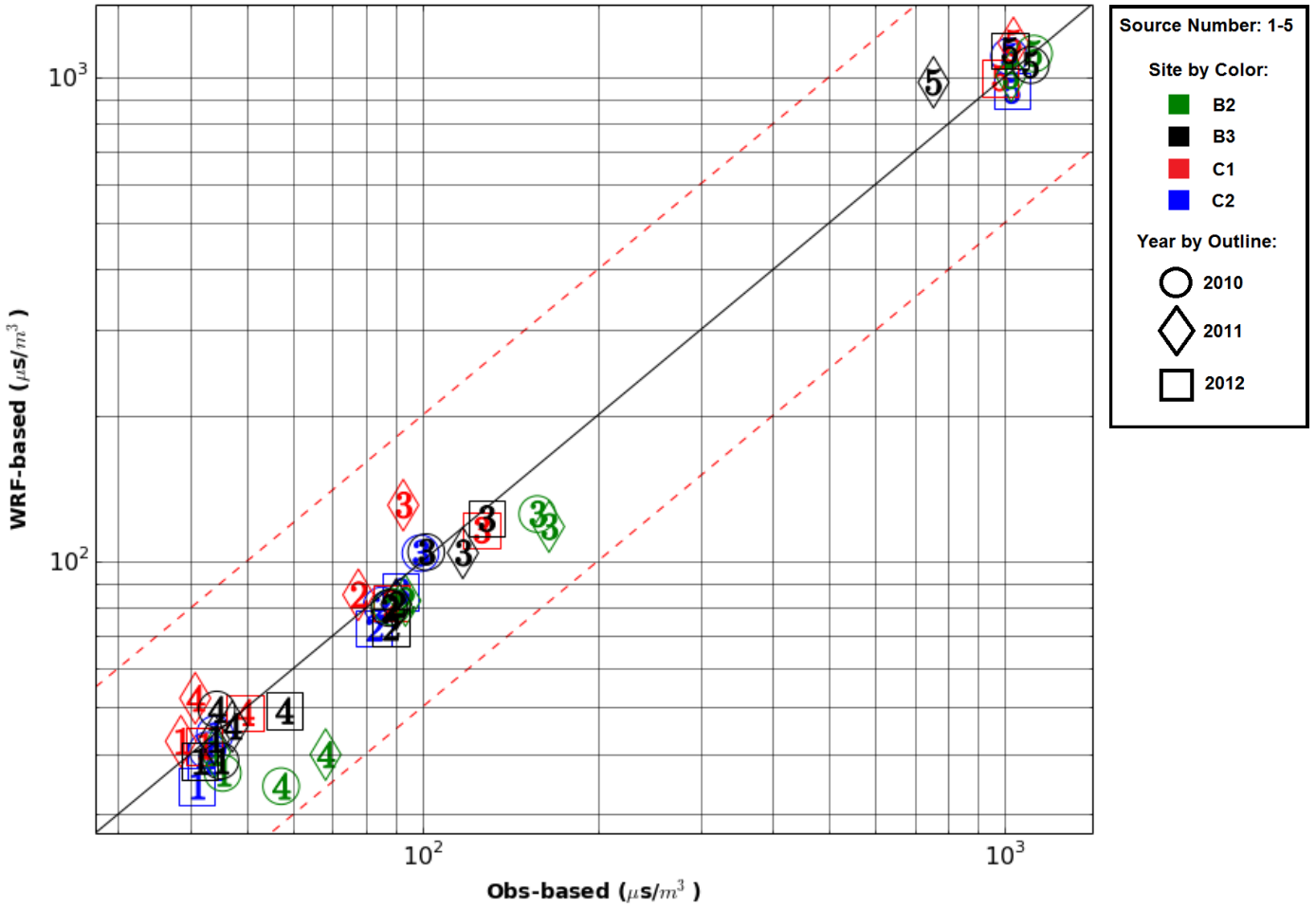

Figure 90. Robust high concentration results for MMIF.RCALF AERMOD 3-hour averaging times.

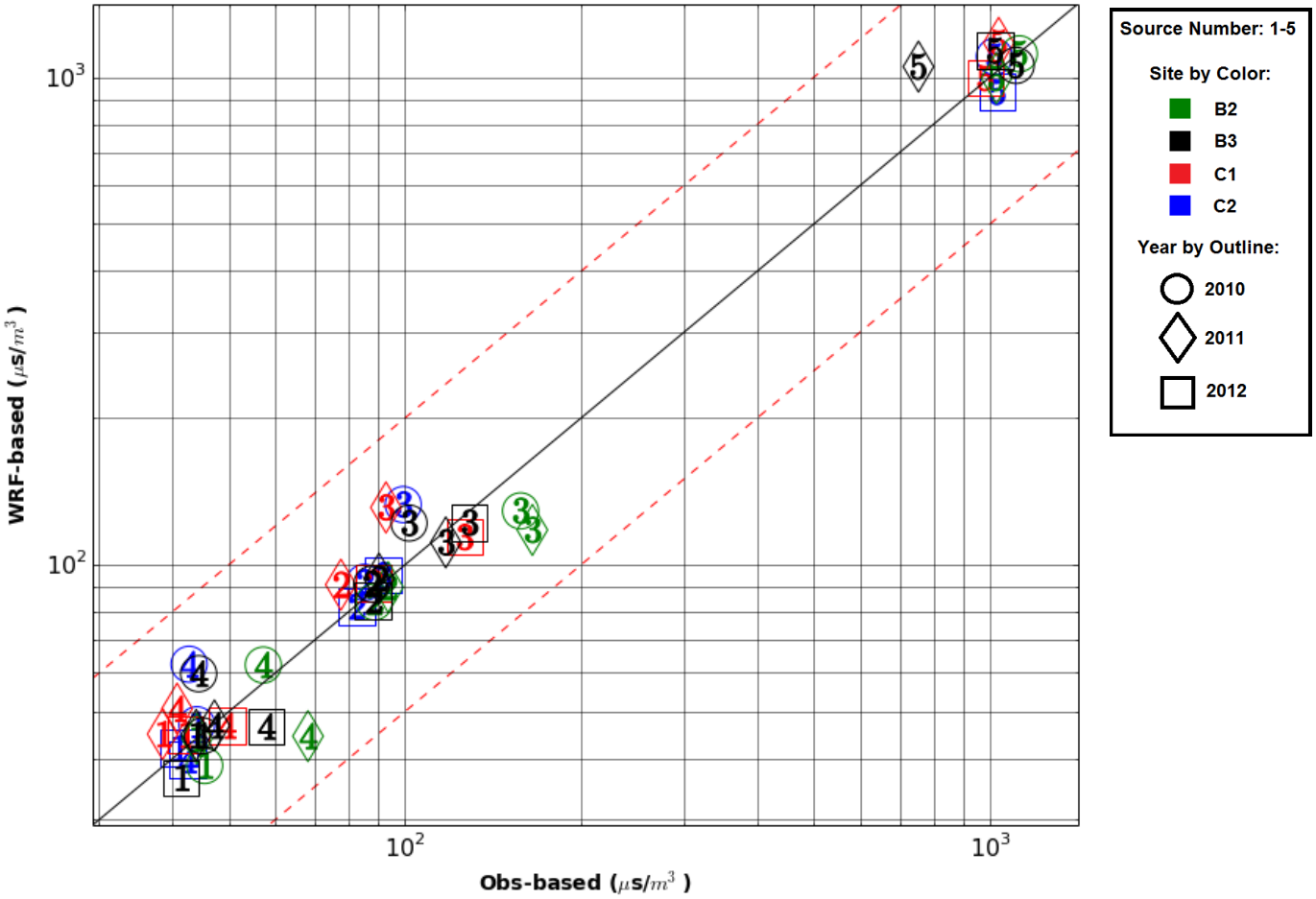

Figure 91. Robust high concentration results for MMIF.RCALT AERMOD 3-hour averaging times.

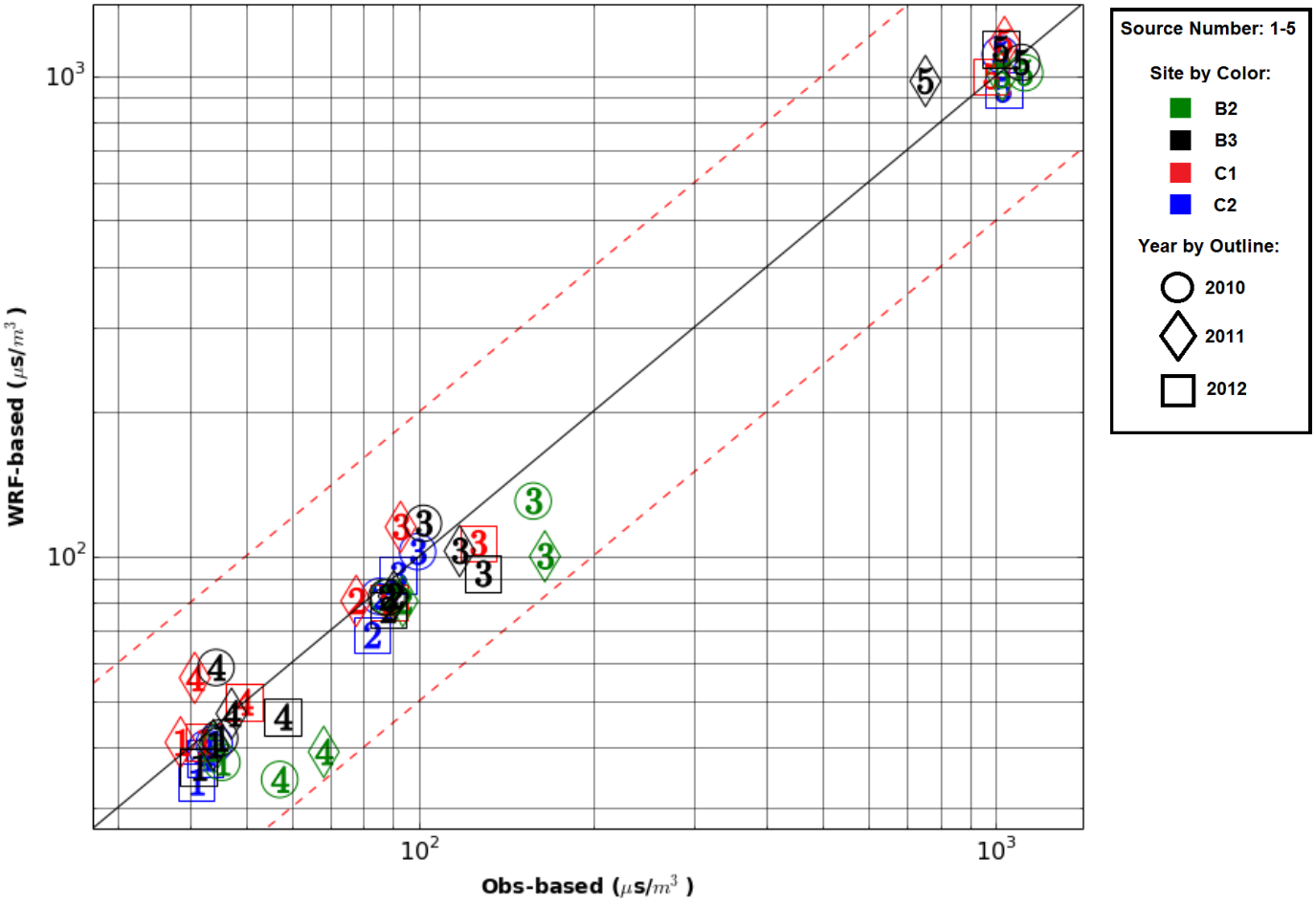

Figure 92. Robust high concentration results for AERC.RCALF AERMOD 3-hour averaging times.

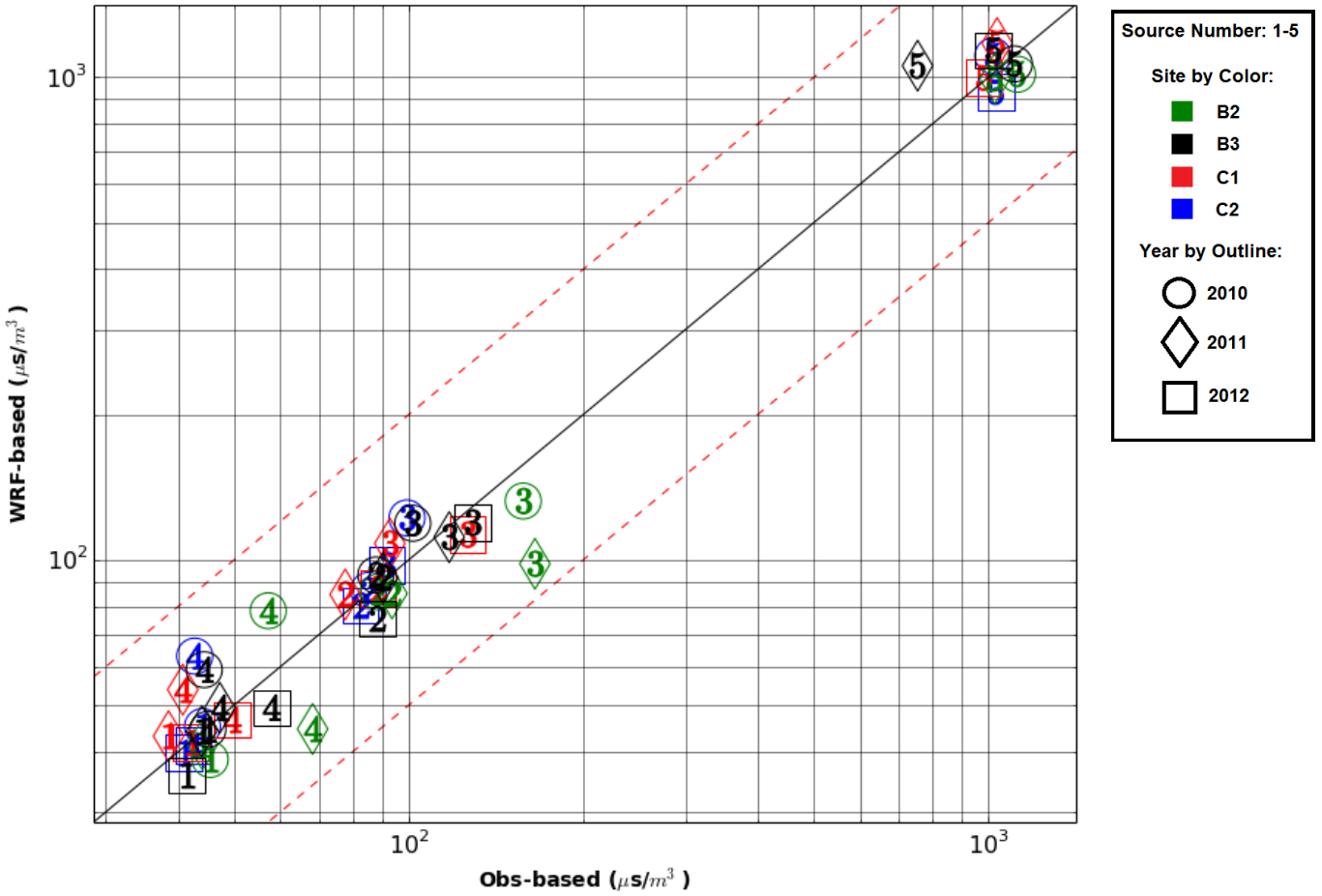

Figure 93. Robust high concentration results for AERC.RCALT AERMOD 3-hour averaging times.

6.2.2 Fraction-factor-of-two

The FF2 results for 3-hour averaging times are plotted in Figure 94 - Figure 97. Source Group #5 simulations had the highest average FF2 (0.99), and Source Group #4 simulations had the lowest average FF2 (0.76). The AERC simulations result in higher FF2 scores overall at site C1. The AERC site C1 and C2 FF2 scores were higher overall than the B2 and B3 AERC cases, but the Chukchi Sea FF2 scores were similar to the Beaufort Sea FF2 scores for the MMIF cases.

6.2.3 Discussion

The 2011 B2 Source Group #4 FF2 scores were consistently low and 2010 B2 Source Group #4 RHC scores consistently varied the most from the observation-based RHCs. Source Group #4 tall stacks were a poorer performer for the short term average simulations, particularly at site B2. These cases were selected for a deeper investigation.

A plot of the maximum concentrations with distance for the 2010 B2 Source Group #4 simulations is shown in Figure 98. The near-source concentrations from the WRF simulations were much lower than the observation-based simulations. After about 300 m, the WRF-based AERMOD concentrations matched the observation-based concentrations more closely. The wide differences in the near-source are the cause of the comparatively low FF2 scores for the 2010 B2 Source Group #4 simulations. The plot of PBL heights relating to the concentrations plotted in Figure 98 are shown in Figure 99. From 0 to 80 m distance, the WRF maximum concentrations occur during highly stable periods (PBL heights of 25 m for both RCALT and RCALF cases) while the observation-based near-source maximums occurred during unstable periods (PBL heights of 250 m).

A single event on August 31 near sunset resulted in the unstable conditions that lead to the higher observation-based concentrations. The observed ASTD was about -1.7ºC while WRF ASTD was about +0.3ºC. The observed ASTD supported unstable atmospheric conditions that lead to the higher PBL heights observed. The erroneous WRF ASTD supported stable conditions. The observation-based meteorology during this period resulted in L values of -5.0 m and light northerly winds about 1 m/s. The WRF meteorology included L values about + 70 m and northerly winds about 3.5 m/s. This type of event, where the measurements result in a negative ASTD while WRF supports a positive ASTD, occurred frequently in August of 2010 at site B2, as seen in Figure 47.

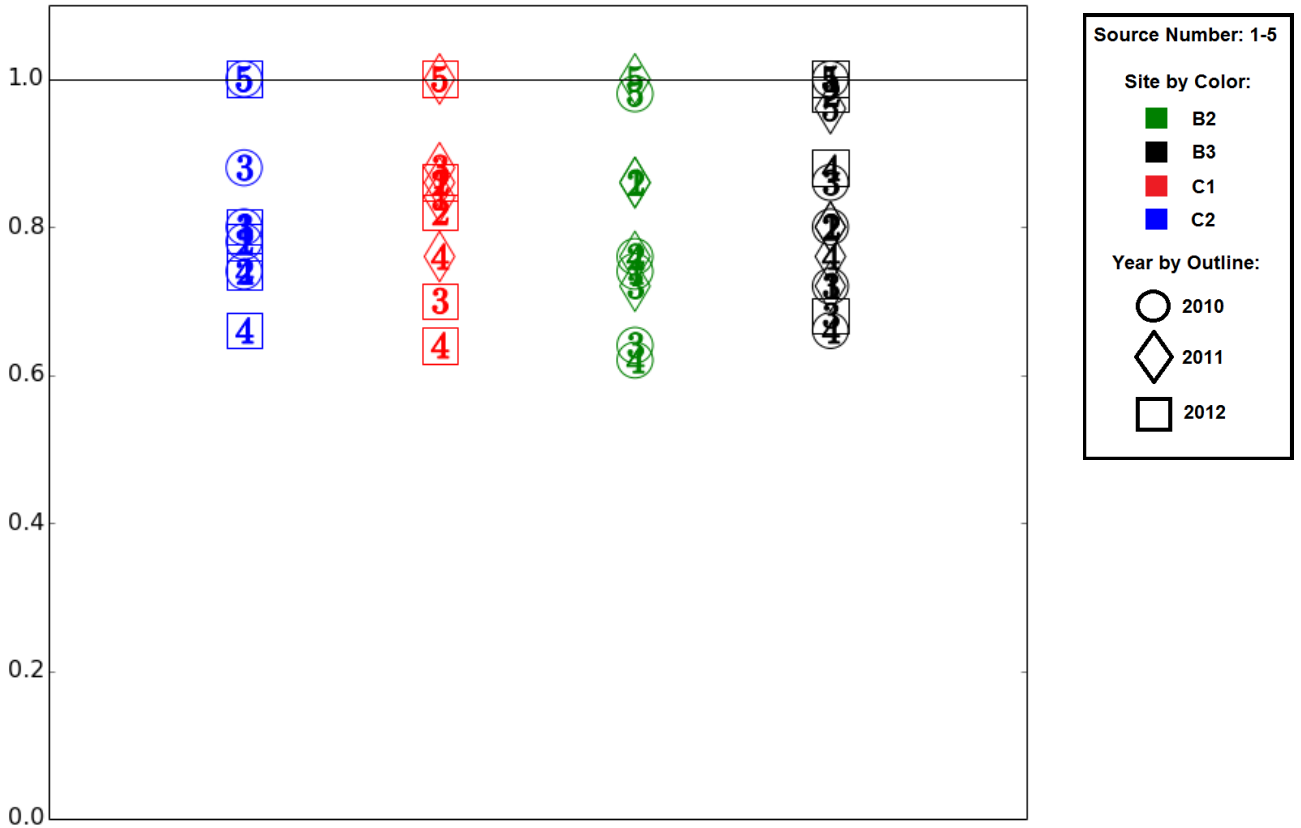

Figure 94. Fraction-factor-of-two MMIF.RCALF AERMOD results for 3-hour averaging times.

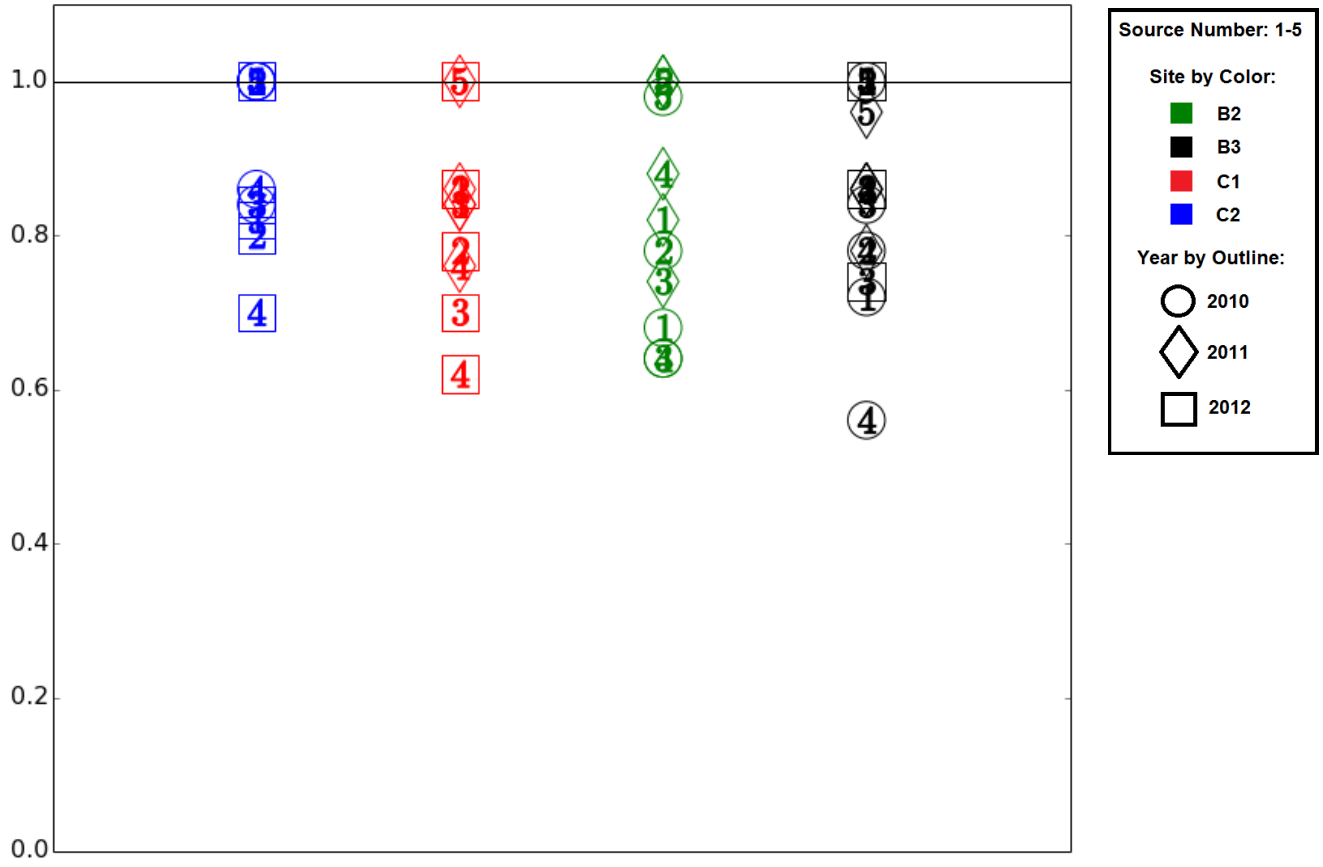

Figure 95 Fraction-factor-of-two MMIF.RCALT AERMOD results for 3-hour averaging times.

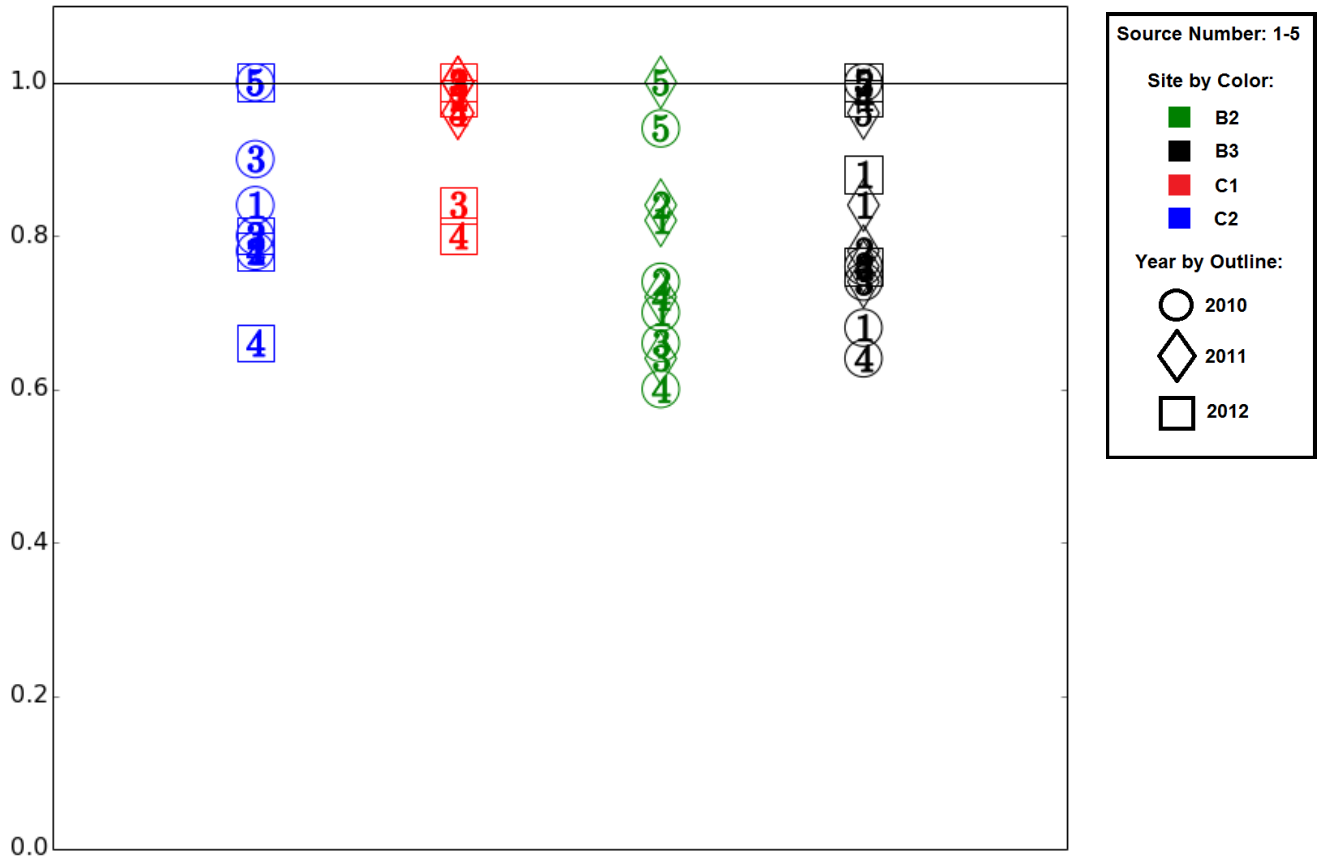

Figure 96. Fraction-factor-of-two AERC.RCALF AERMOD results for 3-hour averaging times.

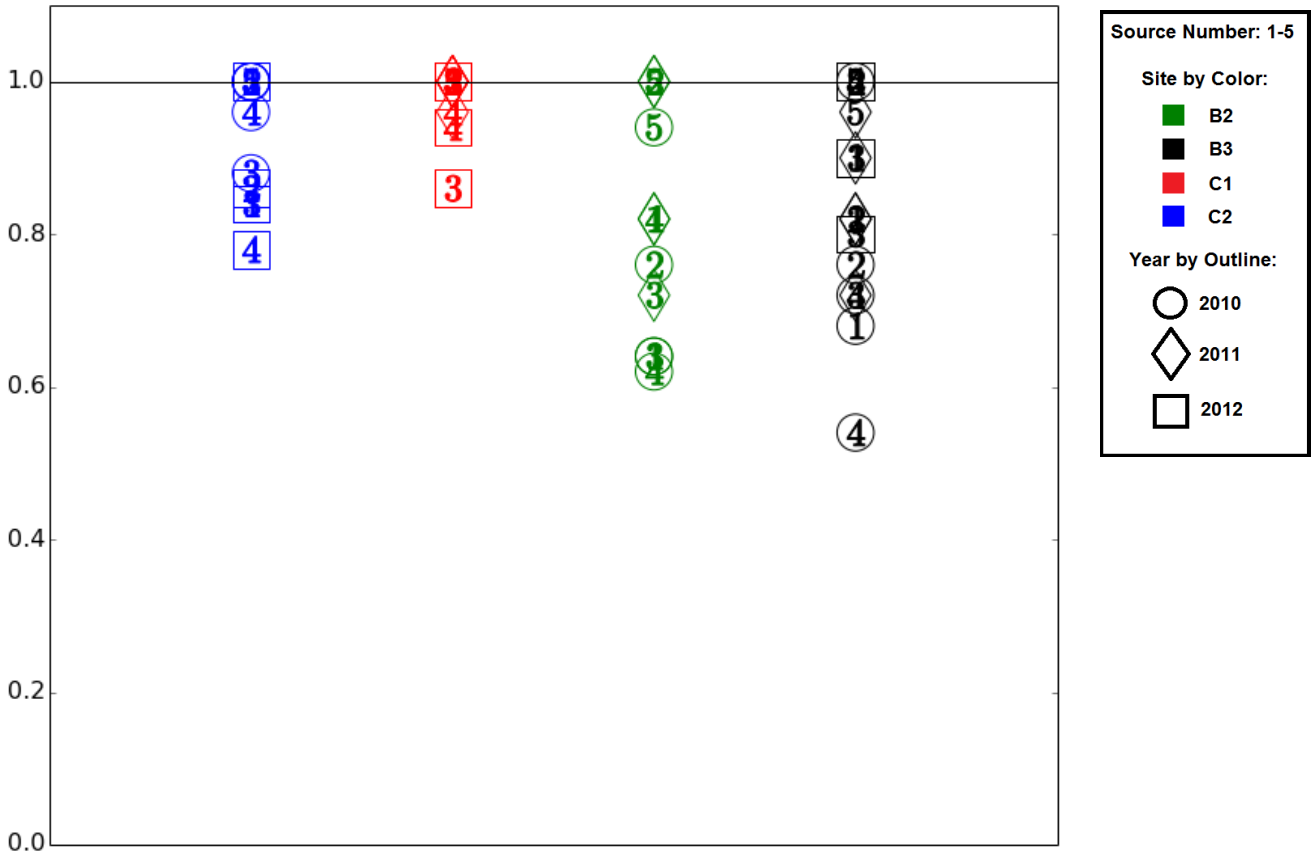

Figure 97. Fraction-factor-of-two AERC.RCALT AERMOD results for 3-hour averaging times.

Periods of unstable conditions occur in the WRF dataset also and it was expected that these periods would result in maximum near-source concentrations. A period of comparable meteorology was identified in the WRF RCALT meteorology on Sept. 18, 2010 where L values were consistently – 5.0 m and winds were light, about 1 – 1.5 m/s, and from the north. Despite the strongly unstable conditions at the surface, the PBL heights were maintained at the minimum 25 m throughout the period. During this same period, the observations resulted in L values in the range of -10 to -20 m and PBL heights around 100 m. The L values of -5.0 indicate strongly unstable conditions, supported by the negative ASTD during this period. The low PBL heights seemed unphysical given the conditions.

Plots of WRF and profiler temperature gradients during this period at the Endeavor Island profiler site are shown in Figure 100. The plot shows that the region was dominated by a warm layer aloft. WRF surface temperatures were much cooler, resulting in a much stronger inversion near the surface. Despite the strongly unstable conditions right at the surface, the related forcing is unable to penetrate significantly into the strong inversion and the low PBL height is retained.

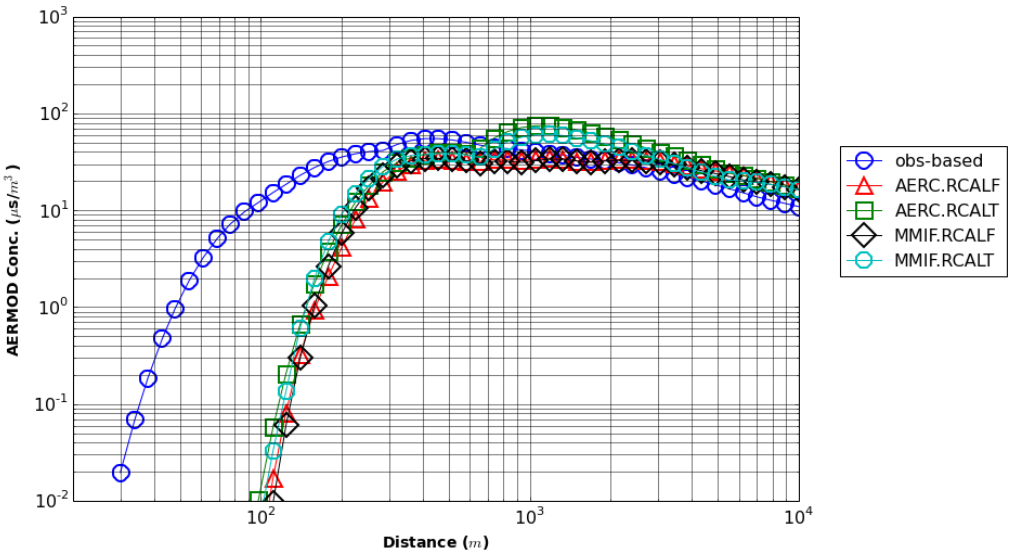

Figure 98. Concentration vs. distance, Site B2, 2010, Source Group #4, 3-hr. avg.

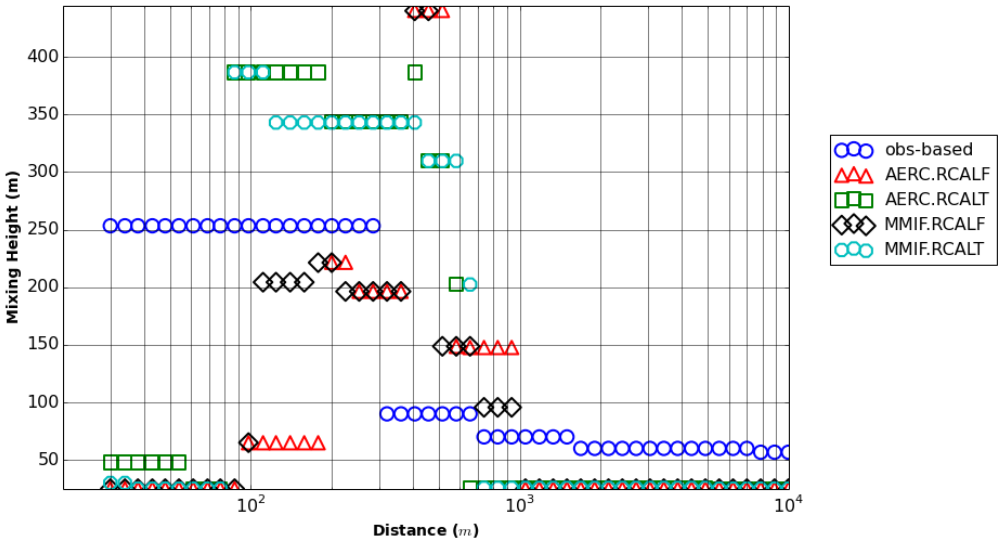

Figure 99. PBL height of concentration maxima vs. distance for Site B2, Source Group #4, 3-hr avg.

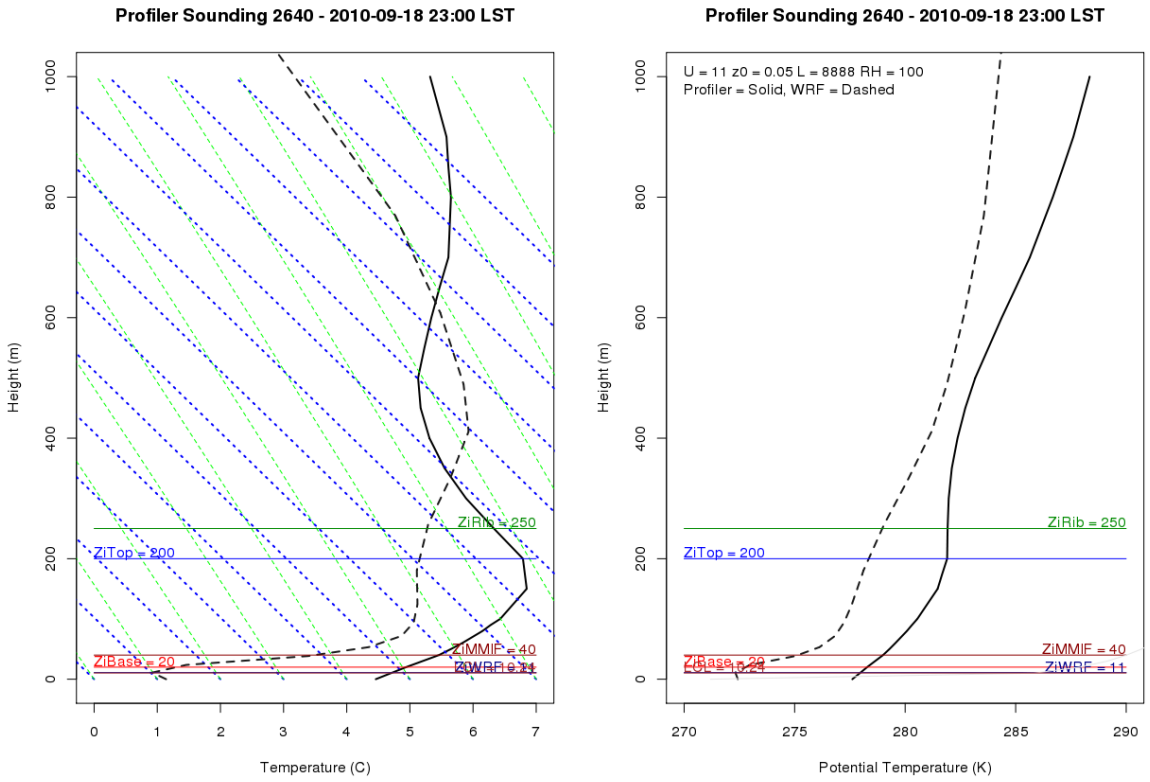

Figure 100. WRF and Profiler soundings (temperature vs. height) at Endeavor Island Sept. 18th, 2010. Temperature (left) and potential temperature (right) are plotted for both the profiler (solid line) and WRF solution (dashed line). PBL heights estimates by WRF (ZiWRF), WRF-MMIF recalculation (ZiMMIF), bulk Richardson method for the profiler data (ZiRib), and subjective "hand analyzed" PBL height as determined by a qualified meteorologist (ZiTop) are listed on the plot.

6.3 8-hour Averages

6.3.1 Robust high concentration

The RHC results for all of the 8-hour averaging time simulations are shown in Figure 101 - Figure 104 for the four WRF extraction methods, respectively. There was very little difference in scores between the simulations using different meteorological extraction methods. The most notable difference was a slight increase of RHC score with the recalculation of PBL height for all source groups except #5. RHC scores for the RCALT (both AERC and MMIF) simulations were slightly less accurate, but more conservative on average.

6.3.2 Fraction-factor-of-two

The 8-hour average FF2 scores from all simulations are plotted in Figure 105 - Figure 108. Many of the site B2 simulations perform poorly based on these scores, especially Source Group #3 2010 simulations. Despite the low FF2 scores at some of these sites, the magnitude of the maximum concentrations agree well, resulting in the good agreement between WRF and observation-based RHC scores. Further analysis of the site B2 Source Group #3 2010 case revealed WRF-based concentrations were overpredicted downwind of 1000 m and underpredicted upwind of 200 m, as shown in Figure 109. In the 200 – 1000 m range, where all the maximum concentrations occur, the concentrations agree well. This pattern was the result of WRF and WRF-MMIF predicting lower PBL heights, as shown in Figure 110. The low PBL heights lead to underpredicted near-source concentrations and overpredicted concentrations in the far-source. However, as seen in the near-source region, both observation-based and WRF-based maximum concentrations occurred during unstable periods based on L values shown in Figure 111. Again, as seen with the 1-hour and 3-hour results, WRF restricted the growth of the PBL due to a warm layer aloft. An implication of these results is that if RHC was evaluated for just the near-source or far-source the RHC results would be less favorable since WRF-based concentrations did not match the observation-based concentrations at these distances at this site.

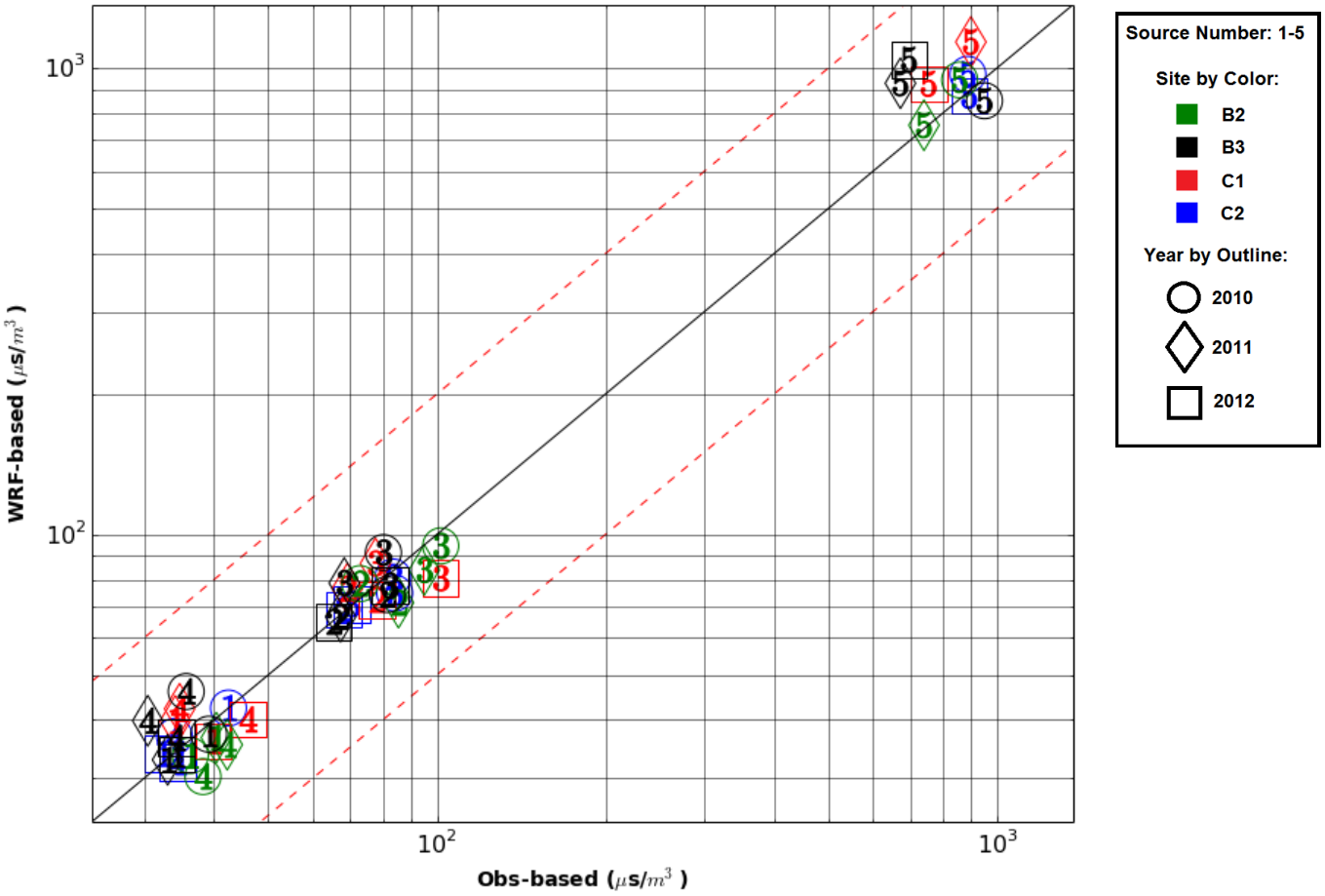

Figure 101. Robust high concentration results for MMIF.RCALF AERMOD 8-hour averaging times.

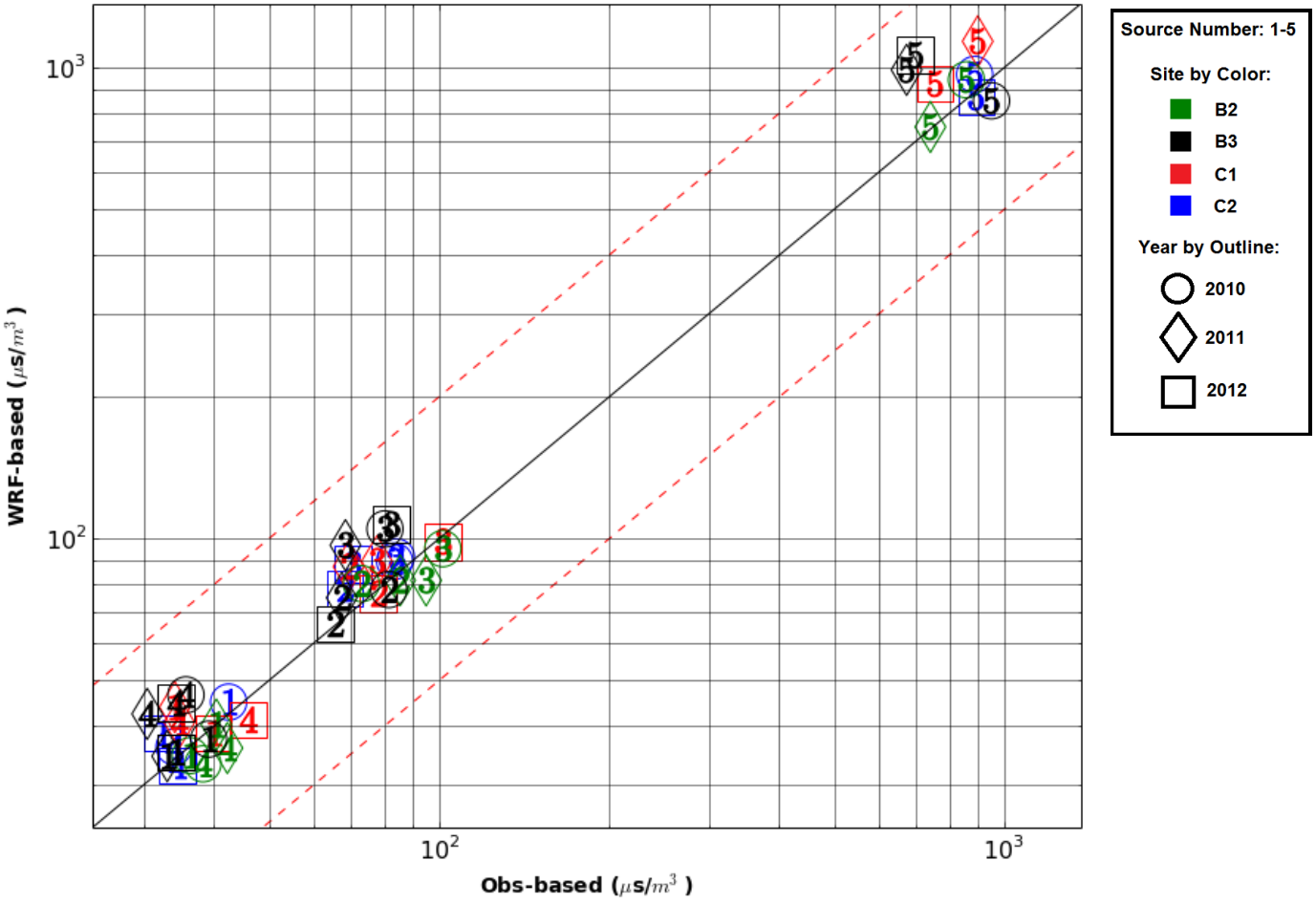

Figure 102. Robust high concentration results for MMIF.RCALT AERMOD 8-hour averaging times.

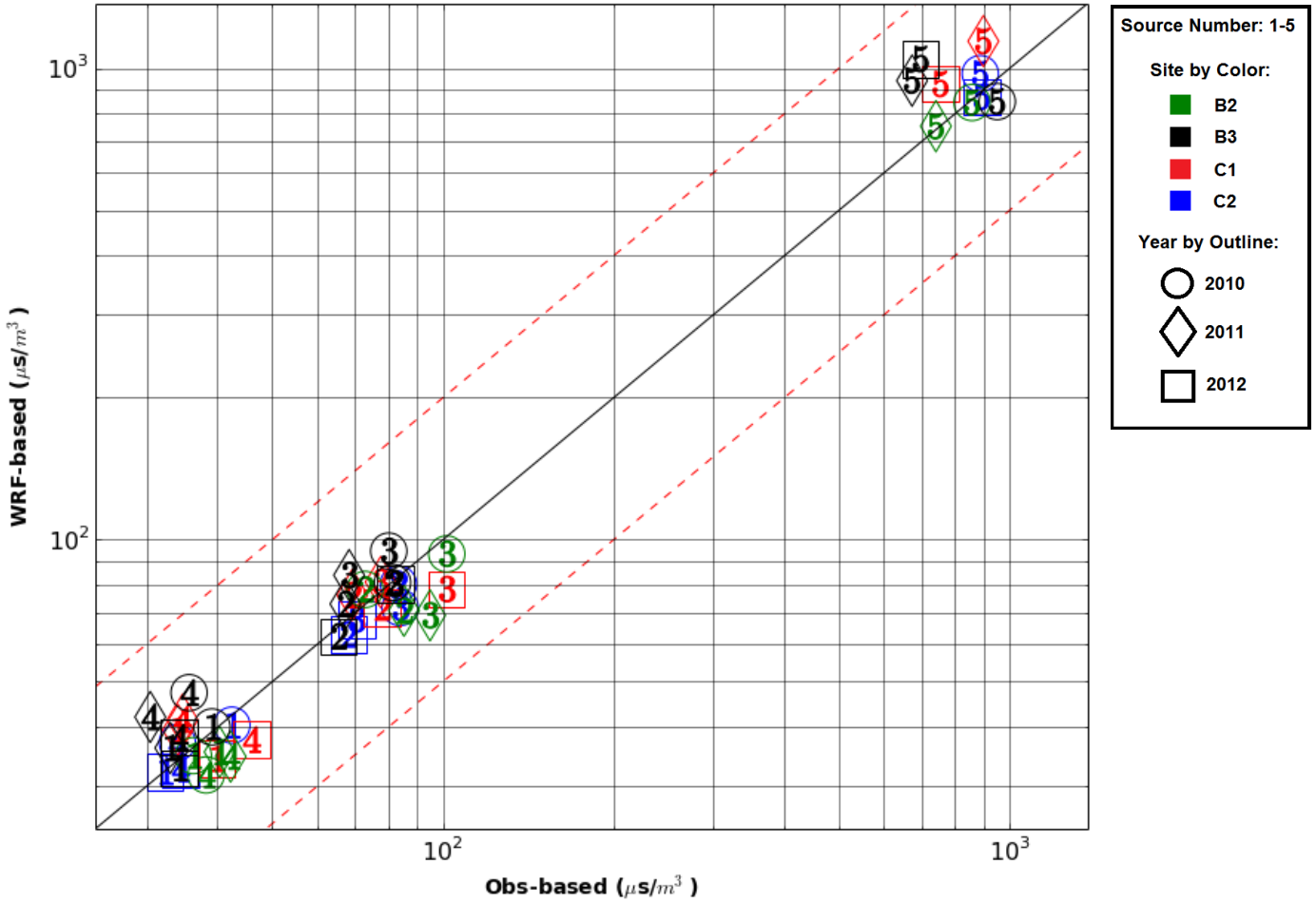

Figure 103. Robust high concentration results for AERC.RCALF AERMOD 8-hour averaging times.

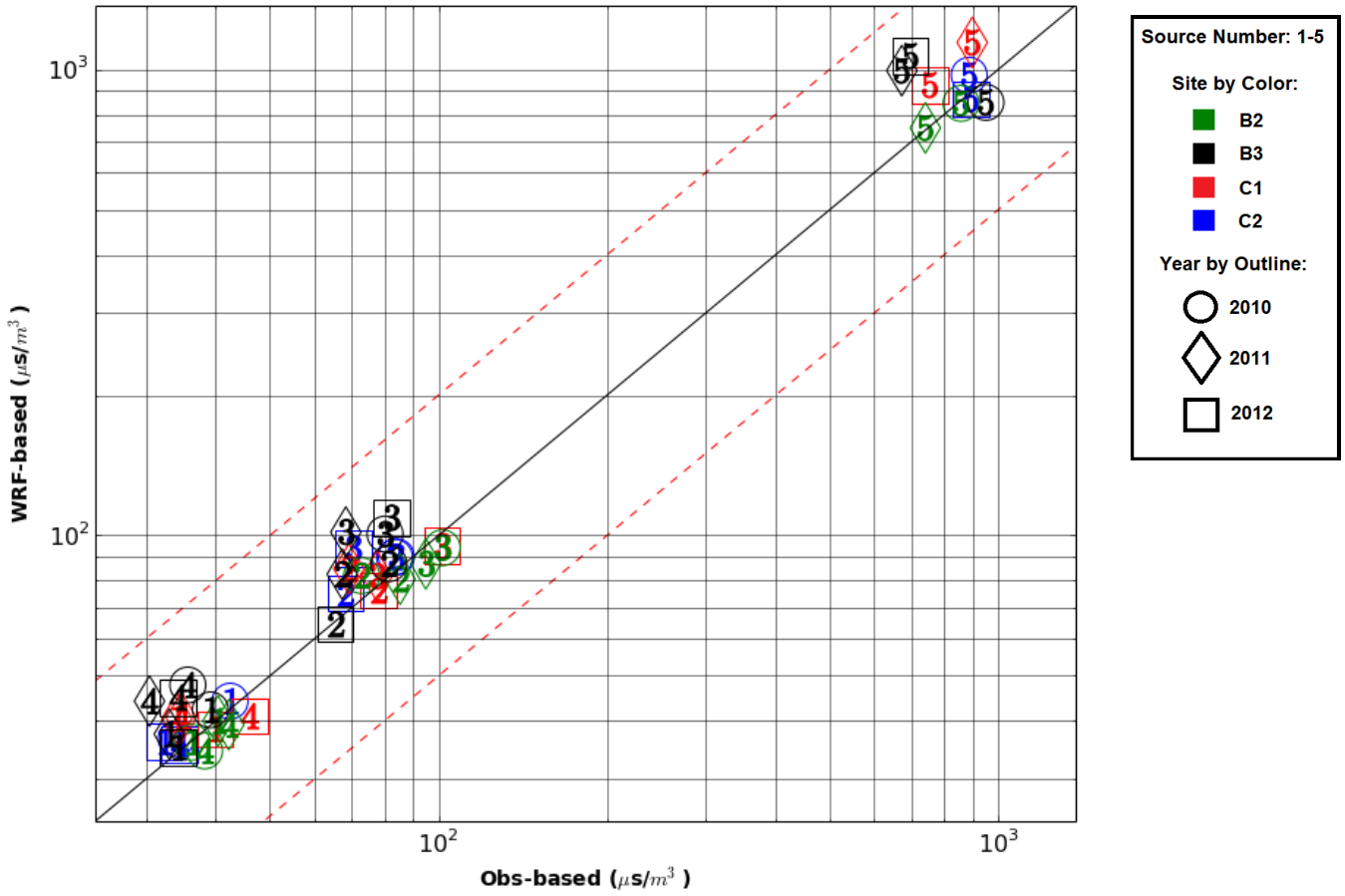

Figure 104. Robust high concentration results for AERC.RCALT AERMOD 8-hour averaging times.

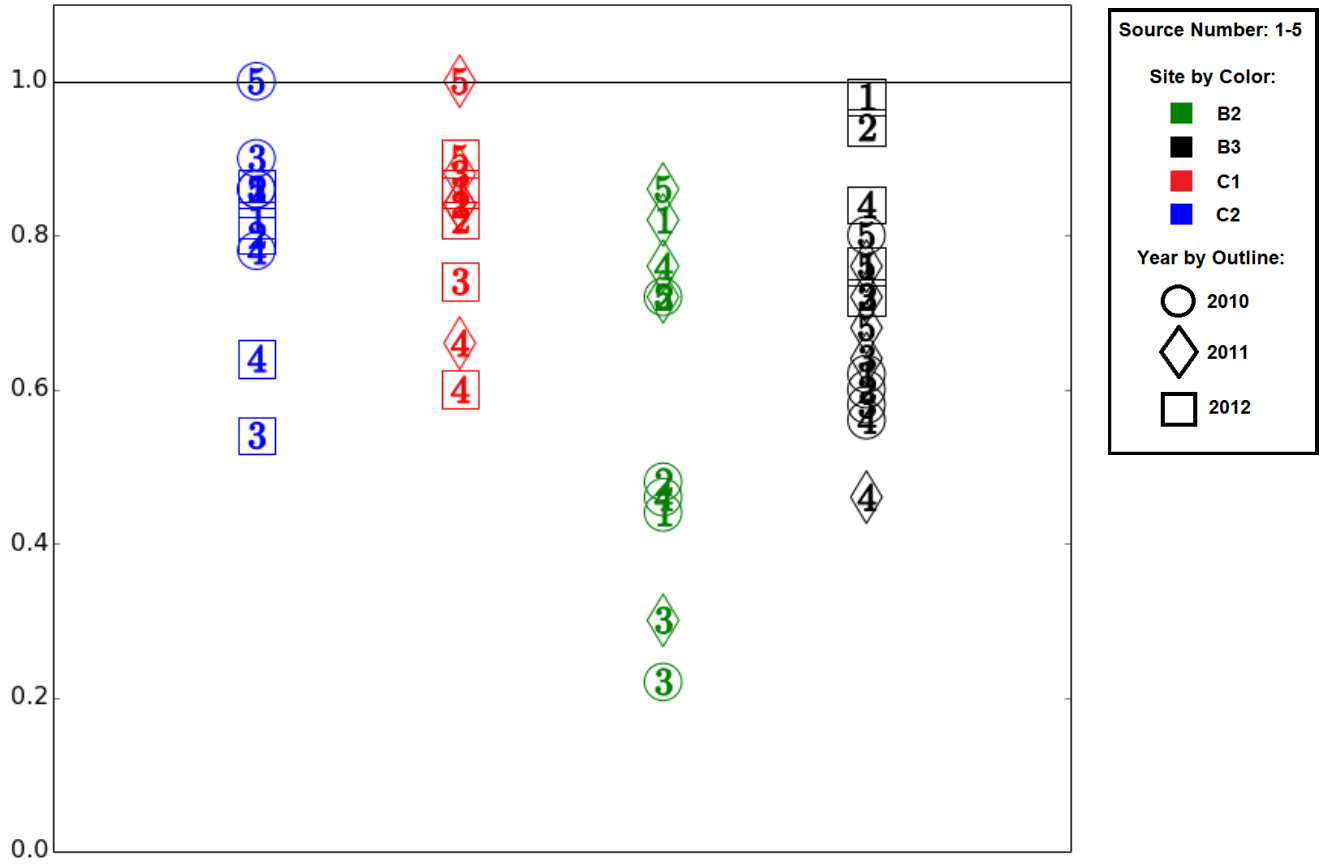

Figure 105. Fraction-factor-of-two MMIF.RCALF AERMOD results for 8-hour averaging times.

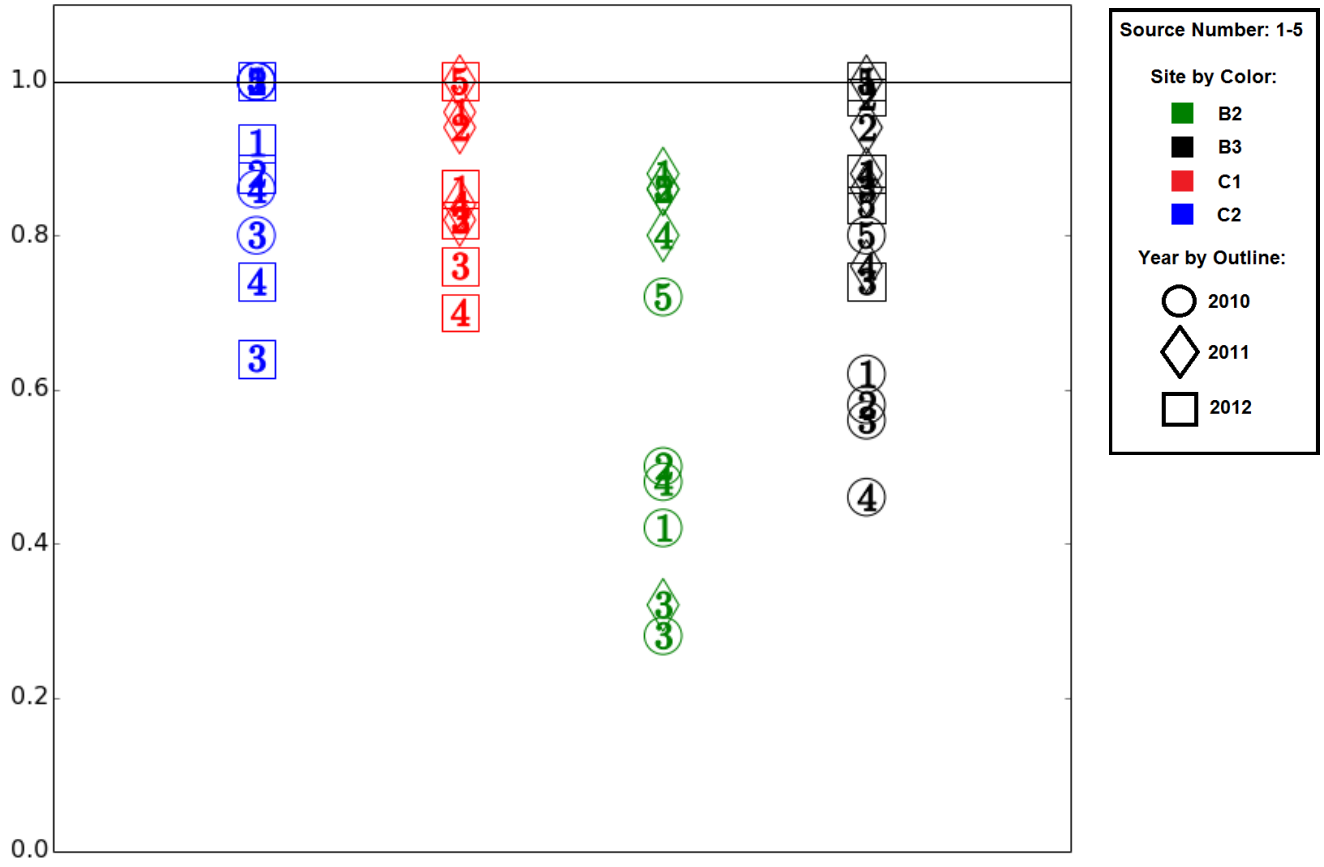

Figure 106. Fraction-factor-of-two MMIF.RCALT AERMOD results for 8-hour averaging times.

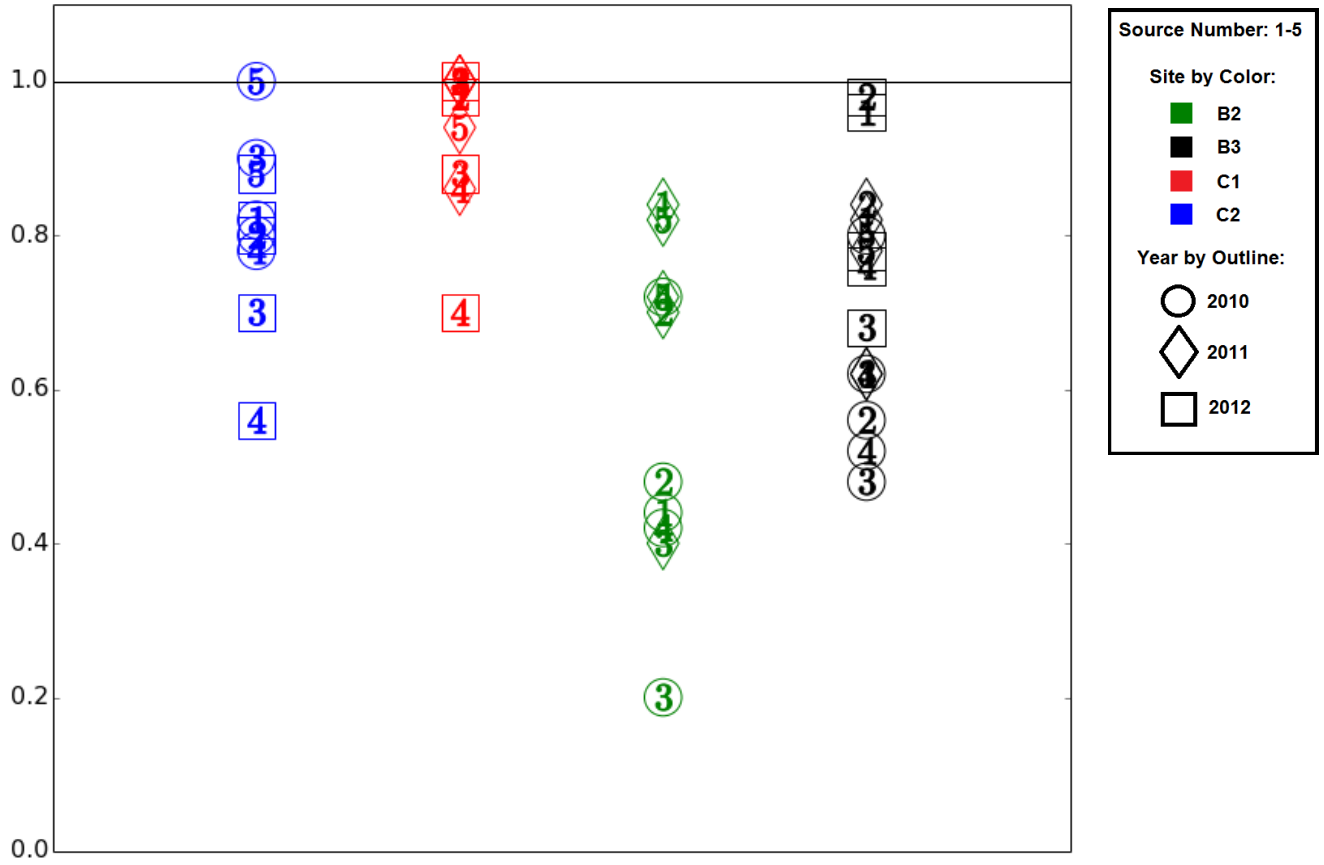

Figure 107. Fraction-factor-of-two AERC.RCALF AERMOD results for 8-hour averaging times.

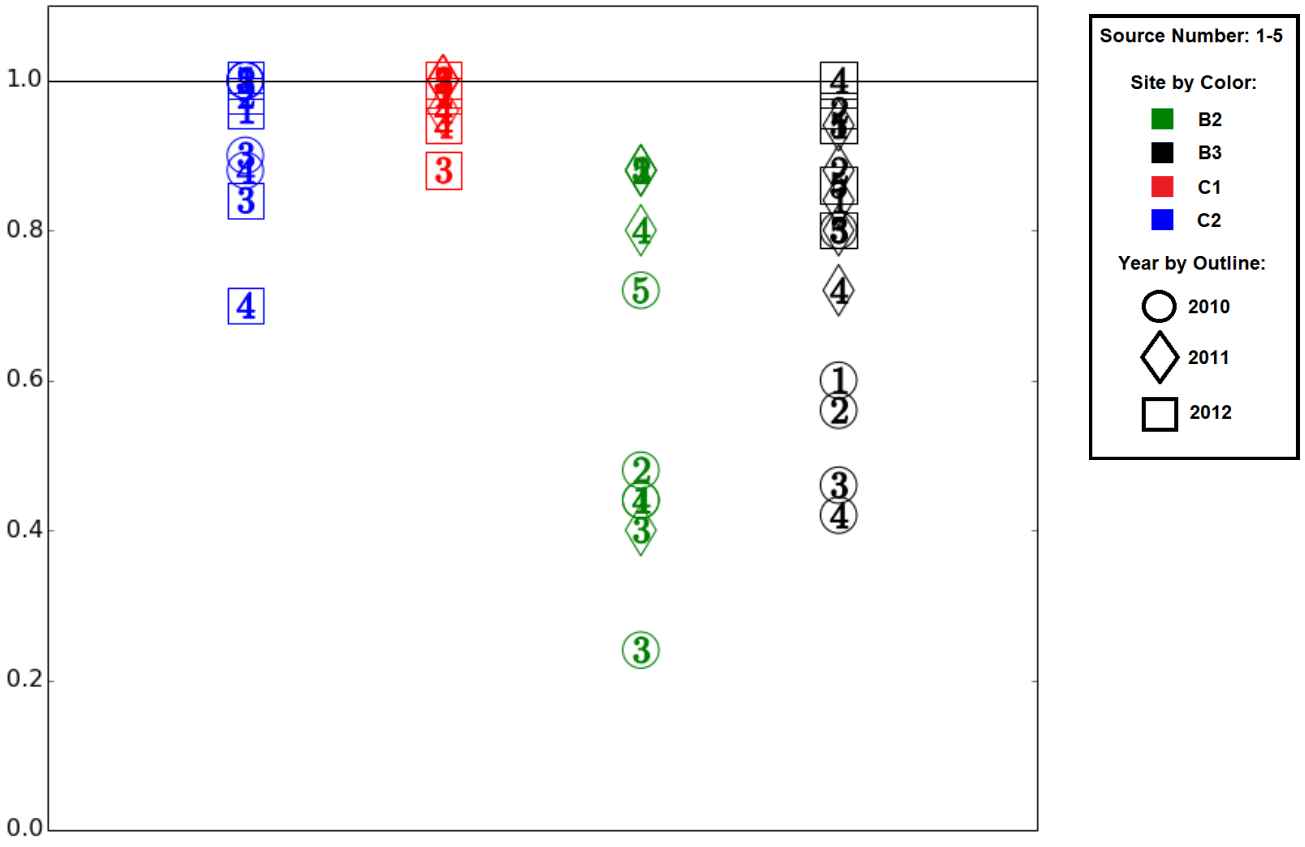

Figure 108. Fraction-factor-of-two AERC.RCALT AERMOD results for 8-hour averaging times.

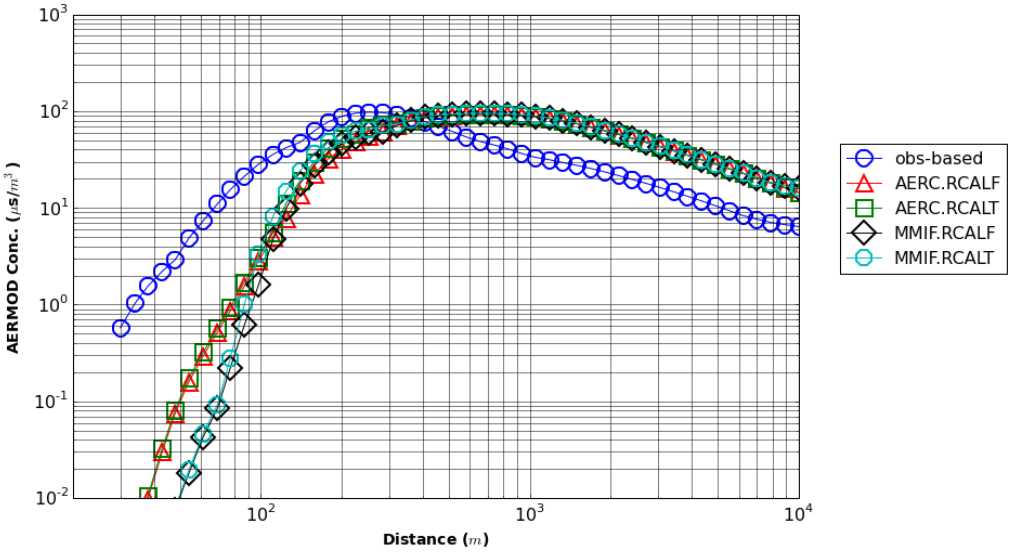

Figure 109. Concentration vs. distance, Site B2, 2010, Source Group #3, 8-hr. avg.

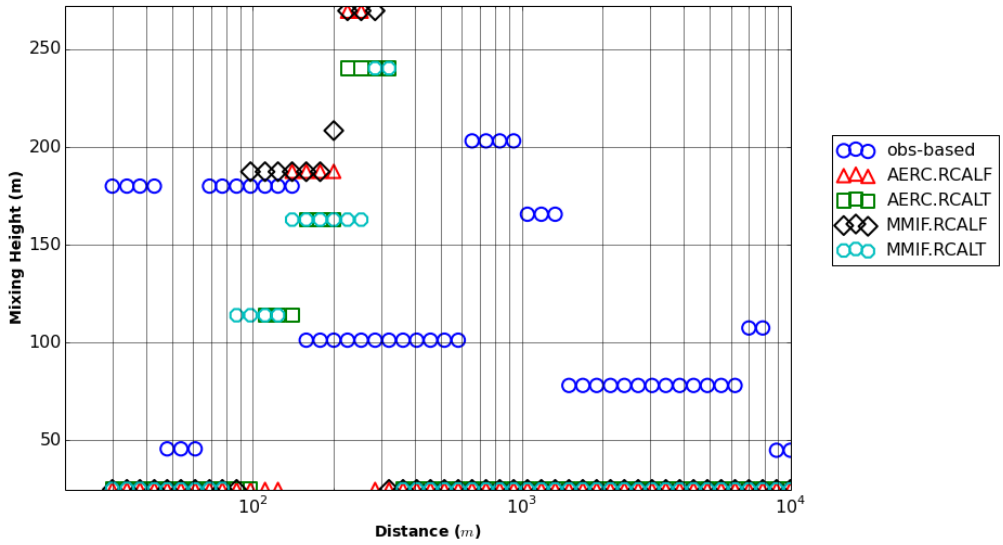

Figure 110. PBL height of concentration maxima vs. distance for Site B2, 2010, Source Group #3, 8-hr avg.

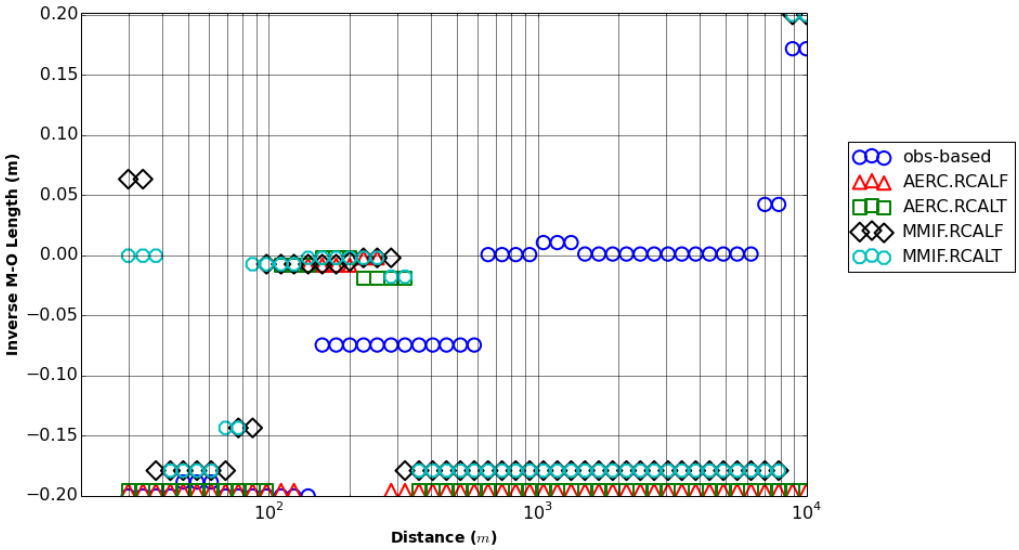

Figure 111. 1/*L* of the concentration maxima vs. distance for Site B2, 2010, Source Group #3, 8-hr avg.

6.4 24-hour Averages

6.4.1 Robust high concentration

The 24-hour average RHCs from all simulations are plotted in Figure 112 - Figure 115, with more variance in RHC scores, on average, than the simulations at shorter averaging times. All RHC scores were within the factor-of-two boundaries, suggesting WRF-based simulations provided a similar range of maximum concentrations as the observation-driven AERMOD simulations. There were no substantial differences in the average RHC values between the simulations using different WRF meteorology extraction methods.

Site C1 2011, Source Group #5 was selected for further investigation since the RHC scores from this case varied the most from the observation-based RHC scores. The Q-Q plot of concentration for this case is shown in Figure 116. The WRF-based runs overpredicted concentration throughout the entire distribution. All concentration maxima occurred in the near-source within 30 – 60 m of the source. As seen in Figure 117, both the observations and WRF exhibited strong negative ASTD for near-source maxima but the far-source observation-based maxima occurred during stable conditions (positive ASTD) while the WRF-based far-source maxima occurred during unstable conditions (negative ASTD). Despite this difference, observed and WRF PBL heights (shown in Figure 118) were low, from 25 – 100 m, characteristic of stable conditions. The low PBL height during strongly unstable conditions (as indicated by the value of *L)* is the same phenomenon identified at site B2 for the 1-hour and 3-hour cases examined.

Both the observation-based and WRF-based maximums occurred on the same day, Sept. 5th, 2011. The range of *L* and PBL height in the AERMOD surface meteorology files were similar for

both the observation-based and WRF-based runs. The sensible heat flux varied with a WRF-based value averaging about +45 W/m^2 and observation-based value averaging about 60 W/m^2. Also, the WRF wind speed average was lower at about 8 m/s compared to the observation-based 9 m/s. The additional heat flux and wind speed contributed to more mixing resulting in lower concentrations in the observation-based simulations. Despite the differences, the WRF-based maximum concentrations were within a factor of two of the observation-based concentrations.

6.4.2 Fraction-factor-of-two

The FF2 scores for the 24-hour averaging simulations are plotted in Figure 119 - Figure 122. Highest average FF2 values were achieved by the AERC.RCALT simulations. Site C1 simulations had notably better average FF2 scores using recalculated PBL height values. Site C2 simulations had notably better average FF2 scores using AERCOARE and recalculated PBL heights. This was most evident for Source Group #3 2012 simulations where FF2 jumped from 0.44 in the MMIF.RCALF simulation to 0.78 in the AERC.RCALT simulation. Concentration maxima for this case are plotted on Figure 123. All WRF-based simulations resulted in underpredicted concentrations from 30 – 150 m and overpredicted concentrations beyond 1000 m. The AERC.RCALT simulation resulted in less overprediction and underprediction in the near-source and far-source, respectively. Figure 124 shows the PBL heights corresponding to the concentration maxima. The MMIF rediagnosed PBL heights corresponded better with PBL heights used for the observation-based simulations in the near-source and far-source (note that MMIF PBL heights were used at sites C1 and C2, however). These results highlight the sensitivity of AERMOD results to PBL height.

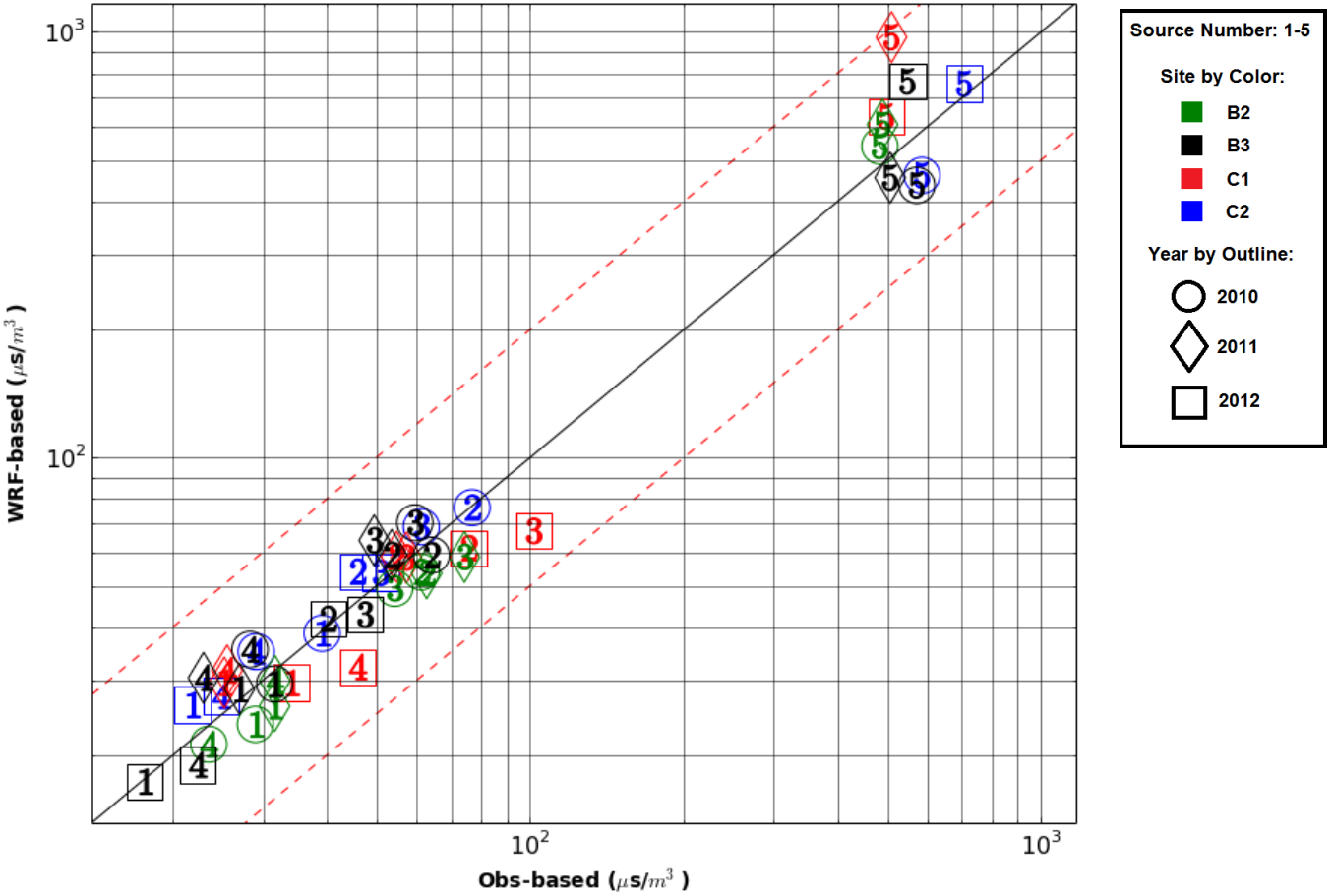

Figure 112. Robust high concentration results for MMIF.RCALF AERMOD 24-hour averaging times.

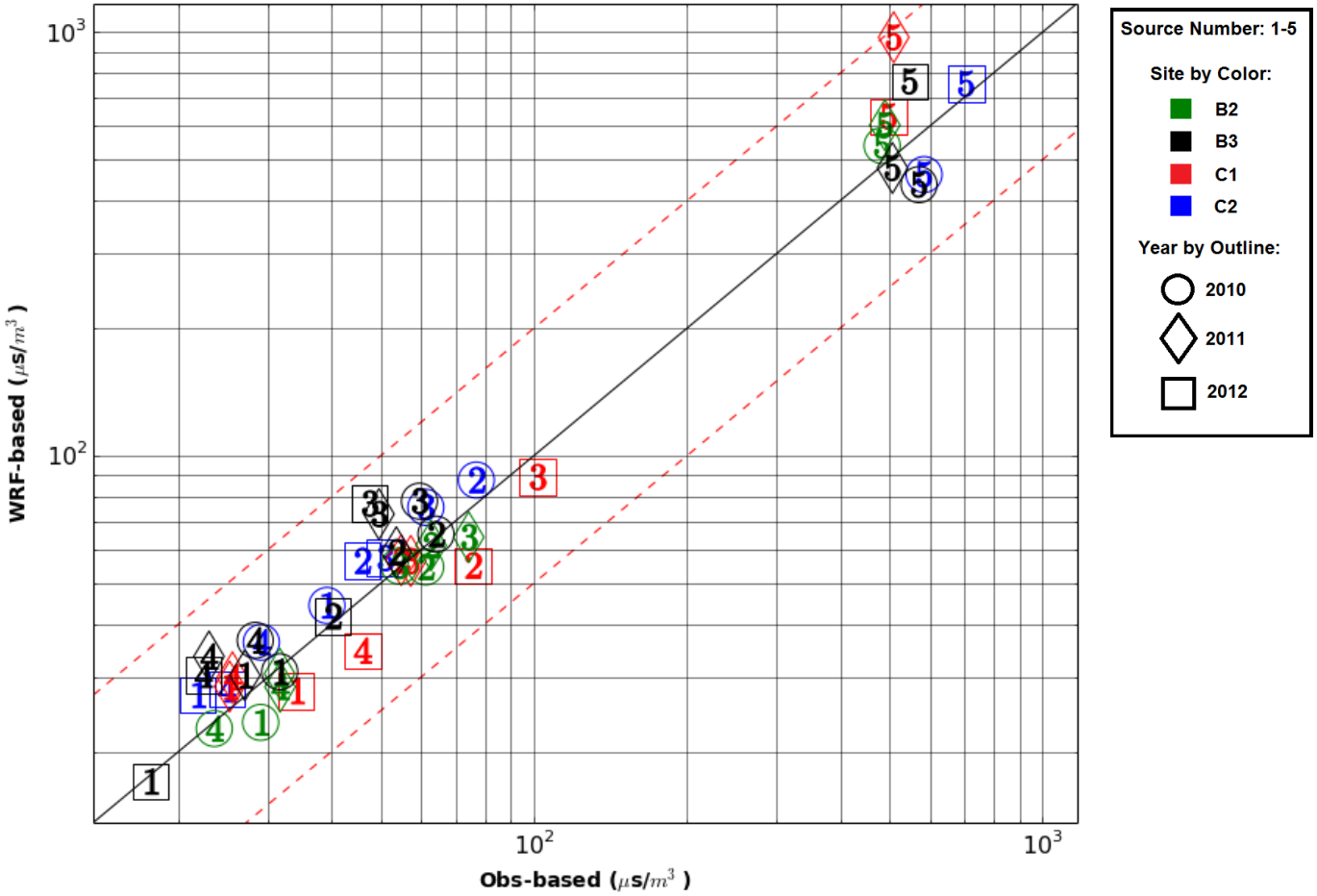

Figure 113. Robust high concentration results for MMIF.RCALT AERMOD 24-hour averaging times.

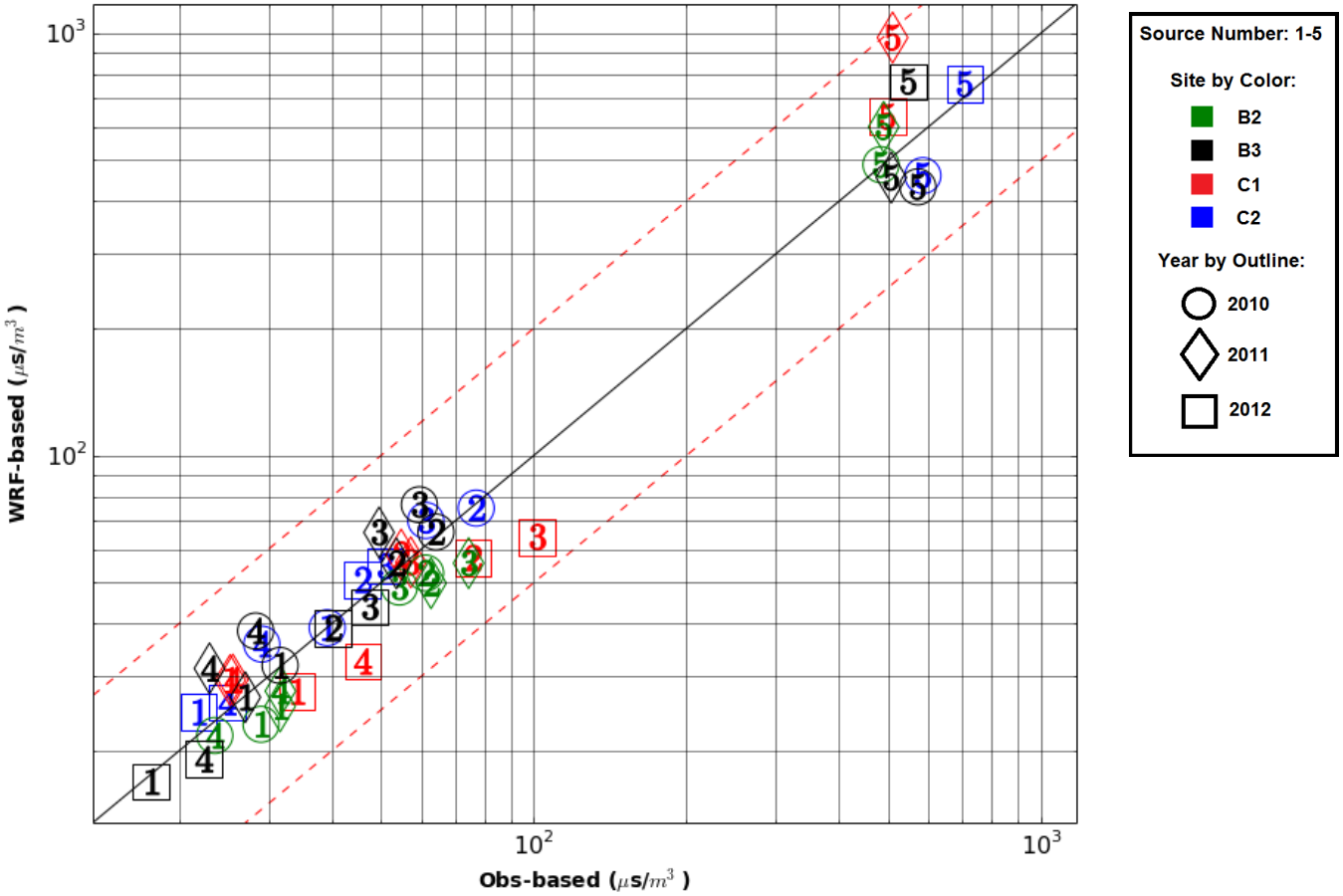

Figure 114. Robust high concentration results for AERC.RCALF AERMOD 24-hour averaging times.

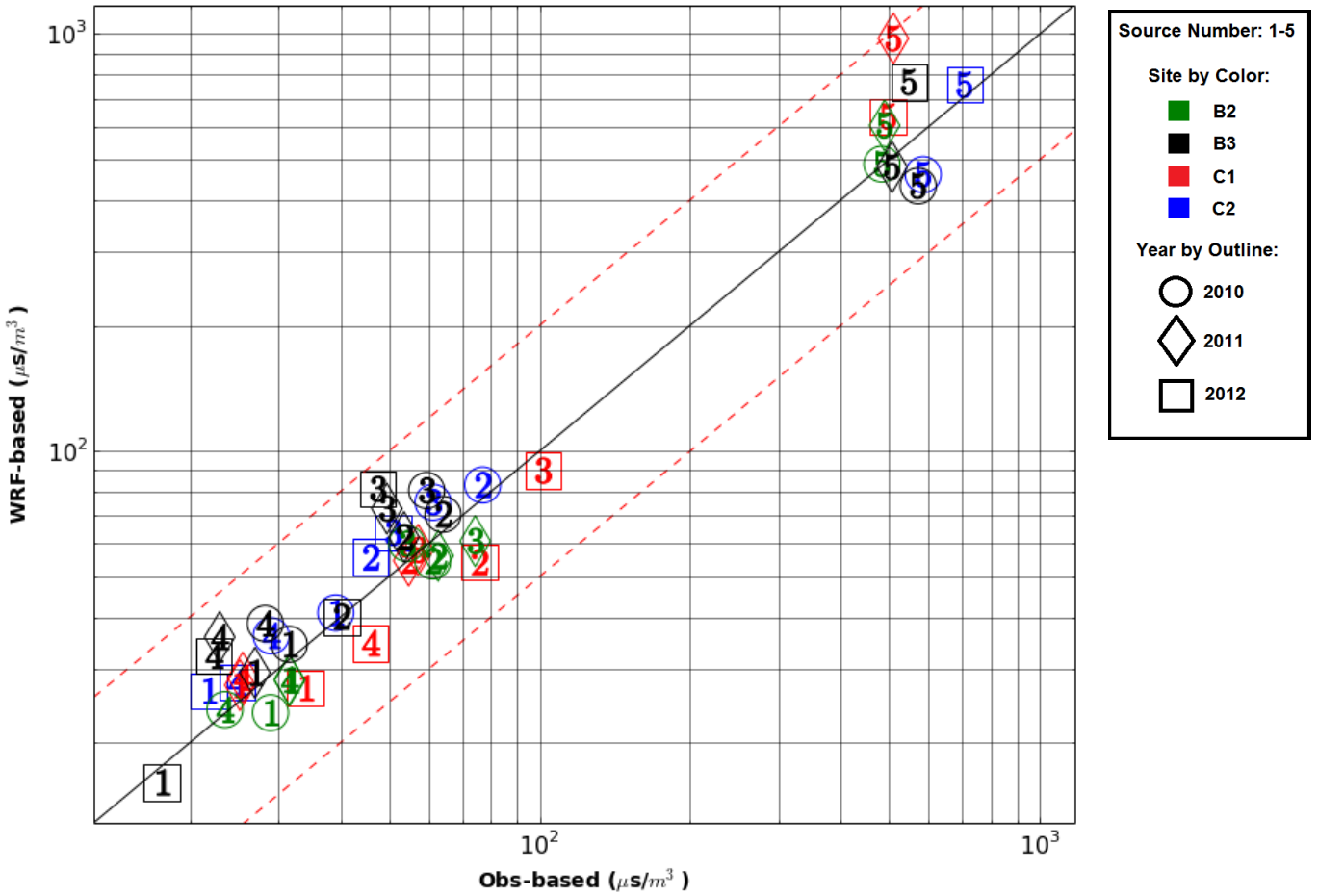

Figure 115. Robust high concentration results for AERC.RCALT AERMOD 24-hour averaging times.

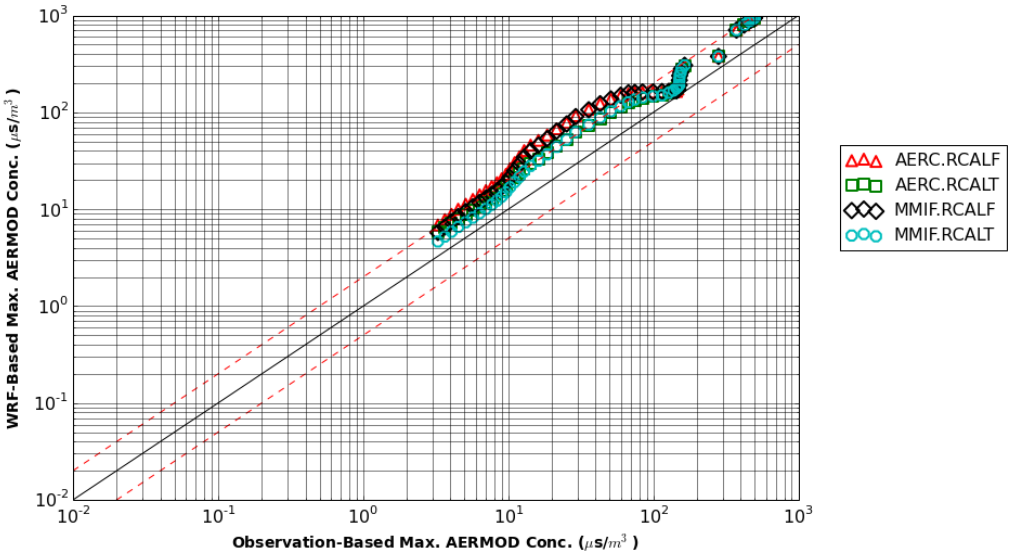

Figure 116. Q-Q plot for Site C1, 2011, Source Group #5, 24-hr avg.

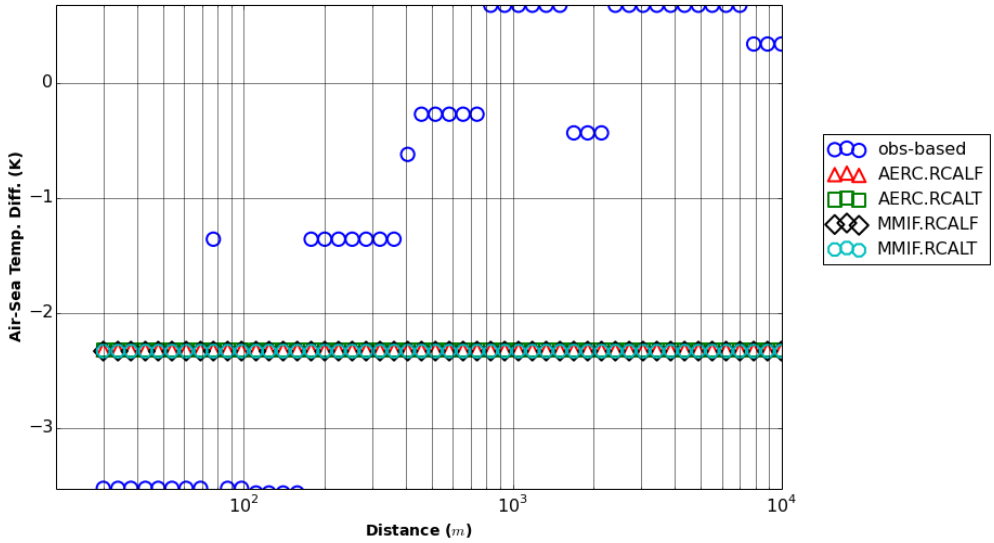

Figure 117. Air-sea temperature difference corresponding to concentration maxima, Site C1, 2011, Source Group #5, 24-hr avg.

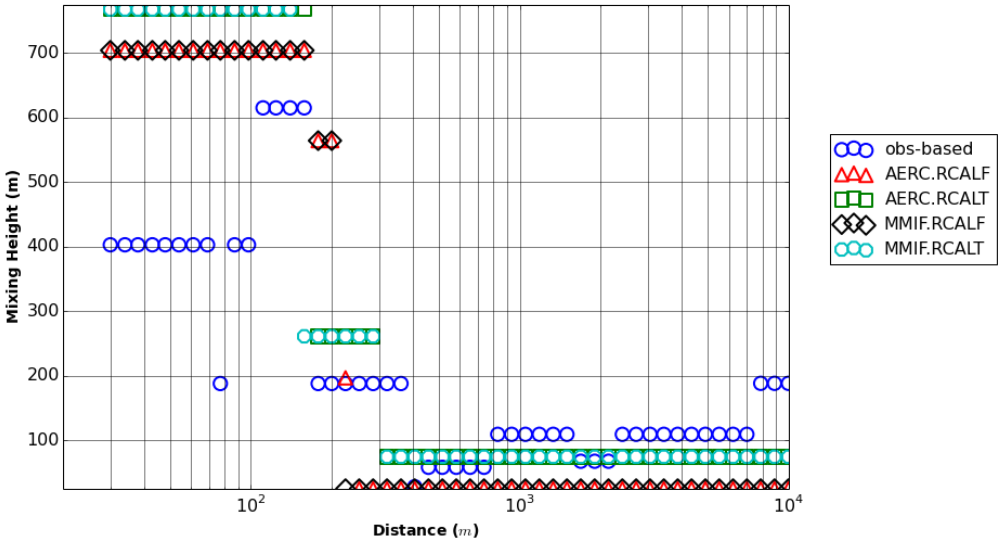

Figure 118. PBL height corresponding to concentration maxima for Site C2, 2012, Source Group #5, 24-hr avg.

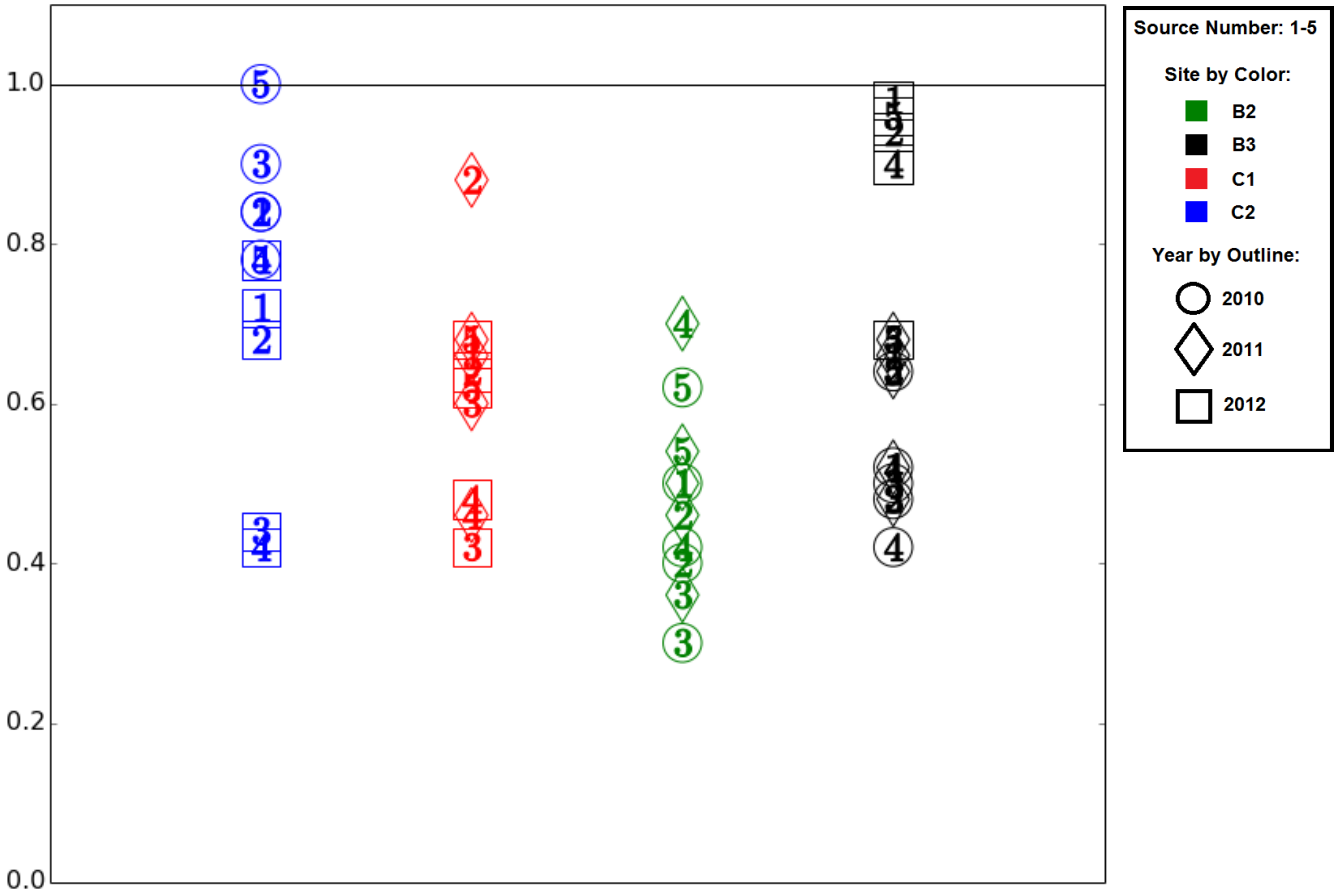

Figure 119. Fraction-factor-of-two MMIF.RCALF AERMOD results for 24-hour averaging times.

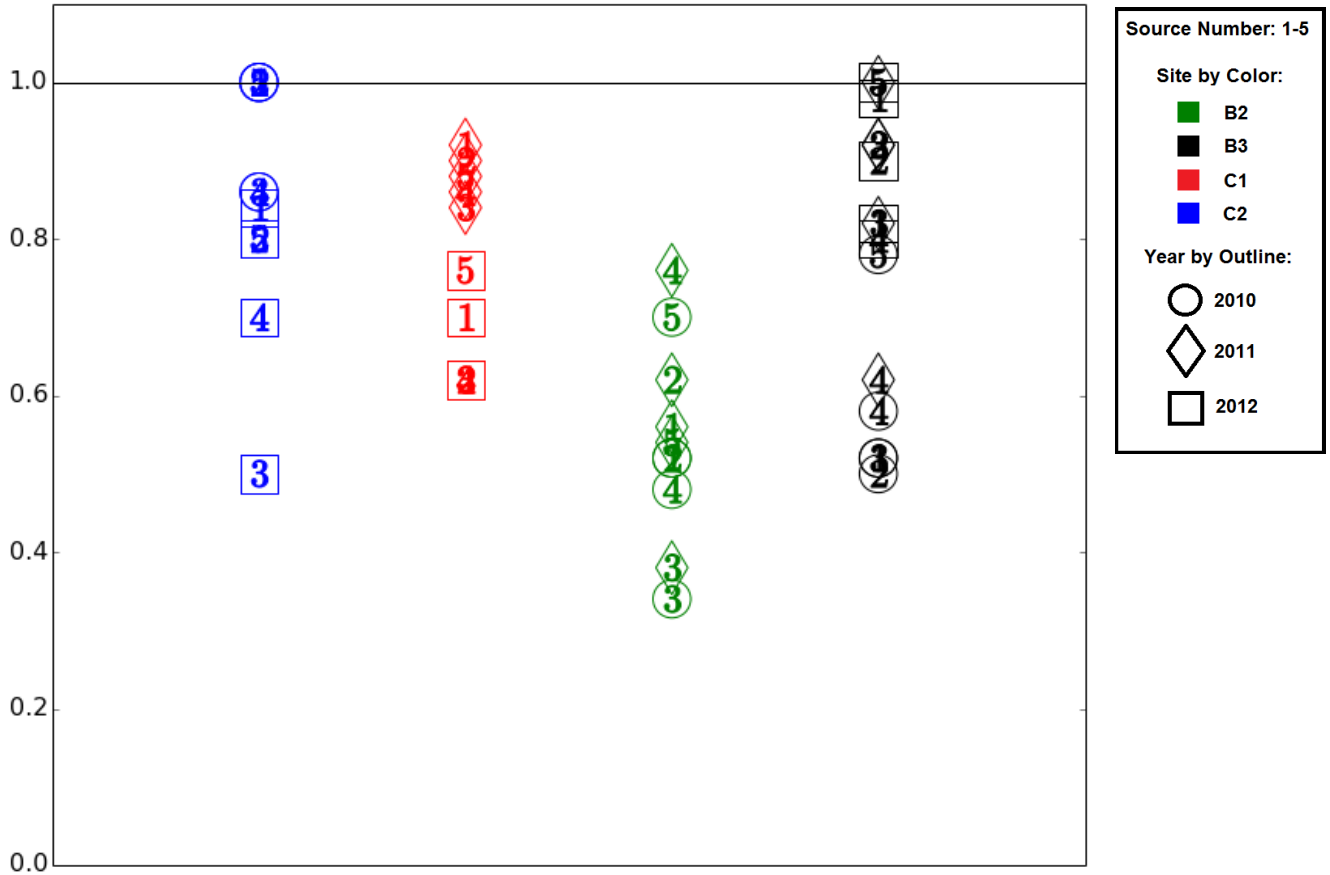

Figure 120. Fraction-factor-of-two MMIF.RCALT AERMOD results for 24-hour averaging times.

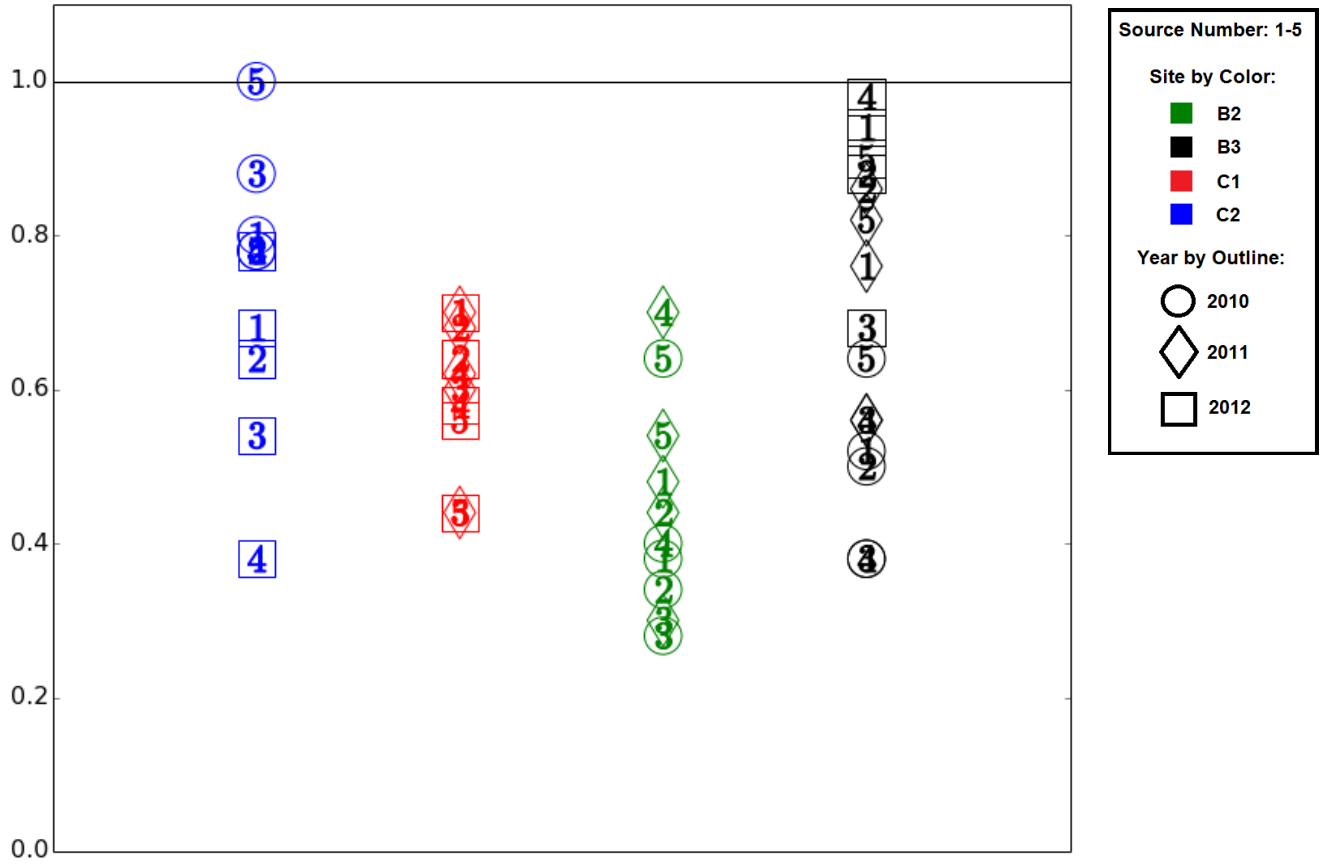

Figure 121. Fraction-factor-of-two AERC.RCALF AERMOD results for 24-hour averaging times.

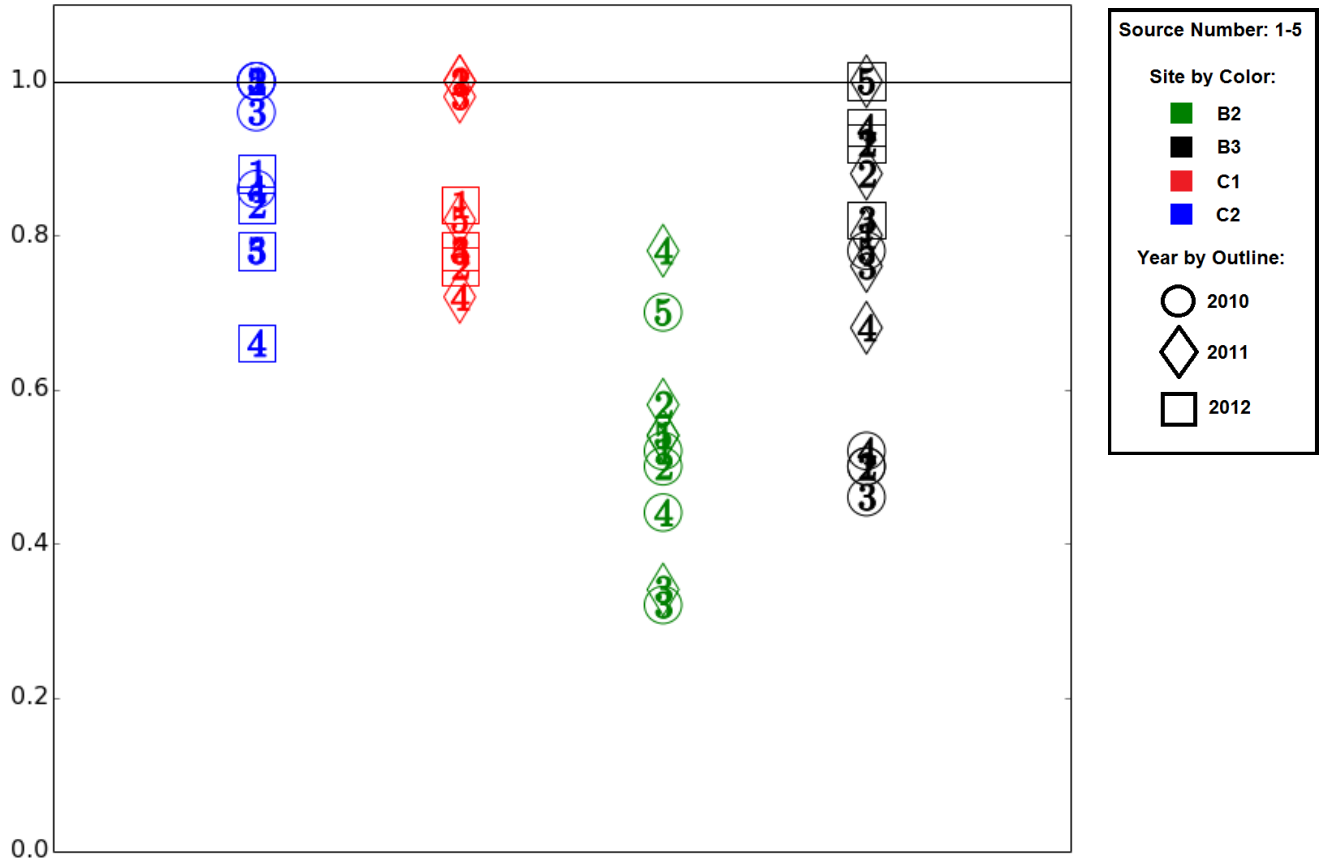

Figure 122. Fraction-factor-of-two AERC.RCALT AERMOD results for 24-hour averaging times.

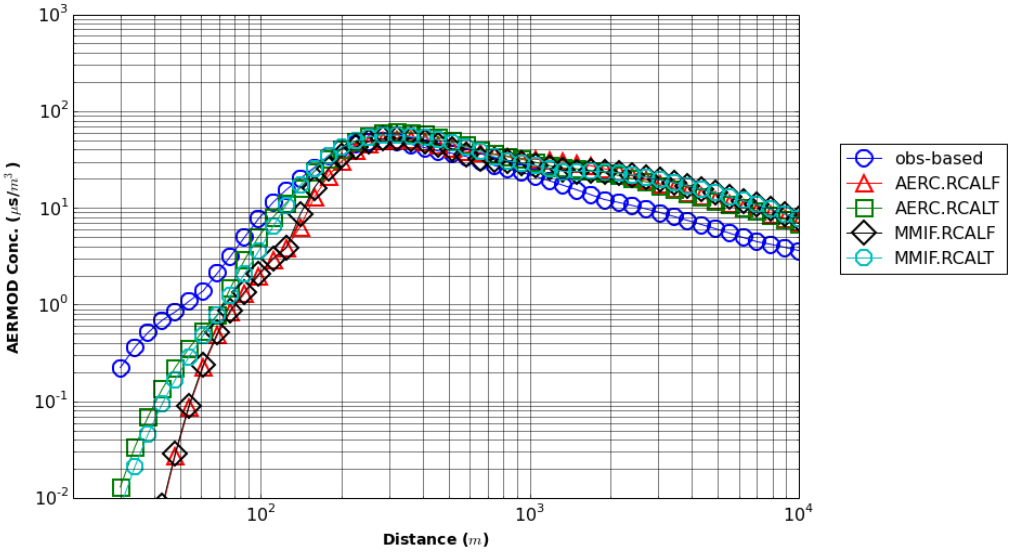

Figure 123. Concentration maxima vs. distance, Site C2, 2012, Source #3, 24-hr avg.

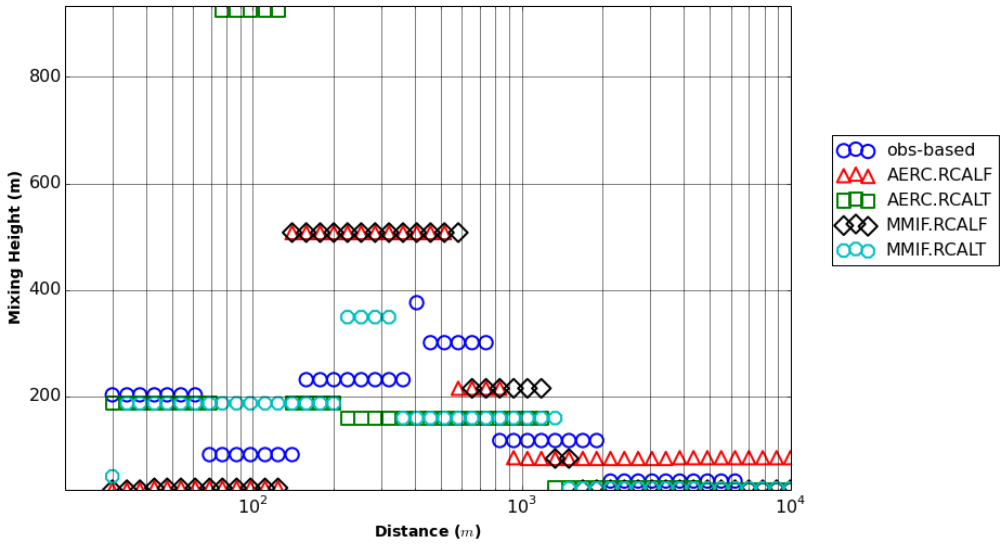

Figure 124. PBL height corresponding to concentration maxima, Site C2, 2012, Source Group #3, 24-hr avg.

6.5 Period Averages

6.5.1 Robust high concentration

The period-average RHC scores are plotted on Figure 125 - Figure 128. All WRF-based RHC values were within the factor-of-two of the observation-based RHC values. A majority of the RCALF simulations predicted lower RHCs than the observation-based simulations. The RCALT simulations were more conservative and matched the observation-driven RHC better. There was no discernible difference in RHC value between the MMIF and AERC based runs.

For RCALF simulations, PBL height was biased low during stable and unstable periods. The high frequency of minimum PBL heights (25 m) that occurred with RCALF simulations contributed to the negative RHC bias. The highly stable conditions limited vertical mixing, resulting in lower average concentrations in the near-source, given that most of the stack heights were well above the surface. Plume height was also above the minimum PBL height of 25 m in cases with tall stacks, such as Source Group #4, or cases with sufficient thermal and mechanical buoyancy, such as Source Groups #1 and #2.

Source Group #1 2012 WRF-based RHC values were consistently lower than observation-based values at Sites C1 and B3. Plots of maximum concentration with distance are plotted in Figure 129 and Figure 130. Both set of results have a similar trend, with near-source and far-source WRF-based concentrations of similar magnitude as the observation-based concentrations and the most deviation from 100 to 500 m. At both sites, WRF underpredicts seasonal wind speed (by -0.5 m/s at both sites). Observed seasonal PBL height at site B3 was about 200 m. WRF underpredicted PBL height with seasonal averages of 180 m and 160 m for RCALT and RCALF simulations, respectively. At site C1 the observation-based dataset had the same seasonal PBL height as the RCALT simulations (about 400 m) and the RCALF simulations resulted in a seasonal average of 270 m.

Combined, the WRF seasonal underprediction of wind speed and PBL height would presumably result in overprediction of concentration. At site B3, this was the case in the near-source and far-source but not in the 100 – 500 m range. At site C1 WRF-based concentrations were overpredicted only in the far-source. The pattern cannot be entirely an artifact of WRF low PBL predictions because the C1 RCALT simulations resulted in a similar pattern as the RCALF simulations (the observation-based simulations used the RCALT PBL heights).

The seasonal concentration profiles for these sites for the tall stack groups (Source Groups #3 and #4) appear similar, with greatest underprediction in the 100 – 1000 m range. Therefore, the pattern isn't a trait of the short stack group (#1). Further investigation would be warranted to discover the cause of the differences in maximum concentration in the mid-range of distance from the source.

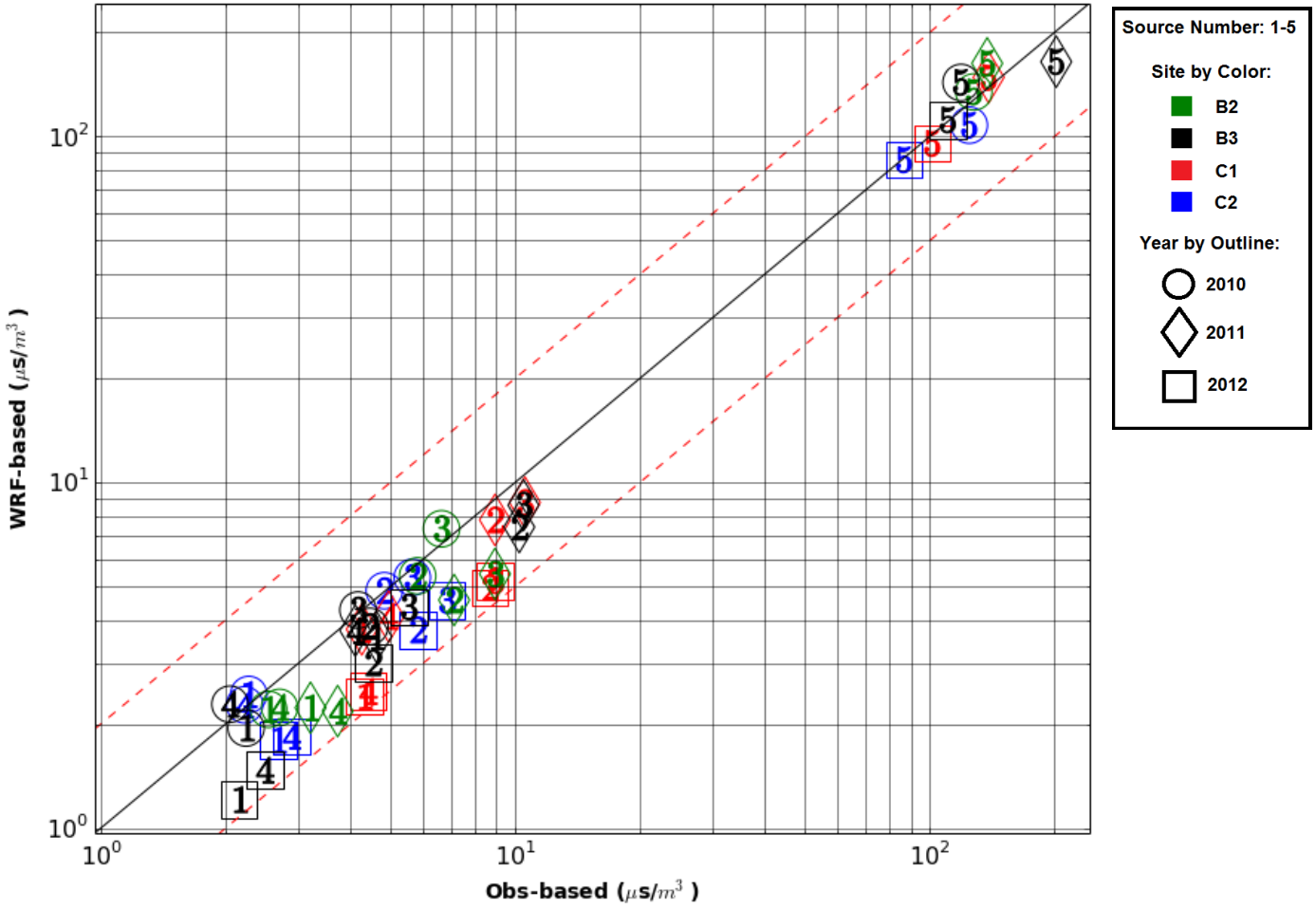

Figure 125. Robust high concentration results for MMIF.RCALF AERMOD Period averaging times.

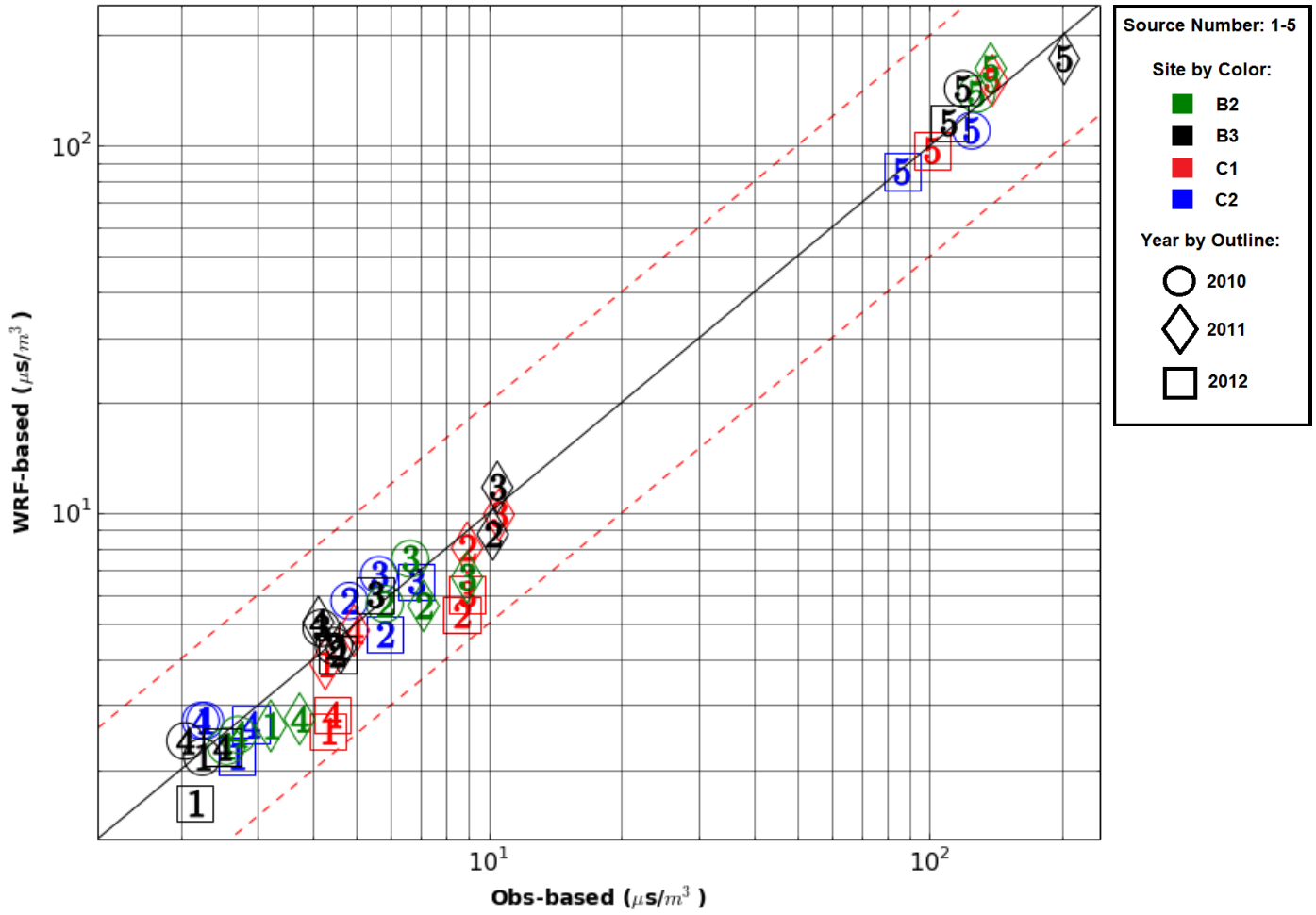

Figure 126. Robust high concentration results for MMIF.RCALT AERMOD period averaging times.

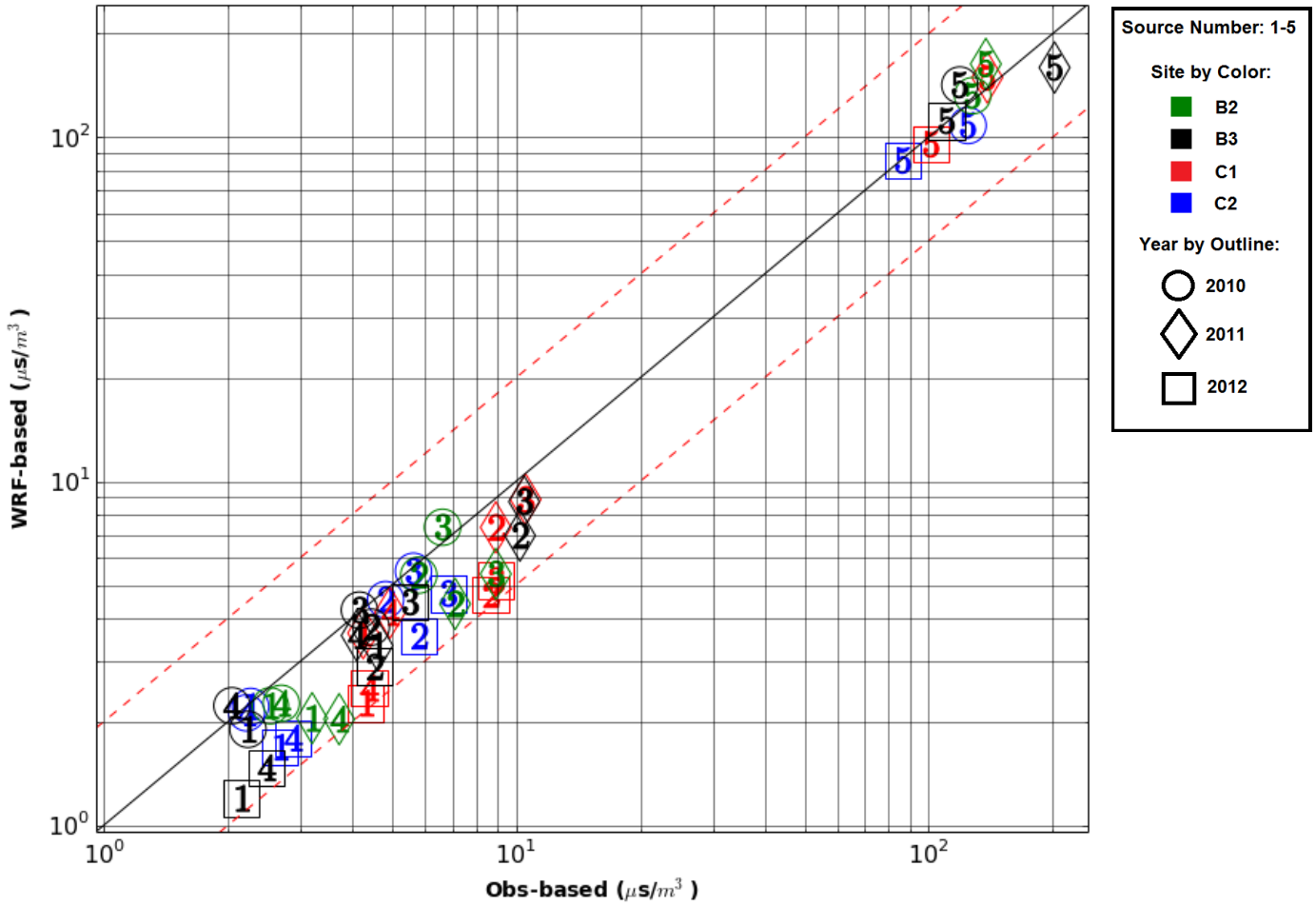

Figure 127. Robust high concentration results for AERC.RCALF AERMOD period averaging times.

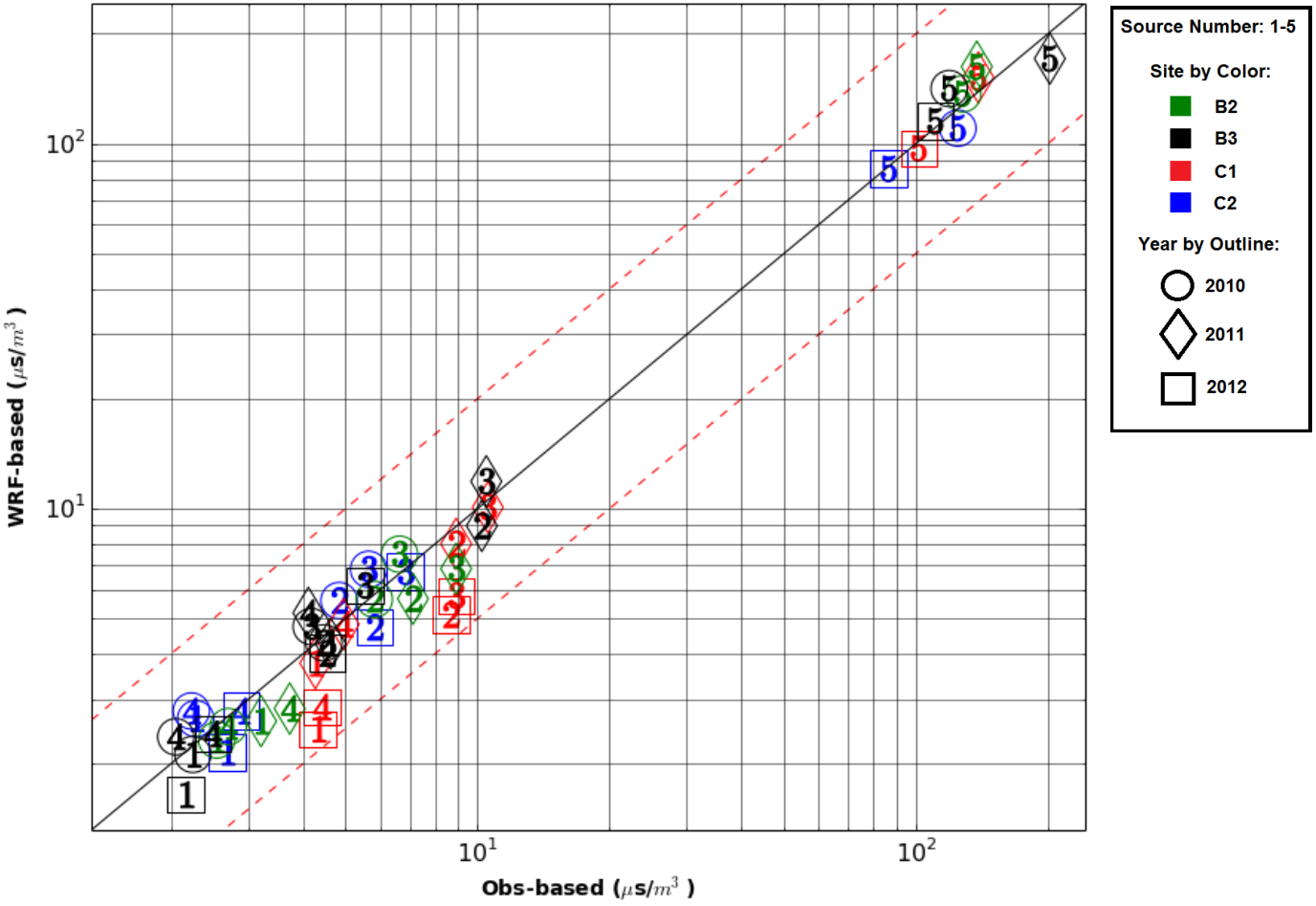

Figure 128. Robust high concentration results for AERC.RCALT AERMOD period averaging times.

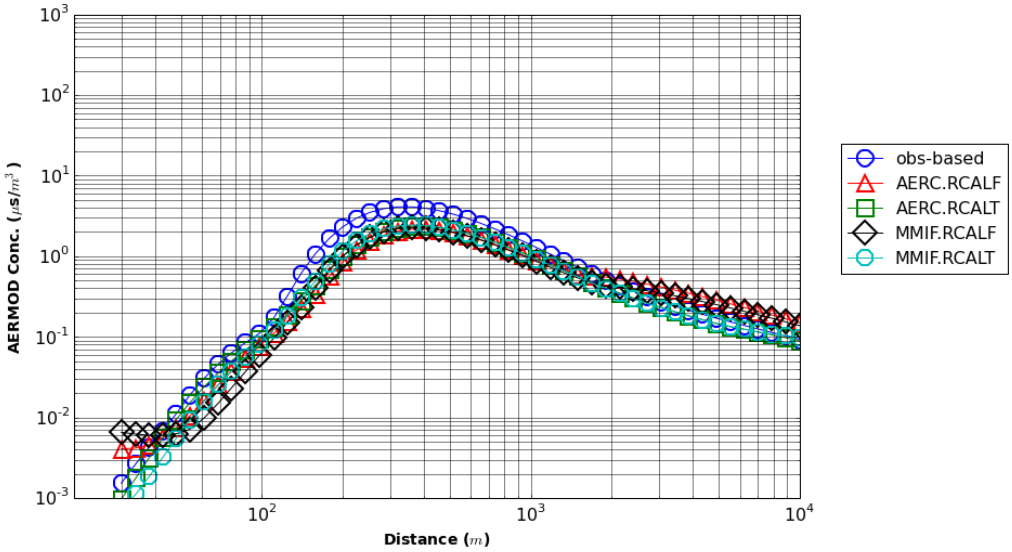

Figure 129. Concentration maxima vs. distance, Site C1, 2012, Source Group #1, Period average.

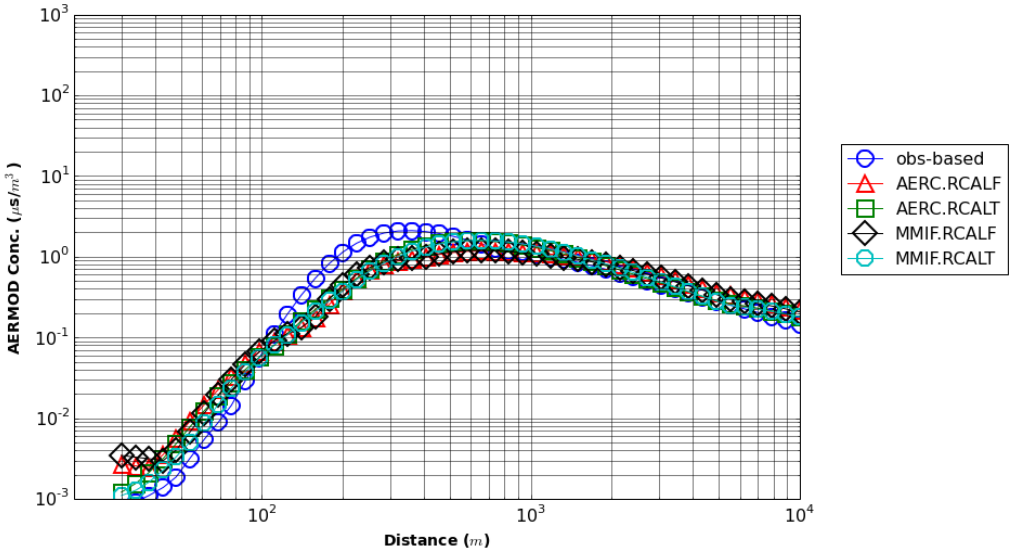

Figure 130. Concentration maxima vs. distance, Site B3, 2012, Source Group #1, Period average.

6.5.2 Fraction-factor-of-two

The period-average FF2 results are plotted in Figure 131 - Figure 134. Again, the Source Group #4 results have the lowest FF2 values and Source Group #5 results have the highest values. This correlated with the previous observation that sources with higher stack heights were more sensitive to differences in meteorology. The RCALT simulations result in a large increase in FF2 score for most of the site C1, compared to the RCALF simulations. FF2 scores are relatively low at site B2 with Source Groups #3 and #4 simulations as low as 0.3 - 0.4.

The Site B2 2010 plot of concentration by distance for the season is shown in Figure 135. All WRF-based simulations resulted in an underestimate of concentration in the near-source and overprediction of concentration in the far-source. These results are consistent with the case where PBL height is consistently underpredicted. The repressed mixing rate in stable conditions prevents the exhaust plume from reaching the ground-level receptors in the near-source and results in higher concentrations in the far-source. The WRF seasonal wind speed was lower than the observed value (4.7 and 4.0 m/s, respectively).

6.6 Site B2 Results

The statistical score results for site B2 1-hour averaging time simulations are listed in Table 11. The TMS provided an effective summary statistic to compare the performance of the four WRF meteorology extraction methods. The accuracy of the upper-end of the concentration distribution can be judged based on RHC score.

Most of the WRF-based B2 simulations slightly underpredicted RHC overall with an average RHC value 81% that of the observation-based RHC, and the recalculated PBL height (RCALT) simulations performed slightly better that RCALF runs. The RCALT simulations predicted an average RHC 84% that of the observation-based RHC, while the average RCALF simulation was 77% of the observation-based RHC. The simulations using the WRF meteorology directly (MMIF.RCALF and MMIF.RCALT) performed slightly better overall with an average TMS score of 0.74 and 0.69 between all applicable scores, respectively. The simulations where WRF meteorology was processed with AERCOARE (AERC.RCALF and AERC.RCALT) resulted in overall average scores of 0.72 and 0.69, respectively.

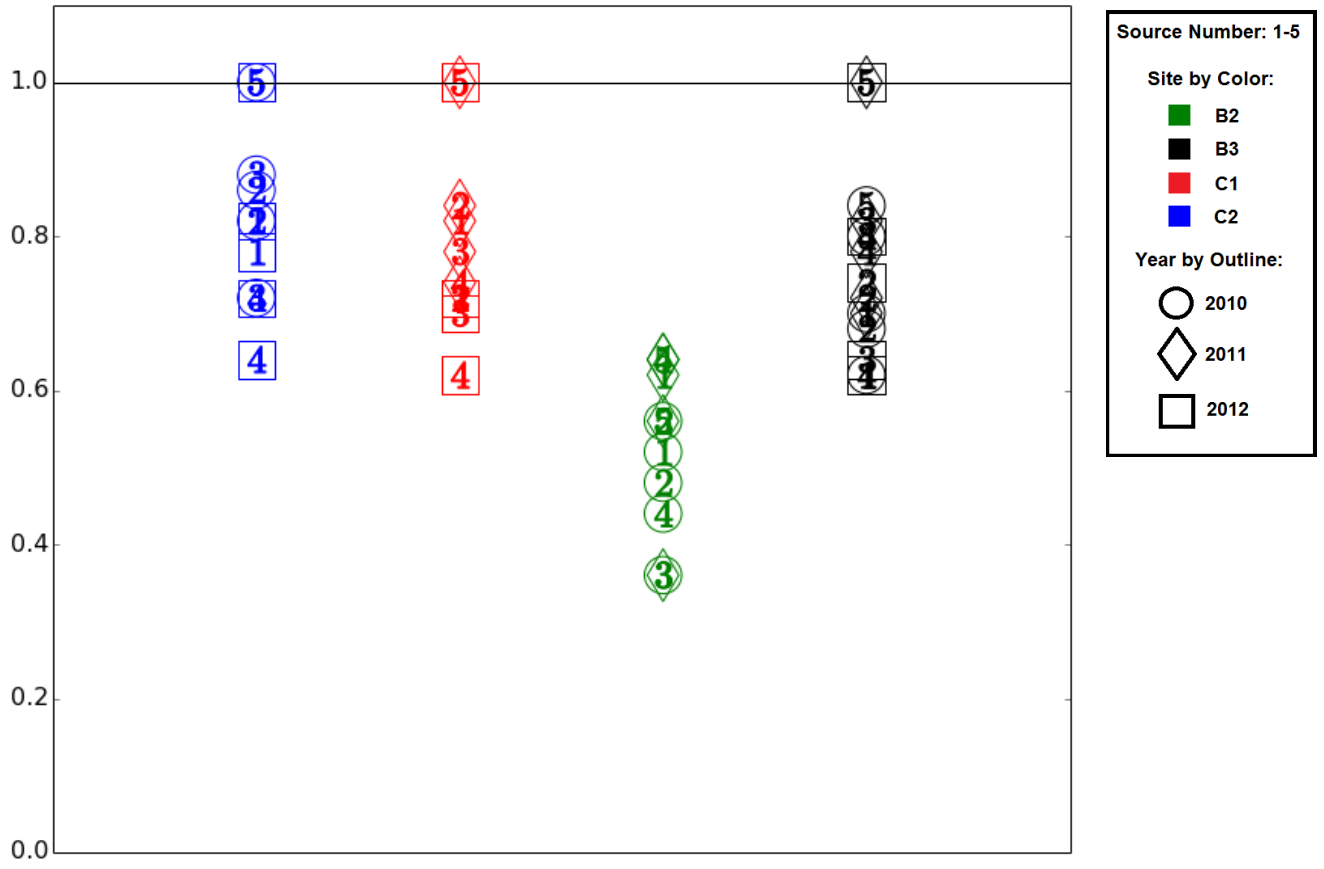

Figure 131. Fraction-factor-of-two MMIF.RCALF AERMOD results for period averaging times.

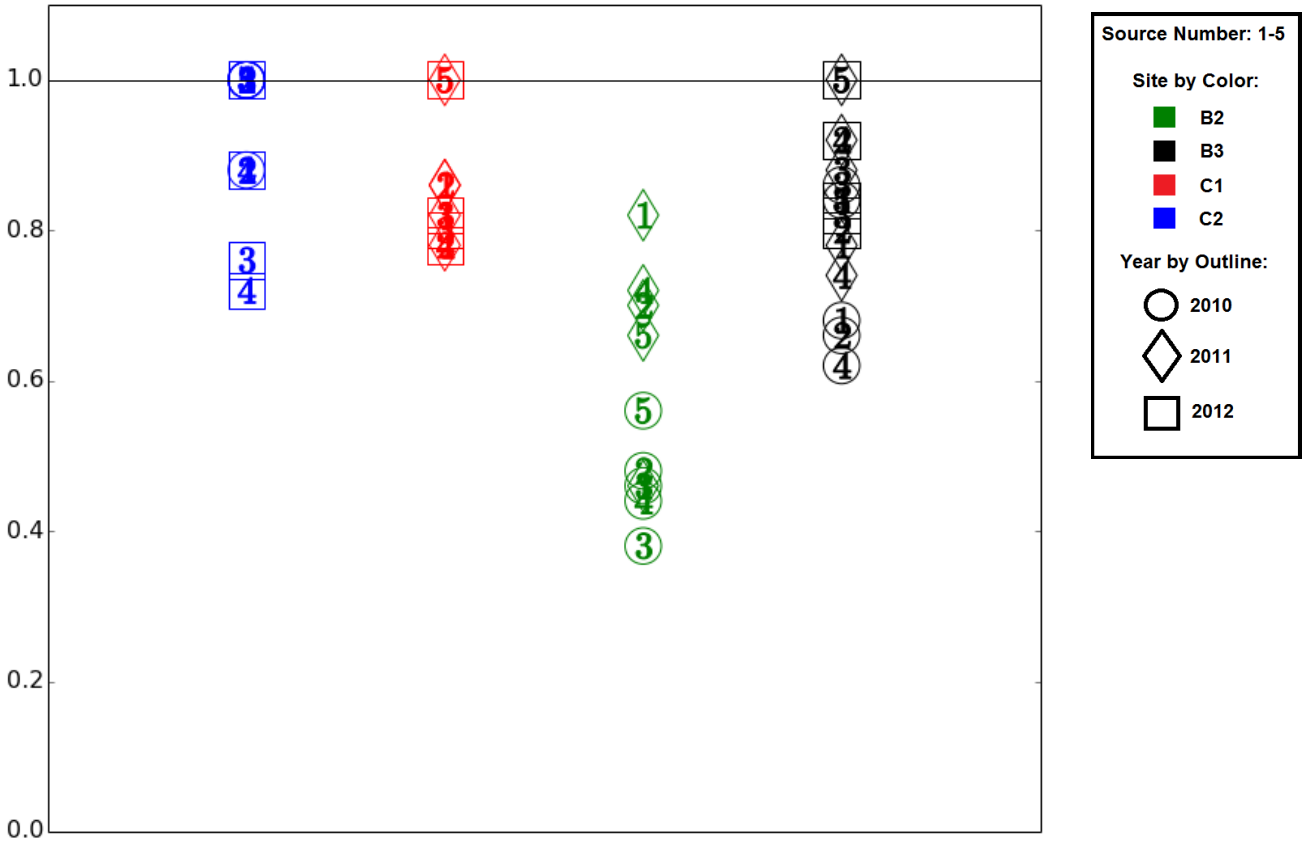

Figure 132. Fraction-factor-of-two MMIF.RCALT AERMOD results for period averaging times.

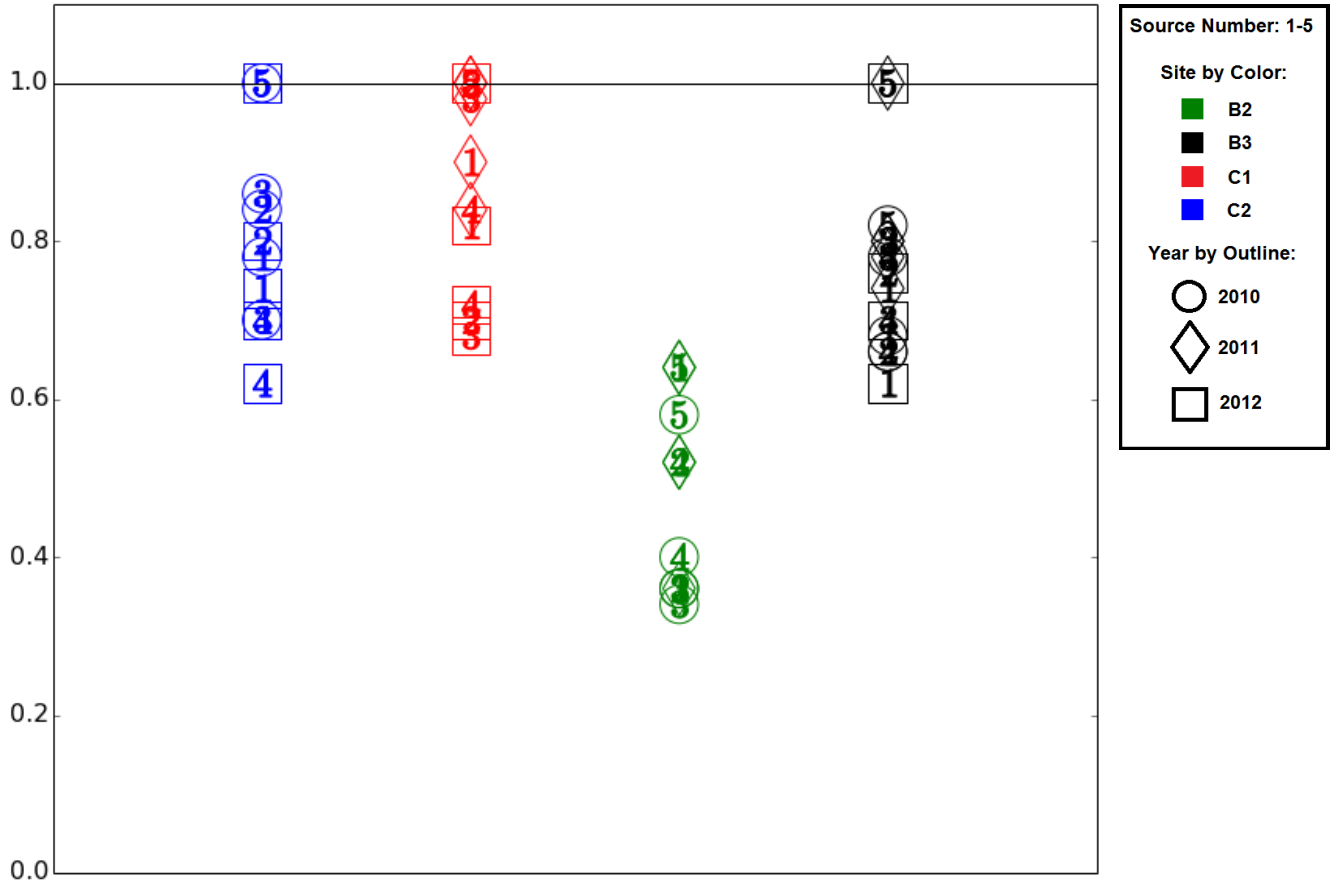

Figure 133. Fraction-factor-of-two AERC.RCALF AERMOD results for Period averaging times.

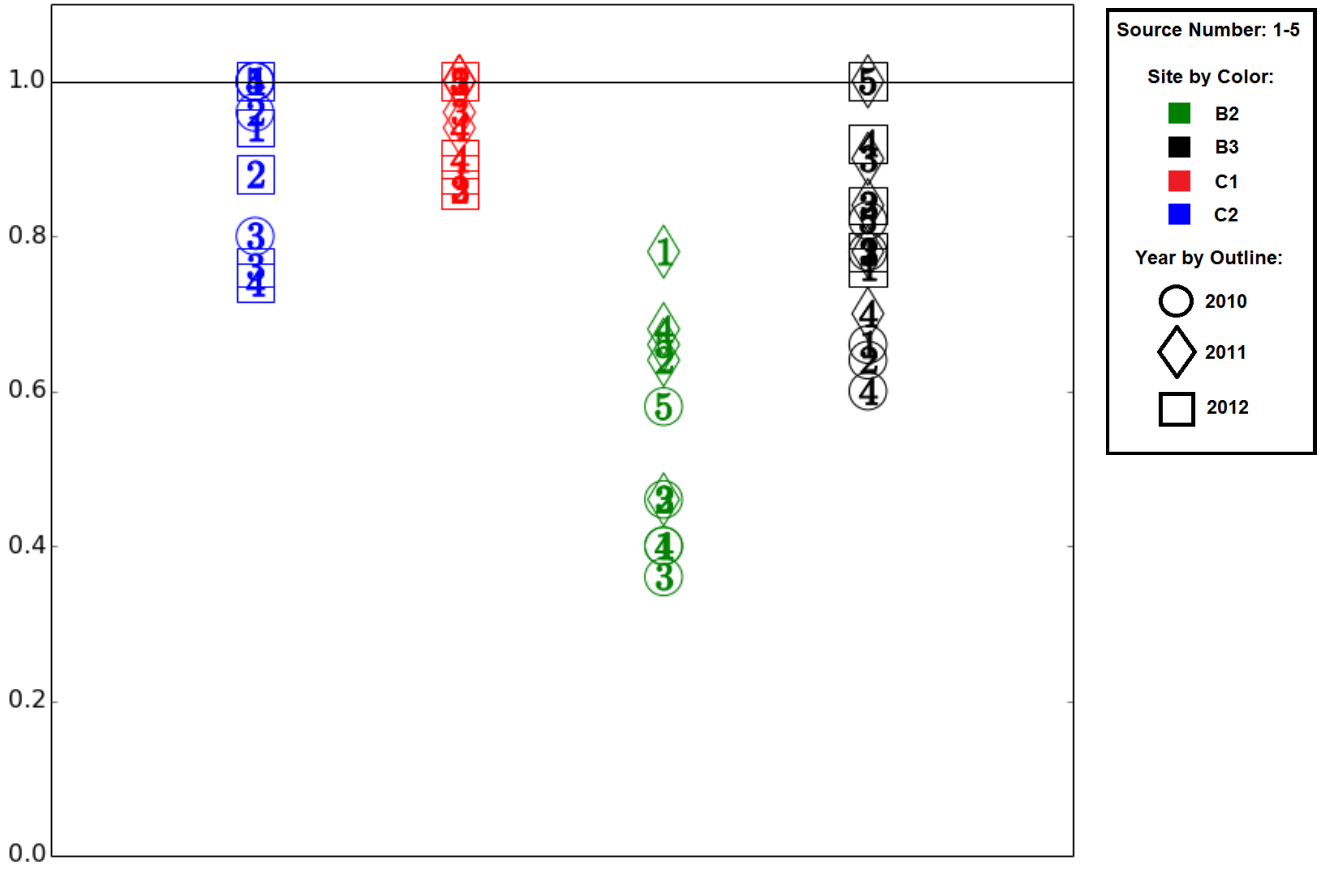

Figure 134. Fraction-factor-of-two AERC.RCALT AERMOD results for Period averaging times.

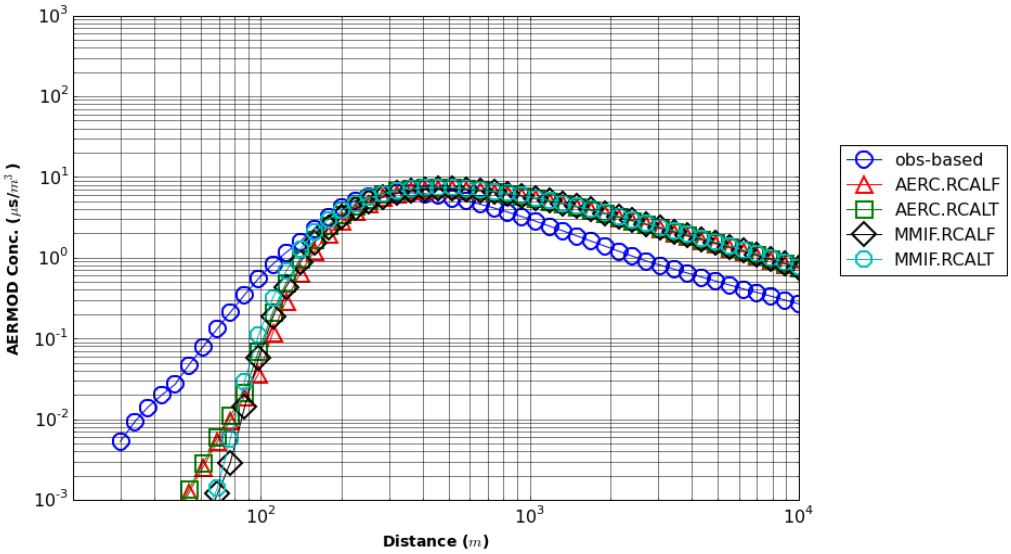

Figure 135. Concentration maxima vs. distance for the Period average, Site B2, 2010, Source Group #3.

Table 11. Site B2 1-hour average statistics scores.

Year	Src.	Run	Geo Mean	Geo. St. Dev.	MG	VG	RHC	Geo. R	FF2	TMS
2010	1	obs	17.20	2.57	1.00	1.00	50.02	1.00	1.00	0.90
		AERC.RCALT	7.38	9.31	2.33	19.93	41.24	0.85	0.70	0.57
		AERC.RCALF	7.68	8.73	2.24	15.04	39.17	0.86	0.72	0.61
		MMIF.RCALF	7.90	8.38	2.18	13.84	38.67	0.85	0.72	0.62
		MMIF.RCALT	7.96	8.59	2.16	14.83	40.47	0.84	0.72	0.61
	2	obs	42.74	2.31	1.00	1.00	101.31	1.00	1.00	0.80
		AERC.RCALT	18.58	8.53	2.30	18.59	87.11	0.86	0.76	0.59
		AERC.RCALF	19.75	7.56	2.16	11.37	86.14	0.87	0.76	0.63
		MMIF.RCALF	19.85	7.46	2.15	11.28	85.99	0.86	0.76	0.63
		MMIF.RCALT	20.63	7.58	2.07	11.04	88.59	0.86	0.76	0.63
	3	obs	65.40	2.40	1.00	1.00	190.48	1.00	1.00	0.81
		AERC.RCALT	29.37	10.84	2.23	42.05	170.50	0.80	0.72	0.58
		AERC.RCALF	27.37	10.90	2.39	46.94	166.69	0.81	0.72	0.59
		MMIF.RCALF	17.70	17.44	3.69	1078.48	133.95	0.73	0.68	0.50
		MMIF.RCALT	18.39	17.58	3.56	1092.87	138.34	0.72	0.66	0.53
	4	obs	22.75	4.47	1.00	1.00	79.69	1.00	1.00	0.82
		AERC.RCALT	2.24	111.84	10.14	>5000	86.05	0.80	0.60	0.49
		AERC.RCALF	1.72	113.43	13.21	>5000	47.48	0.81	0.62	0.41
		MMIF.RCALF	1.78	90.33	12.81	>5000	45.01	0.77	0.60	0.48
		MMIF.RCALT	2.35	89.86	9.70	>5000	79.21	0.79	0.60	0.41

Table 11, continued. Site B2 1-hour average statistics scores.

Year	Src.	Run	Geo Mean	Geo. St. Dev.	MG	VG	RHC	Geo. R	FF2	TMS
		obs	237.59	3.27	1.00	1.00	1224.60	1.00	1.00	0.80
		AERC.RCALT	247.27	3.09	0.96	1.01	1131.49	1.00	1.00	0.98
	5	AERC.RCALF	247.71	3.08	0.96	1.01	1131.49	1.00	1.00	0.99
		MMIF.RCALF	253.77	3.23	0.94	1.01	1221.71	1.00	1.00	0.97
		MMIF.RCALT	253.77	3.23	0.94	1.01	1221.71	1.00	1.00	0.98
		obs	10.67	5.43	1.00	1.00	48.74	1.00	1.00	0.87
		AERC.RCALT	14.05	3.39	0.76	1.42	42.31	0.99	0.82	0.83
	1	AERC.RCALF	9.00	7.00	1.19	1.53	42.08	0.95	0.88	0.86
		MMIF.RCALF	9.94	6.62	1.07	1.40	45.18	0.95	0.90	0.89
		MMIF.RCALT	14.13	3.72	0.76	1.32	45.63	0.99	0.86	0.87
		obs	30.51	3.98	1.00	1.00	116.19	1.00	1.00	0.80
		AERC.RCALT	32.28	3.30	0.95	1.06	89.03	1.00	1.00	0.93
	2	AERC.RCALF	20.56	6.85	1.48	2.13	85.86	0.94	0.82	0.77
		MMIF.RCALF	22.43	6.37	1.36	1.78	90.39	0.95	0.84	0.81
		MMIF.RCALT	32.11	3.59	0.95	1.04	90.33	0.99	1.00	0.98
		obs	64.45	2.88	1.00	1.00	186.80	1.00	1.00	0.81
		AERC.RCALT	30.24	6.54	2.13	6.81	122.01	0.83	0.68	0.56
2011	3	AERC.RCALF	14.68	19.57	4.39	3469.96	122.01	0.64	0.58	0.49
		MMIF.RCALF	17.12	16.42	3.77	958.47	130.24	0.65	0.62	0.49
		MMIF.RCALT	29.14	7.68	2.21	11.02	138.14	0.81	0.70	0.60
		obs	10.60	16.71	1.00	1.00	84.14	1.00	1.00	0.82
		AERC.RCALT	11.40	8.78	0.93	1.92	46.12	0.98	0.76	0.75
	4	AERC.RCALF	3.02	45.55	3.51	199.55	45.36	0.87	0.66	0.56
		MMIF.RCALF	3.61	34.86	2.93	62.10	46.62	0.88	0.60	0.56
		MMIF.RCALT	10.95	10.06	0.97	1.54	62.37	0.99	0.76	0.82
		obs	220.04	3.26	1.00	1.00	1135.76	1.00	1.00	0.80
		AERC.RCALT	237.45	3.00	0.93	1.02	1021.43	1.00	1.00	0.96
	5	AERC.RCALF	237.53	2.99	0.93	1.02	1021.43	1.00	1.00	0.98
		MMIF.RCALF	220.92	3.01	1.00	1.01	1017.11	1.00	1.00	1.00
		MMIF.RCALT	218.45	2.99	1.01	1.01	1008.37	1.00	1.00	0.99

The 2010 Source Group #4 simulations were selected for further investigation. All of the 2010 Source Group #4 WRF simulations resulted in low FF2 scores of 0.6, and TMS scores of 0.41 to 0.49. However, the RCALT simulations resulted in RHC scores very near to the observation-based value of 79 μs/m^3. The two RCALF simulations resulted in RHC scores of 45 and 47 μs/m^3.

The concentration maxima are shown in Figure 136 for these simulations. Note that the RCALF simulations underpredicted concentration within the 1000 – 3,000 m range of receptor distances while the RCALT simulations overpredicted concentration within this range. All of the simulations underpredict concentration from 30 to 500 m. The difference in RHC occurs because the RCALT simulations produced a peak concentration at about 1,000 m downwind of the source that matches the magnitude of the observation-based peak that occurs at roughly 450 m.

Figure 137 reveals that both the RCALT and RCALF maxima occurred when PBL heights were the minimum 25 m. Figure 138 shows the inverse *L* values corresponding to the maximum concentrations. The values are at or near the minimum 1/*L* value of -0.2 m, indicating highly unstable conditions. Observation -based maxima occurred during neutral stability conditions at these distances. Figure 139 shows the wind speed for the same cases. The RCALT concentration maxima occurred mostly during wind speeds of about 1 m/s, while RCALF maxima occurred during wind speeds ranging from 0.5 to 3.5 m/s. The combination of low wind speed and low PBL height resulted in higher concentrations for RCALT simulations.

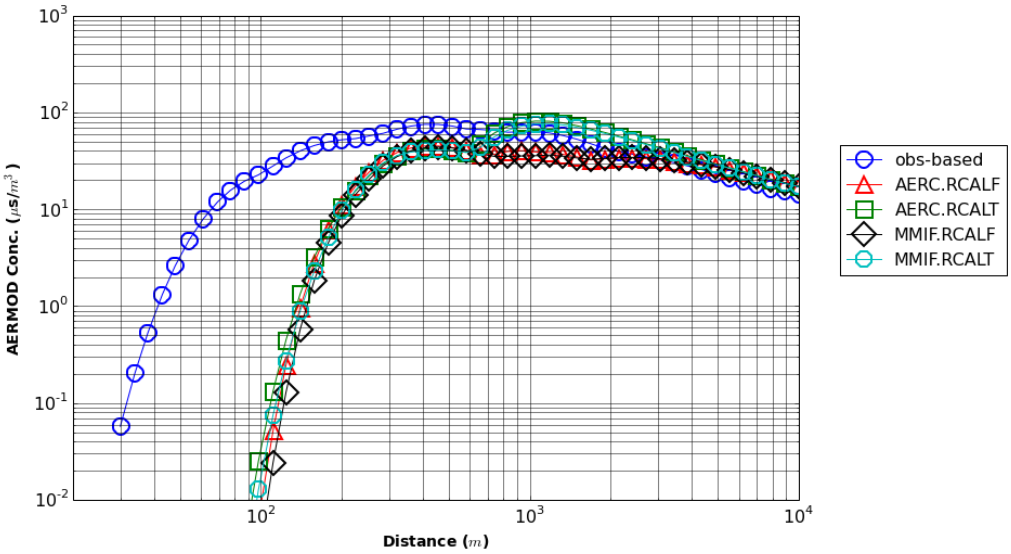

Figure 136. Concentration maxima vs. distance, Site B2, 2010, Source Group #4.

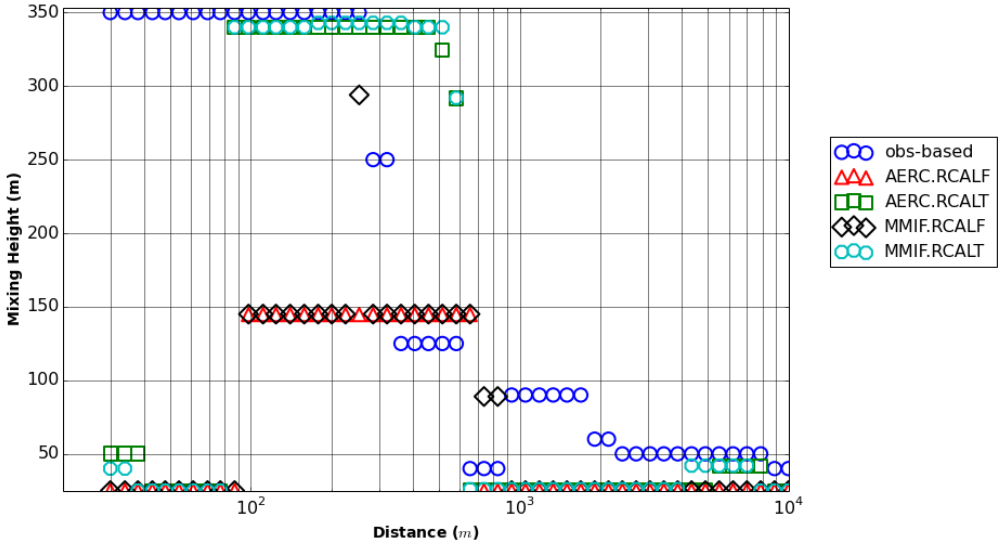

Figure 137. PBL height corresponding to concentration maxima, Site B2, 2010, Source Group #4.

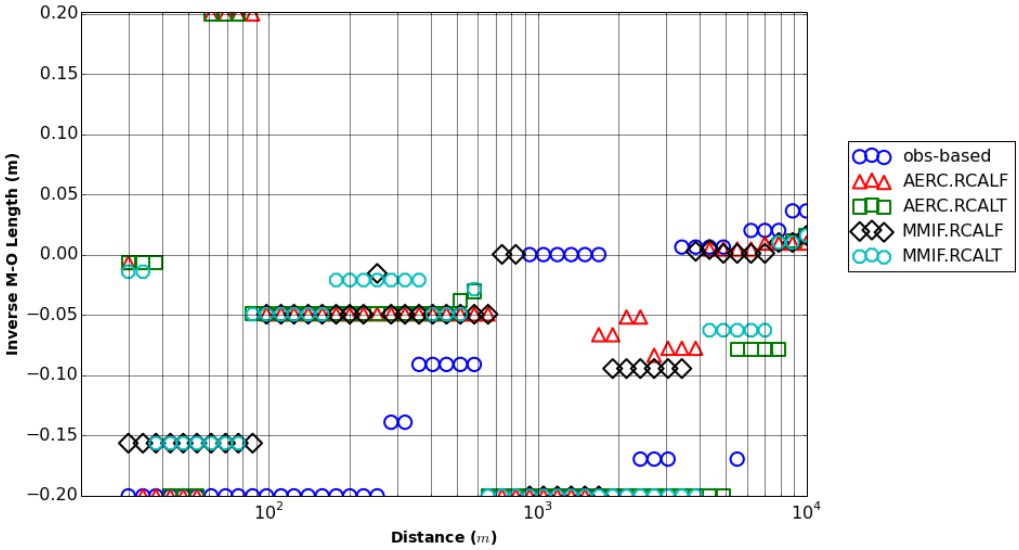

Figure 138. Inverse L corresponding to concentration maxima, Site B2, 2010, Source Group #4.

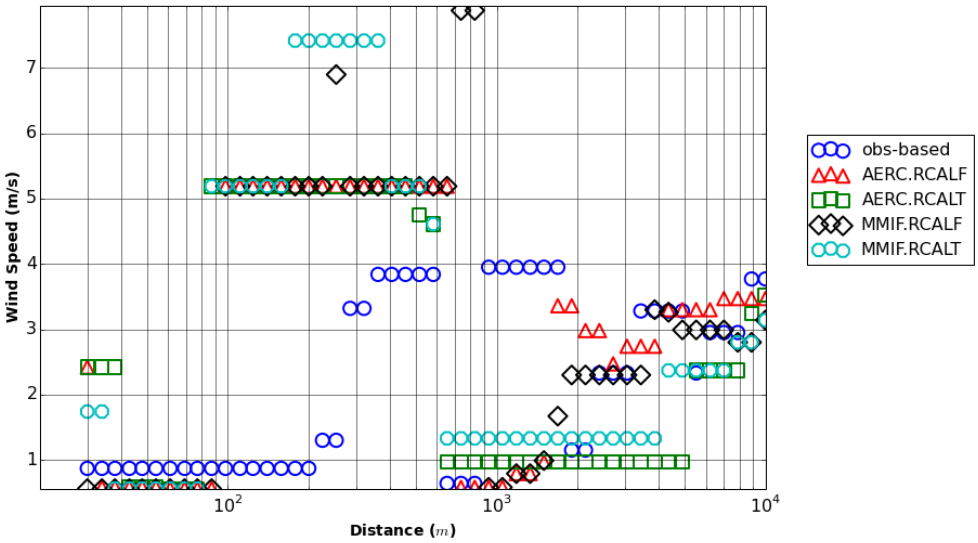

Figure 139. Wind speed corresponding to concentration maxima, Site B2, 2010, Source Group #4.

6.7 Site B3 Results

The statistical score results for site B3 1-hour averaging time simulations are listed in Table 12. For site B3, the MMIF.RCALT simulations resulted in slightly better TMS scores than the other simulations. MMIF.RCALT simulations resulted in average RHC values of 0.84, compared to the average scores of 0.81, 0.80 and 0.81 for MMIF.RCALT, AERC.RCALF, and AERC.RCALT, respectively. Source Group #5 performed the best overall (average TMS of 0.99) and Source Group #4 performed the worst overall (average TMS of 0.69) in terms of TMS score.

Most of the simulations resulted in RHC scores that were close in magnitude to the observation-driven RHC score results. The average WRF RHC score was 92% of the observation-based RHC (slight underprediction on average). Source Group #5 average WRF RHCs were 98% of the observation-based scores. Source Group #3 average RHC scores were the lowest at 86% of the observation-based value. Source Group #4 (the tallest set of stacks) simulations resulted in an average RHC score 92% of the observation-based RHC, but resulted in the greatest extremes with 2012 MMIF.RCALF at 66% of the observation-based RHC and 2010 MMIF.RCALT at 118% of the observation-based RHC.

The 2011 Source Group #3 simulations were selected for further investigation due to a large gap in TMS score between the different runs. The MMIF.RCALT simulation resulted in a TMS score of 0.95 while the MMIF.RCALF simulation resulted in a TMS score of 0.67 Both these simulations resulted in a similar TMS score, but the MMIF.RCALF had a much lower FF2 score

(0.76 versus 0.94) and a geometric mean of 24.6 compared to the MMIF.RCALT value of 41.3 (observation-based geometric mean was 42.1).

The concentration maxima values are plotted with respect to distance in Figure 140. It is evident that the RCALT simulations agree better with the observation-based simulations in the near-source region. At 200 m and beyond, all of the WRF simulations resulted in concentrations that agree well with the predictions of the observation-based simulations. In the near-source, the RCALF simulations underpredicted concentration. The Q-Q plot of these simulations is shown in Figure 141, further illustrating the RCALF underprediction leading to the low FF2. The observation-based simulation maximum occurred at about 200 m downwind of the source, while the WRF simulation maxima occurred roughly 500 – 700 m downwind.

Figure 142 shows PBL height versus distance for the Source Group #3 B3 2011 simulations. The RCALT simulations resulted in high PBL heights, greater than 500 m, in the near-source region corresponding to unstable conditions (L is negative in RCALT simulations, confirming this). However, these PBL heights were greater than the observation-based PBL heights that ranged from 100 to 200 m in the near-source region. The RCALF PBL heights agreed better with the observations with PBL heights of 150 m at a distance of 50 to 200 m and both RCALF and observation-based inverse *L* was -0.2.

Figure 143 is a plot of wind speed versus distance for these simulations. The RCALT simulations near-source maxima occurred during light wind speeds of 0.5 m/s, while the RCALF simulations maxima occurred during winds greater than 3.0 m/s (observation-based maxima occurred during wind speeds of 1.0 - 1.5 m/s).

Again, it is evident that WRF's tendency to predict minimum PBL heights even during unstable periods (when L < 0) is the cause of the discrepancies in near-source maxima. The MMIF rediagnosis resulted in PBL heights more characteristic of unstable conditions, improving the AERMOD performance.

Table 12. Site B3 1-hour average statistics scores.

Year	Src.	Run	Geo Mean	Geo. St. Dev.	MG	VG	RHC	Geo. R	FF2	TMS
2010	1	obs	12.54	4.47	1.00	1.00	47.32	1.00	1.00	0.86
		AERC.RCALT	26.79	1.50	0.47	7.59	44.94	0.79	0.76	0.62
		AERC.RCALF	25.74	1.50	0.49	6.94	41.33	0.81	0.76	0.62
		MMIF.RCALF	21.14	1.88	0.59	3.08	40.89	0.95	0.80	0.73
		MMIF.RCALT	21.93	1.96	0.57	2.98	44.56	0.95	0.80	0.72
	2	obs	34.58	3.41	1.00	1.00	96.26	1.00	1.00	0.80
		AERC.RCALT	57.85	1.47	0.60	3.47	90.62	0.71	0.80	0.67
		AERC.RCALF	54.89	1.51	0.63	2.95	83.60	0.80	0.80	0.70
		MMIF.RCALF	46.38	1.75	0.75	1.85	82.83	0.94	0.84	0.81
		MMIF.RCALT	48.48	1.77	0.71	1.90	87.36	0.93	0.84	0.79

Table 12, continued. Site B3 1-hour average statistics scores.

Year	Src.	Run	Geo Mean	Geo. St. Dev.	MG	VG	RHC	Geo. R	FF2	TMS
2010	3	obs	50.37	3.59	1.00	1.00	157.18	1.00	1.00	0.81
		AERC.RCALT	84.50	1.61	0.60	3.68	139.96	0.68	0.82	0.65
		AERC.RCALF	76.22	1.72	0.66	2.86	142.12	0.76	0.82	0.71
		MMIF.RCALF	63.99	2.07	0.79	1.55	122.45	0.96	0.86	0.82
		MMIF.RCALT	72.18	1.90	0.70	1.91	125.70	0.93	0.84	0.79
	4	obs	10.63	14.23	1.00	1.00	62.18	1.00	1.00	0.82
		AERC.RCALT	40.30	1.74	0.26	1117.46	68.67	0.72	0.72	0.52
		AERC.RCALF	33.80	1.69	0.32	785.50	69.92	0.71	0.72	0.55
		MMIF.RCALF	27.16	2.15	0.39	122.15	56.53	0.91	0.74	0.57
		MMIF.RCALT	31.76	2.42	0.34	116.46	73.54	0.91	0.74	0.55
	5	obs	249.72	3.16	1.00	1.00	1236.04	1.00	1.00	0.80
		AERC.RCALT	248.69	3.12	1.00	1.00	1244.94	1.00	1.00	1.00
		AERC.RCALF	248.75	3.12	1.00	1.00	1244.94	1.00	1.00	1.00
		MMIF.RCALF	248.76	3.20	1.00	1.00	1190.27	1.00	1.00	0.99
		MMIF.RCALT	248.95	3.20	1.00	1.00	1193.66	1.00	1.00	1.00
2011	1	obs	13.89	3.98	1.00	1.00	45.51	1.00	1.00	0.86
		AERC.RCALT	18.54	2.07	0.75	1.83	45.11	0.96	0.84	0.82
		AERC.RCALF	9.95	5.73	1.40	1.87	41.35	0.92	0.80	0.78
		MMIF.RCALF	10.31	5.78	1.35	1.84	43.44	0.92	0.80	0.79
		MMIF.RCALT	15.94	2.80	0.87	1.28	45.10	0.96	0.86	0.89
	2	obs	32.76	3.42	1.00	1.00	90.78	1.00	1.00	0.81
		AERC.RCALT	42.60	2.01	0.77	1.52	90.68	0.96	0.86	0.85
		AERC.RCALF	23.89	5.22	1.37	1.69	83.61	0.94	0.76	0.79
		MMIF.RCALF	24.57	5.28	1.33	1.67	90.70	0.94	0.78	0.80
		MMIF.RCALT	37.24	2.66	0.88	1.18	91.87	0.97	0.90	0.92
	3	obs	42.07	3.90	1.00	1.00	139.03	1.00	1.00	0.81
		AERC.RCALT	54.66	2.42	0.77	1.40	120.83	0.98	0.88	0.84
		AERC.RCALF	23.39	11.78	1.80	8.21	121.60	0.92	0.74	0.67
		MMIF.RCALF	24.57	11.11	1.71	6.88	130.21	0.92	0.76	0.67
		MMIF.RCALT	41.32	3.99	1.02	1.12	135.59	0.97	0.94	0.95
	4	obs	11.72	13.49	1.00	1.00	61.43	1.00	1.00	0.84
		AERC.RCALT	26.24	2.74	0.45	27.69	62.91	0.98	0.76	0.64
		AERC.RCALF	4.99	30.16	2.35	18.59	53.40	0.91	0.68	0.58
		MMIF.RCALF	5.37	25.76	2.18	15.12	53.07	0.90	0.68	0.62
		MMIF.RCALT	18.90	4.61	0.62	4.44	68.31	0.99	0.82	0.69
	5	obs	163.62	3.39	1.00	1.00	1116.54	1.00	1.00	0.80
		AERC.RCALT	169.68	3.11	0.96	1.04	1072.03	0.99	1.00	0.98
		AERC.RCALF	189.57	3.14	0.86	1.07	1016.64	0.99	1.00	0.95
		MMIF.RCALF	190.37	3.14	0.86	1.07	1007.06	0.99	1.00	0.95
		MMIF.RCALT	160.45	3.08	1.02	1.03	1066.92	0.99	1.00	0.98
2012	1	obs	14.65	3.26	1.00	1.00	42.63	1.00	1.00	0.85
		AERC.RCALT	15.56	2.95	0.94	1.06	36.87	0.98	0.98	0.94
		AERC.RCALF	15.58	3.02	0.94	1.08	39.34	0.98	0.94	0.94
		MMIF.RCALF	13.47	3.62	1.09	1.05	40.40	0.99	1.00	0.97
		MMIF.RCALT	13.42	3.64	1.09	1.06	38.47	0.99	1.00	0.96
	2	obs	38.33	2.65	1.00	1.00	90.59	1.00	1.00	0.80
		AERC.RCALT	36.21	2.60	1.06	1.02	85.46	0.99	1.00	0.97
		AERC.RCALF	35.84	2.65	1.07	1.02	80.39	0.99	1.00	0.97
		MMIF.RCALF	31.69	3.12	1.21	1.10	80.23	0.99	0.98	0.94
		MMIF.RCALT	32.27	3.22	1.19	1.11	94.42	0.98	0.96	0.91

Table 12, continued. Site B3 1-hour average statistics scores.

Year	Src.	Run	Geo Mean	Geo. St. Dev.	MG	VG	RHC	Geo. R	FF2	TMS
2012	3	obs	67.63	2.19	1.00	1.00	162.17	1.00	1.00	0.81
		AERC.RCALT	51.15	2.99	1.32	1.37	125.46	0.92	0.82	0.80
		AERC.RCALF	42.07	4.18	1.61	2.53	128.83	0.87	0.76	0.72
		MMIF.RCALF	35.88	5.43	1.89	5.30	137.85	0.83	0.72	0.64
		MMIF.RCALT	38.31	5.35	1.77	4.59	132.11	0.85	0.76	0.67
	4	obs	17.15	7.59	1.00	1.00	74.14	1.00	1.00	0.82
		AERC.RCALT	15.61	7.35	1.10	1.04	54.01	1.00	1.00	0.92
		AERC.RCALF	16.03	7.49	1.07	1.09	52.29	0.99	0.98	0.96
		MMIF.RCALF	11.21	10.92	1.53	1.49	48.99	0.99	0.88	0.83
		MMIF.RCALT	11.51	11.54	1.49	1.50	56.02	0.99	0.78	0.80
	5	obs	243.59	3.16	1.00	1.00	1187.88	1.00	1.00	0.80
		AERC.RCALT	242.22	3.09	1.01	1.00	1200.45	1.00	1.00	1.00
		AERC.RCALF	242.20	3.09	1.01	1.00	1199.78	1.00	1.00	1.00
		MMIF.RCALF	243.06	3.18	1.00	1.00	1195.56	1.00	1.00	1.00
		MMIF.RCALT	243.08	3.18	1.00	1.00	1196.11	1.00	1.00	1.00

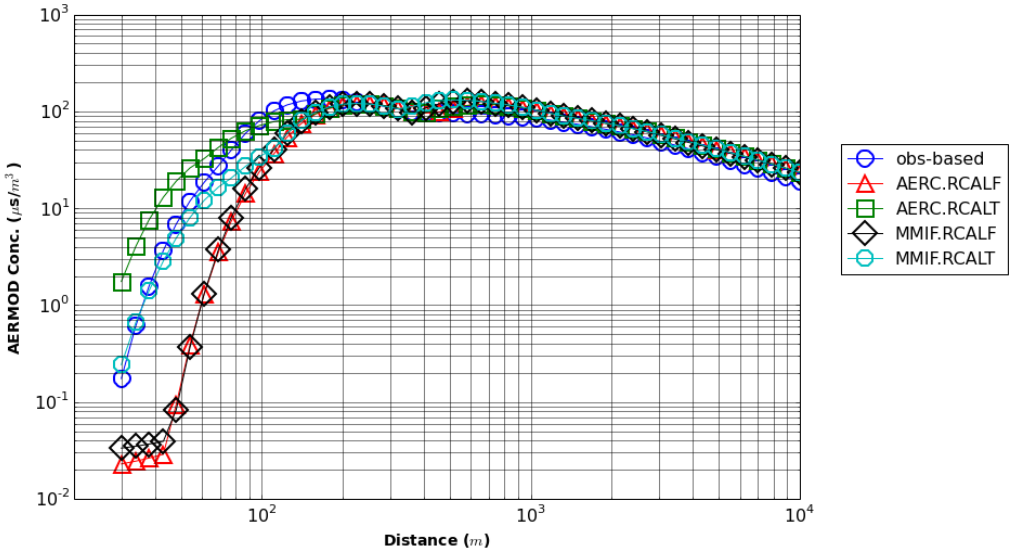

Figure 140. Concentration maxima vs. distance, Site B3, 2011, Source Group #3.

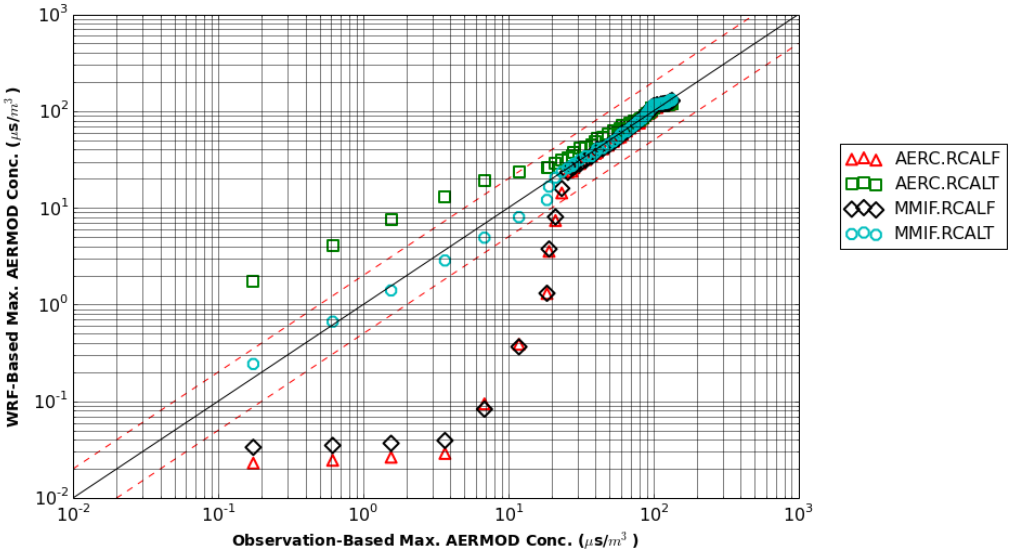

Figure 141. Q-Q plot of WRF-based AERMOD concentration results versus observation-based results, Site B3, 2011, Source Group #3.

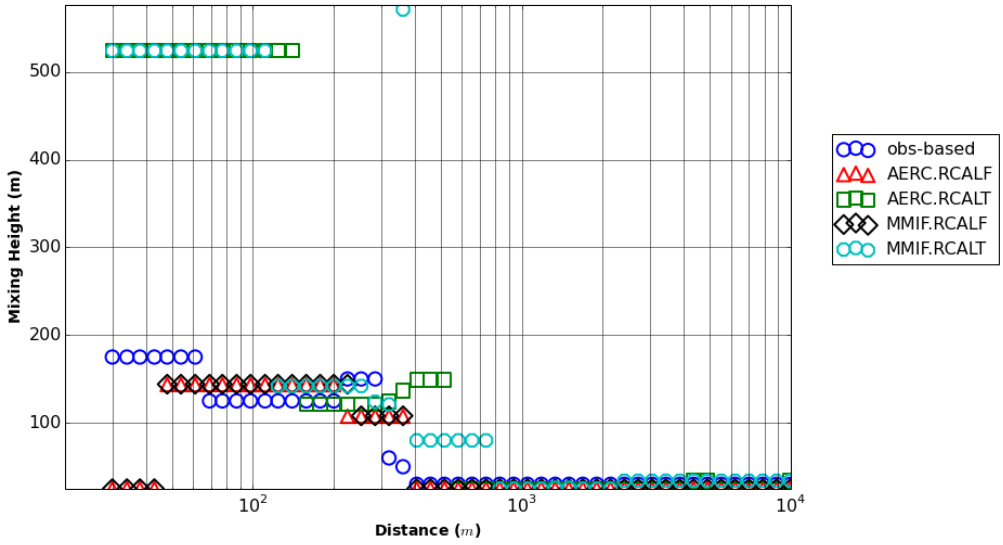

Figure 142. PBL height vs. distance for concentration maxima, Site B3, 2011, Source Group #3.

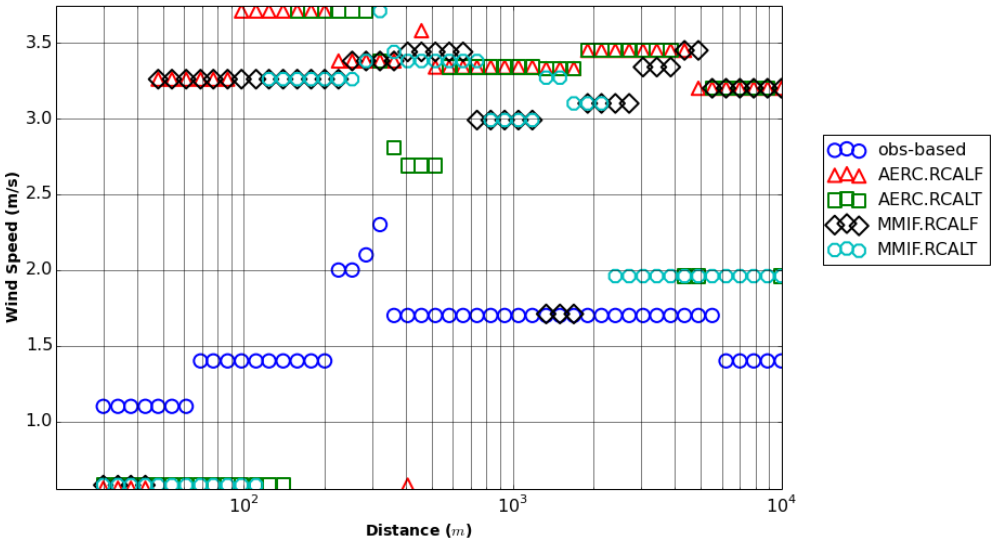

Figure 143. Wind speed vs. distance for concentration maxima, Site B3, 2011, Source Group #3.

6.8 Site C1 Results

The 1-hour average statistic scores for site C1 are listed in Table 13. The average TMS score of the AERC simulations was 0.94 while the average TMS score of the MMIF simulations was 0.84. Again, the taller stack groups (Source Groups #3 and #4) result in the lowest TMS scores, with an average of 0.80 and 0.83, respectively while the other source groups result in average TMS scores of 0.93.

None of the simulations resulted in RHC scores less than 85% of the respective observation-based RHC score. Geometric correlation coefficients are high, greater than 0.9, except for 2012 Source Group #3 simulations.

The 2010 Source Group #3 simulations were selected for further examination because these resulted in the lowest FF2 scores and TMS scores, despite RHC scores that were roughly 90% of the observation-based RHC scores. . Figure 144 shows the concentration maxima with respect to distance. The AERC simulations resulted in concentrations nearer to the observation-based simulation results, but underpredicted. The MMIF simulations highly underpredicted concentration in the near-source region.

PBL heights plotted in Figure 145 and wind speeds plotted in Figure 146 are shown to be favorable for producing high concentrations near the source for all of the WRF simulations. PBL heights are high, greater or equal to 600 m, compared to the measured PBL heights of 170 m in the near-source region. Although all of the WRF-based maximum concentrations occur at about

the same wind speed, the AERC maxima occur at u_* values of about 0.11 m/s compared to the MMIF values of about 0.08 m/s (observation-based u_* values were about 0.06 m/s).

It appears in this case that the AERC simulation near-source results may be fortuitous. Both MMIF and AERC maxima occurred in highly unstable conditions at about the same wind speed and PBL height. Higher u_* in the AERC simulations resulted in increased plume spread that resulted in higher maximum concentrations in the near-source. The observation-based simulation near-source maxima occurred with lower PBL heights and lower u_* than the WRF-based simulations.

Table 13. Site C1 1-hour average statistics scores.

Year	Src.	Run	Geo Mean	Geo. St. Dev.	MG	VG	RHC	Geo. R	FF2	TMS
2011	1	obs	22.90	1.64	1.00	1.00	42.62	1.00	1.00	0.90
		AERC.RCALT	23.25	1.60	0.99	1.01	44.02	0.98	1.00	0.99
		AERC.RCALF	22.82	1.59	1.00	1.01	43.41	0.98	1.00	0.99
		MMIF.RCALF	18.57	2.16	1.23	1.20	44.76	0.92	0.86	0.88
		MMIF.RCALT	19.03	2.13	1.20	1.16	45.99	0.94	0.92	0.90
	2	obs	53.56	1.57	1.00	1.00	91.27	1.00	1.00	0.81
		AERC.RCALT	54.47	1.53	0.98	1.01	88.60	0.98	1.00	0.99
		AERC.RCALF	53.82	1.48	1.00	1.01	83.99	0.97	1.00	0.98
		MMIF.RCALF	44.54	1.90	1.20	1.12	84.81	0.93	0.94	0.92
		MMIF.RCALT	45.53	1.93	1.18	1.12	90.63	0.93	0.94	0.91
	3	obs	76.33	1.66	1.00	1.00	137.67	1.00	1.00	0.81
		AERC.RCALT	75.99	1.76	1.00	1.03	133.93	0.96	1.00	0.98
		AERC.RCALF	79.95	1.72	0.96	1.03	153.77	0.96	1.00	0.95
		MMIF.RCALF	67.49	2.02	1.13	1.14	135.53	0.89	0.92	0.89
		MMIF.RCALT	62.97	2.21	1.21	1.30	134.48	0.82	0.88	0.86
	4	obs	37.58	1.58	1.00	1.00	64.63	1.00	1.00	0.83
		AERC.RCALT	34.16	1.84	1.10	1.09	63.70	0.91	0.96	0.94
		AERC.RCALF	34.14	1.86	1.10	1.11	63.74	0.88	0.96	0.93
		MMIF.RCALF	24.58	2.90	1.53	2.09	63.05	0.81	0.86	0.76
		MMIF.RCALT	26.47	2.82	1.42	1.85	62.64	0.84	0.86	0.79
	5	obs	203.91	3.30	1.00	1.00	1214.21	1.00	1.00	0.80
		AERC.RCALT	235.84	3.09	0.87	1.08	1231.18	0.98	0.92	0.93
		AERC.RCALF	236.12	3.09	0.86	1.08	1234.44	0.98	0.92	0.94
		MMIF.RCALF	238.63	3.18	0.85	1.08	1229.09	0.98	0.94	0.94
		MMIF.RCALT	238.57	3.18	0.86	1.08	1226.75	0.98	0.94	0.94
2012	1	obs	18.40	2.31	1.00	1.00	44.65	1.00	1.00	0.86
		AERC.RCALT	17.56	2.64	1.05	1.03	43.26	0.99	0.98	0.97
		AERC.RCALF	17.13	2.73	1.07	1.06	41.33	0.99	0.96	0.96
		MMIF.RCALF	14.55	3.59	1.27	1.38	43.96	0.97	0.84	0.85
		MMIF.RCALT	14.72	3.44	1.25	1.29	45.00	0.98	0.84	0.87
	2	obs	42.13	2.21	1.00	1.00	89.88	1.00	1.00	0.81
		AERC.RCALT	39.85	2.47	1.06	1.03	87.34	0.99	0.98	0.97
		AERC.RCALF	38.68	2.55	1.09	1.05	82.20	0.99	0.98	0.96
		MMIF.RCALF	32.34	3.49	1.30	1.39	85.39	0.98	0.84	0.85
		MMIF.RCALT	33.95	3.15	1.24	1.24	88.30	0.98	0.86	0.88

Table 13, continued. Site C1 1-hour average statistics scores.

Year	Src.	Run	Geo Mean	Geo. St. Dev.	MG	VG	RHC	Geo. R	FF2	TMS
2012	3	obs	71.36	1.83	1.00	1.00	149.29	1.00	1.00	0.81
		AERC.RCALT	51.14	3.23	1.40	1.96	130.75	0.83	0.82	0.75
		AERC.RCALF	50.63	3.32	1.41	2.06	127.26	0.83	0.82	0.76
		MMIF.RCALF	35.43	6.25	2.02	13.94	131.36	0.71	0.74	0.60
		MMIF.RCALT	36.52	5.98	1.95	11.77	136.11	0.72	0.74	0.60
	4	obs	21.74	3.90	1.00	1.00	58.66	1.00	1.00	0.82
		AERC.RCALT	18.77	5.10	1.16	1.12	51.73	1.00	0.94	0.92
		AERC.RCALF	18.37	5.50	1.18	1.18	61.86	1.00	0.90	0.88
		MMIF.RCALF	12.29	10.08	1.77	3.90	57.34	0.98	0.74	0.69
		MMIF.RCALT	12.93	9.21	1.68	3.16	49.27	0.98	0.74	0.70
	5	obs	167.73	3.26	1.00	1.00	1193.22	1.00	1.00	0.80
		AERC.RCALT	213.14	3.11	0.79	1.11	1258.86	0.98	1.00	0.92
		AERC.RCALF	215.91	3.11	0.78	1.12	1248.61	0.98	1.00	0.93
		MMIF.RCALF	204.43	3.14	0.82	1.07	1235.46	0.99	1.00	0.95
		MMIF.RCALT	198.55	3.12	0.85	1.06	1243.41	0.99	1.00	0.95

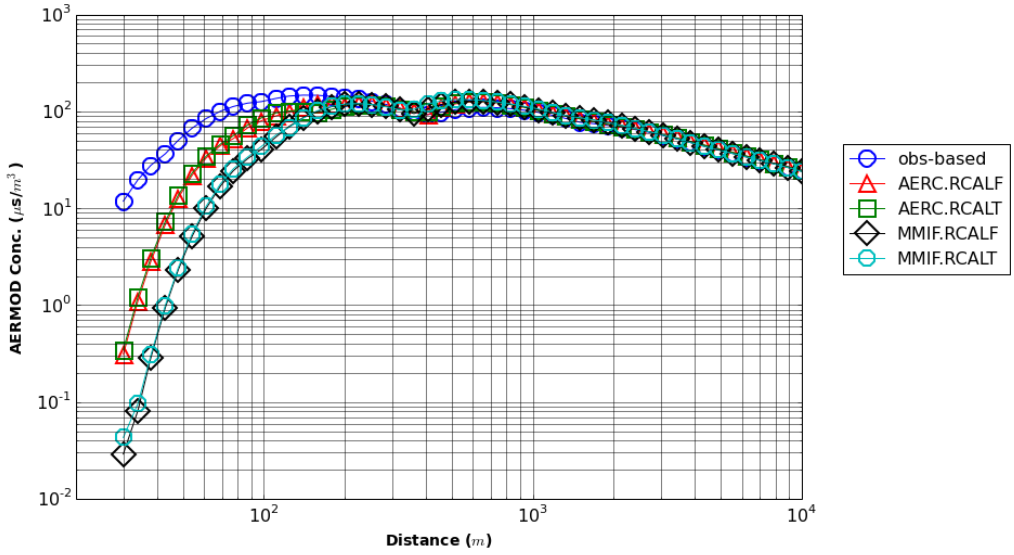

Figure 144. Concentration maxima vs. distance for Site C1, 2010, Source Group #3.

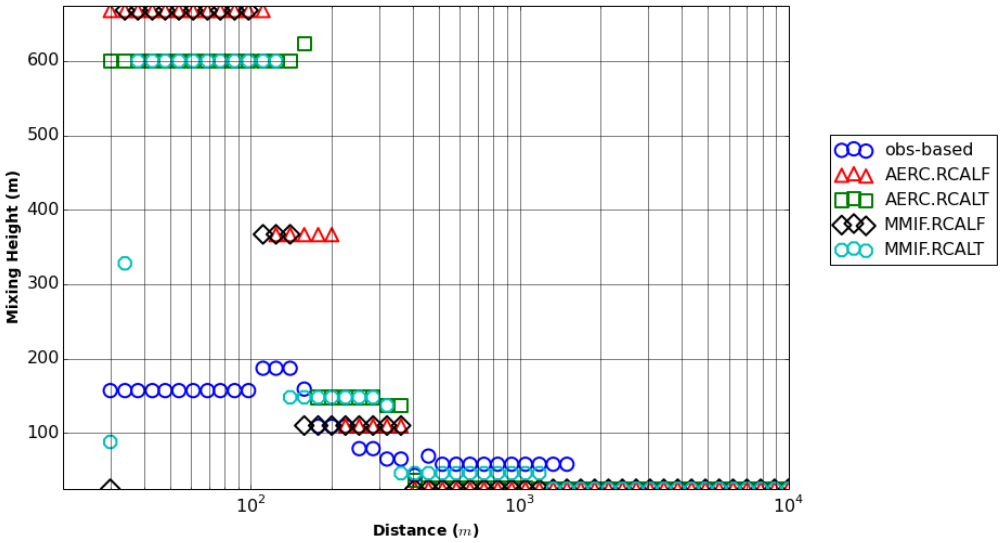

Figure 145. PBL height corresponding to concentration maxima, Site C1, 2011, Source Group #3.

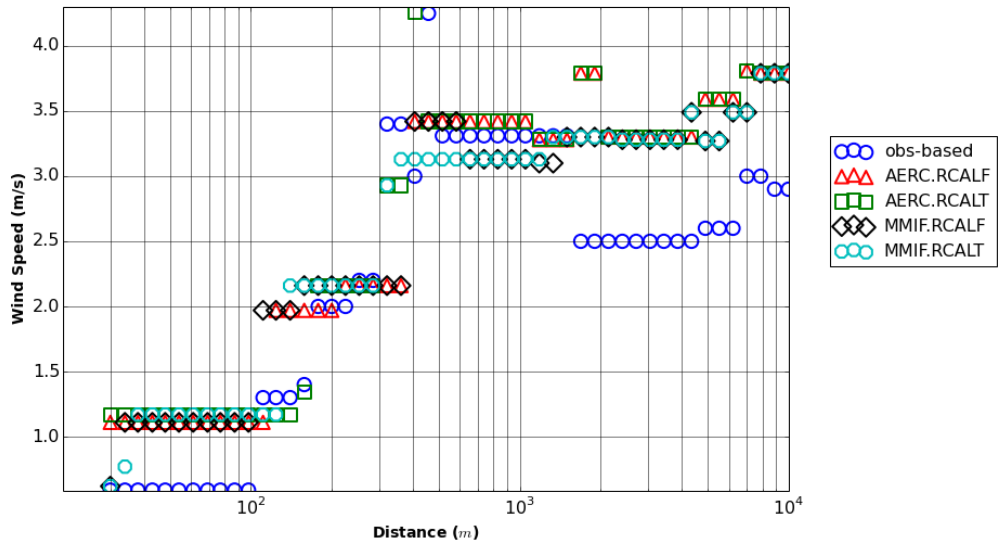

Figure 146. Wind speed corresponding to concentration maxima, Site C1, 2011, Source Group #3.

6.9 Site C2 Results

The site C2 statistical score results are listed in Table 14. The RCALT simulations produced more favorable results with an average TMS score of 0.86 compared to the RCALF TMS score of 0.78. Most simulations produced RHC scores that were accurate and slightly conservative, resulting in an overall average RHC 101% of corresponding observation-based RHC values. The maximum RHC value was 145% of the corresponding observation-based RHC for Source Group #4, 2010 RCALT simulations at site C2. The tall stack group, Source Group #4, resulted in the lowest TMS scores (0.64) compared to the other stack groups (0.80 to 0.97). The Source Group #1 simulations slightly underestimated RHC on average, resulting in an average RHC score 96% of the corresponding observation-based RHC scores while the other stack groups resulted in average RHC scores greater than observation-based RHC scores.

Table 14. Site C2 1-hour average statistics scores.

Year	Src.	Run	Geo Mean	Geo. St. Dev.	MG	VG	RHC	Geo. R	FF2	TMS
2010	1	obs	18.04	2.34	1.00	1.00	45.51	1.00	1.00	1.00
		AERC.RCALT	17.67	2.90	1.02	1.10	45.06	0.97	1.00	0.97
		AERC.RCALF	13.36	4.56	1.35	1.92	42.25	0.95	0.82	0.79
		MMIF.RCALF	13.09	4.66	1.38	2.02	42.46	0.95	0.76	0.79
		MMIF.RCALT	16.09	3.62	1.12	1.30	45.55	0.97	0.82	0.88
	2	obs	41.16	2.30	1.00	1.00	88.95	1.00	1.00	0.81
		AERC.RCALT	39.87	2.51	1.03	1.03	91.15	0.99	1.00	0.98
		AERC.RCALF	31.60	3.65	1.30	1.39	89.15	0.98	0.84	0.86
		MMIF.RCALF	31.34	3.83	1.31	1.46	90.76	0.98	0.82	0.85
		MMIF.RCALT	36.33	3.12	1.13	1.15	91.75	0.98	0.86	0.92
	3	obs	47.91	3.04	1.00	1.00	120.94	1.00	1.00	0.81
		AERC.RCALT	60.21	2.67	0.80	1.08	134.54	1.00	0.96	0.91
		AERC.RCALF	43.77	5.04	1.10	1.33	130.93	0.99	0.90	0.91
		MMIF.RCALF	42.05	5.52	1.14	1.49	130.10	0.99	0.88	0.88
		MMIF.RCALT	48.02	4.06	1.00	1.11	130.72	0.99	0.92	0.96
	4	obs	20.92	3.56	1.00	1.00	52.92	1.00	1.00	0.83
		AERC.RCALT	21.01	4.71	1.00	1.14	76.10	0.99	0.94	0.90
		AERC.RCALF	8.48	18.59	2.47	43.51	46.15	0.97	0.76	0.55
		MMIF.RCALF	8.81	15.31	2.38	25.88	45.74	0.95	0.74	0.63
		MMIF.RCALT	14.59	8.95	1.43	2.96	76.99	0.98	0.74	0.67
	5	obs	197.72	3.03	1.00	1.00	1164.51	1.00	1.00	0.80
		AERC.RCALT	216.21	3.07	0.92	1.01	1228.07	1.00	1.00	0.97
		AERC.RCALF	219.05	3.08	0.90	1.02	1229.25	1.00	1.00	0.98
		MMIF.RCALF	211.01	3.10	0.94	1.01	1225.01	1.00	1.00	0.99
		MMIF.RCALT	206.13	3.08	0.96	1.01	1224.13	1.00	1.00	0.99
2012	1	obs	15.12	2.77	1.00	1.00	41.90	1.00	1.00	0.88
		AERC.RCALT	11.86	4.22	1.27	1.34	40.58	0.98	0.78	0.85
		AERC.RCALF	9.27	6.02	1.63	2.76	36.82	0.95	0.76	0.72
		MMIF.RCALF	9.20	5.85	1.64	2.67	38.37	0.95	0.76	0.73
		MMIF.RCALT	11.29	4.60	1.34	1.52	42.99	0.98	0.78	0.81

Table 14, continued. Site C2 1-hour average statistics scores.

Year	Src.	Run	Geo Mean	Geo. St. Dev.	MG	VG	RHC	Geo. R	FF2	TMS
2012	2	obs	36.19	2.62	1.00	1.00	92.68	1.00	1.00	0.80
		AERC.RCALT	28.58	3.81	1.27	1.27	90.74	0.98	0.78	0.86
		AERC.RCALF	24.22	5.11	1.49	1.96	86.95	0.98	0.80	0.78
		MMIF.RCALF	23.86	5.02	1.52	1.94	91.43	0.98	0.80	0.78
		MMIF.RCALT	27.74	4.11	1.31	1.38	92.20	0.98	0.78	0.85
	3	obs	58.62	2.13	1.00	1.00	131.37	1.00	1.00	0.81
		AERC.RCALT	38.19	3.72	1.54	1.96	125.13	0.91	0.68	0.74
		AERC.RCALF	29.51	9.95	1.99	24.94	137.90	0.89	0.82	0.63
		MMIF.RCALF	30.66	8.86	1.91	16.22	135.46	0.90	0.82	0.66
		MMIF.RCALT	35.12	4.29	1.67	2.61	135.27	0.91	0.70	0.72
	4	obs	19.08	4.23	1.00	1.00	62.56	1.00	1.00	0.82
		AERC.RCALT	8.98	12.10	2.12	5.94	55.29	0.99	0.66	0.63
		AERC.RCALF	4.42	43.19	4.32	4042.10	51.89	0.93	0.70	0.56
		MMIF.RCALF	5.34	27.99	3.58	408.55	49.03	0.92	0.70	0.57
		MMIF.RCALT	8.16	13.16	2.34	8.78	53.37	0.98	0.64	0.62
	5	obs	191.96	3.09	1.00	1.00	1112.40	1.00	1.00	0.80
		AERC.RCALT	234.80	3.05	0.82	1.06	1106.07	0.99	1.00	0.95
		AERC.RCALF	235.54	3.05	0.82	1.07	1106.12	0.99	1.00	0.95
		MMIF.RCALF	203.59	3.08	0.94	1.02	1102.10	1.00	1.00	0.98
		MMIF.RCALT	201.47	3.08	0.95	1.01	1102.02	1.00	1.00	0.99

6.10 Far-Source Results

The results of this study have shown the highest concentrations typically occur immediately downwind of a source, generally within a kilometer of the stacks. Offshore air pollutant sources may be located a greater distance from shore. To address far-source model performance, the maximum concentrations at 10,000 m (the most distant ring of receptors from the stacks) were extracted for evaluation. The 1-hour averaging time simulation results are shown in Figure 147 - Figure 150.

The WRF 1-hour average simulations resulted in far-source concentrations that were accurate and slightly conservative on average That is, the simulations predicted concentrations that were similar and slightly higher than concentrations predicted by the observation-based simulations. In the far-source, there was little difference in results between AERC and MMIF simulations or RCALT and RCALF simulations. No simulations underpredicted concentration and site B2 and B3 simulations were the most conservative, resulting in overpredicted concentrations for all source groups. The overpredicted concentrations were likely due to the high frequency of minimum PBL heights predicted by WRF and MMIF at Sites B2 and B3. The high frequency provided more opportunities for high far-source concentrations.

The period-average simulations at 10,000 m, shown in Figure 151 - Figure 154, resulted in larger differences in WRF- and measurement-based AERMOD concentrations than found for the 1-hour average simulations maxima. For the period average simulations, the influence of stack height was less of a factor for simulation accuracy. There was little difference between the

RCALF and RCALT simulations at all Sites except C1. The C1 predictions were improved (values are nearer to the observation-based concentrations) using the MMIF rediagnosed mixing heights (RCALT). There was little noticeable difference between AERC and MMIF simulations. Site B2 and B3 maximum concentrations were overpredicted consistently. These results were consistent with the negative wind speed and PBL height bias at these sites.

The 2010 WRF-based C2 concentration predictions were less than the observation-based concentrations. WRF predicted lower wind speed on average at C2 which could account for the lower concentrations in the far-source due to the lower u_*.

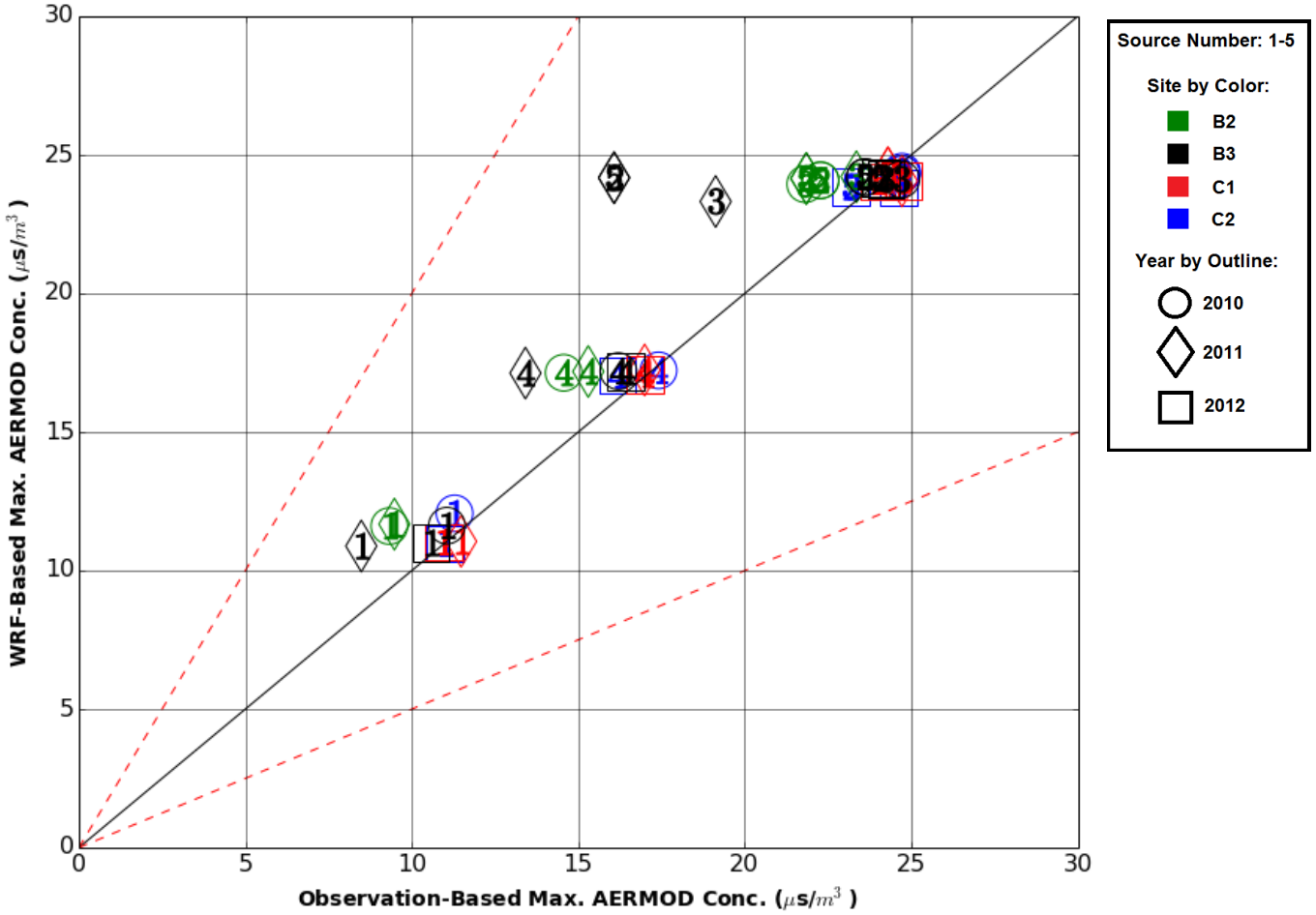

Figure 147. Far-source at 10,000 m 1-hour average maximum concentrations MMIF.RCALF simulations.

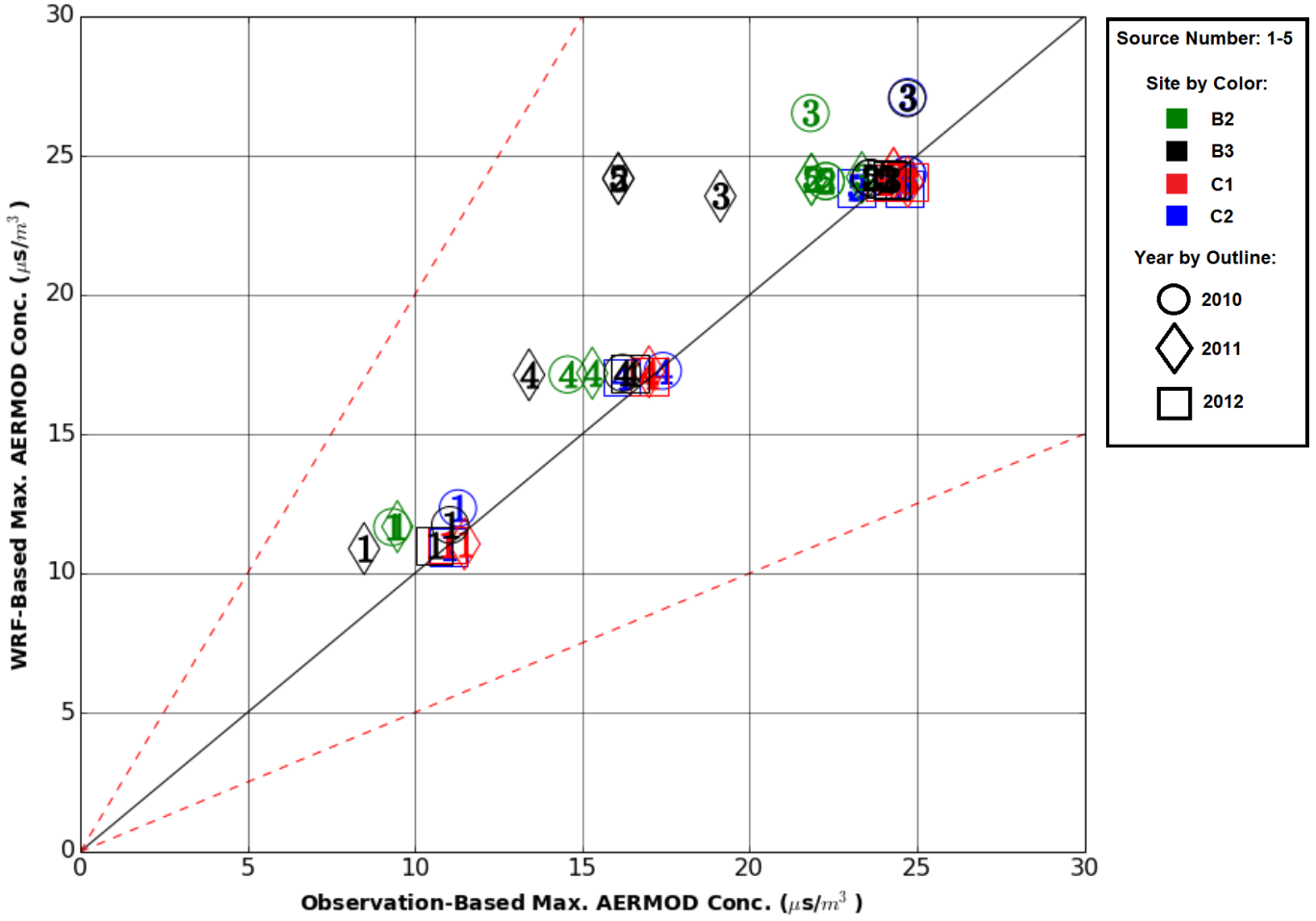

Figure 148. Far-source at 10,000 m 1-hour average maximum concentrations MMIF.RCALT simulations.

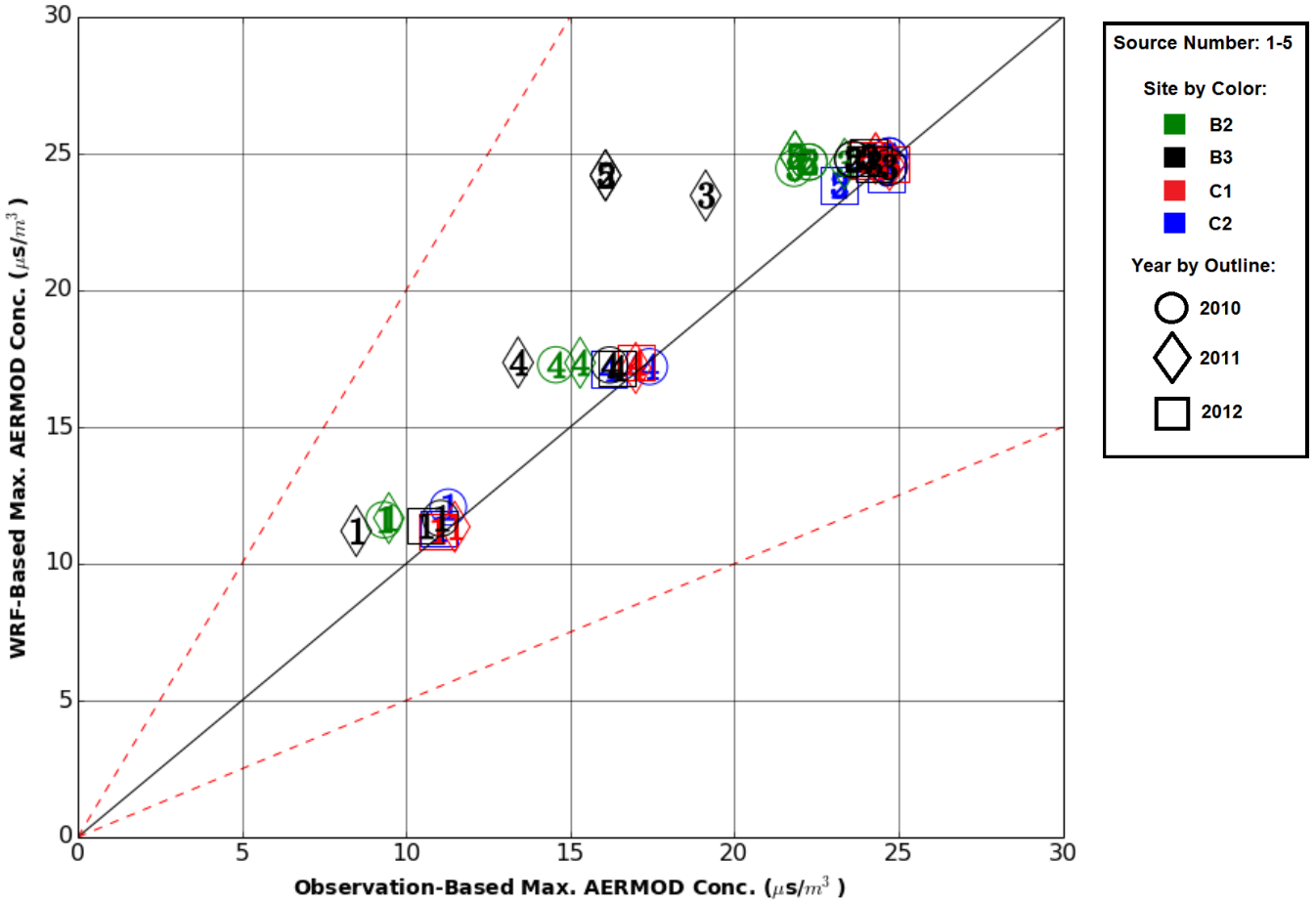

Figure 149. Far-source at 10,000 m 1-hour average maximum concentrations AERC.RCALF simulations.

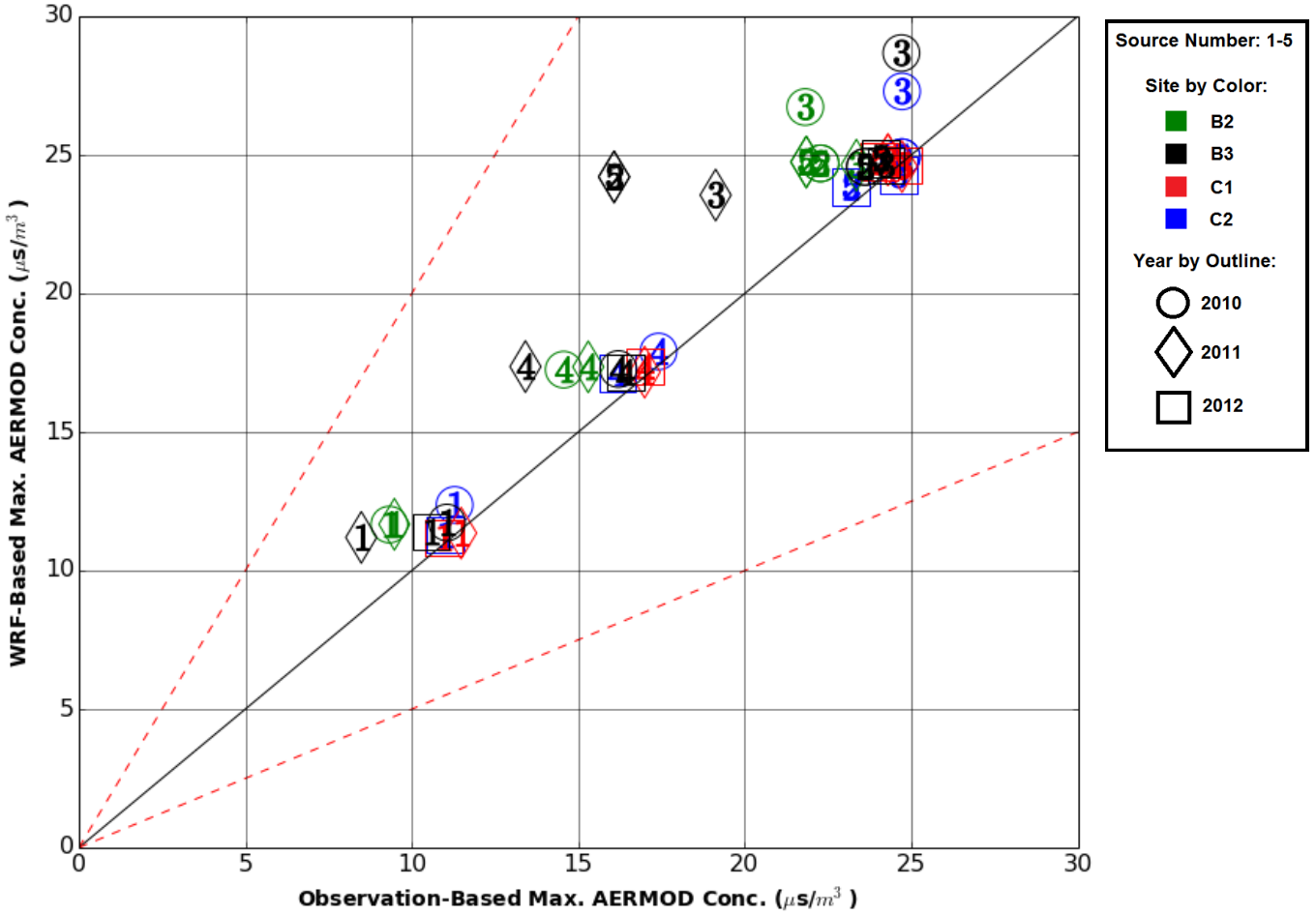

Figure 150. Far-source at 10,000 m 1-hour average maximum concentrations AERC.RCALT simulations.

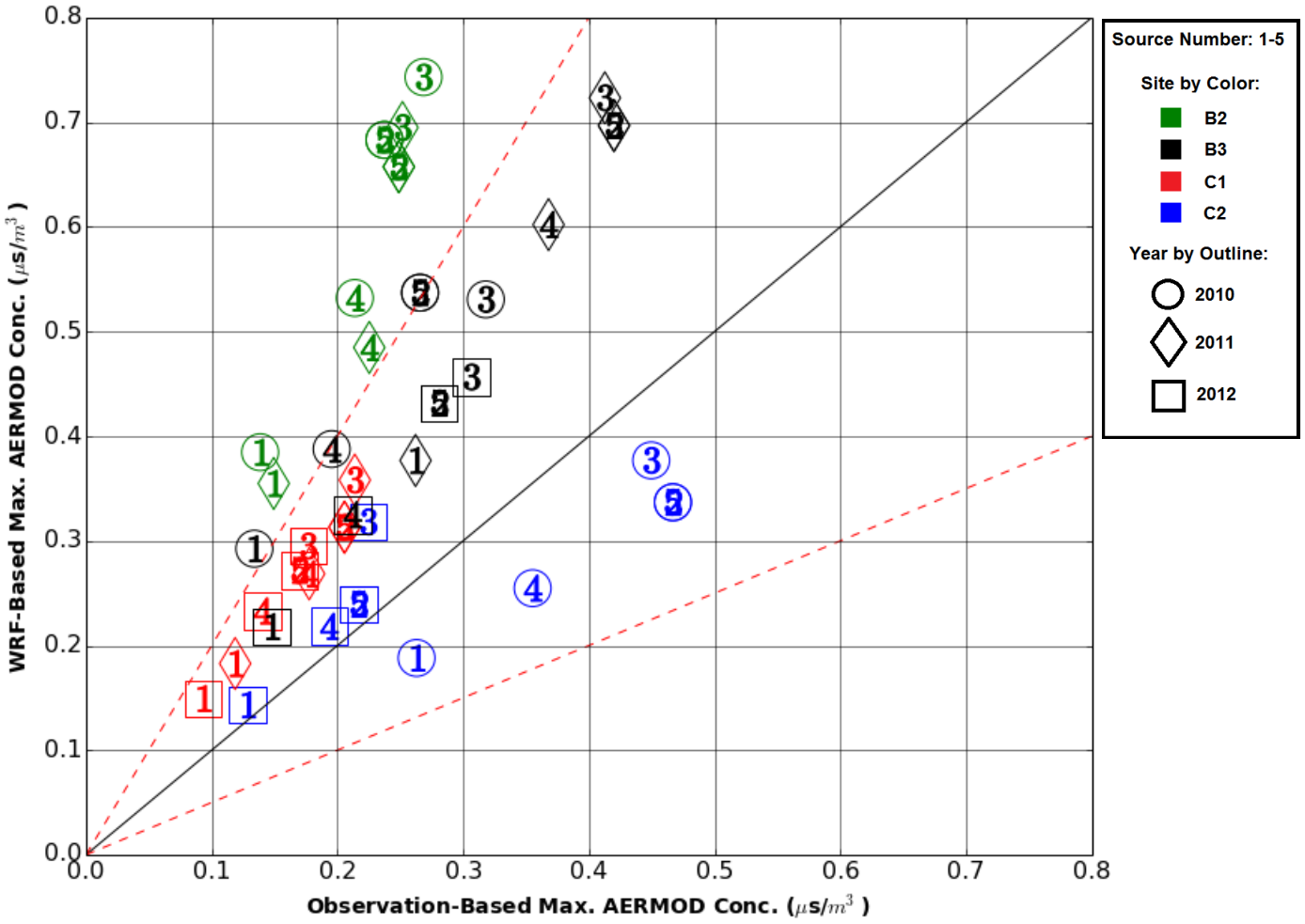

Figure 151. Far-source at 10,000 m Period average maximum concentrations for MMIF.RCALF simulations.

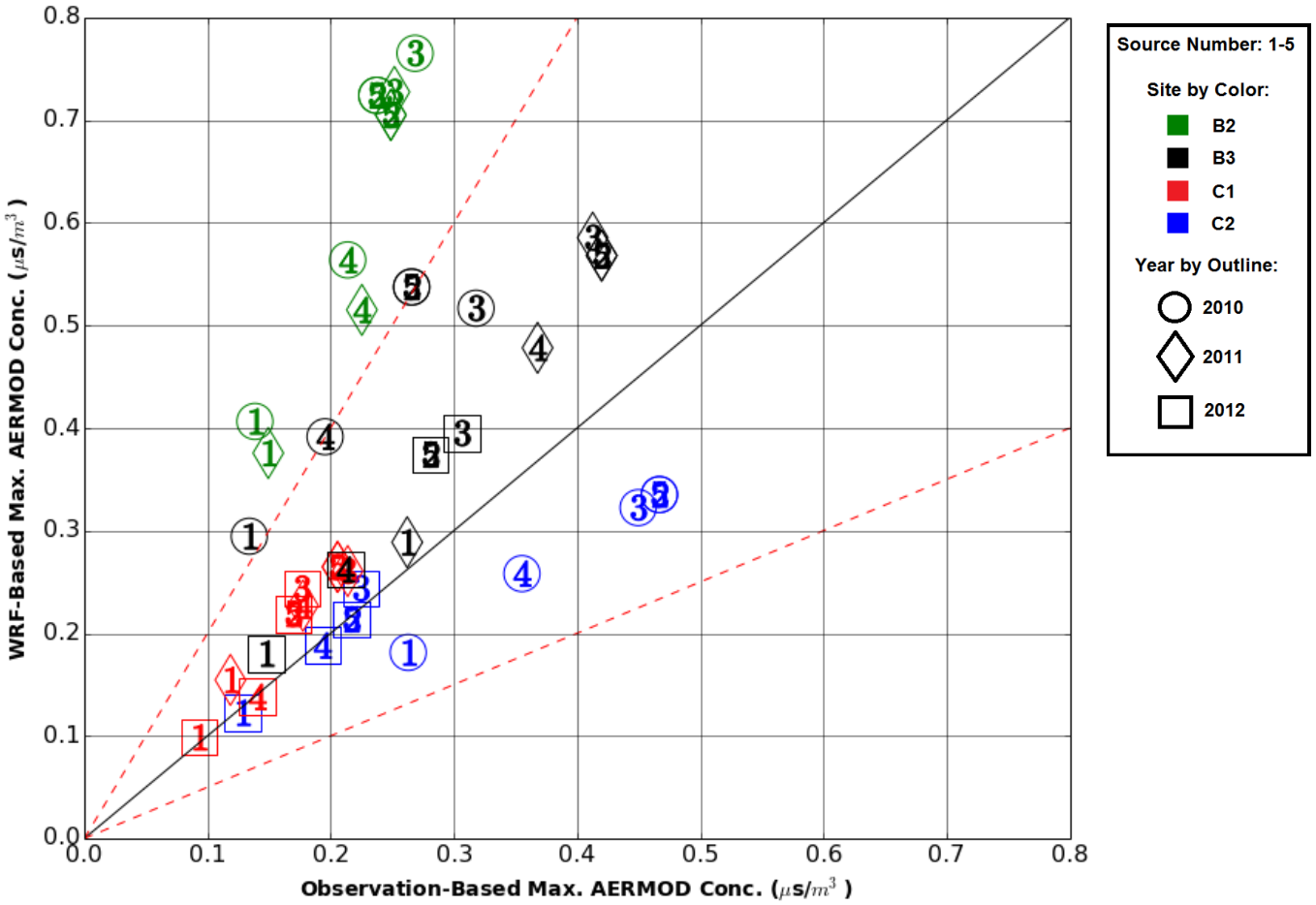

Figure 152. Far-source at 10,000 m Period average maximum concentrations for MMIF.RCALT simulations.

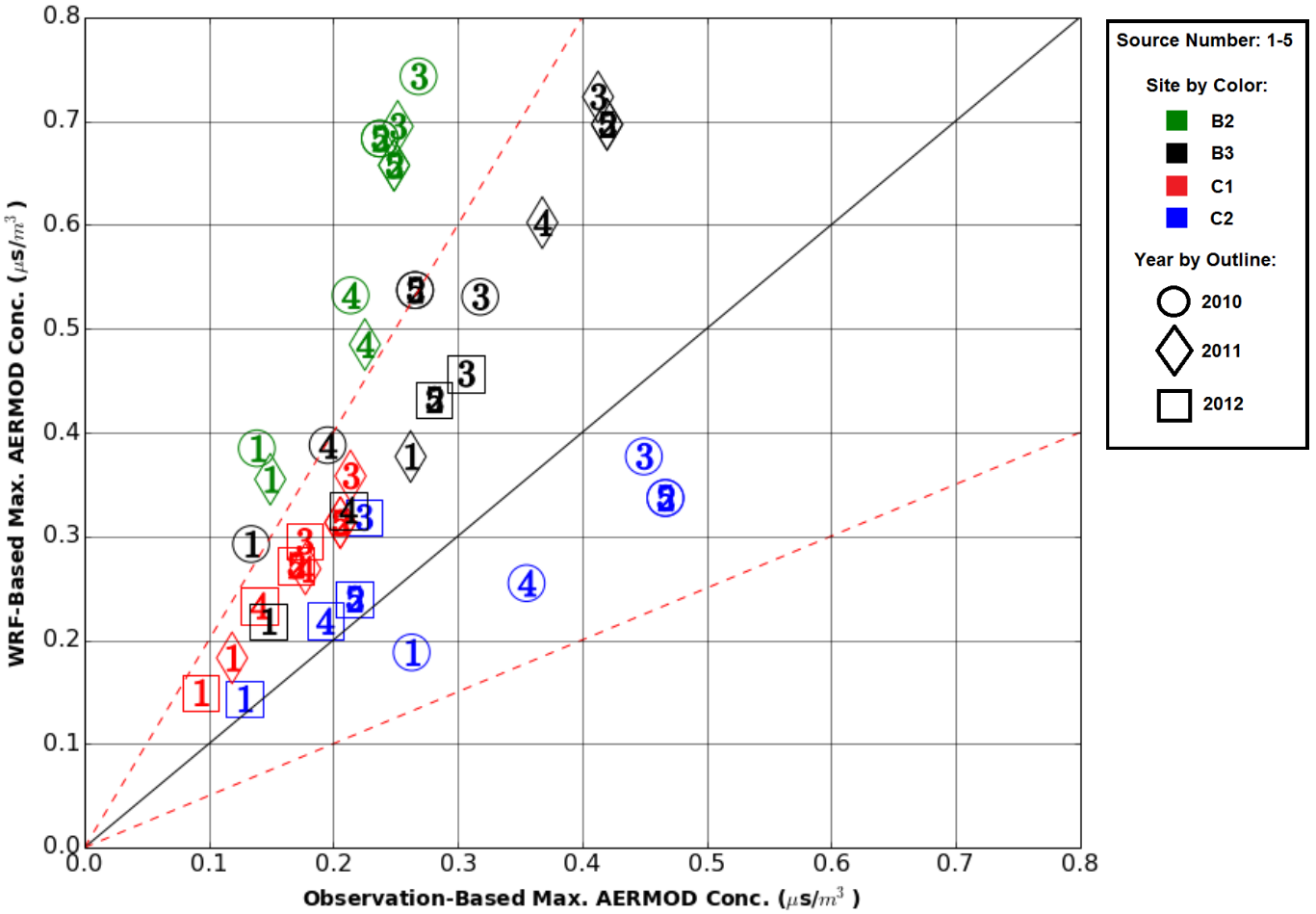

Figure 153. Far-source at 10,000 m Period average maximum concentrations for AERC.RCALF simulations.

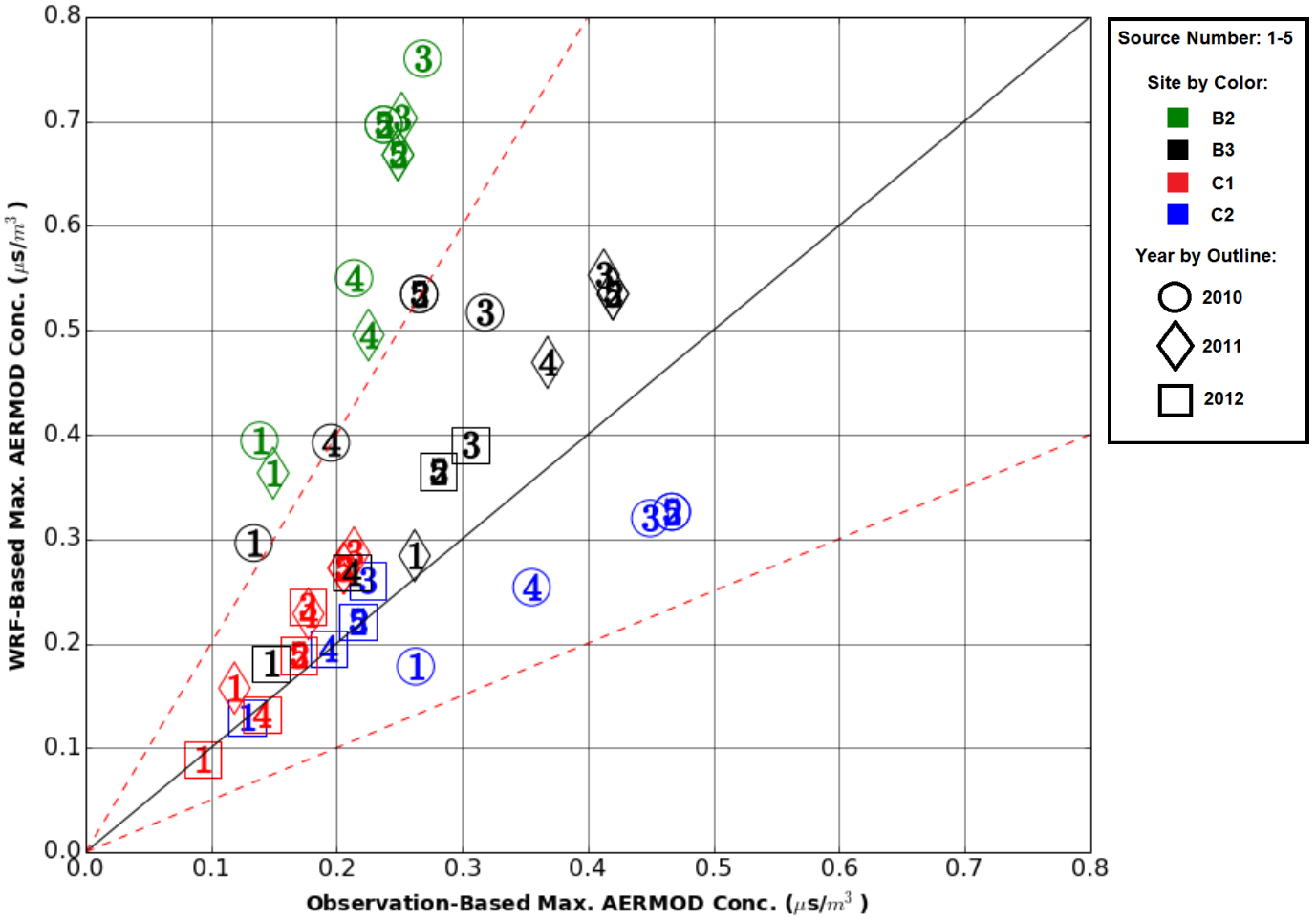

Figure 154. Far-source at 10,000 m Period average maximum concentrations for AERC.RCALT simulations.

[Blank]

7 CONCLUSIONS

The METSTAT and site-specific meteorological analyses suggest WRF was able to produce hourly meteorological datasets that compared favorably to land-based and overwater measurements. The regional METSTAT analyses found temperature and wind speed were within simple-terrain criteria for the majority of periods. Wind speed at overwater sites was biased high in October only. Overall, WRF meteorology at all four sites agreed with measured data, but with some biases. Average wind speed was underpredicted at all sites, more so at Beaufort buoy locations. PBL height was underpredicted on average. Minimum PBL heights (25 m) occurred too frequently in WRF results at the Beaufort buoy locations. WRF had a tendency to produce minimum PBL heights even during strongly unstable conditions when L was -5.0 m. It was found in these cases that although the local ASTD supported unstable conditions, a warm layer aloft prevented the growth of the PBL. The MMIF rediagnosed PBL height (RCALT) improved the PBL height predictions, especially at site B3.

Overall, most AERMOD concentration results using WRF meteorology were favorable, falling within a factor of two of the observation-based concentrations and producing RHC values that corresponded well with observation-driven AERMOD results. Maximum concentrations in the far-source (greater than 1,000 m) tended to be conservative. Maximum concentrations in the near-source (within 1,000 m) were underpredicted for the tall stack simulations (Source Groups #3 and #4) due to the persistence of overly stable conditions that prevented near-source mixing to the surface. Maximum concentrations tended to occur in the near-source anywhere from 100 m to 1,000 m. Near-source maxima tended to occur during unstable conditions characterized by higher PBL heights due to the increased rate of vertical mixing. The WRF-based concentration predictions of Source Group #5 (downwash cases) were consistently the most comparable to the observation-based predictions of all the source groups.

WRF-based AERMOD concentrations agreed better with observation-based concentrations at Sites C1 and C2 overall. This was mostly attributed to the fact that the WRF-MMIF RCALT PBL heights were used for the observation-based simulations. Site B2 consistently had the lowest FF2 scores of the four sites at all averaging periods due to the persistence of minimum PBL heights both in the RCALF and RCALT cases. The persistence of low PBL heights resulted in far-source period averages at B2 that were highly conservative resulting in RHC values that were more than a factor of two than the observation-based RHC values. Period average far-source RHC values at site C2 were underpredicted with respect to the observation-based RHC values, but still within a factor of two of the observation-based values.

The negative wind speed bias at sites B2 and B3 supported conservative maximum concentrations values in the far-source at long-term averaging periods due to the lower rate of diffusion associated with lower speeds. The MMIF recalculated PBL heights (RCALT) were more comparable than the WRF (RCALF) PBL heights to the observed PBL heights.

The main conclusions of the study are summarized as responses to the set of questions below:

- Is there a consistent bias across source type and/or location (e.g. Chukchi vs. Beaufort)? In particular are there any instances where the WRF simulations result in a bias towards underprediction compared to using the buoy observations?

  For the sources considered in this study, the absolute maximum concentrations occurred in the near-source during unstable conditions. There was no consistent bias at the Chukchi or Beaufort sites for maximum short term average concentrations. Prediction accuracy (with respect to observation-based predictions) was better at the Chukchi sites because the WRF-MMIF PBL heights were used for the observation-based simulations (no PBL height measurements were available for these sites). With respect to averaging time, the long-term period-averaged concentrations were underpredicted in some instances. For example, the simulations using the MMIF recalculated PBL heights underpredicted the long-term maximum concentrations at the site C2.

  The FF2 scores were persistently lower at site B2 than the other sites. Concentrations were typically overpredicted at this site in the far-source and underpredicted in the near-source due to the high frequency of minimum PBL height.

  WRF-based Source Group #4 simulations underpredicted concentration in the near-source consistently, with respect to observation-based simulations. It was found that the taller stack groups (Source Groups #3 and #4) were more sensitive to differences in meteorology than the other groups. Far-source tall-stack maximum concentrations were underpredicted in cases where PBL height was overpredicted. High PBL height corresponded to unstable conditions that promote vertical mixing. These conditions could therefore promote higher concentration maxima for tall stacks in the near-source but promote lower concentrations in the far-source. Near-source tall-stack concentrations were underpredicted when PBL height was underpredicted.

  The MMIF-rediagnosis (RCALT) of PBL height tended to improve WRF-based AERMOD performance by producing more accurate PBL heights.

- For locations where WRF performed better, does that ultimately translate to different dispersion model results?

  The short term maximum concentrations were less sensitive to bias in the WRF results. This was likely because the concentration maxima occurred during the extreme atmospheric stability conditions (either stable or unstable). The MMIF PBL height and *L* limits result in observation- and WRF-based meteorological simulations that are quite similar during the most extreme conditions.

  The long-term far-source maximum concentrations were the most sensitive to the meteorological bias over the period modeled. Underpredicted wind speeds at Sites B2 and B3 favored conservative period-averaged concentrations in the far-source. Site B2 period average far-source concentrations were highly conservative with RHC values greater than a factor of two of the observation-based concentrations.

It is highly recommended that FNMOC SST analysis, or a similar high-resolution SST dataset based on both remotely-sensed and in-situ measurements, be used instead of alternative datasets such as the NCEP RTG for simulations of open-water periods in the Beaufort Sea. The MacKenzie River warm-water outflow plume is a prevalent feature on the Beaufort Sea in summer. Low resolution SST analysis or excessive smoothing may result in erroneous air-sea temperature difference estimates. The FNMOC SST analyses gave a better spatial and temporal description of the SST distribution and gradient across the Beaufort Sea over the 2010-2012 periods analyzed.

- Did it make any difference when WRF predictions were processed by AERCOARE as opposed to directly for predictions of the surface energy fluxes?

  Overall, there was little discernable advantage in using AERCOARE. Considering average TMS, the “MMIF” runs (direct extraction from WRF without AERCOARE processing) resulted in slightly higher scores. Total average TMS was a fraction higher for AERC simulations at site C1 only (0.94 versus 0.84) The MMIF recalculation of PBL height (RCALT) has a much greater influence than AERCOARE processing on the accuracy of the simulations.

- Does it make any difference when PBL heights are rediagnosed by MMIF?

  Overall, maximum concentration results were more accurate and more conservative when the MMIF rediagnosis was applied.

  The concentration results from the shorter stack groups and downwash-affected sources were less sensitive to differences in the PBL height. If the plume is already near ground level, maximum concentrations at ground level will occur in the near-source and are less sensitive to the height of the PBL. Concentration maxima from taller stacks are much more sensitive to the PBL height. Note that the height of the tall stacks used in this study is near to the minimum PBL height (25 m). If the minimum PBL height was greater than the tallest stack, it is likely that concentration estimates would be more comparable.

Given the results of this study, a few recommendations can be made:

The use of WRF meteorology for AERMOD dispersion modeling resulted in similar concentrations compared to the measurement-based modeling. The WRF-based concentrations were within a factor-of-two of the predictions from the measured meteorology simulations. WRF tended to underpredict PBL height during unstable periods and underpredict wind speed. These biases, in general, contributed to overpredictions of concentration in the far-source (> 1 km). In the tall stack cases, these biases contributed to underprediction of concentration in the near-source. However, there was no scenario modeled in this study where the maximum RHC values predicted by WRF were underpredicted (in comparison to measurement-based RHC results) by more than a factor of two. This suggests WRF extracted meteorology can be used as an alternative to offshore observations for air permitting in such areas. It is likely that

near-source underprediction could be impeded if a higher minimum PBL height was applied.

The WRF simulated datasets should undergo considerable scrutiny prior to their application. We recommend at minimum, an evaluation against measurements in the offshore or coastal areas of the study domain using METSTAT. Comparisons of air-sea temperature difference to measurements should be made where possible.

The MMIF PBL height rediagnosis (RCALT) option should be applied to obtain more accurate and conservative maximum AERMOD predictions. The rediagnosis option provides a consistent way to define the PBL height as opposed to the multiple definitions used by the various WRF PBL schemes. In several instances the rediagnosed PBL heights also agreed more closely with observations and also resulted in conservative predicted maxima concentrations, despite a tendency to overpredict PBL height during unstable periods on average.

The downwash algorithm should be used where applicable. It is assumed that most offshore stacks will be mounted on ships or platforms that will form a wake. Concentration estimates using downwash were less sensitive to meteorological biases. Underprediction of concentration in the near-source will be prevented if downwash is accounted for.

There is no discernable benefit in using AERCOARE to process meteorology extracted from WRF. AERMOD results were similar overall with and without AERCOARE processing. The only exception might be when offshore sigma-theta observations are available. WRF does not provide either lateral or vertical turbulence parameters that might better characterize dispersion in some instances. However, in this study other differences between measured and simulated meteorology tended to mask the benefits of having such measurements.

A high resolution SST dataset is recommended to capture near-shore temperature gradients. Avoid using the coarse SST data typically available in the meteorological reanalysis datasets. In this study, the SST spatial gradients are high in the Beaufort Sea due to the prevalence of the Mackenzie River outflow plume. Due to the smoothing in the reanalysis datasets, the influence of the river plume affected a much larger area than suggested by buoy measurements and more refined SST datasets. This bias resulted in WRF predicting a different PBL structure than was observed in some cases.

When used by AERMOD, we recommend WRF-extracted meteorology be filtered to avoid extreme conditions not typically observed over water. In our study, we defined calm conditions as 0.5 m/s, required mixing heights to be greater than 25 m, and did not allow the absolute value of the Monin-Obukhov length (L) to be less than 5 m.

In conclusion, this study compared WRF meteorological predictions and WRF-driven AERMOD simulations to AERMOD applications prepared with measurements. Such datasets in the Arctic

are limited to a few locations, a couple seasons, and in some instances patched together with assumptions that were difficult to assess. WRF should be used to account for locations and seasons outside of the available datasets and the MMIF extractions likely provide a more robust and consistent meteorological database to simulate sources in the Arctic.

[Blank]

8 REFERENCES

AECOM Environment, 2009. *Reindeer Island Ambient Air Quality and Meteorological Monitoring Station Quality Assurance Project Plan,* Anchorage, Alaska: Prepared for Shell Exploration and Production Company.

Air Sciences Inc., 2010. *Chukchi and Beaufort Seas Oceanographic and Meteorological Monitoring Station Quality Assurance Project Plan,* Anchorage, Alaska: prepared for Shell Exploration and Production Company.

Air Sciences Inc., 2011. *Supplemental Outer Continental Shelf (OCS) Operating Permit Application, Shell Beaufort Sea, Alaska Exploratory Program: Conical Drilling Unit Kulluk, Attachment C: ENVIRON Profiler,* Anchorage: Shell Offshore Inc.

Arya, P., 1988. *Introduction to Micrometeorology.* London: Academic Press.

Brashers, B. & Emery, C., 2014. *The Mesoscale Model Interface Program (MMIF) Draft User's Manual,* Novato, CA: ENVIRON Int. Corp. Air Sciences Group, Prepared for U.S. EPA Air Quality Assessment Division.

Bridgers, G., 2011. *Model Clearinghouse Review of AERMOD-COARE as an Alternative Model for Application in an Arctic Marine Ice Free Environment.* Research Triangle Park(North Carolina): U.S. EPA.

Bromwich, D., Hines, K. & Bai, L.-S., 2009. Development and Testing of Polar WRF, Part 2: Arctic Ocean. *J. Geophys. Res.,* p. D08122.

Bromwich, D. et al., 2013. Comprehensive Evaluation of Polar Weather Research and Forecasting Performance in the Antarctic. *J. Geophys. Res.,* Volume 118, pp. 274-292.

Carsey, F., 1978. Character of Arctic PBL Structure as Determined by Acoustic Radar.. *AIDJEX Bulletin,* pp. 132-150.

Chen, F., Janjic, Z. & Mitchell, K., 1997. Impact of atmospheric surface layer parameterization in the new land-surface scheme of the NCEP Mesoscale Eta numerical model.. *Bound.-Layer Meteor.,* Volume 185, pp. 391-421.

Cimorelli, A. et al., 2004. *AERMOD: Description of Model Formulation,* s.l.: Environmental Protection Agency, EPA-454/R-03-004.

Cole, J. & Summerhays, J., 1979. A Review of Techniques Available for Estimation of Short-Term NO2 Concentrations. *Journal of the Air Pollution Control Association,* 29(8), pp. 812-817.

DiCristofaro, D. & Hanna, S., 1989. *OCD: The Offshore and Coastal Dispersion Model,* s.l.: Prepared for U.S. Dept. of Interior MMS, , Report #A085-1.

Emery, C., Tai, E. & Yarwood, G., 2001. *Enhanced meteorological modeling and performance evaulation for two Texas ozone episodes,* Novato, CA: Prepared for the Texas Nat. Res. Cons. Commission by ENVIRON Int. Corp..

ENVIRON Int. Corp., 2014. *METSTAT.* [Online]
Available at: http://www.camx.com/download/support-software.apx

EPA, 1998. *Interagency Workgroup on Air Quality Modeling (IWAQM) Phase 2 Summary Report and Recommendations for Modeling Long Range Transport Impacts,* Research Triangle Park, NC, EPA-454/R-98-019: U.S. EPA Office of Air Quality Planning and Standards.

Fairall, C. et al., 2003. Bulk Parameterization of Air-Sea Fluxes: Updates and Verification for the COARE Algorithm. *J. Climate,* Volume 16, pp. 571-591.

Garratt, J., 1992. *The Atmospheric Boundary Layer.* New York: Cambridge University Press.

Gryning, S. & Batchvarova, E., 2003. Marine atmospheric boundary-layer height estimated from NWP model output. *Int. Jour. of Environ. and Pollution,* pp. 147-153.

Hanna, S. et al., 1985. Development and Evaluation of the Offshore and Coastal Dispersion Model. *J. Air Poll. Contr. Assoc.,* Volume 35, pp. 1039-1047.

Hanrahan, P., 1999. The Plume Volume Molar Ratio Method for Determining NO2/NOx Ratios for Modeling, Part 1: Methodology. *Journal of the Air & Waste Management Association,* Volume 49, pp. 1324-1331.

Hines, K. & Bromwich, D., 2008. Development and testing of Polar WRF, Part 1: Greenland ice sheet meteorology.. *Mon. Wea. Rev.,* pp. 1971-1989.

Hines, K. et al., 2015. Sea ice enhancements to Polar WRF. *Mon. Wea. Rev., (in press).*

Hsu, S., 1988. *Coastal Meteorology.* San Diego: Academic Press, Inc..

Janjic, Z., 1994. The step-mountain eta coordinate model: further developments of the convection, viscous sublayer and turbulence closure schemes. *Mon. Weather Rev.,* Volume 122, pp. 927-945.

Kemball-Cook, S., Jia, Y., Emery, C. & Morris, R., 2005. *Alaska MM5 Modeling for the 2002 Annual Period to Support Visibility Modeling,* Novato, CA: Prepared for the Western Regional Air Partnership by ENVIRON Int. Corp..

Leavitt, E., Albright, M. & Baumann, R., 1978. Variations in Planetary Boundary Layer Parameters Observed During AIDJEX. *AIDJEX Bulletin,* Volume 39, pp. 149-163.

Louis, J., 1979. A Parameteric Model of Vertical Eddy Fluxes in the Atmosphere. *J. Atmos. Sci.,* Volume 35, pp. 187-202.

Mellor, G. & Yamada, T., 1982. Development of a turbulence closure model for geophysical fluid problems. *Rev. Geophys. Space Phys.,* Volume 20, pp. 851-875.

NCAR, 2014. *Weather Research & Forecasting (WRF) ARW Version 3 Modeling System User's Guide,* s.l.: Nat. Center for Atmos. Research Mesoscale & Meteorology Division.

NOAA-NCDC, 2014. *NOAA NCDC Integrated Surface Database.* [Online]
Available at: www.ncdc.noaa.gov/isd

Richmond, K. & Morris, R., 2012. *Evaluation of the Combined AERCOARE/AERMOD Modeling Approach for Offshore Sources,* s.l.: ENVIRON Int. Corp. Prepared for USEPA R.10, EPA-910-R-12-007.

Schulman, L., Strimaitis, D. & Scire, J., 2002. Development and Evaluation of the PRIME plume rise and building downwash model.. *Journal of the Air & Waste Management Association,* Volume 50, pp. 278-390.

Simmons, A., Uppala, S., Dee, D. & Kobayashi, S., 2006. ERA-Interim: New ECMWF reanalysis products from 1989 onwards.. *ECMWF Newsletter*, pp. 26-35.

SLR, Inc., 2011. *Quality Assurance Project Plan for the Endeavor Island (Endicott) Meteorological Monitoring Program,* Anchorage, Alaska: Prepared for Shell Offshore, Inc..

Stauffer, D., Seaman, N. & Binkowski, F., 1991. Use of four-dimensional data assimilation in a limited-area mesoscale model. Part II: effects of data assimilation within the planetary boundary layer. *Mon. Weather Rev.,* Volume 119, pp. 734-754.

US Navy, 2014. *Fleet Numerical Meteorology and Oceanography Center (FNMOC) Naval Oceanography Portal - Met. and Ocean. Products.* [Online]
Available at: http://www.usno.navy.mil/FNMOC/

USEPA, 2003. *AERMOD: Latest Features and Evaluation Results,* Research Triangle Park, NC: U.S. EPA, OAQPA, EPA-454/R-03-003.

USEPA, 2004a. *AERMOD: Description of model formulation,* Research Triangle Park, North Carolina: U.S. Environ. Protection Agency, EPA-454/R-03-004.

USEPA, 2004b. *User's Guide for the AERMOD Meteorological Preprocessor AERMET,* Research Triangle Park, North Carolina: U.S. Environ. Protection Agency, EPA-454/B03-002.

USEPA, 2004c. *User's Guide for the AMS/EPA Regulatory Model AERMOD,* Research Triangle Park, North Carolina: U.S. Environ. Protection Agency, EPA-454/B-03-001.

USEPA, 2012. *User's Manual AERCOARE Version 1.0,* Seattle, WA: U.S. Environ. Protection Agency Region 10, EPA-910-R-12-008.

USN, 2014. *Fleet Numerical Meteorology and Oceanography Center (FNMOC) Naval Oceanography Portal - Met. and Ocean. Products.* [Online]
Available at: http://www.usno.navy.mil/FNMOC/

Venkatram, A., 1980. Estimating the Monin-Obukhov Length in the Stable Boundary Layer for Dispersion Calculations. *Boundary Layer Meteor.,* Volume 19, pp. 481-485.

Vogelezang, D. & Holtslag, A., 1996. Evaluation and model impacts of alternative boundary-layer height formulations. *Boundary Layer Meteor.,* Volume 81, pp. 245-269.

Wilson, A., Bromwich, D., Hines, K. & Landis, C., 2009. *Enhancement of Polar WRF Arctic Atmospheric and Surface Processes..* 18-21 May 2009, Madison, WI, American Meteorological Society.

Wong, H., 2011. *COARE Bulk Flux Algorithm to Generate Hourly Meteorological Data for use with AERMOD.* Seattle(WA): U.S. EPA Region 10.

Wong, H., 2012. *(personal communication).* s.l.:s.n.

Xu, F. & Ignatov, A., 2010. Evaluation of in situ sea surface temperatures for use in the calibration and validation of satellite retrievals. *J. Geophys. Res.,* Volume 115, pp. 1-18.

APPENDIX A: TASK 3 PROTOCOL

Evaluate the AERMOD Performance Using Predicted or Measured Meteorology
Task 3 Protocol

AMEC RFP # 12-6480110233-TC-3902
Federal Prime Contract # EP-W-09-028

Prepared for:
AMEC Environment & Infrastructure, Inc.
502 W. Germantown Pike, Suite 850
Plymouth Meeting, PA 19462-1308
Attention: Thomas Carr

Prepared by:
ENVIRON International Corporation
773 San Marin Drive, Suite 2115
Novato, California, 94945
www.environcorp.com
P-415-899-0700
F-415-899-0707

July 2, 2013

ENVIRON

INTRODUCTION

The primary objective of the current study is to test and evaluate AERMOD on the outer continental shelf (OCS). The current modeling procedures for sources on land use the AERMOD modeling system. The meteorological AERMET processor included in the system is inappropriate for OCS sources because the energy fluxes over water are not strongly driven by diurnal heating and cooling. In addition, the meteorological observations necessary to drive the dispersion models are commonly not available, especially in the Arctic Ocean. For applications in the Arctic, the remote location and seasonal sea-ice pose logistical problems for the deployment of buoys or offshore measurement platforms.

This study evaluates a combined modeling approach where the meteorological variables are provided by a numerical weather prediction model, and then processed by a combination of a new Mesoscale Model Interface program (MMIF) and, optionally, AERCOARE (a replacement for AERMET suitable for overwater conditions). Given an appropriate overwater meteorological dataset, AERMOD can then be applied for New Source Review following the same procedures as used for sources over land.

The remainder of this document presents a protocol for Task 3 of the study. Task 3 generates a WRF meteorological dataset for 2009-2011 suitable for dispersion modeling in the Arctic, employs various combinations of MMIF and AERCOARE to extract modeled and observational meteorology overwater, and uses that to drive AERMOD simulations.

The modeling period in the current protocol is 2009-2011 allowing for one year of overlap with the BOEM/UAF 30-year WRF and Observational dataset. This overlapping period would allow for a “reanalysis vs. hind-cast” comparison. It also allows for an approximately 1.5 year overlap with the profiler data collected at Endeavor Island (Jun 2010 to Dec 2011). Extending the simulation and meteorological analysis through 2012 would provide an extra year of comparison with the profiler and may be considered if additional funding is available.

Task 3: Evaluate the use of WRF Solutions with AERMOD

AMEC and ENVIRON prepared a Work Plan outlining the various tasks and objectives of the current study. As directed by EPA and AMEC, the third task protocol includes additional information on data, options, and issues that were not fully described in the Work Plan. With an approved protocol, ENVIRON staff will perform the following subtasks:

Task 3a: Generate WRF simulations for calendar years 2009 through 2011.

For these simulations, ENVIRON has selected the National Center for Atmospheric Research’s (NCAR’s) community-developed WRF model (dynamical core version 3.4.1). WRF is a limited-area, non-hydrostatic, terrain-following eta-coordinate mesoscale model.

ENVIRON’s 3-year WRF simulation (2009-2011) will include 5.5 day simulation blocks (starting December 15th, 2008), with 12 hours overlapping to account for model spin-up. The spin-up time allows for the model to develop sub-grid scale processes, including vorticity and moisture fields. Given the high latitude, the domains are defined on a polar stereographic map projection. The outermost 36 km domain encompasses all of Alaska and parts of Northern Canada and Russia;

a 12 km nest including most of interior Alaska, the Bering, Chukchi, and Beaufort seas; and the 4 km nest focuses on the regions of the Chukchi and Beaufort seas containing active lease sites and the entirety of Alaska's North Slope (see Figure 1). EPA guidance recommends a 50 km buffer around CALPUFF sources and receptors, to allow for re-circulation of the puffs. Additionally, the first five grid points on the edge of a nested WRF grid are contaminated by the numerical down-scaling in WRF, and should not be used. Figure 2 illustrates 70 km (5 × 4km + 50km) buffers around the active lease areas with yellow dots (National Park Service, 2010).

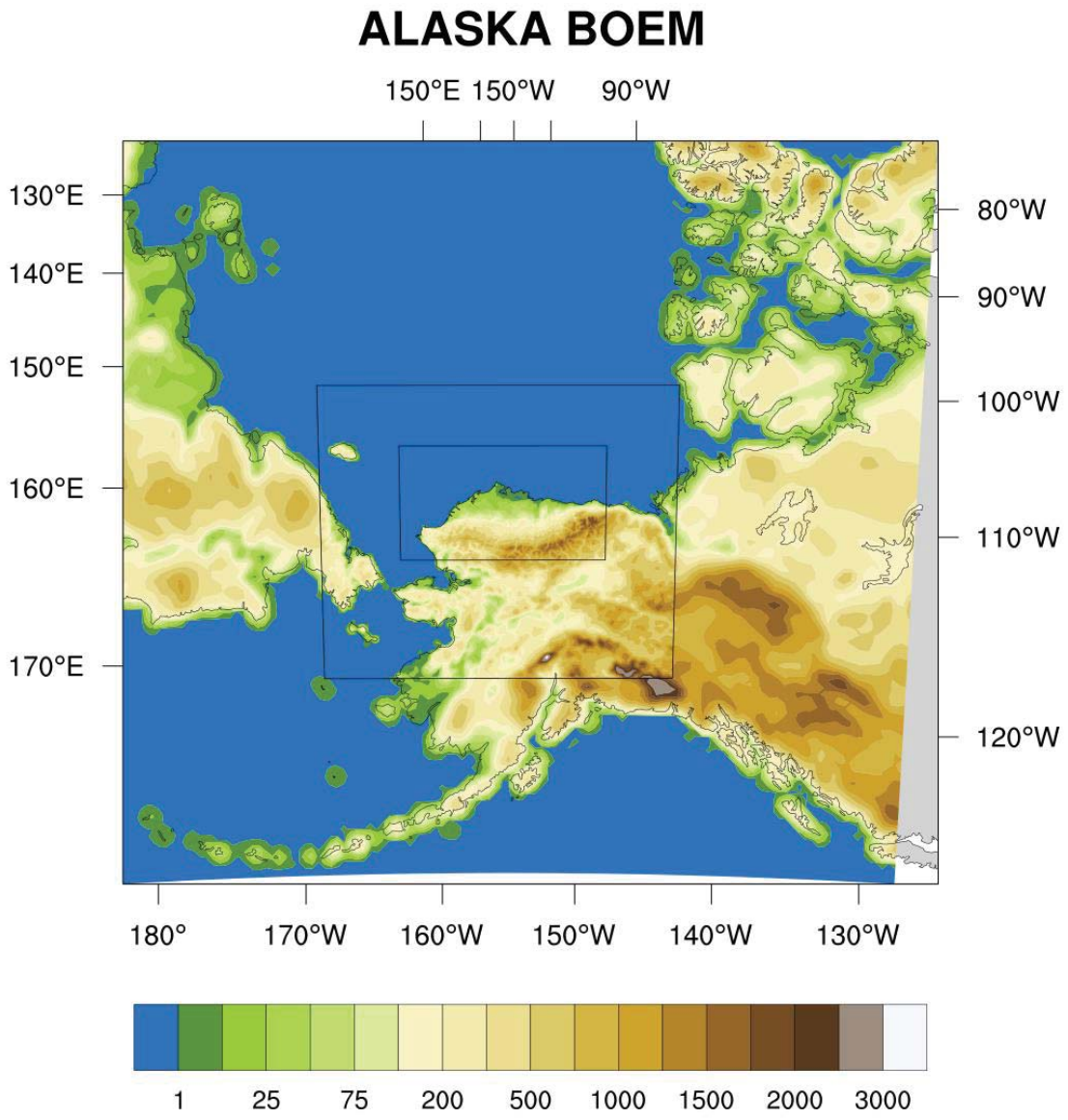

Figure 1. Proposed WRF 36km, 12km, and 4 km domains.

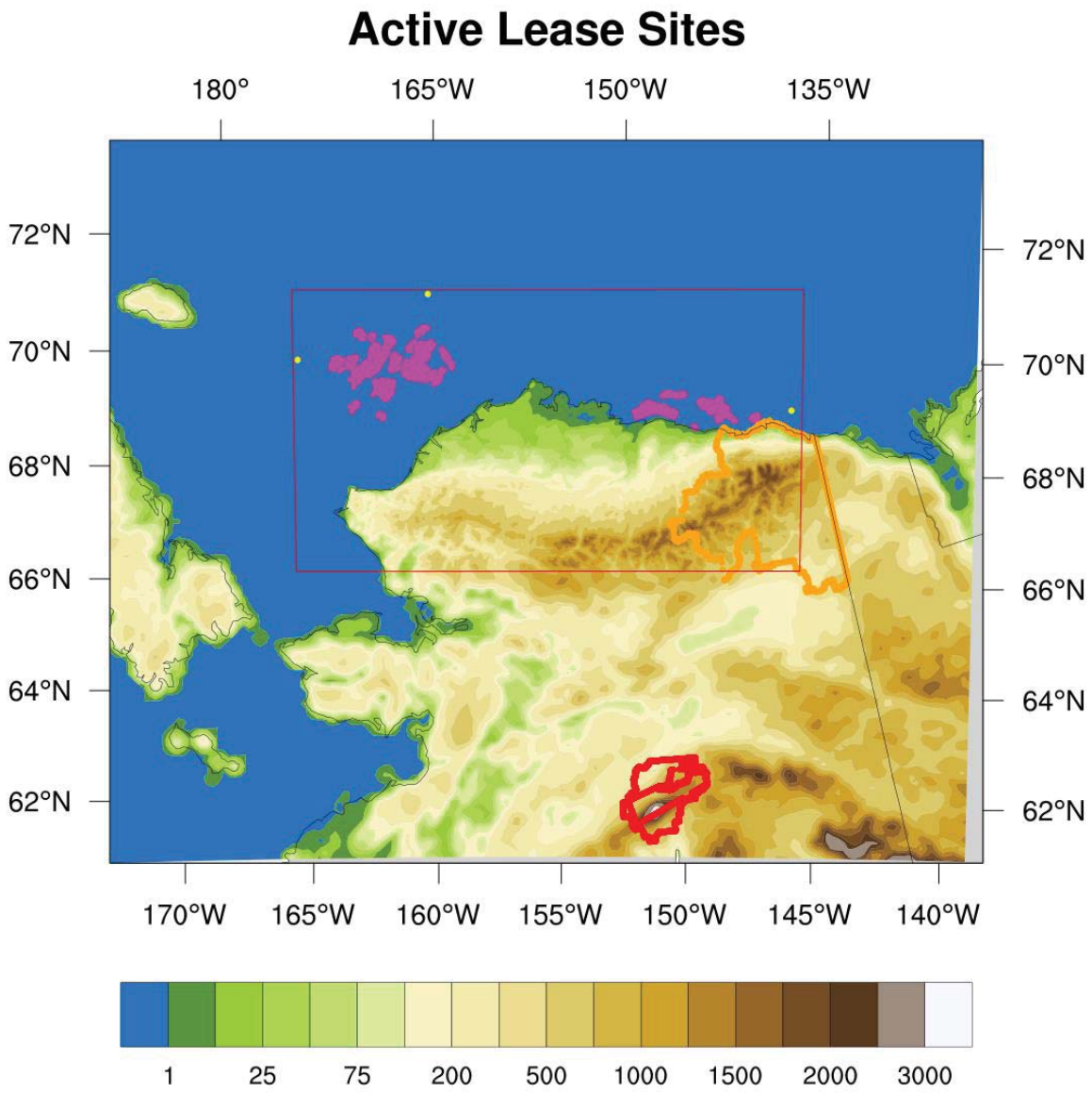

Figure 2. 12 km and 4 km WRF domains, with lease sites (magenta), the Arctic National Wildlife Refuge (orange), Class I Areas (red), and 70 km buffers from active lease sites (yellow dots).

The planned model vertical structure maintains the 37 vertical levels from the Task 2 WRF modeling. Layers are stacked toward the surface to capture the coastal boundary layer and sharp arctic wintertime temperature inversions (see Table 1). ENVIRON anticipates that the fine vertical spacing will help winds and temperatures respond more explicitly to dynamical influences.

Table 1. WRF model 37 vertical levels with approximate heights AGL.

Level	eta	Pressure (mb)	Level Height (m)	Mid-layer Height (m)	Layer Thickness (m)
1	1	1000	0.0		
2	0.9985	999	10.8	5.4	10.8
3	0.997	997	21.6	16.2	10.8
4	0.995	996	36.0	28.8	14.4
5	0.993	994	50.5	43.3	14.5
6	0.991	992	65.0	57.7	14.5
7	0.988	989	86.7	75.9	21.8
8	0.985	987	108.5	97.6	21.8
9	0.98	982	145.0	126.8	36.4
10	0.97	973	218.3	181.6	73.3
11	0.96	964	292.1	255.2	73.8
12	0.95	955	366.5	329.3	74.4
13	0.94	946	441.5	404.0	75.0
14	0.93	937	517.1	479.3	75.6
15	0.91	919	670.0	593.5	152.9
16	0.89	901	825.3	747.6	155.3
17	0.87	883	983.2	904.3	157.9
18	0.84	856	1225.0	1104.1	241.8
19	0.8	820	1557.1	1391.0	332.2
20	0.76	784	1901.3	1729.2	344.2
21	0.72	748	2258.5	2079.9	357.2
22	0.68	712	2630.0	2444.3	371.4
23	0.64	676	3016.9	2823.5	387.0
24	0.6	640	3421.0	3219.0	404.0
25	0.55	595	3952.7	3686.9	531.8
26	0.5	550	4518.1	4235.4	565.4
27	0.45	505	5122.3	4820.2	604.2
28	0.4	460	5771.8	5447.1	649.5
29	0.35	415	6475.0	6123.4	703.2
30	0.3	370	7242.8	6858.9	767.9
31	0.25	325	8090.5	7666.7	847.6
32	0.2	280	9039.1	8564.8	948.7
33	0.15	235	10120.5	9579.8	1081.4
34	0.1	190	11385.0	10752.8	1264.5
35	0.06	154	12585.4	11985.2	1200.4
36	0.027	124	13761.3	13173.4	1175.9
37	0	100	14907.1	14334.2	1145.8
Note: Calculated using P_0=1000mb, P_{top}=100mb, T_0=0.00C, and dT/dx=-6.5C/km.					

WRF must be optimized to simulate coastal arctic weather. To do this, ENVIRON's model configuration should include the most accurate initial inputs, regionally applicable physics choices, and effective nudging, combined with the best SST's, sea ice, and land surface models available. ENVIRON's WRF will build upon the successful application of WRF to reanalyze 30 years (1979-2009) of arctic meteorology prepared by BOEM-UAF specifically to study surface winds (Krieger, Zhang, Shulski, Fuhong, & Tao, 2012). UAF's method used data assimilation to generate hourly reanalyses. By contrast, ENVIRON proposes running WRF as a hind-cast, initializing the model from ECMWF reanalysis grids and running it for a 5.5-day period, using a combination of 3D analysis nudging and observational nudging. ENVIRON's approach is very similar to many other WRF model applications used to support photochemical grid modeling in many parts of the country.

Table 2 shows ENVIRON's proposed WRF hind-cast treatments relative to the BOEM-UAF reanalysis. The treatment of sea ice is critical to WRF modeling success. The BOEM-UAF reanalysis employs modifications from a variant of WRF named "Polar WRF (Byrd Polar Research Center, 2013) to the standard WRF package, which ENVRON also proposes to use. Although WRFv3.5 has been released, the Polar WRF modifications have not yet been made to v3.5, and ENVIRON proposes to use Polar WRFv3.4.1 instead.

ENVIRON will also improve upon the 24 km CMC sea ice by ingesting ~4 km gridded snow and sea ice dataset from the National Ice Center (NIC) Ice Mapping System (IMS) available post-2004 (National Ice Center, 2008). ENVIRON will employ the Morrison microphysics scheme, which was designed specifically for arctic applications but has documented success at mid-latitudes as well. ENVIRON concurs with the BOEM-UAF selection of the Rapid Radiative Transfer Model for GCMs (RRTMG) radiation option, Monin-Obukhov (Janjic) surface layer scheme, NOAH land surface model (with polar modifications), and the TKE-based Mellor-Yamada-Janjic (MYJ) planetary boundary layer scheme. Other ENVIRON sensitivity studies for stable boundary layers in Alaska (for a confidential client) and Wyoming (Hahn, Brashers, Emery, & McNally, 2012) indicated superior vertical profiles of temperature and moisture using MYJ compared to YSU and other planetary boundary layer schemes. The BOEM-UAF reanalysis employs the relatively un-tested Grell-3D cumulus scheme. ENVIRON performed sensitivity studies in the four corners region, and found the Grell-3D scheme produced extremely minimal convection during the summer compared to PRISM data. Thus, ENVIRON proposes to use the Kain-Fritch cumulus scheme on the 36 and 12 km domains, with explicit convection (no parameterized scheme) on the 4km domain. ENVIRON will update SST's daily, calculate the skin SST, and update deep soil temperatures following the usual WRF procedures.

Model inputs will use the ERA-interim European Center for Medium Range Weather Forecast's ERA-Interim dataset (ERA-I, 6-hourly analysis output, ~0.75^0x0.75^0 degree resolution). Traditionally, ENVIRON recommends 3-D nudging toward analysis grids for wind, temperature, and moisture for the 36 and 12 km domains. Analysis nudging within the PBL can prevent the natural, dynamic development of boundary layer processes. Therefore, ENVIRON's strategy

involves 3-D analysis nudging above the PBL for the 36km domain, and observational nudging against DS-3505[1] data on the 4km domain. 3-D analysis nudging of the 12 km using the 0.75° ERA-I data directly would likely degrade model performance. Recent ENVIRON experience with the WRF system's OBSGRID program in the data-sparse Four Corners region showed that model performance was degraded when analysis nudging with OBSGRID output was used.

Table 2. BOEM-UAF 30-year vs ENVIRON proposed Model Options

Treatment	BOEM-UAF REANALYSIS	ENVIRON 2009-2011
WRF Version	V3.2.1	V3.4.1
Snow/sea ice	BOEM modified version of Polar WRF codes for snow/sea ice processes	All Polar WRF modules
Boundary Conditions	ERA-Interim (0.75^0 grid spacing)	ERA-Interim (0.75^0 grid spacing)
Snow	Canadian Meteorological Centre (CMC) daily snow depth (24 km)	IMS 4-km NH daily snow
Sea Ice	AMSR-E daily sea ice concentration/thickness (12.5 km)	IMS 4-km NH daily (sea ice)
Microphysics	Morrison	Morrison
Radiation	RRTMG shortwave and longwave	RRTMG shortwave and longwave
Surface Layer	Monin-Obukhov (Janjic) scheme	Monin-Obukhov (Janjic) scheme
Land Surface Model	Noah with Polar WRF modifications	Noah with Polar WRF modifications
PBL	MYJ TKE	MYJ TKE
Cumulus	Grell-3D	Kain-Fritch (36/12km only)
Time-varying SST	On	On
Calculate skin SST	On	On
Update Deep Soil Temp	Yes	Yes
Fractional Sea Ice	Yes	IMS 4-km dataset
Tice2tsk_if2cold	True	True
Nudging	Spectral	Spectral (u, v, theta, geopotential, and moisture)
FDDA	Yes	No
Obs. nudging	No	Nudge toward DS-3505 data

[1] DS-3505 integrated surface hourly (ISH) worldwide station data includes extensive automated QC on all data and additional manual QC for USAF, NAVY, and NWS stations. It integrates all data from DS9956, DS3280, and DS3240. 10,000 currently active stations report wind speed and direction, wind gust, temperature, dew point, cloud data, sea level pressure, altimeter setting, station pressure, present weather, visibility, precipitation amounts for various tie periods, snow depth, and various other elements as observed by each station. (NOAA/NCDC, 2010)

Successful application of spectral nudging in the BOEM-UAF 30-year reanalysis dataset warrants an attempt in this study. Spectral nudging is relatively new in WRF, and ENVIRON proposes a limited nudging sensitivity test for February and August 2009 evaluating spectral versus analysis nudging (Table 3). Spectral nudging configurations will be guided by the parameters in Otte et al. (2012), that suggest limiting nudging above the tropopause and adopting a ~6 hour timescale. One other limited sensitivity study will be performed comparing analysis nudging both with and without using objectively analyzed input files during February and August 2009. ENVIRON will also perform observational nudging (winds only) using NCDC DS-3505 data on the 4 km domain, using a 50 km radius of influence. ENVIRON excludes nudging of temperature because in coastal areas it may weaken land-sea temperature contrasts and adversely affect model performance; the majority of North Slope observational assets reside along the coastline. Table 3 presents proposed relevant nudging parameters.

Table 3. Proposed WRF nudging coefficients

Nudging	Domains Applied	Nudging Strengths (1/s)		
		Wind	Temperature (no PBL)	Humidity (no PBL)
Spectral	36/12/4 km	~6 h timescale	~6 h timescale	~6 h timescale
3-D Analysis (if required)	36 km	3×10^{-4}	3×10^{-4}	3×10^{-4}
2-D Surface	None			
Observational	4 km	6×10^{-4}	None	None

The 2009-2011 WRF simulation will be subjected to a model performance evaluation using the METSTAT program to evaluate temperatures, winds, and humidity. METSTAT uses surface meteorological observations and extracted WRF data (paired in time and space) to calculate a series of statistical measures designed to examine WRF's ability to characterize the observations. ENVIRON will evaluate the model against as full an observed dataset as feasible, including DS-3505 data for 2009-2011 and the BOEM-UAF observational dataset for 2009 (extended as feasible) if obtained from UAF. Data contained in the BOEM-UAF dataset, but not in the DS-3505 data will serve as an independent verification of model performance as this data was not used for nudging. Additionally, the off-shore buoys analyzed in Task 1 represent independent verification as they are not contained in the DS-3505 dataset.

Additionally, ENVIRON will employ METSTAT to evaluate the single overlapping year, 2009, from the 30-year BOEM-UAF simulation. This will enable a direct comparison of the meteorology for that year.

Task 3b: Extract meteorological datasets using WRF solutions for sites with overwater observations in the Arctic

ENVIRON will extract WRF solutions from five buoy locations in the Arctic (two sites in the Chukchi Sea and three in the Beaufort Sea) as well as for the Endeavor Island profiler location

(Figure 3). As proposed in Task 1, ENVIRON will evaluate the four extractions and processing options as follows:

1. MMIF will be applied to extract and prepare data sets for direct use by AERMOD. All variables will be as-predicted by the WRF simulations including the surface energy fluxes, surface roughness and planetary boundary layer (PBL) height.
2. As in Option 1), but the PBL height will be re-diagnosed from the wind speed and potential temperature profiles using the Bulk-Richardson algorithm within MMIF. Based on the August to October 2010 monitoring data collected by Shell in the Beaufort Sea, PBL heights range from 10 m to 700 m, with a median height of 80 m. AERMOD simulations can be very sensitive to the PBL height (Richmond & Morris, 2012) and MMIF-processed PBL heights may provide significantly different predicted concentrations than the PBL height diagnosed by WRF.
3. MMIF will be applied to extract the key meteorological variables of overwater wind speed, wind direction, temperature, humidity, and PBL height. AERCOARE will use these variables to predict the surface energy fluxes, surface roughness length and other variables needed for the AERMOD simulations. AERCOARE has a surface layer scheme developed specifically to predict surface fluxes from overwater measurements. In this application, the WRF simulations provide model-derived alternatives for variables measured by a buoy, ship or offshore platform. AERCOARE can also be applied using a number of different options. For the current study, we propose to apply AERCOARE using the defaults recommended in the AECOARE model evaluations study (Richmond & Morris, 2012).
4. As in Option 3), but the PBL height will be re-diagnosed using the Bulk-Richardson algorithm within MMIF. AERCOARE will be applied as in Option 3.

Figure 3. Buoy sites in the Chukchi and Beaufort Seas; Endeavor Island profiler location.

Task 3c: AERCOARE using buoy and profiler data

ENVIRON will use surface input from the buoys in Figure 3 to drive AERCOARE. The buoys provide wind speed, wind direction, temperature (at various heights), relative humidity, and sea surface temperature.

The vertical temperature profiler at Endeavor Island will be used to extract hourly mixing heights from April 2010 (when the profiler was installed) through 2011. These mixing heights will be provided to AERCOARE to replace WRF-diagnosed and AERCOARE-diagnosed mixing heights options 3 and 4, respectively, of Task 3b.

Task 3d: AERMOD

ENVIRON will conduct AERMOD simulations for the six OCS hypothetical sources using the output from the modeling-based approaches (MMIF/AERCOARE as described in Task 3b) to drive AERMOD. These will be compared directly against AERMOD driven by the buoy and profiler extraction in Task 3c. Simulations involving AERCOARE will be confined to the open water time periods of 2009-2011, whereas MMIF/AERMOD runs will be performed for all months. The analysis will calculate the predicted concentrations over relevant averaging periods for the criteria pollutants (e.g., 1-hour, 8-hour, 24-hour, and period) for OCS sources. As in Task 1, the sources will be modeled at the buoy and profiler location, with a polar grid of receptors located along 360 equidistant radii at radial distances (30 m, 50 m, 75 m, 100 m, 125 m, 150 m,

175 m, 200 m, 300 m, 400 m, 500 m, 750 m, 1 km, 1.5 km, 2 km, 3 km, 4 km, 5 km, 6 km, 7 km, 8 km, 9 km, and 10 km) from the source.

Task 3e: AERMOD evaluation

ENVIRON will evaluate the model-driven AERMOD performance in Task 3d against the observationally-driven AERMOD runs using contour plots, scatter diagrams, Q-Q plots, and statistics as necessary.

Task 3f: Conclusion from evaluation

ENVIRON will diagnose how various aspects of the modeling procedures influenced the prediction of concentration (in particular maximum concentration) by assessing (1) the meteorology and modeling performance influence, (2) MMIF recalculated PBL height vs WRF PBL height, and (3) MMIF with AERCOARE or MMIF fed directly into AERMOD.

REFERENCES

NOAA/NCDC. (2010, 09 15). Retrieved 02 15, 2013, from http://www.ncdc.noaa.gov/oa/climate/rcsg/datasets.html#surface

Bowden, J. H., Otte, T. L., Nolte, C. G., & Otte, M. J. (2012). Examining interior grid nudging techniques using two-way nesting in the wrf model for regional climate modeling. *J. Climate, 25*, 2805-2823.

Byrd Polar Research Center. (2013, 03 06). *The Polar WRF*. Retrieved 06 24, 2013, from Ohio State University: http://polarmet.osu.edu/PolarMet/pwrf.html

Environ. (2010). *Evaluation of the COARE-AERMOD Alternative Modeling Approach Support for Simulation of Shell Exploratory Drilling Sources In the Beaufort and Chukchi Seas.*

Hahn, R., Brashers, B., Emery, C., & McNally, D. (2012). *Winter 2008 WRF Modeling of the Upper Green River Basin.* Novato, CA: ENVIRON.

Krieger, J., Zhang, J., Shulski, M., Fuhong, L., & Tao, W. a. (2012). *Toward Producing a Beaufort/Chukchi Seas Regional Reanalysis.* Retrieved 06 12, 2013, from Beaufort/Chukchi Seas Mesoscale Meteorology Modeling Study: http://mms-meso.gi.alaska.edu/pub/amss12-krieger-presentation.pdf

McNally, D., & Wilkinson, J. G. (2011). *Model Application and Evaluation: ConocoPhillips Chukchi Sea WRF Model Application.* Arvada, Colorado: Alpine Geophysics, LLC.

National Ice Center, 2008. u. (n.d.). *IMS daily Northern Hemisphere snow and ice analysis at 4 km and 24 km resolution.* Retrieved 06 18, 2013, from National Snow and Ice Data Center.: http://dx.doi.org/10.7265/N52R3PMC

National Park Service. (2010). *Federal Land Managers' Air Quality Related Values Work Group (FLAG) Phase 1 Report—Revised.* Retrieved 06 19, 2013, from http://www.nature.nps.gov/air/Pubs/pdf/flag/FLAG_2010.pdf

Otte, T. L., Otte, M. J., Bowden, J. H., & Nolte, C. G. (2012). *Sensitivity of Spectral Nudging Toward Moisture.* US Environmental Protection Agency.

Richmond, K., & Morris, R. (2012, 10). *Evaluation of the Combined AERCOARE/AERMOD Modeling Approach for Offshore Sources.* Retrieved 06 19, 2013, from EPA: http://www.epa.gov/ttn/scram/models/relat/aercoare/AERCOARE-Model-Evaluation.pdf

Zhang, J. (2011). *Beaufort and Chukchi Seas Mesoscale Meteorology Model Study.*

APPENDIX B: AERMOD RESULTS STATISTICAL SCORES

AERMOD results statistical scores: 1-hour average concentrations.

site	year	source	avg time	Simulation type	geo mean	geo stddev	MG	VG	RHC	geo R	ff2	TMS
B2	2010	1	1hr	obs	17.20	2.57	1.00	1.00	50.02	1.00	1.00	0.90
B2	2010	1	1hr	AERC.RCALT	7.38	9.31	2.33	19.93	41.24	0.85	0.70	0.57
B2	2010	1	1hr	AERC.RCALF	7.68	8.73	2.24	15.04	39.17	0.86	0.72	0.61
B2	2010	1	1hr	MMIF.RCALF	7.90	8.38	2.18	13.84	38.67	0.85	0.72	0.62
B2	2010	1	1hr	MMIF.RCALT	7.96	8.59	2.16	14.83	40.47	0.84	0.72	0.61
B2	2010	2	1hr	obs	42.74	2.31	1.00	1.00	101.31	1.00	1.00	0.80
B2	2010	2	1hr	AERC.RCALT	18.58	8.53	2.30	18.59	87.11	0.86	0.76	0.59
B2	2010	2	1hr	AERC.RCALF	19.75	7.56	2.16	11.37	86.14	0.87	0.76	0.63
B2	2010	2	1hr	MMIF.RCALF	19.85	7.46	2.15	11.28	85.99	0.86	0.76	0.63
B2	2010	2	1hr	MMIF.RCALT	20.63	7.58	2.07	11.04	88.59	0.86	0.76	0.63
B2	2010	3	1hr	obs	65.40	2.40	1.00	1.00	190.48	1.00	1.00	0.81
B2	2010	3	1hr	AERC.RCALT	29.37	10.84	2.23	42.05	170.50	0.80	0.72	0.58
B2	2010	3	1hr	AERC.RCALF	27.37	10.90	2.39	46.94	166.69	0.81	0.72	0.59
B2	2010	3	1hr	MMIF.RCALF	17.70	17.44	3.69	1078.48	133.95	0.73	0.68	0.50
B2	2010	3	1hr	MMIF.RCALT	18.39	17.58	3.56	1092.87	138.34	0.72	0.66	0.53
B2	2010	4	1hr	obs	22.75	4.47	1.00	1.00	79.69	1.00	1.00	0.82
B2	2010	4	1hr	AERC.RCALT	2.24	111.84	10.14	>5000	86.05	0.80	0.60	0.49
B2	2010	4	1hr	AERC.RCALF	1.72	113.43	13.21	>5000	47.48	0.81	0.62	0.41
B2	2010	4	1hr	MMIF.RCALF	1.78	90.33	12.81	>5000	45.01	0.77	0.60	0.48
B2	2010	4	1hr	MMIF.RCALT	2.35	89.86	9.70	>5000	79.21	0.79	0.60	0.41
B2	2010	5	1hr	obs	237.59	3.27	1.00	1.00	1224.60	1.00	1.00	0.80
B2	2010	5	1hr	AERC.RCALT	247.27	3.09	0.96	1.01	1131.49	1.00	1.00	0.98
B2	2010	5	1hr	AERC.RCALF	247.71	3.08	0.96	1.01	1131.49	1.00	1.00	0.99
B2	2010	5	1hr	MMIF.RCALF	253.77	3.23	0.94	1.01	1221.71	1.00	1.00	0.97
B2	2010	5	1hr	MMIF.RCALT	253.77	3.23	0.94	1.01	1221.71	1.00	1.00	0.98

site	year	source	avg time	Simulation type	geo mean	geo stddev	MG	VG	RHC	geo R	ff2	TMS
B2	2011	1	1hr	obs	10.67	5.43	1.00	1.00	48.74	1.00	1.00	0.87
B2	2011	1	1hr	AERC.RCALT	14.05	3.39	0.76	1.42	42.31	0.99	0.82	0.83
B2	2011	1	1hr	AERC.RCALF	9.00	7.00	1.19	1.53	42.08	0.95	0.88	0.86
B2	2011	1	1hr	MMIF.RCALF	9.94	6.62	1.07	1.40	45.18	0.95	0.90	0.89
B2	2011	1	1hr	MMIF.RCALT	14.13	3.72	0.76	1.32	45.63	0.99	0.86	0.87
B2	2011	2	1hr	obs	30.51	3.98	1.00	1.00	116.19	1.00	1.00	0.80
B2	2011	2	1hr	AERC.RCALT	32.28	3.30	0.95	1.06	89.03	1.00	1.00	0.93
B2	2011	2	1hr	AERC.RCALF	20.56	6.85	1.48	2.13	85.86	0.94	0.82	0.77
B2	2011	2	1hr	MMIF.RCALF	22.43	6.37	1.36	1.78	90.39	0.95	0.84	0.81
B2	2011	2	1hr	MMIF.RCALT	32.11	3.59	0.95	1.04	90.33	0.99	1.00	0.98
B2	2011	3	1hr	obs	64.45	2.88	1.00	1.00	186.80	1.00	1.00	0.81
B2	2011	3	1hr	AERC.RCALT	30.24	6.54	2.13	6.81	122.01	0.83	0.68	0.56
B2	2011	3	1hr	AERC.RCALF	14.68	19.57	4.39	3469.96	122.01	0.64	0.58	0.49
B2	2011	3	1hr	MMIF.RCALF	17.12	16.42	3.77	958.47	130.24	0.65	0.62	0.49
B2	2011	3	1hr	MMIF.RCALT	29.14	7.68	2.21	11.02	138.14	0.81	0.70	0.60
B2	2011	4	1hr	obs	10.60	16.71	1.00	1.00	84.14	1.00	1.00	0.82
B2	2011	4	1hr	AERC.RCALT	11.40	8.78	0.93	1.92	46.12	0.98	0.76	0.75
B2	2011	4	1hr	AERC.RCALF	3.02	45.55	3.51	199.55	45.36	0.87	0.66	0.56
B2	2011	4	1hr	MMIF.RCALF	3.61	34.86	2.93	62.10	46.62	0.88	0.60	0.56
B2	2011	4	1hr	MMIF.RCALT	10.95	10.06	0.97	1.54	62.37	0.99	0.76	0.82
B2	2011	5	1hr	obs	220.04	3.26	1.00	1.00	1135.76	1.00	1.00	0.80
B2	2011	5	1hr	AERC.RCALT	237.45	3.00	0.93	1.02	1021.43	1.00	1.00	0.96
B2	2011	5	1hr	AERC.RCALF	237.53	2.99	0.93	1.02	1021.43	1.00	1.00	0.98
B2	2011	5	1hr	MMIF.RCALF	220.92	3.01	1.00	1.01	1017.11	1.00	1.00	1.00
B2	2011	5	1hr	MMIF.RCALT	218.45	2.99	1.01	1.01	1008.37	1.00	1.00	0.99
B3	2010	1	1hr	obs	12.54	4.47	1.00	1.00	47.32	1.00	1.00	0.86
B3	2010	1	1hr	AERC.RCALT	26.79	1.50	0.47	7.59	44.94	0.79	0.76	0.62

site	year	source	avg time	Simulation type	geo mean	geo stddev	MG	VG	RHC	geo R	ff2	TMS
B3	2010	1	1hr	AERC.RCALF	25.74	1.50	0.49	6.94	41.33	0.81	0.76	0.62
B3	2010	1	1hr	MMIF.RCALF	21.14	1.88	0.59	3.08	40.89	0.95	0.80	0.73
B3	2010	1	1hr	MMIF.RCALT	21.93	1.96	0.57	2.98	44.56	0.95	0.80	0.72
B3	2010	2	1hr	obs	34.58	3.41	1.00	1.00	96.26	1.00	1.00	0.80
B3	2010	2	1hr	AERC.RCALT	57.85	1.47	0.60	3.47	90.62	0.71	0.80	0.67
B3	2010	2	1hr	AERC.RCALF	54.89	1.51	0.63	2.95	83.60	0.80	0.80	0.70
B3	2010	2	1hr	MMIF.RCALF	46.38	1.75	0.75	1.85	82.83	0.94	0.84	0.81
B3	2010	2	1hr	MMIF.RCALT	48.48	1.77	0.71	1.90	87.36	0.93	0.84	0.79
B3	2010	3	1hr	obs	50.37	3.59	1.00	1.00	157.18	1.00	1.00	0.81
B3	2010	3	1hr	AERC.RCALT	84.50	1.61	0.60	3.68	139.96	0.68	0.82	0.65
B3	2010	3	1hr	AERC.RCALF	76.22	1.72	0.66	2.86	142.12	0.76	0.82	0.71
B3	2010	3	1hr	MMIF.RCALF	63.99	2.07	0.79	1.55	122.45	0.96	0.86	0.82
B3	2010	3	1hr	MMIF.RCALT	72.18	1.90	0.70	1.91	125.70	0.93	0.84	0.79
B3	2010	4	1hr	obs	10.63	14.23	1.00	1.00	62.18	1.00	1.00	0.82
B3	2010	4	1hr	AERC.RCALT	40.30	1.74	0.26	1117.46	68.67	0.72	0.72	0.52
B3	2010	4	1hr	AERC.RCALF	33.80	1.69	0.32	785.50	69.92	0.71	0.72	0.55
B3	2010	4	1hr	MMIF.RCALF	27.16	2.15	0.39	122.15	56.53	0.91	0.74	0.57
B3	2010	4	1hr	MMIF.RCALT	31.76	2.42	0.34	116.46	73.54	0.91	0.74	0.55
B3	2010	5	1hr	obs	249.72	3.16	1.00	1.00	1236.04	1.00	1.00	0.80
B3	2010	5	1hr	AERC.RCALT	248.69	3.12	1.00	1.00	1244.94	1.00	1.00	1.00
B3	2010	5	1hr	AERC.RCALF	248.75	3.12	1.00	1.00	1244.94	1.00	1.00	1.00
B3	2010	5	1hr	MMIF.RCALF	248.76	3.20	1.00	1.00	1190.27	1.00	1.00	0.99
B3	2010	5	1hr	MMIF.RCALT	248.95	3.20	1.00	1.00	1193.66	1.00	1.00	1.00
B3	2011	1	1hr	obs	13.89	3.98	1.00	1.00	45.51	1.00	1.00	0.86
B3	2011	1	1hr	AERC.RCALT	18.54	2.07	0.75	1.83	45.11	0.96	0.84	0.82
B3	2011	1	1hr	AERC.RCALF	9.95	5.73	1.40	1.87	41.35	0.92	0.80	0.78
B3	2011	1	1hr	MMIF.RCALF	10.31	5.78	1.35	1.84	43.44	0.92	0.80	0.79

site	year	source	avg time	Simulation type	geo mean	geo stddev	MG	VG	RHC	geo R	ff2	TMS
B3	2011	1	1hr	MMIF.RCALT	15.94	2.80	0.87	1.28	45.10	0.96	0.86	0.89
B3	2011	2	1hr	obs	32.76	3.42	1.00	1.00	90.78	1.00	1.00	0.81
B3	2011	2	1hr	AERC.RCALT	42.60	2.01	0.77	1.52	90.68	0.96	0.86	0.85
B3	2011	2	1hr	AERC.RCALF	23.89	5.22	1.37	1.69	83.61	0.94	0.76	0.79
B3	2011	2	1hr	MMIF.RCALF	24.57	5.28	1.33	1.67	90.70	0.94	0.78	0.80
B3	2011	2	1hr	MMIF.RCALT	37.24	2.66	0.88	1.18	91.87	0.97	0.90	0.92
B3	2011	3	1hr	obs	42.07	3.90	1.00	1.00	139.03	1.00	1.00	0.81
B3	2011	3	1hr	AERC.RCALT	54.66	2.42	0.77	1.40	120.83	0.98	0.88	0.84
B3	2011	3	1hr	AERC.RCALF	23.39	11.78	1.80	8.21	121.60	0.92	0.74	0.67
B3	2011	3	1hr	MMIF.RCALF	24.57	11.11	1.71	6.88	130.21	0.92	0.76	0.67
B3	2011	3	1hr	MMIF.RCALT	41.32	3.99	1.02	1.12	135.59	0.97	0.94	0.95
B3	2011	4	1hr	obs	11.72	13.49	1.00	1.00	61.43	1.00	1.00	0.84
B3	2011	4	1hr	AERC.RCALT	26.24	2.74	0.45	27.69	62.91	0.98	0.76	0.64
B3	2011	4	1hr	AERC.RCALF	4.99	30.16	2.35	18.59	53.40	0.91	0.68	0.58
B3	2011	4	1hr	MMIF.RCALF	5.37	25.76	2.18	15.12	53.07	0.90	0.68	0.62
B3	2011	4	1hr	MMIF.RCALT	18.90	4.61	0.62	4.44	68.31	0.99	0.82	0.69
B3	2011	5	1hr	obs	163.62	3.39	1.00	1.00	1116.54	1.00	1.00	0.80
B3	2011	5	1hr	AERC.RCALT	169.68	3.11	0.96	1.04	1072.03	0.99	1.00	0.98
B3	2011	5	1hr	AERC.RCALF	189.57	3.14	0.86	1.07	1016.64	0.99	1.00	0.95
B3	2011	5	1hr	MMIF.RCALF	190.37	3.14	0.86	1.07	1007.06	0.99	1.00	0.95
B3	2011	5	1hr	MMIF.RCALT	160.45	3.08	1.02	1.03	1066.92	0.99	1.00	0.98
B3	2012	1	1hr	obs	14.65	3.26	1.00	1.00	42.63	1.00	1.00	0.85
B3	2012	1	1hr	AERC.RCALT	15.56	2.95	0.94	1.06	36.87	0.98	0.98	0.94
B3	2012	1	1hr	AERC.RCALF	15.58	3.02	0.94	1.08	39.34	0.98	0.94	0.94
B3	2012	1	1hr	MMIF.RCALF	13.47	3.62	1.09	1.05	40.40	0.99	1.00	0.97
B3	2012	1	1hr	MMIF.RCALT	13.42	3.64	1.09	1.06	38.47	0.99	1.00	0.96
B3	2012	2	1hr	obs	38.33	2.65	1.00	1.00	90.59	1.00	1.00	0.80

site	year	source	avg time	Simulation type	geo mean	geo stddev	MG	VG	RHC	geo R	ff2	TMS
B3	2012	2	1hr	AERC.RCALT	36.21	2.60	1.06	1.02	85.46	0.99	1.00	0.97
B3	2012	2	1hr	AERC.RCALF	35.84	2.65	1.07	1.02	80.39	0.99	1.00	0.97
B3	2012	2	1hr	MMIF.RCALF	31.69	3.12	1.21	1.10	80.23	0.99	0.98	0.94
B3	2012	2	1hr	MMIF.RCALT	32.27	3.22	1.19	1.11	94.42	0.98	0.96	0.91
B3	2012	3	1hr	obs	67.63	2.19	1.00	1.00	162.17	1.00	1.00	0.81
B3	2012	3	1hr	AERC.RCALT	51.15	2.99	1.32	1.37	125.46	0.92	0.82	0.80
B3	2012	3	1hr	AERC.RCALF	42.07	4.18	1.61	2.53	128.83	0.87	0.76	0.72
B3	2012	3	1hr	MMIF.RCALF	35.88	5.43	1.89	5.30	137.85	0.83	0.72	0.64
B3	2012	3	1hr	MMIF.RCALT	38.31	5.35	1.77	4.59	132.11	0.85	0.76	0.67
B3	2012	4	1hr	obs	17.15	7.59	1.00	1.00	74.14	1.00	1.00	0.82
B3	2012	4	1hr	AERC.RCALT	15.61	7.35	1.10	1.04	54.01	1.00	1.00	0.92
B3	2012	4	1hr	AERC.RCALF	16.03	7.49	1.07	1.09	52.29	0.99	0.98	0.96
B3	2012	4	1hr	MMIF.RCALF	11.21	10.92	1.53	1.49	48.99	0.99	0.88	0.83
B3	2012	4	1hr	MMIF.RCALT	11.51	11.54	1.49	1.50	56.02	0.99	0.78	0.80
B3	2012	5	1hr	obs	243.59	3.16	1.00	1.00	1187.88	1.00	1.00	0.80
B3	2012	5	1hr	AERC.RCALT	242.22	3.09	1.01	1.00	1200.45	1.00	1.00	1.00
B3	2012	5	1hr	AERC.RCALF	242.20	3.09	1.01	1.00	1199.78	1.00	1.00	1.00
B3	2012	5	1hr	MMIF.RCALF	243.06	3.18	1.00	1.00	1195.56	1.00	1.00	1.00
B3	2012	5	1hr	MMIF.RCALT	243.08	3.18	1.00	1.00	1196.11	1.00	1.00	1.00
C1	2011	1	1hr	obs	22.90	1.64	1.00	1.00	42.62	1.00	1.00	0.90
C1	2011	1	1hr	AERC.RCALT	23.25	1.60	0.99	1.01	44.02	0.98	1.00	0.99
C1	2011	1	1hr	AERC.RCALF	22.82	1.59	1.00	1.01	43.41	0.98	1.00	0.99
C1	2011	1	1hr	MMIF.RCALF	18.57	2.16	1.23	1.20	44.76	0.92	0.86	0.88
C1	2011	1	1hr	MMIF.RCALT	19.03	2.13	1.20	1.16	45.99	0.94	0.92	0.90
C1	2011	2	1hr	obs	53.56	1.57	1.00	1.00	91.27	1.00	1.00	0.81
C1	2011	2	1hr	AERC.RCALT	54.47	1.53	0.98	1.01	88.60	0.98	1.00	0.99
C1	2011	2	1hr	AERC.RCALF	53.82	1.48	1.00	1.01	83.99	0.97	1.00	0.98

site	year	source	avg time	Simulation type	geo mean	geo stddev	MG	VG	RHC	geo R	ff2	TMS
C1	2011	2	1hr	MMIF.RCALF	44.54	1.90	1.20	1.12	84.81	0.93	0.94	0.92
C1	2011	2	1hr	MMIF.RCALT	45.53	1.93	1.18	1.12	90.63	0.93	0.94	0.91
C1	2011	3	1hr	obs	76.33	1.66	1.00	1.00	137.67	1.00	1.00	0.81
C1	2011	3	1hr	AERC.RCALT	75.99	1.76	1.00	1.03	133.93	0.96	1.00	0.98
C1	2011	3	1hr	AERC.RCALF	79.95	1.72	0.96	1.03	153.77	0.96	1.00	0.95
C1	2011	3	1hr	MMIF.RCALF	67.49	2.02	1.13	1.14	135.53	0.89	0.92	0.89
C1	2011	3	1hr	MMIF.RCALT	62.97	2.21	1.21	1.30	134.48	0.82	0.88	0.86
C1	2011	4	1hr	obs	37.58	1.58	1.00	1.00	64.63	1.00	1.00	0.83
C1	2011	4	1hr	AERC.RCALT	34.16	1.84	1.10	1.09	63.70	0.91	0.96	0.94
C1	2011	4	1hr	AERC.RCALF	34.14	1.86	1.10	1.11	63.74	0.88	0.96	0.93
C1	2011	4	1hr	MMIF.RCALF	24.58	2.90	1.53	2.09	63.05	0.81	0.86	0.76
C1	2011	4	1hr	MMIF.RCALT	26.47	2.82	1.42	1.85	62.64	0.84	0.86	0.79
C1	2011	5	1hr	obs	203.91	3.30	1.00	1.00	1214.21	1.00	1.00	0.80
C1	2011	5	1hr	AERC.RCALT	235.84	3.09	0.87	1.08	1231.18	0.98	0.92	0.93
C1	2011	5	1hr	AERC.RCALF	236.12	3.09	0.86	1.08	1234.44	0.98	0.92	0.94
C1	2011	5	1hr	MMIF.RCALF	238.63	3.18	0.85	1.08	1229.09	0.98	0.94	0.94
C1	2011	5	1hr	MMIF.RCALT	238.57	3.18	0.86	1.08	1226.75	0.98	0.94	0.94
C1	2012	1	1hr	obs	18.40	2.31	1.00	1.00	44.65	1.00	1.00	0.86
C1	2012	1	1hr	AERC.RCALT	17.56	2.64	1.05	1.03	43.26	0.99	0.98	0.97
C1	2012	1	1hr	AERC.RCALF	17.13	2.73	1.07	1.06	41.33	0.99	0.96	0.96
C1	2012	1	1hr	MMIF.RCALF	14.55	3.59	1.27	1.38	43.96	0.97	0.84	0.85
C1	2012	1	1hr	MMIF.RCALT	14.72	3.44	1.25	1.29	45.00	0.98	0.84	0.87
C1	2012	2	1hr	obs	42.13	2.21	1.00	1.00	89.88	1.00	1.00	0.81
C1	2012	2	1hr	AERC.RCALT	39.85	2.47	1.06	1.03	87.34	0.99	0.98	0.97
C1	2012	2	1hr	AERC.RCALF	38.68	2.55	1.09	1.05	82.20	0.99	0.98	0.96
C1	2012	2	1hr	MMIF.RCALF	32.34	3.49	1.30	1.39	85.39	0.98	0.84	0.85
C1	2012	2	1hr	MMIF.RCALT	33.95	3.15	1.24	1.24	88.30	0.98	0.86	0.88

site	year	source	avg time	Simulation type	geo mean	geo stddev	MG	VG	RHC	geo R	ff2	TMS
C1	2012	3	1hr	obs	71.36	1.83	1.00	1.00	149.29	1.00	1.00	0.81
C1	2012	3	1hr	AERC.RCALT	51.14	3.23	1.40	1.96	130.75	0.83	0.82	0.75
C1	2012	3	1hr	AERC.RCALF	50.63	3.32	1.41	2.06	127.26	0.83	0.82	0.76
C1	2012	3	1hr	MMIF.RCALF	35.43	6.25	2.02	13.94	131.36	0.71	0.74	0.60
C1	2012	3	1hr	MMIF.RCALT	36.52	5.98	1.95	11.77	136.11	0.72	0.74	0.60
C1	2012	4	1hr	obs	21.74	3.90	1.00	1.00	58.66	1.00	1.00	0.82
C1	2012	4	1hr	AERC.RCALT	18.77	5.10	1.16	1.12	51.73	1.00	0.94	0.92
C1	2012	4	1hr	AERC.RCALF	18.37	5.50	1.18	1.18	61.86	1.00	0.90	0.88
C1	2012	4	1hr	MMIF.RCALF	12.29	10.08	1.77	3.90	57.34	0.98	0.74	0.69
C1	2012	4	1hr	MMIF.RCALT	12.93	9.21	1.68	3.16	49.27	0.98	0.74	0.70
C1	2012	5	1hr	obs	167.73	3.26	1.00	1.00	1193.22	1.00	1.00	0.80
C1	2012	5	1hr	AERC.RCALT	213.14	3.11	0.79	1.11	1258.86	0.98	1.00	0.92
C1	2012	5	1hr	AERC.RCALF	215.91	3.11	0.78	1.12	1248.61	0.98	1.00	0.93
C1	2012	5	1hr	MMIF.RCALF	204.43	3.14	0.82	1.07	1235.46	0.99	1.00	0.95
C1	2012	5	1hr	MMIF.RCALT	198.55	3.12	0.85	1.06	1243.41	0.99	1.00	0.95
C2	2010	1	1hr	obs	18.04	2.34	1.00	1.00	45.51	1.00	1.00	1.00
C2	2010	1	1hr	AERC.RCALT	17.67	2.90	1.02	1.10	45.06	0.97	1.00	0.97
C2	2010	1	1hr	AERC.RCALF	13.36	4.56	1.35	1.92	42.25	0.95	0.82	0.79
C2	2010	1	1hr	MMIF.RCALF	13.09	4.66	1.38	2.02	42.46	0.95	0.76	0.79
C2	2010	1	1hr	MMIF.RCALT	16.09	3.62	1.12	1.30	45.55	0.97	0.82	0.88
C2	2010	2	1hr	obs	41.16	2.30	1.00	1.00	88.95	1.00	1.00	0.81
C2	2010	2	1hr	AERC.RCALT	39.87	2.51	1.03	1.03	91.15	0.99	1.00	0.98
C2	2010	2	1hr	AERC.RCALF	31.60	3.65	1.30	1.39	89.15	0.98	0.84	0.86
C2	2010	2	1hr	MMIF.RCALF	31.34	3.83	1.31	1.46	90.76	0.98	0.82	0.85
C2	2010	2	1hr	MMIF.RCALT	36.33	3.12	1.13	1.15	91.75	0.98	0.86	0.92
C2	2010	3	1hr	obs	47.91	3.04	1.00	1.00	120.94	1.00	1.00	0.81
C2	2010	3	1hr	AERC.RCALT	60.21	2.67	0.80	1.08	134.54	1.00	0.96	0.91

site	year	source	avg time	Simulation type	geo mean	geo stddev	MG	VG	RHC	geo R	ff2	TMS
C2	2010	3	1hr	AERC.RCALF	43.77	5.04	1.10	1.33	130.93	0.99	0.90	0.91
C2	2010	3	1hr	MMIF.RCALF	42.05	5.52	1.14	1.49	130.10	0.99	0.88	0.88
C2	2010	3	1hr	MMIF.RCALT	48.02	4.06	1.00	1.11	130.72	0.99	0.92	0.96
C2	2010	4	1hr	obs	20.92	3.56	1.00	1.00	52.92	1.00	1.00	0.83
C2	2010	4	1hr	AERC.RCALT	21.01	4.71	1.00	1.14	76.10	0.99	0.94	0.90
C2	2010	4	1hr	AERC.RCALF	8.48	18.59	2.47	43.51	46.15	0.97	0.76	0.55
C2	2010	4	1hr	MMIF.RCALF	8.81	15.31	2.38	25.88	45.74	0.95	0.74	0.63
C2	2010	4	1hr	MMIF.RCALT	14.59	8.95	1.43	2.96	76.99	0.98	0.74	0.67
C2	2010	5	1hr	obs	197.72	3.03	1.00	1.00	1164.51	1.00	1.00	0.80
C2	2010	5	1hr	AERC.RCALT	216.21	3.07	0.92	1.01	1228.07	1.00	1.00	0.97
C2	2010	5	1hr	AERC.RCALF	219.05	3.08	0.90	1.02	1229.25	1.00	1.00	0.98
C2	2010	5	1hr	MMIF.RCALF	211.01	3.10	0.94	1.01	1225.01	1.00	1.00	0.99
C2	2010	5	1hr	MMIF.RCALT	206.13	3.08	0.96	1.01	1224.13	1.00	1.00	0.99
C2	2012	1	1hr	obs	15.12	2.77	1.00	1.00	41.90	1.00	1.00	0.88
C2	2012	1	1hr	AERC.RCALT	11.86	4.22	1.27	1.34	40.58	0.98	0.78	0.85
C2	2012	1	1hr	AERC.RCALF	9.27	6.02	1.63	2.76	36.82	0.95	0.76	0.72
C2	2012	1	1hr	MMIF.RCALF	9.20	5.85	1.64	2.67	38.37	0.95	0.76	0.73
C2	2012	1	1hr	MMIF.RCALT	11.29	4.60	1.34	1.52	42.99	0.98	0.78	0.81
C2	2012	2	1hr	obs	36.19	2.62	1.00	1.00	92.68	1.00	1.00	0.80
C2	2012	2	1hr	AERC.RCALT	28.58	3.81	1.27	1.27	90.74	0.98	0.78	0.86
C2	2012	2	1hr	AERC.RCALF	24.22	5.11	1.49	1.96	86.95	0.98	0.80	0.78
C2	2012	2	1hr	MMIF.RCALF	23.86	5.02	1.52	1.94	91.43	0.98	0.80	0.78
C2	2012	2	1hr	MMIF.RCALT	27.74	4.11	1.31	1.38	92.20	0.98	0.78	0.85
C2	2012	3	1hr	obs	58.62	2.13	1.00	1.00	131.37	1.00	1.00	0.81
C2	2012	3	1hr	AERC.RCALT	38.19	3.72	1.54	1.96	125.13	0.91	0.68	0.74
C2	2012	3	1hr	AERC.RCALF	29.51	9.95	1.99	24.94	137.90	0.89	0.82	0.63
C2	2012	3	1hr	MMIF.RCALF	30.66	8.86	1.91	16.22	135.46	0.90	0.82	0.66

site	year	source	avg time	Simulation type	geo mean	geo stddev	MG	VG	RHC	geo R	ff2	TMS
C2	2012	3	1hr	MMIF.RCALT	35.12	4.29	1.67	2.61	135.27	0.91	0.70	0.72
C2	2012	4	1hr	obs	19.08	4.23	1.00	1.00	62.56	1.00	1.00	0.82
C2	2012	4	1hr	AERC.RCALT	8.98	12.10	2.12	5.94	55.29	0.99	0.66	0.63
C2	2012	4	1hr	AERC.RCALF	4.42	43.19	4.32	4042.10	51.89	0.93	0.70	0.56
C2	2012	4	1hr	MMIF.RCALF	5.34	27.99	3.58	408.55	49.03	0.92	0.70	0.57
C2	2012	4	1hr	MMIF.RCALT	8.16	13.16	2.34	8.78	53.37	0.98	0.64	0.62
C2	2012	5	1hr	obs	191.96	3.09	1.00	1.00	1112.40	1.00	1.00	0.80
C2	2012	5	1hr	AERC.RCALT	234.80	3.05	0.82	1.06	1106.07	0.99	1.00	0.95
C2	2012	5	1hr	AERC.RCALF	235.54	3.05	0.82	1.07	1106.12	0.99	1.00	0.95
C2	2012	5	1hr	MMIF.RCALF	203.59	3.08	0.94	1.02	1102.10	1.00	1.00	0.98
C2	2012	5	1hr	MMIF.RCALT	201.47	3.08	0.95	1.01	1102.02	1.00	1.00	0.99

AERMOD results statistical scores: 3-hour average concentrations.

site	year	source	avg time	Simulation type	geo mean	geo stddev	MG	VG	RHC	geo R	ff2	TMS
B2	2010	1	3hr	AERC.RCALT	5.85	12.46	1.93	26.10	38.56	0.85	0.64	0.58
B2	2010	1	3hr	AERC.RCALF	5.75	11.97	1.96	23.50	37.20	0.85	0.70	0.61
B2	2010	1	3hr	MMIF.RCALF	6.29	11.00	1.80	16.80	36.54	0.84	0.74	0.64
B2	2010	1	3hr	MMIF.RCALT	6.46	11.14	1.75	16.69	38.74	0.85	0.68	0.62
B2	2010	2	3hr	obs	26.13	2.64	1.00	1.00	88.59	1.00	1.00	1.00
B2	2010	2	3hr	AERC.RCALT	15.98	10.08	1.64	15.12	85.79	0.85	0.76	0.65
B2	2010	2	3hr	AERC.RCALF	15.16	9.80	1.72	14.95	82.16	0.85	0.74	0.64
B2	2010	2	3hr	MMIF.RCALF	15.78	9.60	1.66	13.50	80.51	0.85	0.76	0.65
B2	2010	2	3hr	MMIF.RCALT	17.30	9.30	1.51	10.64	83.86	0.86	0.78	0.67
B2	2010	3	3hr	obs	39.12	2.86	1.00	1.00	157.50	1.00	1.00	0.98
B2	2010	3	3hr	AERC.RCALT	18.79	14.90	2.08	69.55	132.33	0.83	0.64	0.56
B2	2010	3	3hr	AERC.RCALF	17.33	14.90	2.26	78.62	130.23	0.83	0.66	0.59
B2	2010	3	3hr	MMIF.RCALF	12.78	24.66	3.06	1380.89	125.11	0.80	0.64	0.55
B2	2010	3	3hr	MMIF.RCALT	14.16	23.38	2.76	828.81	128.93	0.81	0.64	0.56
B2	2010	4	3hr	obs	14.24	5.52	1.00	1.00	57.22	1.00	1.00	0.94
B2	2010	4	3hr	AERC.RCALT	1.60	156.61	8.89	>5000	78.38	0.84	0.62	0.46
B2	2010	4	3hr	AERC.RCALF	1.08	162.74	13.16	>5000	34.29	0.83	0.60	0.39
B2	2010	4	3hr	MMIF.RCALF	1.19	133.89	11.93	>5000	34.32	0.81	0.62	0.50
B2	2010	4	3hr	MMIF.RCALT	1.60	127.76	8.88	>5000	62.26	0.83	0.64	0.43
B2	2010	5	3hr	obs	162.50	4.00	1.00	1.00	1121.56	1.00	1.00	0.98
B2	2010	5	3hr	AERC.RCALT	223.13	3.08	0.73	1.21	1014.09	0.99	0.94	0.88
B2	2010	5	3hr	AERC.RCALF	223.10	3.08	0.73	1.21	1014.09	0.99	0.94	0.90
B2	2010	5	3hr	MMIF.RCALF	231.47	3.25	0.70	1.21	1116.13	0.99	0.98	0.88
B2	2010	5	3hr	MMIF.RCALT	231.55	3.25	0.70	1.21	1116.13	0.99	0.98	0.90
B2	2011	1	3hr	obs	7.04	7.31	1.00	1.00	44.06	1.00	1.00	0.99
B2	2011	1	3hr	AERC.RCALT	10.15	4.82	0.69	1.44	41.45	0.99	0.82	0.83

site	year	source	avg time	Simulation type	geo mean	geo stddev	MG	VG	RHC	geo R	ff2	TMS
B2	2011	1	3hr	AERC.RCALF	6.76	8.69	1.04	1.50	39.78	0.96	0.82	0.87
B2	2011	1	3hr	MMIF.RCALF	7.45	7.90	0.95	1.40	40.28	0.96	0.86	0.89
B2	2011	1	3hr	MMIF.RCALT	10.36	5.06	0.68	1.38	43.94	0.99	0.82	0.83
B2	2011	2	3hr	obs	19.70	5.07	1.00	1.00	93.54	1.00	1.00	0.99
B2	2011	2	3hr	AERC.RCALT	23.89	4.68	0.83	1.12	85.14	0.99	1.00	0.92
B2	2011	2	3hr	AERC.RCALF	16.06	8.55	1.23	1.95	80.57	0.95	0.84	0.81
B2	2011	2	3hr	MMIF.RCALF	17.49	7.53	1.13	1.58	82.91	0.96	0.86	0.86
B2	2011	2	3hr	MMIF.RCALT	23.72	4.95	0.83	1.11	89.91	0.99	1.00	0.93
B2	2011	3	3hr	obs	37.52	3.43	1.00	1.00	165.01	1.00	1.00	0.97
B2	2011	3	3hr	AERC.RCALT	21.30	9.14	1.76	9.45	98.08	0.82	0.72	0.56
B2	2011	3	3hr	AERC.RCALF	10.57	26.59	3.55	4594.08	99.89	0.67	0.64	0.52
B2	2011	3	3hr	MMIF.RCALF	12.42	23.07	3.02	1390.74	117.82	0.69	0.72	0.52
B2	2011	3	3hr	MMIF.RCALT	20.84	10.70	1.80	14.76	117.82	0.82	0.74	0.64
B2	2011	4	3hr	obs	6.19	20.38	1.00	1.00	68.23	1.00	1.00	0.98
B2	2011	4	3hr	AERC.RCALT	7.36	12.31	0.84	1.71	44.60	0.98	0.82	0.78
B2	2011	4	3hr	AERC.RCALF	2.14	63.36	2.90	132.40	39.13	0.90	0.72	0.57
B2	2011	4	3hr	MMIF.RCALF	2.55	50.11	2.43	44.94	39.88	0.91	0.76	0.62
B2	2011	4	3hr	MMIF.RCALT	6.92	13.79	0.90	1.38	44.50	0.99	0.88	0.88
B2	2011	5	3hr	obs	137.45	3.84	1.00	1.00	1024.79	1.00	1.00	1.00
B2	2011	5	3hr	AERC.RCALT	163.26	3.13	0.84	1.09	993.64	0.99	1.00	0.94
B2	2011	5	3hr	AERC.RCALF	171.12	3.17	0.80	1.11	1001.01	0.99	1.00	0.94
B2	2011	5	3hr	MMIF.RCALF	166.92	3.20	0.82	1.10	1003.52	0.99	1.00	0.94
B2	2011	5	3hr	MMIF.RCALT	155.72	3.15	0.88	1.09	994.70	0.99	1.00	0.96
B3	2010	1	3hr	obs	8.17	6.14	1.00	1.00	45.03	1.00	1.00	1.00
B3	2010	1	3hr	AERC.RCALT	21.69	1.91	0.38	12.00	44.52	0.93	0.68	0.61
B3	2010	1	3hr	AERC.RCALF	20.79	1.94	0.39	10.67	41.80	0.93	0.68	0.61
B3	2010	1	3hr	MMIF.RCALF	16.55	2.56	0.49	3.79	38.72	0.98	0.72	0.68

site	year	source	avg time	Simulation type	geo mean	geo stddev	MG	VG	RHC	geo R	ff2	TMS
B3	2010	1	3hr	MMIF.RCALT	17.40	2.63	0.47	3.83	44.56	0.99	0.72	0.66
B3	2010	2	3hr	obs	21.49	4.58	1.00	1.00	87.71	1.00	1.00	1.00
B3	2010	2	3hr	AERC.RCALT	46.22	1.80	0.47	4.93	93.01	0.92	0.76	0.66
B3	2010	2	3hr	AERC.RCALF	43.74	1.87	0.49	4.17	82.09	0.94	0.76	0.66
B3	2010	2	3hr	MMIF.RCALF	35.75	2.32	0.60	2.18	80.05	0.98	0.80	0.76
B3	2010	2	3hr	MMIF.RCALT	37.81	2.32	0.57	2.27	91.27	0.98	0.78	0.73
B3	2010	3	3hr	obs	26.63	4.21	1.00	1.00	101.57	1.00	1.00	0.96
B3	2010	3	3hr	AERC.RCALT	61.88	1.87	0.43	4.73	119.00	0.90	0.72	0.62
B3	2010	3	3hr	AERC.RCALF	57.06	2.01	0.47	3.69	116.99	0.91	0.74	0.67
B3	2010	3	3hr	MMIF.RCALF	45.67	2.66	0.58	1.75	104.42	0.98	0.86	0.78
B3	2010	3	3hr	MMIF.RCALT	50.50	2.40	0.53	2.17	121.69	0.98	0.84	0.73
B3	2010	4	3hr	obs	5.37	17.02	1.00	1.00	44.37	1.00	1.00	0.92
B3	2010	4	3hr	AERC.RCALT	29.24	2.23	0.18	1673.38	59.17	0.91	0.54	0.48
B3	2010	4	3hr	AERC.RCALF	24.83	2.17	0.22	1090.49	58.62	0.91	0.64	0.55
B3	2010	4	3hr	MMIF.RCALF	19.05	2.93	0.28	132.88	49.42	0.97	0.66	0.55
B3	2010	4	3hr	MMIF.RCALT	21.86	3.26	0.25	140.42	59.75	0.96	0.56	0.52
B3	2010	5	3hr	obs	186.57	3.63	1.00	1.00	1107.59	1.00	1.00	0.99
B3	2010	5	3hr	AERC.RCALT	203.41	3.24	0.92	1.03	1065.28	1.00	1.00	0.97
B3	2010	5	3hr	AERC.RCALF	203.53	3.23	0.92	1.03	1065.28	1.00	1.00	0.98
B3	2010	5	3hr	MMIF.RCALF	202.35	3.30	0.92	1.04	1056.55	0.99	1.00	0.97
B3	2010	5	3hr	MMIF.RCALT	202.18	3.31	0.92	1.04	1056.55	0.99	1.00	0.98
B3	2011	1	3hr	obs	8.88	5.42	1.00	1.00	43.94	1.00	1.00	0.99
B3	2011	1	3hr	AERC.RCALT	14.15	2.65	0.63	2.15	44.17	0.99	0.82	0.78
B3	2011	1	3hr	AERC.RCALF	8.02	6.54	1.11	1.38	40.45	0.96	0.84	0.87
B3	2011	1	3hr	MMIF.RCALF	8.77	6.47	1.01	1.45	42.84	0.95	0.80	0.87
B3	2011	1	3hr	MMIF.RCALT	12.70	3.59	0.70	1.41	44.75	0.99	0.86	0.84
B3	2011	2	3hr	obs	21.57	4.45	1.00	1.00	90.23	1.00	1.00	1.00

site	year	source	avg time	Simulation type	geo mean	geo stddev	MG	VG	RHC	geo R	ff2	TMS
B3	2011	2	3hr	AERC.RCALT	32.37	2.58	0.67	1.63	91.82	0.99	0.82	0.81
B3	2011	2	3hr	AERC.RCALF	19.42	5.87	1.11	1.40	82.60	0.95	0.78	0.85
B3	2011	2	3hr	MMIF.RCALF	21.00	5.91	1.03	1.43	81.45	0.95	0.80	0.88
B3	2011	2	3hr	MMIF.RCALT	29.50	3.45	0.73	1.26	93.64	0.98	0.86	0.85
B3	2011	3	3hr	obs	25.43	4.87	1.00	1.00	117.38	1.00	1.00	0.97
B3	2011	3	3hr	AERC.RCALT	38.83	3.15	0.66	1.53	111.38	0.98	0.90	0.83
B3	2011	3	3hr	AERC.RCALF	16.63	15.24	1.53	8.88	102.49	0.92	0.74	0.67
B3	2011	3	3hr	MMIF.RCALF	17.71	13.87	1.44	7.23	103.99	0.91	0.72	0.69
B3	2011	3	3hr	MMIF.RCALT	29.73	5.31	0.86	1.26	111.08	0.96	0.86	0.88
B3	2011	4	3hr	obs	6.16	16.38	1.00	1.00	47.21	1.00	1.00	0.94
B3	2011	4	3hr	AERC.RCALT	16.61	3.47	0.37	31.18	49.34	0.99	0.72	0.61
B3	2011	4	3hr	AERC.RCALF	3.65	40.75	1.69	11.39	47.01	0.94	0.76	0.67
B3	2011	4	3hr	MMIF.RCALF	4.01	32.83	1.54	8.91	45.60	0.92	0.76	0.68
B3	2011	4	3hr	MMIF.RCALT	12.13	5.99	0.51	4.66	46.79	0.99	0.78	0.69
B3	2011	5	3hr	obs	103.68	3.62	1.00	1.00	754.22	1.00	1.00	0.94
B3	2011	5	3hr	AERC.RCALT	140.91	3.33	0.74	1.13	1056.16	0.99	0.96	0.86
B3	2011	5	3hr	AERC.RCALF	156.32	3.39	0.66	1.22	974.76	0.99	0.96	0.87
B3	2011	5	3hr	MMIF.RCALF	162.36	3.27	0.64	1.25	973.79	1.00	0.96	0.88
B3	2011	5	3hr	MMIF.RCALT	140.50	3.26	0.74	1.13	1050.48	0.99	0.96	0.90
B3	2012	1	3hr	obs	9.43	4.45	1.00	1.00	41.38	1.00	1.00	0.99
B3	2012	1	3hr	AERC.RCALT	11.57	3.79	0.82	1.21	35.74	0.97	0.90	0.87
B3	2012	1	3hr	AERC.RCALF	11.75	3.83	0.80	1.21	36.33	0.97	0.88	0.89
B3	2012	1	3hr	MMIF.RCALF	10.55	4.54	0.89	1.09	38.64	0.98	1.00	0.95
B3	2012	1	3hr	MMIF.RCALT	10.34	4.78	0.91	1.11	36.54	0.98	1.00	0.95
B3	2012	2	3hr	obs	24.30	3.49	1.00	1.00	88.12	1.00	1.00	0.99
B3	2012	2	3hr	AERC.RCALT	27.59	3.32	0.88	1.13	75.43	0.97	1.00	0.92
B3	2012	2	3hr	AERC.RCALF	26.86	3.57	0.91	1.14	77.31	0.96	1.00	0.95

site	year	source	avg time	Simulation type	geo mean	geo stddev	MG	VG	RHC	geo R	ff2	TMS
B3	2012	2	3hr	MMIF.RCALF	23.98	4.27	1.01	1.15	73.02	0.97	0.98	0.95
B3	2012	2	3hr	MMIF.RCALT	25.29	4.07	0.96	1.14	84.44	0.97	1.00	0.93
B3	2012	3	3hr	obs	39.52	2.49	1.00	1.00	128.79	1.00	1.00	0.99
B3	2012	3	3hr	AERC.RCALT	35.77	3.90	1.11	1.51	119.37	0.92	0.80	0.84
B3	2012	3	3hr	AERC.RCALF	28.13	5.39	1.41	2.92	91.94	0.88	0.76	0.69
B3	2012	3	3hr	MMIF.RCALF	25.07	7.42	1.58	6.65	122.37	0.86	0.68	0.62
B3	2012	3	3hr	MMIF.RCALT	29.78	6.99	1.33	4.36	121.95	0.91	0.74	0.73
B3	2012	4	3hr	obs	8.53	9.19	1.00	1.00	57.93	1.00	1.00	0.99
B3	2012	4	3hr	AERC.RCALT	10.30	9.50	0.83	1.11	49.37	0.99	1.00	0.91
B3	2012	4	3hr	AERC.RCALF	10.45	9.64	0.82	1.18	46.28	0.99	0.98	0.91
B3	2012	4	3hr	MMIF.RCALF	7.89	14.67	1.08	1.40	49.12	0.99	0.88	0.89
B3	2012	4	3hr	MMIF.RCALT	7.70	15.65	1.11	1.48	46.54	0.99	0.86	0.88
B3	2012	5	3hr	obs	138.38	3.53	1.00	1.00	1019.43	1.00	1.00	0.97
B3	2012	5	3hr	AERC.RCALT	177.72	3.35	0.78	1.10	1136.96	0.99	1.00	0.92
B3	2012	5	3hr	AERC.RCALF	182.22	3.37	0.76	1.11	1136.26	0.99	1.00	0.93
B3	2012	5	3hr	MMIF.RCALF	184.40	3.34	0.75	1.11	1131.73	0.99	1.00	0.93
B3	2012	5	3hr	MMIF.RCALT	181.10	3.33	0.76	1.10	1132.36	0.99	1.00	0.93
C1	2011	1	3hr	obs	15.04	1.92	1.00	1.00	38.51	1.00	1.00	0.97
C1	2011	1	3hr	AERC.RCALT	18.15	2.05	0.83	1.08	43.11	0.97	1.00	0.92
C1	2011	1	3hr	AERC.RCALF	17.41	2.01	0.86	1.07	40.95	0.95	1.00	0.94
C1	2011	1	3hr	MMIF.RCALF	14.17	2.87	1.06	1.32	42.48	0.92	0.84	0.89
C1	2011	1	3hr	MMIF.RCALT	15.30	2.69	0.98	1.21	44.95	0.94	0.84	0.91
C1	2011	2	3hr	obs	35.08	1.76	1.00	1.00	77.67	1.00	1.00	0.97
C1	2011	2	3hr	AERC.RCALT	41.75	1.94	0.84	1.06	84.73	0.97	1.00	0.93
C1	2011	2	3hr	AERC.RCALF	41.02	1.86	0.86	1.05	80.66	0.96	1.00	0.94
C1	2011	2	3hr	MMIF.RCALF	33.85	2.53	1.04	1.22	85.22	0.93	0.86	0.90
C1	2011	2	3hr	MMIF.RCALT	35.18	2.56	1.00	1.22	90.97	0.95	0.86	0.91

site	year	source	avg time	Simulation type	geo mean	geo stddev	MG	VG	RHC	geo R	ff2	TMS
C1	2011	3	3hr	obs	48.58	1.77	1.00	1.00	92.74	1.00	1.00	0.94
C1	2011	3	3hr	AERC.RCALT	52.39	1.97	0.93	1.04	108.08	0.98	1.00	0.94
C1	2011	3	3hr	AERC.RCALF	55.40	1.85	0.88	1.04	114.99	0.98	1.00	0.95
C1	2011	3	3hr	MMIF.RCALF	47.20	2.50	1.03	1.23	130.50	0.92	0.88	0.89
C1	2011	3	3hr	MMIF.RCALT	44.43	2.84	1.09	1.42	131.02	0.90	0.84	0.87
C1	2011	4	3hr	obs	21.55	1.73	1.00	1.00	40.76	1.00	1.00	0.93
C1	2011	4	3hr	AERC.RCALT	22.54	2.26	0.96	1.10	53.81	0.98	0.96	0.91
C1	2011	4	3hr	AERC.RCALF	23.31	2.28	0.92	1.12	55.79	0.96	0.96	0.94
C1	2011	4	3hr	MMIF.RCALF	16.53	3.86	1.30	2.24	52.12	0.94	0.76	0.77
C1	2011	4	3hr	MMIF.RCALT	18.00	3.70	1.20	1.98	50.65	0.95	0.76	0.80
C1	2011	5	3hr	obs	138.06	3.34	1.00	1.00	1034.29	1.00	1.00	0.97
C1	2011	5	3hr	AERC.RCALT	169.12	3.29	0.82	1.06	1176.23	0.99	1.00	0.93
C1	2011	5	3hr	AERC.RCALF	181.49	3.21	0.76	1.13	1174.92	0.99	0.96	0.92
C1	2011	5	3hr	MMIF.RCALF	179.21	3.27	0.77	1.11	1174.31	0.99	1.00	0.93
C1	2011	5	3hr	MMIF.RCALT	172.22	3.31	0.80	1.07	1175.49	0.99	1.00	0.95
C1	2012	1	3hr	obs	12.26	3.08	1.00	1.00	42.16	1.00	1.00	0.99
C1	2012	1	3hr	AERC.RCALT	13.45	3.32	0.91	1.08	41.81	0.98	1.00	0.96
C1	2012	1	3hr	AERC.RCALF	13.01	3.49	0.94	1.10	41.08	0.97	0.98	0.96
C1	2012	1	3hr	MMIF.RCALF	11.01	4.49	1.11	1.39	41.49	0.95	0.86	0.88
C1	2012	1	3hr	MMIF.RCALT	11.18	4.55	1.10	1.32	44.81	0.97	0.86	0.88
C1	2012	2	3hr	obs	28.32	2.77	1.00	1.00	88.40	1.00	1.00	1.00
C1	2012	2	3hr	AERC.RCALT	30.84	3.12	0.92	1.11	87.04	0.97	1.00	0.95
C1	2012	2	3hr	AERC.RCALF	29.34	3.24	0.97	1.14	79.97	0.96	0.98	0.94
C1	2012	2	3hr	MMIF.RCALF	24.45	4.50	1.16	1.58	82.04	0.94	0.82	0.85
C1	2012	2	3hr	MMIF.RCALT	26.50	4.23	1.07	1.41	91.76	0.95	0.78	0.85
C1	2012	3	3hr	obs	40.94	2.24	1.00	1.00	126.30	1.00	1.00	0.99
C1	2012	3	3hr	AERC.RCALT	36.70	3.86	1.12	2.01	112.73	0.82	0.86	0.79

site	year	source	avg time	Simulation type	geo mean	geo stddev	MG	VG	RHC	geo R	ff2	TMS
C1	2012	3	3hr	AERC.RCALF	35.69	4.07	1.15	2.19	106.28	0.82	0.84	0.79
C1	2012	3	3hr	MMIF.RCALF	25.69	8.20	1.59	15.75	115.84	0.75	0.70	0.61
C1	2012	3	3hr	MMIF.RCALT	26.53	7.84	1.54	13.28	113.88	0.75	0.70	0.63
C1	2012	4	3hr	obs	12.35	4.93	1.00	1.00	49.59	1.00	1.00	1.00
C1	2012	4	3hr	AERC.RCALT	13.04	6.45	0.95	1.19	46.56	0.98	0.94	0.93
C1	2012	4	3hr	AERC.RCALF	12.96	7.25	0.95	1.33	49.67	0.98	0.80	0.88
C1	2012	4	3hr	MMIF.RCALF	8.42	13.72	1.47	4.53	48.71	0.96	0.64	0.70
C1	2012	4	3hr	MMIF.RCALT	8.50	12.14	1.45	3.57	46.77	0.96	0.62	0.70
C1	2012	5	3hr	obs	114.85	3.65	1.00	1.00	981.53	1.00	1.00	0.96
C1	2012	5	3hr	AERC.RCALT	156.59	3.16	0.73	1.13	997.98	1.00	1.00	0.92
C1	2012	5	3hr	AERC.RCALF	164.48	3.17	0.70	1.18	997.52	0.99	1.00	0.91
C1	2012	5	3hr	MMIF.RCALF	164.71	3.13	0.70	1.19	994.08	0.99	1.00	0.91
C1	2012	5	3hr	MMIF.RCALT	153.98	3.15	0.75	1.12	995.07	1.00	1.00	0.93
C2	2010	1	3hr	obs	12.41	3.30	1.00	1.00	44.06	1.00	1.00	0.99
C2	2010	1	3hr	AERC.RCALT	13.85	3.58	0.90	1.04	45.11	0.99	1.00	0.97
C2	2010	1	3hr	AERC.RCALF	9.97	5.51	1.24	1.50	40.67	0.98	0.84	0.84
C2	2010	1	3hr	MMIF.RCALF	9.90	5.62	1.25	1.54	43.96	0.98	0.80	0.83
C2	2010	1	3hr	MMIF.RCALT	13.39	3.97	0.93	1.06	46.95	0.99	1.00	0.96
C2	2010	2	3hr	obs	28.03	3.21	1.00	1.00	85.21	1.00	1.00	0.99
C2	2010	2	3hr	AERC.RCALT	32.18	3.07	0.87	1.04	86.43	0.99	1.00	0.96
C2	2010	2	3hr	AERC.RCALF	23.32	4.76	1.20	1.30	82.44	0.98	0.80	0.87
C2	2010	2	3hr	MMIF.RCALF	23.28	4.91	1.20	1.32	81.07	0.98	0.78	0.87
C2	2010	2	3hr	MMIF.RCALT	31.40	3.42	0.89	1.03	91.99	1.00	1.00	0.95
C2	2010	3	3hr	obs	27.48	3.82	1.00	1.00	99.26	1.00	1.00	0.95
C2	2010	3	3hr	AERC.RCALT	40.09	3.46	0.69	1.19	122.11	0.99	0.88	0.84
C2	2010	3	3hr	AERC.RCALF	27.82	6.35	0.99	1.36	102.13	0.99	0.90	0.89
C2	2010	3	3hr	MMIF.RCALF	28.17	6.73	0.98	1.47	103.84	0.99	0.88	0.90

site	year	source	avg time	Simulation type	geo mean	geo stddev	MG	VG	RHC	geo R	ff2	TMS
C2	2010	3	3hr	MMIF.RCALT	34.81	5.30	0.79	1.25	132.81	0.99	0.84	0.84
C2	2010	4	3hr	obs	12.50	4.74	1.00	1.00	42.73	1.00	1.00	0.91
C2	2010	4	3hr	AERC.RCALT	14.00	6.26	0.89	1.14	63.15	0.99	0.96	0.88
C2	2010	4	3hr	AERC.RCALF	5.48	24.13	2.28	35.98	39.84	0.98	0.78	0.57
C2	2010	4	3hr	MMIF.RCALF	5.58	19.60	2.24	20.45	40.68	0.96	0.74	0.64
C2	2010	4	3hr	MMIF.RCALT	11.35	10.21	1.10	1.95	62.48	0.99	0.86	0.78
C2	2010	5	3hr	obs	138.22	3.34	1.00	1.00	1017.06	1.00	1.00	0.97
C2	2010	5	3hr	AERC.RCALT	157.00	3.19	0.88	1.02	1107.19	1.00	1.00	0.95
C2	2010	5	3hr	AERC.RCALF	166.33	3.24	0.83	1.05	1107.50	1.00	1.00	0.96
C2	2010	5	3hr	MMIF.RCALF	164.81	3.24	0.84	1.04	1101.95	1.00	1.00	0.96
C2	2010	5	3hr	MMIF.RCALT	156.12	3.19	0.89	1.02	1101.91	1.00	1.00	0.97
C2	2012	1	3hr	obs	11.08	3.67	1.00	1.00	40.96	1.00	1.00	0.99
C2	2012	1	3hr	AERC.RCALT	9.24	4.94	1.20	1.19	39.80	0.99	0.84	0.89
C2	2012	1	3hr	AERC.RCALF	6.83	6.34	1.62	2.37	33.88	0.93	0.78	0.72
C2	2012	1	3hr	MMIF.RCALF	7.11	6.23	1.56	2.27	34.33	0.93	0.78	0.76
C2	2012	1	3hr	MMIF.RCALT	9.08	5.16	1.22	1.28	42.08	0.98	0.82	0.84
C2	2012	2	3hr	obs	25.43	3.43	1.00	1.00	82.58	1.00	1.00	0.98
C2	2012	2	3hr	AERC.RCALT	22.14	4.63	1.15	1.14	80.30	0.99	0.86	0.91
C2	2012	2	3hr	AERC.RCALF	16.88	5.84	1.51	1.76	68.47	0.97	0.78	0.77
C2	2012	2	3hr	MMIF.RCALF	17.47	5.76	1.46	1.70	72.75	0.97	0.74	0.79
C2	2012	2	3hr	MMIF.RCALT	22.32	4.76	1.14	1.18	82.11	0.99	0.80	0.88
C2	2012	3	3hr	obs	36.89	2.60	1.00	1.00	91.74	1.00	1.00	0.94
C2	2012	3	3hr	AERC.RCALT	26.29	4.92	1.40	1.75	97.45	0.99	0.84	0.81
C2	2012	3	3hr	AERC.RCALF	17.83	11.19	2.07	17.23	91.22	0.96	0.80	0.65
C2	2012	3	3hr	MMIF.RCALF	19.17	9.54	1.92	9.93	86.55	0.96	0.80	0.67
C2	2012	3	3hr	MMIF.RCALT	25.93	5.60	1.42	2.16	95.10	0.98	0.84	0.78
C2	2012	4	3hr	obs	11.08	5.30	1.00	1.00	42.45	1.00	1.00	0.96

site	year	source	avg time	Simulation type	geo mean	geo stddev	MG	VG	RHC	geo R	ff2	TMS
C2	2012	4	3hr	AERC.RCALT	6.19	16.28	1.79	5.18	41.21	1.00	0.78	0.70
C2	2012	4	3hr	AERC.RCALF	2.88	48.71	3.85	1698.01	37.98	0.95	0.66	0.56
C2	2012	4	3hr	MMIF.RCALF	3.60	30.66	3.08	170.11	38.65	0.93	0.66	0.58
C2	2012	4	3hr	MMIF.RCALT	5.50	15.80	2.02	6.18	39.77	0.99	0.70	0.66
C2	2012	5	3hr	obs	145.35	3.35	1.00	1.00	1029.30	1.00	1.00	0.99
C2	2012	5	3hr	AERC.RCALT	172.77	3.33	0.84	1.07	932.64	0.99	1.00	0.93
C2	2012	5	3hr	AERC.RCALF	175.77	3.32	0.83	1.08	936.43	0.99	1.00	0.95
C2	2012	5	3hr	MMIF.RCALF	159.54	3.16	0.91	1.06	936.25	0.99	1.00	0.97
C2	2012	5	3hr	MMIF.RCALT	153.97	3.17	0.94	1.03	932.35	0.99	1.00	0.98

AERMOD results statistical scores: 8-hour average concentrations.

site	year	source	avg time	Simulation type	geo	geo	MG	VG	RHC	geo	ff2	TMS
B2	2010	1	8hr	obs	6.93	4.05	1.00	1.00	36.29	1.00	1.00	0.99
B2	2010	1	8hr	AERC.RCALT	4.46	13.55	1.55	13.27	36.00	0.87	0.44	0.60
B2	2010	1	8hr	AERC.RCALF	4.31	13.41	1.61	13.80	34.85	0.87	0.44	0.59
B2	2010	1	8hr	MMIF.RCALF	4.74	12.52	1.46	9.99	33.56	0.88	0.44	0.61
B2	2010	1	8hr	MMIF.RCALT	4.72	13.47	1.47	12.31	34.65	0.87	0.42	0.60
B2	2010	2	8hr	obs	16.08	3.50	1.00	1.00	72.89	1.00	1.00	0.97
B2	2010	2	8hr	AERC.RCALT	12.29	10.80	1.31	8.12	81.99	0.87	0.48	0.63
B2	2010	2	8hr	AERC.RCALF	11.00	10.97	1.46	9.82	78.44	0.86	0.48	0.62
B2	2010	2	8hr	MMIF.RCALF	11.69	10.92	1.38	9.08	78.43	0.87	0.48	0.64
B2	2010	2	8hr	MMIF.RCALT	13.30	10.44	1.21	6.90	80.29	0.88	0.50	0.67
B2	2010	3	8hr	obs	19.82	3.39	1.00	1.00	101.58	1.00	1.00	0.96
B2	2010	3	8hr	AERC.RCALT	12.01	16.83	1.65	57.41	94.09	0.82	0.24	0.52
B2	2010	3	8hr	AERC.RCALF	11.26	16.99	1.76	69.60	93.32	0.81	0.20	0.52
B2	2010	3	8hr	MMIF.RCALF	8.45	29.46	2.35	1231.88	94.52	0.79	0.22	0.49
B2	2010	3	8hr	MMIF.RCALT	9.40	27.67	2.11	700.16	95.27	0.80	0.28	0.51
B2	2010	4	8hr	obs	6.62	6.13	1.00	1.00	38.22	1.00	1.00	0.92
B2	2010	4	8hr	AERC.RCALT	0.92	176.71	7.23	>5000	34.49	0.85	0.44	0.47
B2	2010	4	8hr	AERC.RCALF	0.68	206.08	9.78	>5000	31.71	0.84	0.42	0.46
B2	2010	4	8hr	MMIF.RCALF	0.77	174.23	8.64	>5000	30.26	0.83	0.46	0.47
B2	2010	4	8hr	MMIF.RCALT	0.94	146.86	7.04	>5000	33.28	0.84	0.48	0.47
B2	2010	5	8hr	obs	93.13	4.72	1.00	1.00	857.68	1.00	1.00	0.95
B2	2010	5	8hr	AERC.RCALT	143.87	3.38	0.65	1.35	845.55	1.00	0.72	0.82
B2	2010	5	8hr	AERC.RCALF	143.82	3.39	0.65	1.35	845.55	1.00	0.72	0.82
B2	2010	5	8hr	MMIF.RCALF	152.79	3.51	0.61	1.40	942.90	1.00	0.72	0.79
B2	2010	5	8hr	MMIF.RCALT	152.49	3.52	0.61	1.39	942.90	1.00	0.72	0.81
B2	2011	1	8hr	obs	4.72	8.54	1.00	1.00	40.38	1.00	1.00	0.98

site	year	source	avg time	Simulation type	geo	geo	MG	VG	RHC	geo	ff2	TMS
B2	2011	1	8hr	AERC.RCALT	6.81	6.61	0.69	1.32	40.00	0.99	0.88	0.86
B2	2011	1	8hr	AERC.RCALF	4.56	10.77	1.04	1.58	35.48	0.96	0.84	0.86
B2	2011	1	8hr	MMIF.RCALF	5.10	9.38	0.93	1.47	36.67	0.96	0.82	0.87
B2	2011	1	8hr	MMIF.RCALT	6.94	6.87	0.68	1.29	40.31	0.99	0.88	0.85
B2	2011	2	8hr	obs	12.91	6.04	1.00	1.00	85.39	1.00	1.00	0.99
B2	2011	2	8hr	AERC.RCALT	16.51	6.30	0.78	1.19	80.58	0.98	0.88	0.89
B2	2011	2	8hr	AERC.RCALF	11.31	10.23	1.14	2.09	70.70	0.95	0.70	0.78
B2	2011	2	8hr	MMIF.RCALF	12.58	8.93	1.03	1.73	71.41	0.95	0.72	0.84
B2	2011	2	8hr	MMIF.RCALT	16.79	6.61	0.77	1.21	81.63	0.98	0.86	0.86
B2	2011	3	8hr	obs	21.01	3.82	1.00	1.00	94.91	1.00	1.00	0.96
B2	2011	3	8hr	AERC.RCALT	13.86	11.77	1.52	9.97	86.94	0.87	0.40	0.59
B2	2011	3	8hr	AERC.RCALF	6.91	34.23	3.04	4318.91	69.14	0.75	0.40	0.46
B2	2011	3	8hr	MMIF.RCALF	8.26	29.35	2.55	1302.06	83.91	0.76	0.30	0.46
B2	2011	3	8hr	MMIF.RCALT	13.76	13.75	1.53	15.79	81.59	0.87	0.32	0.58
B2	2011	4	8hr	obs	3.44	24.33	1.00	1.00	42.23	1.00	1.00	0.99
B2	2011	4	8hr	AERC.RCALT	4.47	15.96	0.77	1.74	39.28	0.98	0.80	0.81
B2	2011	4	8hr	AERC.RCALF	1.34	86.66	2.57	149.37	34.69	0.91	0.72	0.58
B2	2011	4	8hr	MMIF.RCALF	1.63	68.20	2.11	49.91	35.42	0.92	0.76	0.63
B2	2011	4	8hr	MMIF.RCALT	4.23	18.11	0.81	1.46	35.95	0.99	0.80	0.85
B2	2011	5	8hr	obs	84.38	4.13	1.00	1.00	740.68	1.00	1.00	0.95
B2	2011	5	8hr	AERC.RCALT	115.09	3.11	0.73	1.22	748.85	0.99	0.88	0.88
B2	2011	5	8hr	AERC.RCALF	122.31	3.20	0.69	1.28	753.36	0.99	0.82	0.85
B2	2011	5	8hr	MMIF.RCALF	121.42	3.11	0.70	1.28	753.85	0.99	0.86	0.86
B2	2011	5	8hr	MMIF.RCALT	114.04	3.04	0.74	1.23	748.77	0.99	0.86	0.88
B3	2010	1	8hr	obs	5.40	7.40	1.00	1.00	39.14	1.00	1.00	0.98
B3	2010	1	8hr	AERC.RCALT	15.47	2.28	0.35	13.32	42.26	0.97	0.60	0.58
B3	2010	1	8hr	AERC.RCALF	14.45	2.28	0.37	11.30	40.09	0.98	0.62	0.60

site	year	source	avg time	Simulation type	geo	geo	MG	VG	RHC	geo	ff2	TMS
B3	2010	1	8hr	MMIF.RCALF	11.66	3.08	0.46	4.13	37.31	0.99	0.62	0.65
B3	2010	1	8hr	MMIF.RCALT	12.48	3.15	0.43	4.36	37.56	0.99	0.62	0.65
B3	2010	2	8hr	obs	13.78	5.58	1.00	1.00	81.51	1.00	1.00	0.98
B3	2010	2	8hr	AERC.RCALT	34.15	2.16	0.40	6.07	86.99	0.97	0.56	0.61
B3	2010	2	8hr	AERC.RCALF	31.07	2.21	0.44	4.95	81.15	0.97	0.56	0.62
B3	2010	2	8hr	MMIF.RCALF	25.86	2.82	0.53	2.64	74.30	0.97	0.60	0.68
B3	2010	2	8hr	MMIF.RCALT	28.20	2.83	0.49	2.84	78.01	0.98	0.58	0.67
B3	2010	3	8hr	obs	15.37	4.81	1.00	1.00	80.26	1.00	1.00	0.93
B3	2010	3	8hr	AERC.RCALT	40.24	2.12	0.38	5.70	100.68	0.94	0.46	0.55
B3	2010	3	8hr	AERC.RCALF	37.58	2.22	0.41	4.46	94.62	0.96	0.48	0.60
B3	2010	3	8hr	MMIF.RCALF	29.63	3.12	0.52	1.99	91.43	0.98	0.58	0.71
B3	2010	3	8hr	MMIF.RCALT	32.34	2.85	0.48	2.45	104.93	0.98	0.56	0.66
B3	2010	4	8hr	obs	3.05	19.95	1.00	1.00	35.67	1.00	1.00	0.92
B3	2010	4	8hr	AERC.RCALT	18.17	2.49	0.17	2503.48	47.78	0.95	0.42	0.46
B3	2010	4	8hr	AERC.RCALF	16.67	2.51	0.18	1703.87	47.39	0.96	0.52	0.53
B3	2010	4	8hr	MMIF.RCALF	12.65	3.57	0.24	168.78	46.06	0.98	0.56	0.55
B3	2010	4	8hr	MMIF.RCALT	13.67	3.79	0.22	177.99	46.62	0.98	0.46	0.53
B3	2010	5	8hr	obs	101.97	4.40	1.00	1.00	950.13	1.00	1.00	0.98
B3	2010	5	8hr	AERC.RCALT	138.18	3.25	0.74	1.21	849.58	1.00	0.80	0.85
B3	2010	5	8hr	AERC.RCALF	140.34	3.26	0.73	1.22	849.58	1.00	0.80	0.87
B3	2010	5	8hr	MMIF.RCALF	141.03	3.29	0.72	1.22	850.73	1.00	0.80	0.87
B3	2010	5	8hr	MMIF.RCALT	139.30	3.29	0.73	1.21	850.73	1.00	0.80	0.87
B3	2011	1	8hr	obs	6.13	6.41	1.00	1.00	33.05	1.00	1.00	0.95
B3	2011	1	8hr	AERC.RCALT	9.36	3.29	0.66	2.04	37.48	0.98	0.84	0.77
B3	2011	1	8hr	AERC.RCALF	5.91	6.97	1.04	1.46	36.19	0.95	0.82	0.88
B3	2011	1	8hr	MMIF.RCALF	6.17	6.57	0.99	1.61	32.88	0.93	0.76	0.84
B3	2011	1	8hr	MMIF.RCALT	8.31	4.34	0.74	1.39	34.55	0.98	0.88	0.85

site	year	source	avg time	Simulation type	geo	geo	MG	VG	RHC	geo	ff2	TMS
B3	2011	2	8hr	obs	14.89	5.05	1.00	1.00	67.31	1.00	1.00	0.94
B3	2011	2	8hr	AERC.RCALT	20.12	3.15	0.74	1.45	82.58	0.99	0.88	0.82
B3	2011	2	8hr	AERC.RCALF	13.74	6.16	1.08	1.35	73.08	0.96	0.84	0.87
B3	2011	2	8hr	MMIF.RCALF	14.72	6.01	1.01	1.45	66.62	0.94	0.72	0.85
B3	2011	2	8hr	MMIF.RCALT	19.08	4.20	0.78	1.21	74.93	0.98	0.94	0.88
B3	2011	3	8hr	obs	15.29	5.39	1.00	1.00	68.32	1.00	1.00	0.92
B3	2011	3	8hr	AERC.RCALT	23.79	3.73	0.64	1.56	101.66	0.98	0.80	0.75
B3	2011	3	8hr	AERC.RCALF	11.04	16.59	1.39	8.00	84.12	0.93	0.62	0.64
B3	2011	3	8hr	MMIF.RCALF	11.85	15.23	1.29	6.62	78.65	0.92	0.64	0.68
B3	2011	3	8hr	MMIF.RCALT	19.13	6.56	0.80	1.36	96.89	0.97	0.86	0.83
B3	2011	4	8hr	obs	3.59	18.95	1.00	1.00	30.46	1.00	1.00	0.93
B3	2011	4	8hr	AERC.RCALT	11.23	4.43	0.32	35.37	44.12	0.98	0.72	0.55
B3	2011	4	8hr	AERC.RCALF	2.72	48.91	1.32	9.20	42.08	0.95	0.62	0.68
B3	2011	4	8hr	MMIF.RCALF	2.72	42.63	1.32	9.64	39.85	0.93	0.46	0.64
B3	2011	4	8hr	MMIF.RCALT	8.00	7.54	0.45	5.36	42.48	0.98	0.76	0.66
B3	2011	5	8hr	obs	72.91	3.98	1.00	1.00	672.27	1.00	1.00	0.93
B3	2011	5	8hr	AERC.RCALT	107.63	4.08	0.68	1.20	993.71	0.99	0.94	0.82
B3	2011	5	8hr	AERC.RCALF	124.78	3.88	0.58	1.40	940.98	0.99	0.78	0.80
B3	2011	5	8hr	MMIF.RCALF	131.01	3.61	0.56	1.45	927.39	0.99	0.68	0.78
B3	2011	5	8hr	MMIF.RCALT	113.73	3.79	0.64	1.23	989.71	1.00	1.00	0.88
B3	2012	1	8hr	obs	6.40	5.46	1.00	1.00	34.28	1.00	1.00	0.99
B3	2012	1	8hr	AERC.RCALT	8.17	4.74	0.78	1.14	35.13	0.99	0.94	0.91
B3	2012	1	8hr	AERC.RCALF	7.98	4.78	0.80	1.11	32.82	0.99	0.96	0.92
B3	2012	1	8hr	MMIF.RCALF	7.74	5.22	0.83	1.09	33.71	0.99	0.98	0.94
B3	2012	1	8hr	MMIF.RCALT	7.71	5.62	0.83	1.08	35.23	0.99	1.00	0.94
B3	2012	2	8hr	obs	15.69	4.22	1.00	1.00	65.46	1.00	1.00	0.96
B3	2012	2	8hr	AERC.RCALT	20.59	3.69	0.76	1.15	64.50	0.99	0.96	0.91

site	year	source	avg time	Simulation type	geo	geo	MG	VG	RHC	geo	ff2	TMS
B3	2012	2	8hr	AERC.RCALF	17.64	4.60	0.89	1.09	62.41	0.99	0.98	0.95
B3	2012	2	8hr	MMIF.RCALF	17.04	5.17	0.92	1.14	65.01	0.98	0.94	0.94
B3	2012	2	8hr	MMIF.RCALT	19.27	4.30	0.81	1.11	65.95	0.99	0.98	0.93
B3	2012	3	8hr	obs	21.50	3.05	1.00	1.00	82.37	1.00	1.00	0.94
B3	2012	3	8hr	AERC.RCALT	23.92	4.79	0.90	1.53	109.15	0.94	0.80	0.81
B3	2012	3	8hr	AERC.RCALF	17.90	6.89	1.20	3.31	80.49	0.88	0.68	0.69
B3	2012	3	8hr	MMIF.RCALF	15.98	8.86	1.35	6.01	77.64	0.88	0.72	0.70
B3	2012	3	8hr	MMIF.RCALT	18.95	7.85	1.14	3.67	107.21	0.92	0.74	0.71
B3	2012	4	8hr	obs	4.82	10.96	1.00	1.00	34.24	1.00	1.00	0.95
B3	2012	4	8hr	AERC.RCALT	6.64	12.11	0.73	1.16	44.90	1.00	1.00	0.87
B3	2012	4	8hr	AERC.RCALF	6.90	12.56	0.70	1.28	38.09	0.99	0.76	0.82
B3	2012	4	8hr	MMIF.RCALF	5.51	18.57	0.88	1.48	36.62	0.99	0.84	0.87
B3	2012	4	8hr	MMIF.RCALT	5.07	19.64	0.95	1.49	44.83	1.00	0.88	0.86
B3	2012	5	8hr	obs	79.31	3.82	1.00	1.00	696.49	1.00	1.00	0.92
B3	2012	5	8hr	AERC.RCALT	131.58	3.79	0.60	1.33	1067.65	0.99	0.86	0.77
B3	2012	5	8hr	AERC.RCALF	135.11	3.81	0.59	1.38	1045.50	0.99	0.78	0.81
B3	2012	5	8hr	MMIF.RCALF	137.46	3.75	0.58	1.41	1041.22	0.99	0.76	0.81
B3	2012	5	8hr	MMIF.RCALT	133.43	3.73	0.59	1.35	1063.68	0.99	0.84	0.83
C1	2011	1	8hr	obs	9.65	2.58	1.00	1.00	34.09	1.00	1.00	0.95
C1	2011	1	8hr	AERC.RCALT	12.11	2.59	0.80	1.08	40.45	0.99	1.00	0.91
C1	2011	1	8hr	AERC.RCALF	11.21	2.65	0.86	1.07	39.52	0.97	1.00	0.95
C1	2011	1	8hr	MMIF.RCALF	9.07	3.83	1.06	1.35	39.82	0.95	0.84	0.89
C1	2011	1	8hr	MMIF.RCALT	10.57	3.36	0.91	1.17	43.92	0.96	0.96	0.92
C1	2011	2	8hr	obs	22.02	2.37	1.00	1.00	69.20	1.00	1.00	0.95
C1	2011	2	8hr	AERC.RCALT	27.35	2.53	0.81	1.08	84.78	0.99	1.00	0.91

site	year	source	avg time	Simulation type	geo	geo	MG	VG	RHC	geo	ff2	TMS
C1	2011	2	8hr	AERC.RCALF	25.25	2.45	0.87	1.07	76.36	0.97	1.00	0.94
C1	2011	2	8hr	MMIF.RCALF	21.41	3.38	1.03	1.27	76.57	0.95	0.84	0.91
C1	2011	2	8hr	MMIF.RCALT	24.65	3.20	0.89	1.19	87.25	0.97	0.94	0.90
C1	2011	3	8hr	obs	26.04	2.09	1.00	1.00	77.67	1.00	1.00	0.92
C1	2011	3	8hr	AERC.RCALT	31.08	2.36	0.84	1.08	81.72	0.97	1.00	0.94
C1	2011	3	8hr	AERC.RCALF	32.52	2.18	0.80	1.09	81.31	0.97	1.00	0.94
C1	2011	3	8hr	MMIF.RCALF	27.28	3.06	0.96	1.31	86.62	0.93	0.88	0.89
C1	2011	3	8hr	MMIF.RCALT	25.62	3.48	1.02	1.49	89.61	0.93	0.82	0.87
C1	2011	4	8hr	obs	11.54	2.13	1.00	1.00	34.73	1.00	1.00	0.94
C1	2011	4	8hr	AERC.RCALT	13.44	2.67	0.86	1.13	40.66	0.97	0.96	0.91
C1	2011	4	8hr	AERC.RCALF	14.24	2.86	0.81	1.24	41.52	0.95	0.86	0.88
C1	2011	4	8hr	MMIF.RCALF	9.90	4.96	1.17	2.49	42.28	0.93	0.66	0.77
C1	2011	4	8hr	MMIF.RCALT	10.66	4.19	1.08	1.82	40.73	0.94	0.84	0.84
C1	2011	5	8hr	obs	89.18	3.96	1.00	1.00	898.20	1.00	1.00	0.95
C1	2011	5	8hr	AERC.RCALT	126.21	3.98	0.71	1.14	1141.87	1.00	1.00	0.87
C1	2011	5	8hr	AERC.RCALF	134.91	3.84	0.66	1.22	1141.11	0.99	0.94	0.88
C1	2011	5	8hr	MMIF.RCALF	134.11	3.84	0.67	1.20	1137.41	1.00	1.00	0.90
C1	2011	5	8hr	MMIF.RCALT	126.52	3.91	0.71	1.14	1137.87	1.00	1.00	0.92
C1	2012	1	8hr	obs	8.18	3.88	1.00	1.00	39.90	1.00	1.00	0.98
C1	2012	1	8hr	AERC.RCALT	8.92	4.17	0.92	1.10	38.46	0.98	0.98	0.95
C1	2012	1	8hr	AERC.RCALF	8.70	4.19	0.94	1.11	34.34	0.98	0.98	0.94
C1	2012	1	8hr	MMIF.RCALF	7.55	5.09	1.08	1.32	36.02	0.96	0.86	0.89
C1	2012	1	8hr	MMIF.RCALT	7.34	5.75	1.11	1.36	38.66	0.97	0.86	0.88
C1	2012	2	8hr	obs	19.46	3.41	1.00	1.00	78.12	1.00	1.00	0.97
C1	2012	2	8hr	AERC.RCALT	20.35	3.86	0.96	1.13	76.17	0.97	0.98	0.95

site	year	source	avg time	Simulation type	geo	geo	MG	VG	RHC	geo	ff2	TMS
C1	2012	2	8hr	AERC.RCALF	19.80	4.00	0.98	1.15	71.84	0.97	0.98	0.95
C1	2012	2	8hr	MMIF.RCALF	16.96	5.16	1.15	1.48	72.44	0.95	0.82	0.86
C1	2012	2	8hr	MMIF.RCALT	17.36	5.21	1.12	1.43	76.51	0.96	0.82	0.86
C1	2012	3	8hr	obs	27.35	2.52	1.00	1.00	101.54	1.00	1.00	0.98
C1	2012	3	8hr	AERC.RCALT	23.86	4.81	1.15	2.00	94.91	0.91	0.88	0.82
C1	2012	3	8hr	AERC.RCALF	22.68	4.97	1.21	2.23	78.58	0.90	0.88	0.78
C1	2012	3	8hr	MMIF.RCALF	15.46	9.62	1.77	14.71	80.55	0.86	0.74	0.64
C1	2012	3	8hr	MMIF.RCALT	16.82	9.64	1.63	12.60	98.60	0.88	0.76	0.63
C1	2012	4	8hr	obs	7.66	6.12	1.00	1.00	45.98	1.00	1.00	1.00
C1	2012	4	8hr	AERC.RCALT	7.99	8.02	0.96	1.20	40.93	0.99	0.94	0.92
C1	2012	4	8hr	AERC.RCALF	8.32	9.15	0.92	1.42	37.66	0.98	0.70	0.84
C1	2012	4	8hr	MMIF.RCALF	5.46	17.54	1.40	4.67	40.13	0.97	0.60	0.69
C1	2012	4	8hr	MMIF.RCALT	5.17	15.29	1.48	3.49	41.27	0.97	0.70	0.72
C1	2012	5	8hr	obs	86.00	3.82	1.00	1.00	755.03	1.00	1.00	0.95
C1	2012	5	8hr	AERC.RCALT	127.45	3.44	0.68	1.20	925.14	1.00	1.00	0.86
C1	2012	5	8hr	AERC.RCALF	132.61	3.47	0.65	1.24	925.65	1.00	1.00	0.89
C1	2012	5	8hr	MMIF.RCALF	134.19	3.51	0.64	1.26	924.40	0.99	0.90	0.87
C1	2012	5	8hr	MMIF.RCALT	127.35	3.46	0.68	1.19	924.00	1.00	1.00	0.90
C2	2010	1	8hr	obs	8.62	4.09	1.00	1.00	42.44	1.00	1.00	0.98
C2	2010	1	8hr	AERC.RCALT	9.69	4.19	0.89	1.05	44.11	0.99	1.00	0.96
C2	2010	1	8hr	AERC.RCALF	7.07	6.09	1.22	1.41	40.43	0.97	0.82	0.85
C2	2010	1	8hr	MMIF.RCALF	7.53	5.97	1.14	1.33	42.44	0.98	0.86	0.88
C2	2010	1	8hr	MMIF.RCALT	9.89	4.57	0.87	1.07	45.00	0.99	1.00	0.95
C2	2010	2	8hr	obs	19.91	3.86	1.00	1.00	83.47	1.00	1.00	0.98
C2	2010	2	8hr	AERC.RCALT	23.62	3.68	0.84	1.07	89.80	0.99	1.00	0.94
C2	2010	2	8hr	AERC.RCALF	17.11	5.34	1.16	1.29	80.53	0.97	0.80	0.86
C2	2010	2	8hr	MMIF.RCALF	18.45	5.27	1.08	1.23	81.07	0.98	0.86	0.91

site	year	source	avg time	Simulation type	geo	geo	MG	VG	RHC	geo	ff2	TMS
C2	2010	2	8hr	MMIF.RCALT	24.18	4.01	0.82	1.07	89.63	0.99	1.00	0.93
C2	2010	3	8hr	obs	17.91	4.44	1.00	1.00	84.07	1.00	1.00	0.93
C2	2010	3	8hr	AERC.RCALT	26.35	4.25	0.68	1.24	90.04	0.99	0.90	0.86
C2	2010	3	8hr	AERC.RCALF	17.99	7.44	1.00	1.50	71.82	0.98	0.90	0.87
C2	2010	3	8hr	MMIF.RCALF	18.22	7.49	0.98	1.49	74.86	0.98	0.90	0.90
C2	2010	3	8hr	MMIF.RCALT	23.51	6.36	0.76	1.42	91.54	0.97	0.80	0.81
C2	2010	4	8hr	obs	7.19	5.21	1.00	1.00	33.99	1.00	1.00	0.91
C2	2010	4	8hr	AERC.RCALT	7.74	7.26	0.93	1.21	36.62	0.99	0.88	0.91
C2	2010	4	8hr	AERC.RCALF	3.61	29.40	1.99	44.22	37.14	0.97	0.78	0.65
C2	2010	4	8hr	MMIF.RCALF	4.03	22.16	1.79	17.33	36.91	0.96	0.78	0.67
C2	2010	4	8hr	MMIF.RCALT	6.67	10.85	1.08	1.94	36.18	0.99	0.86	0.85
C2	2010	5	8hr	obs	106.45	3.69	1.00	1.00	886.98	1.00	1.00	0.96
C2	2010	5	8hr	AERC.RCALT	130.00	3.24	0.82	1.07	971.59	1.00	1.00	0.93
C2	2010	5	8hr	AERC.RCALF	135.45	3.28	0.79	1.08	973.56	1.00	1.00	0.94
C2	2010	5	8hr	MMIF.RCALF	135.79	3.25	0.78	1.09	969.45	1.00	1.00	0.94
C2	2010	5	8hr	MMIF.RCALT	130.94	3.21	0.81	1.07	967.85	1.00	1.00	0.95
C2	2012	1	8hr	obs	6.66	4.55	1.00	1.00	32.33	1.00	1.00	0.95
C2	2012	1	8hr	AERC.RCALT	6.70	5.25	0.99	1.08	36.08	0.99	0.96	0.95
C2	2012	1	8hr	AERC.RCALF	4.67	6.87	1.43	2.04	32.22	0.93	0.82	0.77
C2	2012	1	8hr	MMIF.RCALF	4.72	7.17	1.41	1.96	33.87	0.94	0.82	0.79
C2	2012	1	8hr	MMIF.RCALT	6.43	5.94	1.04	1.16	38.66	0.99	0.92	0.92
C2	2012	2	8hr	obs	14.95	4.19	1.00	1.00	68.10	1.00	1.00	0.97
C2	2012	2	8hr	AERC.RCALT	15.46	5.22	0.97	1.09	75.16	0.99	0.98	0.95
C2	2012	2	8hr	AERC.RCALF	11.31	6.61	1.32	1.64	63.00	0.96	0.80	0.79
C2	2012	2	8hr	MMIF.RCALF	11.72	6.96	1.28	1.67	68.94	0.97	0.80	0.81
C2	2012	2	8hr	MMIF.RCALT	15.42	5.65	0.97	1.16	78.33	0.99	0.88	0.92
C2	2012	3	8hr	obs	19.19	3.16	1.00	1.00	70.40	1.00	1.00	0.95

site	year	source	avg time	Simulation type	geo	geo	MG	VG	RHC	geo	ff2	TMS
C2	2012	3	8hr	AERC.RCALT	18.60	6.19	1.03	1.75	93.82	0.97	0.84	0.82
C2	2012	3	8hr	AERC.RCALF	11.22	13.11	1.71	15.02	67.77	0.93	0.70	0.60
C2	2012	3	8hr	MMIF.RCALF	12.79	11.86	1.50	10.69	70.86	0.92	0.54	0.64
C2	2012	3	8hr	MMIF.RCALT	18.82	7.08	1.02	2.38	88.26	0.95	0.64	0.76
C2	2012	4	8hr	obs	6.17	6.54	1.00	1.00	34.45	1.00	1.00	0.97
C2	2012	4	8hr	AERC.RCALT	4.45	20.04	1.38	4.50	35.63	0.99	0.70	0.72
C2	2012	4	8hr	AERC.RCALF	1.84	57.28	3.36	1147.62	32.64	0.94	0.56	0.54
C2	2012	4	8hr	MMIF.RCALF	2.21	36.94	2.79	144.72	32.49	0.93	0.64	0.59
C2	2012	4	8hr	MMIF.RCALT	3.89	19.23	1.59	4.77	32.96	0.98	0.74	0.71
C2	2012	5	8hr	obs	91.87	4.10	1.00	1.00	892.22	1.00	1.00	0.99
C2	2012	5	8hr	AERC.RCALT	112.38	3.64	0.82	1.10	862.70	0.99	1.00	0.94
C2	2012	5	8hr	AERC.RCALF	118.46	3.70	0.78	1.16	869.39	0.98	0.88	0.90
C2	2012	5	8hr	MMIF.RCALF	121.05	3.58	0.76	1.18	871.84	0.98	0.86	0.89
C2	2012	5	8hr	MMIF.RCALT	113.30	3.60	0.81	1.11	865.40	0.99	1.00	0.94

AERMOD results statistical scores: 24-hour average concentrations.

site	year	source	avg time	Simulation type	geo mean	geo stddev	MG	VG	RHC	geo R	ff2	TMS
B2	2010	1	24hr	obs	3.51	5.20	1.00	1.00	28.99	1.00	1.00	0.97
B2	2010	1	24hr	AERC.RCALT	2.24	15.99	1.57	11.88	23.59	0.89	0.52	0.59
B2	2010	1	24hr	AERC.RCALF	2.20	13.82	1.60	8.94	23.10	0.88	0.38	0.60
B2	2010	1	24hr	MMIF.RCALF	2.55	11.68	1.38	5.06	23.63	0.89	0.50	0.66
B2	2010	1	24hr	MMIF.RCALT	2.46	14.97	1.43	8.79	23.43	0.90	0.52	0.64
B2	2010	2	24hr	obs	8.16	4.54	1.00	1.00	61.21	1.00	1.00	0.95
B2	2010	2	24hr	AERC.RCALT	5.99	13.07	1.36	8.87	54.49	0.88	0.50	0.62
B2	2010	2	24hr	AERC.RCALF	5.62	11.90	1.45	8.10	52.69	0.86	0.34	0.60
B2	2010	2	24hr	MMIF.RCALF	6.28	10.69	1.30	5.60	53.88	0.87	0.40	0.64
B2	2010	2	24hr	MMIF.RCALT	6.51	12.56	1.26	7.29	54.57	0.88	0.52	0.66
B2	2010	3	24hr	obs	9.57	3.91	1.00	1.00	54.31	1.00	1.00	0.91
B2	2010	3	24hr	AERC.RCALT	5.40	20.75	1.77	64.26	60.01	0.87	0.32	0.54
B2	2010	3	24hr	AERC.RCALF	4.78	21.14	2.00	94.35	48.81	0.85	0.28	0.49
B2	2010	3	24hr	MMIF.RCALF	3.79	35.49	2.52	1384.36	49.31	0.85	0.30	0.51
B2	2010	3	24hr	MMIF.RCALT	4.48	30.02	2.14	436.12	54.83	0.86	0.34	0.51
B2	2010	4	24hr	obs	3.13	7.35	1.00	1.00	23.51	1.00	1.00	0.94
B2	2010	4	24hr	AERC.RCALT	0.44	225.54	7.18	>5000	24.00	0.88	0.44	0.49
B2	2010	4	24hr	AERC.RCALF	0.00	NA	NA	NA	21.74	0.93	0.40	NA
B2	2010	4	24hr	MMIF.RCALF	0.41	201.14	7.55	>5000	21.22	0.86	0.42	0.48
B2	2010	4	24hr	MMIF.RCALT	0.47	182.97	6.62	>5000	22.66	0.87	0.48	0.49
B2	2010	5	24hr	obs	43.76	5.16	1.00	1.00	483.47	1.00	1.00	0.90
B2	2010	5	24hr	AERC.RCALT	71.66	3.57	0.61	1.47	487.65	1.00	0.70	0.80
B2	2010	5	24hr	AERC.RCALF	73.15	3.65	0.60	1.49	487.65	1.00	0.64	0.78
B2	2010	5	24hr	MMIF.RCALF	76.07	3.72	0.58	1.54	539.44	1.00	0.62	0.75
B2	2010	5	24hr	MMIF.RCALT	73.98	3.66	0.59	1.50	539.44	1.00	0.70	0.79
B2	2011	1	24hr	obs	2.48	10.65	1.00	1.00	31.61	1.00	1.00	0.96

site	year	source	avg time	Simulation type	geo mean	geo stddev	MG	VG	RHC	geo R	ff2	TMS
B2	2011	1	24hr	AERC.RCALT	4.06	8.75	0.61	1.61	28.32	0.98	0.54	0.73
B2	2011	1	24hr	AERC.RCALF	2.73	13.59	0.91	1.99	25.47	0.95	0.48	0.75
B2	2011	1	24hr	MMIF.RCALF	3.14	11.23	0.79	1.77	26.08	0.96	0.50	0.76
B2	2011	1	24hr	MMIF.RCALT	4.10	8.86	0.60	1.54	30.54	0.99	0.56	0.73
B2	2011	2	24hr	obs	6.55	7.57	1.00	1.00	62.73	1.00	1.00	0.95
B2	2011	2	24hr	AERC.RCALT	9.89	8.46	0.66	1.60	56.10	0.97	0.58	0.75
B2	2011	2	24hr	AERC.RCALF	7.01	12.64	0.94	2.71	49.85	0.93	0.44	0.71
B2	2011	2	24hr	MMIF.RCALF	7.88	10.64	0.83	2.15	53.49	0.94	0.46	0.73
B2	2011	2	24hr	MMIF.RCALT	9.96	8.68	0.66	1.58	61.32	0.97	0.62	0.75
B2	2011	3	24hr	obs	10.52	4.81	1.00	1.00	74.38	1.00	1.00	0.98
B2	2011	3	24hr	AERC.RCALT	7.71	15.45	1.37	11.16	60.84	0.89	0.34	0.57
B2	2011	3	24hr	AERC.RCALF	3.80	45.26	2.77	>5000	55.60	0.79	0.30	0.47
B2	2011	3	24hr	MMIF.RCALF	4.30	37.12	2.44	1371.90	58.43	0.80	0.36	0.50
B2	2011	3	24hr	MMIF.RCALT	7.32	17.50	1.44	16.51	64.14	0.89	0.38	0.59
B2	2011	4	24hr	obs	1.71	30.78	1.00	1.00	31.66	1.00	1.00	0.98
B2	2011	4	24hr	AERC.RCALT	2.43	21.14	0.70	1.82	28.20	0.98	0.78	0.78
B2	2011	4	24hr	AERC.RCALF	0.70	115.37	2.44	155.14	27.70	0.92	0.70	0.60
B2	2011	4	24hr	MMIF.RCALF	0.84	89.98	2.03	51.01	29.89	0.93	0.70	0.61
B2	2011	4	24hr	MMIF.RCALT	2.28	23.64	0.75	1.46	28.43	0.99	0.76	0.83
B2	2011	5	24hr	obs	50.85	5.01	1.00	1.00	489.44	1.00	1.00	0.93
B2	2011	5	24hr	AERC.RCALT	86.87	3.28	0.59	1.67	603.29	0.99	0.54	0.70
B2	2011	5	24hr	AERC.RCALF	88.62	3.30	0.57	1.70	599.08	0.99	0.54	0.74
B2	2011	5	24hr	MMIF.RCALF	88.17	3.28	0.58	1.70	605.92	0.99	0.54	0.74
B2	2011	5	24hr	MMIF.RCALT	86.93	3.27	0.59	1.68	602.98	0.99	0.54	0.74
B3	2010	1	24hr	obs	3.14	10.05	1.00	1.00	31.61	1.00	1.00	0.97
B3	2010	1	24hr	AERC.RCALT	8.84	2.89	0.36	15.52	34.42	0.98	0.50	0.56
B3	2010	1	24hr	AERC.RCALF	8.35	2.91	0.38	13.54	31.85	0.98	0.52	0.57

site	year	source	avg time	Simulation type	geo mean	geo stddev	MG	VG	RHC	geo R	ff2	TMS
B3	2010	1	24hr	MMIF.RCALF	6.51	3.99	0.48	4.47	29.41	0.98	0.52	0.63
B3	2010	1	24hr	MMIF.RCALT	6.92	4.04	0.45	4.70	30.86	0.99	0.52	0.63
B3	2010	2	24hr	obs	8.19	7.37	1.00	1.00	64.14	1.00	1.00	0.96
B3	2010	2	24hr	AERC.RCALT	19.30	2.74	0.42	6.28	70.53	0.97	0.50	0.59
B3	2010	2	24hr	AERC.RCALF	17.92	2.80	0.46	5.43	65.90	0.97	0.50	0.61
B3	2010	2	24hr	MMIF.RCALF	14.45	3.67	0.57	2.79	59.01	0.96	0.48	0.65
B3	2010	2	24hr	MMIF.RCALT	15.62	3.65	0.52	2.87	65.20	0.97	0.50	0.65
B3	2010	3	24hr	obs	8.25	6.19	1.00	1.00	59.50	1.00	1.00	0.91
B3	2010	3	24hr	AERC.RCALT	21.67	2.73	0.38	5.57	80.46	0.97	0.46	0.55
B3	2010	3	24hr	AERC.RCALF	20.82	2.83	0.40	4.71	76.45	0.98	0.38	0.58
B3	2010	3	24hr	MMIF.RCALF	15.56	3.98	0.53	2.01	70.31	0.98	0.50	0.69
B3	2010	3	24hr	MMIF.RCALT	16.80	3.67	0.49	2.34	78.02	0.99	0.52	0.66
B3	2010	4	24hr	obs	1.64	26.04	1.00	1.00	28.29	1.00	1.00	0.92
B3	2010	4	24hr	AERC.RCALT	9.20	3.13	0.18	2295.20	38.60	0.96	0.52	0.48
B3	2010	4	24hr	AERC.RCALF	9.30	3.27	0.18	1799.97	38.42	0.98	0.38	0.51
B3	2010	4	24hr	MMIF.RCALF	6.80	4.73	0.24	156.36	35.42	0.99	0.42	0.52
B3	2010	4	24hr	MMIF.RCALT	6.61	4.77	0.25	144.38	36.60	0.99	0.58	0.56
B3	2010	5	24hr	obs	54.21	4.66	1.00	1.00	571.44	1.00	1.00	0.93
B3	2010	5	24hr	AERC.RCALT	76.70	3.41	0.71	1.30	432.19	0.99	0.78	0.80
B3	2010	5	24hr	AERC.RCALF	80.74	3.40	0.67	1.41	432.15	0.98	0.64	0.80
B3	2010	5	24hr	MMIF.RCALF	80.72	3.42	0.67	1.39	436.30	0.98	0.64	0.80
B3	2010	5	24hr	MMIF.RCALT	77.36	3.40	0.70	1.31	436.28	0.99	0.78	0.85
B3	2011	1	24hr	obs	3.37	8.49	1.00	1.00	26.99	1.00	1.00	0.96
B3	2011	1	24hr	AERC.RCALT	5.27	4.56	0.64	2.01	29.43	0.98	0.80	0.77
B3	2011	1	24hr	AERC.RCALF	3.90	7.85	0.87	1.50	26.78	0.96	0.76	0.83
B3	2011	1	24hr	MMIF.RCALF	4.08	7.40	0.83	1.71	28.61	0.94	0.66	0.79
B3	2011	1	24hr	MMIF.RCALT	4.70	6.00	0.72	1.39	30.27	0.99	0.82	0.84

site	year	source	avg time	Simulation type	geo mean	geo stddev	MG	VG	RHC	geo R	ff2	TMS
B3	2011	2	24hr	obs	8.34	6.78	1.00	1.00	53.60	1.00	1.00	0.94
B3	2011	2	24hr	AERC.RCALT	11.26	4.28	0.74	1.46	62.21	0.99	0.88	0.83
B3	2011	2	24hr	AERC.RCALF	8.53	7.09	0.98	1.31	55.55	0.97	0.86	0.89
B3	2011	2	24hr	MMIF.RCALF	9.19	6.94	0.91	1.48	59.10	0.95	0.64	0.82
B3	2011	2	24hr	MMIF.RCALT	10.66	5.59	0.78	1.20	59.10	0.99	0.92	0.90
B3	2011	3	24hr	obs	7.70	6.66	1.00	1.00	49.54	1.00	1.00	0.90
B3	2011	3	24hr	AERC.RCALT	12.62	4.91	0.61	1.52	72.79	0.99	0.76	0.74
B3	2011	3	24hr	AERC.RCALF	6.35	21.22	1.21	7.12	65.72	0.95	0.56	0.68
B3	2011	3	24hr	MMIF.RCALF	6.73	18.58	1.14	5.49	63.93	0.94	0.48	0.69
B3	2011	3	24hr	MMIF.RCALT	10.00	8.53	0.77	1.28	72.73	0.99	0.92	0.87
B3	2011	4	24hr	obs	1.80	23.35	1.00	1.00	22.95	1.00	1.00	0.91
B3	2011	4	24hr	AERC.RCALT	5.57	5.91	0.32	29.37	35.83	0.98	0.68	0.53
B3	2011	4	24hr	AERC.RCALF	1.58	65.53	1.14	8.90	31.32	0.96	0.56	0.68
B3	2011	4	24hr	MMIF.RCALF	1.68	50.92	1.07	7.64	30.38	0.94	0.52	0.70
B3	2011	4	24hr	MMIF.RCALT	4.24	10.23	0.43	5.01	33.53	0.99	0.62	0.63
B3	2011	5	24hr	obs	48.48	4.72	1.00	1.00	506.73	1.00	1.00	0.90
B3	2011	5	24hr	AERC.RCALT	63.47	4.23	0.76	1.14	479.86	0.99	1.00	0.92
B3	2011	5	24hr	AERC.RCALF	73.35	3.86	0.66	1.32	454.63	0.98	0.82	0.83
B3	2011	5	24hr	MMIF.RCALF	75.53	3.54	0.64	1.36	454.58	0.99	0.68	0.81
B3	2011	5	24hr	MMIF.RCALT	67.58	3.91	0.72	1.17	477.57	1.00	1.00	0.90
B3	2012	1	24hr	obs	3.70	6.82	1.00	1.00	17.59	1.00	1.00	0.90
B3	2012	1	24hr	AERC.RCALT	3.50	5.89	1.06	1.13	16.06	0.99	0.92	0.93
B3	2012	1	24hr	AERC.RCALF	3.59	5.59	1.03	1.10	16.89	0.99	0.94	0.95
B3	2012	1	24hr	MMIF.RCALF	3.58	6.10	1.03	1.05	17.34	1.00	0.98	0.97
B3	2012	1	24hr	MMIF.RCALT	3.31	6.98	1.12	1.06	16.98	0.99	0.98	0.96
B3	2012	2	24hr	obs	9.39	5.17	1.00	1.00	40.19	1.00	1.00	0.92
B3	2012	2	24hr	AERC.RCALT	8.76	4.79	1.07	1.12	40.08	0.98	0.92	0.94

site	year	source	avg time	Simulation type	geo mean	geo stddev	MG	VG	RHC	geo R	ff2	TMS
B3	2012	2	24hr	AERC.RCALF	7.76	5.45	1.21	1.11	39.01	0.99	0.88	0.91
B3	2012	2	24hr	MMIF.RCALF	7.80	6.05	1.20	1.13	41.76	0.99	0.94	0.92
B3	2012	2	24hr	MMIF.RCALT	8.25	5.56	1.14	1.13	41.72	0.98	0.90	0.93
B3	2012	3	24hr	obs	12.53	3.67	1.00	1.00	47.48	1.00	1.00	0.89
B3	2012	3	24hr	AERC.RCALT	11.26	6.03	1.11	1.47	81.11	0.97	0.82	0.79
B3	2012	3	24hr	AERC.RCALF	8.02	8.03	1.56	3.19	43.77	0.94	0.68	0.62
B3	2012	3	24hr	MMIF.RCALF	7.09	10.17	1.77	5.79	42.77	0.93	0.68	0.67
B3	2012	3	24hr	MMIF.RCALT	9.64	10.04	1.30	3.65	77.00	0.96	0.82	0.68
B3	2012	4	24hr	obs	2.72	14.17	1.00	1.00	22.36	1.00	1.00	0.90
B3	2012	4	24hr	AERC.RCALT	2.84	14.44	0.96	1.14	32.31	0.99	0.94	0.89
B3	2012	4	24hr	AERC.RCALF	2.92	14.23	0.93	1.17	19.11	0.99	0.98	0.87
B3	2012	4	24hr	MMIF.RCALF	2.39	21.19	1.14	1.38	19.00	0.99	0.90	0.90
B3	2012	4	24hr	MMIF.RCALT	2.18	23.25	1.25	1.48	30.36	0.99	0.80	0.78
B3	2012	5	24hr	obs	60.17	4.09	1.00	1.00	547.74	1.00	1.00	0.90
B3	2012	5	24hr	AERC.RCALT	72.83	4.58	0.83	1.07	766.40	1.00	1.00	0.89
B3	2012	5	24hr	AERC.RCALF	78.20	4.66	0.77	1.16	766.57	0.99	0.90	0.90
B3	2012	5	24hr	MMIF.RCALF	78.36	4.60	0.77	1.15	764.86	0.99	0.96	0.92
B3	2012	5	24hr	MMIF.RCALT	72.85	4.55	0.83	1.07	764.70	1.00	1.00	0.95
C1	2011	1	24hr	obs	4.36	3.22	1.00	1.00	25.20	1.00	1.00	0.91
C1	2011	1	24hr	AERC.RCALT	5.87	3.25	0.74	1.17	27.48	0.97	1.00	0.90
C1	2011	1	24hr	AERC.RCALF	6.32	3.40	0.69	1.32	29.40	0.95	0.70	0.81
C1	2011	1	24hr	MMIF.RCALF	4.95	4.87	0.88	1.48	29.61	0.94	0.66	0.83
C1	2011	1	24hr	MMIF.RCALT	4.95	4.27	0.88	1.22	28.48	0.97	0.92	0.91
C1	2011	2	24hr	obs	9.93	3.02	1.00	1.00	54.77	1.00	1.00	0.93
C1	2011	2	24hr	AERC.RCALT	12.81	3.07	0.78	1.15	54.62	0.97	1.00	0.92
C1	2011	2	24hr	AERC.RCALF	13.81	3.03	0.72	1.28	58.26	0.94	0.68	0.81
C1	2011	2	24hr	MMIF.RCALF	11.17	4.17	0.89	1.35	58.51	0.94	0.88	0.89

site	year	source	avg time	Simulation type	geo mean	geo stddev	MG	VG	RHC	geo R	ff2	TMS
C1	2011	2	24hr	MMIF.RCALT	10.95	4.01	0.91	1.23	56.60	0.96	0.90	0.91
C1	2011	3	24hr	obs	11.86	2.75	1.00	1.00	57.23	1.00	1.00	0.93
C1	2011	3	24hr	AERC.RCALT	15.79	2.97	0.75	1.23	57.95	0.95	0.98	0.90
C1	2011	3	24hr	AERC.RCALF	18.00	2.67	0.66	1.43	55.85	0.91	0.60	0.77
C1	2011	3	24hr	MMIF.RCALF	13.75	3.68	0.86	1.47	58.24	0.90	0.60	0.80
C1	2011	3	24hr	MMIF.RCALT	12.02	4.23	0.99	1.55	56.36	0.91	0.84	0.87
C1	2011	4	24hr	obs	5.37	2.80	1.00	1.00	25.52	1.00	1.00	0.93
C1	2011	4	24hr	AERC.RCALT	7.03	3.53	0.76	1.29	28.62	0.95	0.72	0.82
C1	2011	4	24hr	AERC.RCALF	7.56	3.69	0.71	1.52	29.47	0.92	0.62	0.78
C1	2011	4	24hr	MMIF.RCALF	5.41	6.45	0.99	2.98	31.63	0.90	0.46	0.72
C1	2011	4	24hr	MMIF.RCALT	5.17	5.54	1.04	2.03	29.94	0.93	0.86	0.84
C1	2011	5	24hr	obs	45.89	4.90	1.00	1.00	509.64	1.00	1.00	0.89
C1	2011	5	24hr	AERC.RCALT	79.88	4.78	0.57	1.39	975.60	1.00	0.82	0.73
C1	2011	5	24hr	AERC.RCALF	95.54	4.27	0.48	1.86	975.32	0.99	0.44	0.69
C1	2011	5	24hr	MMIF.RCALF	89.49	4.60	0.51	1.67	972.25	0.99	0.68	0.75
C1	2011	5	24hr	MMIF.RCALT	76.12	5.10	0.60	1.33	972.25	1.00	0.88	0.85
C1	2012	1	24hr	obs	4.35	5.33	1.00	1.00	34.07	1.00	1.00	0.98
C1	2012	1	24hr	AERC.RCALT	4.69	5.14	0.93	1.20	27.03	0.97	0.84	0.87
C1	2012	1	24hr	AERC.RCALF	5.94	5.14	0.73	1.64	27.62	0.93	0.70	0.79
C1	2012	1	24hr	MMIF.RCALF	4.75	5.62	0.92	1.43	29.58	0.94	0.68	0.83
C1	2012	1	24hr	MMIF.RCALT	4.00	6.81	1.09	1.37	27.79	0.96	0.70	0.85
C1	2012	2	24hr	obs	10.36	4.82	1.00	1.00	75.77	1.00	1.00	1.00
C1	2012	2	24hr	AERC.RCALT	10.75	4.74	0.96	1.26	54.11	0.95	0.76	0.84
C1	2012	2	24hr	AERC.RCALF	12.50	4.90	0.83	1.58	57.20	0.92	0.64	0.79
C1	2012	2	24hr	MMIF.RCALF	10.02	5.60	1.03	1.47	61.26	0.93	0.64	0.83
C1	2012	2	24hr	MMIF.RCALT	9.32	6.42	1.11	1.54	55.01	0.94	0.62	0.80
C1	2012	3	24hr	obs	13.79	3.79	1.00	1.00	101.54	1.00	1.00	0.99

site	year	source	avg time	Simulation type	geo mean	geo stddev	MG	VG	RHC	geo R	ff2	TMS
C1	2012	3	24hr	AERC.RCALT	12.97	6.20	1.06	2.08	89.78	0.90	0.78	0.80
C1	2012	3	24hr	AERC.RCALF	15.51	6.62	0.89	3.63	64.10	0.81	0.44	0.63
C1	2012	3	24hr	MMIF.RCALF	9.57	11.97	1.44	15.01	67.25	0.81	0.42	0.59
C1	2012	3	24hr	MMIF.RCALT	9.04	12.40	1.53	12.28	88.92	0.86	0.62	0.60
C1	2012	4	24hr	obs	4.02	8.40	1.00	1.00	45.98	1.00	1.00	0.98
C1	2012	4	24hr	AERC.RCALT	4.31	10.28	0.93	1.28	34.66	0.98	0.78	0.85
C1	2012	4	24hr	AERC.RCALF	5.46	12.31	0.74	2.46	32.52	0.94	0.58	0.72
C1	2012	4	24hr	MMIF.RCALF	3.67	22.78	1.10	6.49	32.23	0.94	0.48	0.69
C1	2012	4	24hr	MMIF.RCALT	2.86	19.84	1.40	3.52	34.61	0.97	0.62	0.70
C1	2012	5	24hr	obs	51.68	5.05	1.00	1.00	497.77	1.00	1.00	0.91
C1	2012	5	24hr	AERC.RCALT	75.94	3.90	0.68	1.27	633.47	1.00	0.78	0.81
C1	2012	5	24hr	AERC.RCALF	92.41	3.58	0.56	1.66	633.64	0.99	0.56	0.74
C1	2012	5	24hr	MMIF.RCALF	87.08	4.09	0.59	1.46	632.25	0.99	0.62	0.78
C1	2012	5	24hr	MMIF.RCALT	75.73	3.88	0.68	1.27	632.17	1.00	0.76	0.85
C2	2010	1	24hr	obs	4.91	5.67	1.00	1.00	39.15	1.00	1.00	0.97
C2	2010	1	24hr	AERC.RCALT	6.09	5.74	0.81	1.12	40.96	0.99	1.00	0.93
C2	2010	1	24hr	AERC.RCALF	4.24	7.71	1.16	1.39	39.10	0.97	0.80	0.86
C2	2010	1	24hr	MMIF.RCALF	4.52	7.32	1.09	1.28	38.67	0.98	0.84	0.90
C2	2010	1	24hr	MMIF.RCALT	6.18	6.05	0.79	1.11	44.25	0.99	1.00	0.91
C2	2010	2	24hr	obs	11.19	5.20	1.00	1.00	76.98	1.00	1.00	0.97
C2	2010	2	24hr	AERC.RCALT	14.38	4.98	0.78	1.12	82.95	0.99	1.00	0.92
C2	2010	2	24hr	AERC.RCALF	9.90	6.92	1.13	1.35	75.07	0.97	0.78	0.86
C2	2010	2	24hr	MMIF.RCALF	10.66	6.56	1.05	1.24	76.33	0.98	0.84	0.91
C2	2010	2	24hr	MMIF.RCALT	14.56	5.24	0.77	1.11	87.52	0.99	1.00	0.91
C2	2010	3	24hr	obs	9.32	5.68	1.00	1.00	61.26	1.00	1.00	0.93
C2	2010	3	24hr	AERC.RCALT	12.73	5.36	0.73	1.14	75.39	1.00	0.96	0.88
C2	2010	3	24hr	AERC.RCALF	8.68	9.28	1.07	1.47	70.16	0.98	0.88	0.88

site	year	source	avg time	Simulation type	geo mean	geo stddev	MG	VG	RHC	geo R	ff2	TMS
C2	2010	3	24hr	MMIF.RCALF	8.97	9.09	1.04	1.39	68.76	0.99	0.90	0.91
C2	2010	3	24hr	MMIF.RCALT	11.27	7.83	0.83	1.28	75.44	0.98	0.86	0.87
C2	2010	4	24hr	obs	3.66	6.82	1.00	1.00	29.09	1.00	1.00	0.96
C2	2010	4	24hr	AERC.RCALT	4.18	9.47	0.88	1.24	36.07	0.99	0.86	0.87
C2	2010	4	24hr	AERC.RCALF	1.95	37.61	1.87	41.77	35.76	0.97	0.78	0.66
C2	2010	4	24hr	MMIF.RCALF	2.17	27.98	1.69	15.54	35.02	0.96	0.78	0.68
C2	2010	4	24hr	MMIF.RCALT	3.62	13.67	1.01	1.90	36.23	0.98	0.86	0.87
C2	2010	5	24hr	obs	59.23	4.39	1.00	1.00	584.72	1.00	1.00	0.92
C2	2010	5	24hr	AERC.RCALT	69.95	3.60	0.85	1.08	460.18	1.00	1.00	0.91
C2	2010	5	24hr	AERC.RCALF	69.22	3.66	0.86	1.07	459.52	1.00	1.00	0.96
C2	2010	5	24hr	MMIF.RCALF	70.85	3.63	0.84	1.08	460.29	1.00	1.00	0.95
C2	2010	5	24hr	MMIF.RCALT	69.80	3.59	0.85	1.08	460.94	1.00	1.00	0.96
C2	2012	1	24hr	obs	3.06	5.62	1.00	1.00	21.80	1.00	1.00	0.91
C2	2012	1	24hr	AERC.RCALT	3.41	6.12	0.90	1.16	26.63	0.98	0.88	0.89
C2	2012	1	24hr	AERC.RCALF	2.61	8.31	1.17	2.20	24.69	0.92	0.68	0.77
C2	2012	1	24hr	MMIF.RCALF	2.56	7.93	1.19	1.93	26.25	0.93	0.72	0.79
C2	2012	1	24hr	MMIF.RCALT	3.34	6.58	0.92	1.22	27.20	0.97	0.84	0.90
C2	2012	2	24hr	obs	6.92	5.23	1.00	1.00	45.93	1.00	1.00	0.92
C2	2012	2	24hr	AERC.RCALT	7.97	6.21	0.87	1.20	55.65	0.98	0.84	0.87
C2	2012	2	24hr	AERC.RCALF	6.09	7.85	1.14	1.84	50.76	0.94	0.64	0.78
C2	2012	2	24hr	MMIF.RCALF	6.33	7.81	1.09	1.75	53.96	0.94	0.68	0.81
C2	2012	2	24hr	MMIF.RCALT	8.08	6.54	0.86	1.26	56.42	0.98	0.80	0.88
C2	2012	3	24hr	obs	9.11	3.96	1.00	1.00	50.95	1.00	1.00	0.92
C2	2012	3	24hr	AERC.RCALT	8.98	7.76	1.02	2.02	63.72	0.96	0.78	0.80
C2	2012	3	24hr	AERC.RCALF	5.72	15.75	1.59	16.28	54.65	0.91	0.54	0.60
C2	2012	3	24hr	MMIF.RCALF	6.15	13.84	1.48	10.61	53.64	0.91	0.44	0.62
C2	2012	3	24hr	MMIF.RCALT	8.59	8.72	1.06	2.67	57.27	0.94	0.50	0.74

site	year	source	avg time	Simulation type	geo mean	geo stddev	MG	VG	RHC	geo R	ff2	TMS
C2	2012	4	24hr	obs	2.81	8.10	1.00	1.00	24.85	1.00	1.00	0.95
C2	2012	4	24hr	AERC.RCALT	2.11	24.70	1.34	4.93	27.89	0.98	0.66	0.70
C2	2012	4	24hr	AERC.RCALF	0.94	70.41	2.99	1041.86	26.04	0.94	0.38	0.52
C2	2012	4	24hr	MMIF.RCALF	1.15	45.98	2.44	137.94	27.56	0.93	0.42	0.54
C2	2012	4	24hr	MMIF.RCALT	1.84	23.12	1.53	4.83	28.05	0.98	0.70	0.70
C2	2012	5	24hr	obs	50.34	5.72	1.00	1.00	707.21	1.00	1.00	0.96
C2	2012	5	24hr	AERC.RCALT	73.76	4.36	0.68	1.28	755.45	1.00	0.78	0.83
C2	2012	5	24hr	AERC.RCALF	75.92	4.33	0.66	1.32	756.41	0.99	0.78	0.84
C2	2012	5	24hr	MMIF.RCALF	76.48	4.29	0.66	1.34	755.74	0.99	0.78	0.84
C2	2012	5	24hr	MMIF.RCALT	73.90	4.31	0.68	1.29	754.92	0.99	0.80	0.85

AERMOD results statistical scores: 24-hour average concentrations.

site	year	source	avg time	Simulation type	geo mean	geo Stddev	MG	VG	RHC	geo R	ff2	TMS
B2	2010	1	PERIOD	obs	0.27	7.33	1.00	1.00	2.54	1.00	1.00	0.82
B2	2010	1	PERIOD	AERC.RCALT	0.20	19.46	1.34	5.55	2.32	0.94	0.40	0.64
B2	2010	1	PERIOD	AERC.RCALF	0.21	16.16	1.28	4.08	2.23	0.94	0.36	0.66
B2	2010	1	PERIOD	MMIF.RCALF	0.25	13.28	1.09	2.69	2.21	0.94	0.52	0.75
B2	2010	1	PERIOD	MMIF.RCALT	0.23	17.27	1.19	3.99	2.32	0.95	0.46	0.69
B2	2010	2	PERIOD	obs	0.66	6.56	1.00	1.00	5.81	1.00	1.00	0.82
B2	2010	2	PERIOD	AERC.RCALT	0.57	16.70	1.16	4.83	5.64	0.94	0.46	0.69
B2	2010	2	PERIOD	AERC.RCALF	0.57	14.11	1.16	3.95	5.34	0.92	0.36	0.67
B2	2010	2	PERIOD	MMIF.RCALF	0.66	12.05	1.00	2.81	5.36	0.93	0.48	0.75
B2	2010	2	PERIOD	MMIF.RCALT	0.65	15.00	1.03	3.65	5.66	0.94	0.48	0.72
B2	2010	3	PERIOD	obs	0.79	6.24	1.00	1.00	6.64	1.00	1.00	0.82
B2	2010	3	PERIOD	AERC.RCALT	0.50	33.36	1.58	48.56	7.49	0.93	0.36	0.57
B2	2010	3	PERIOD	AERC.RCALF	0.44	37.16	1.79	90.02	7.35	0.93	0.34	0.56
B2	2010	3	PERIOD	MMIF.RCALF	0.37	55.68	2.13	690.36	7.34	0.92	0.36	0.55
B2	2010	3	PERIOD	MMIF.RCALT	0.45	44.70	1.76	192.95	7.51	0.92	0.38	0.57
B2	2010	4	PERIOD	obs	0.23	12.37	1.00	1.00	2.70	1.00	1.00	0.82
B2	2010	4	PERIOD	AERC.RCALT	0.00	NA	NA	NA	2.53	0.92	0.40	NA
B2	2010	4	PERIOD	AERC.RCALF	0.00	NA	NA	NA	2.27	0.91	0.40	NA
B2	2010	4	PERIOD	MMIF.RCALF	0.00	NA	NA	NA	2.23	0.91	0.44	NA
B2	2010	4	PERIOD	MMIF.RCALT	0.00	NA	NA	NA	2.49	0.91	0.44	NA
B2	2010	5	PERIOD	obs	6.27	7.02	1.00	1.00	127.75	1.00	1.00	0.85
B2	2010	5	PERIOD	AERC.RCALT	11.15	4.82	0.56	1.61	136.88	1.00	0.58	0.74
B2	2010	5	PERIOD	AERC.RCALF	11.05	4.79	0.57	1.60	131.94	1.00	0.58	0.75
B2	2010	5	PERIOD	MMIF.RCALF	11.33	4.77	0.55	1.66	134.53	1.00	0.56	0.74
B2	2010	5	PERIOD	MMIF.RCALT	11.41	4.79	0.55	1.66	138.55	1.00	0.56	0.74
B2	2011	1	PERIOD	obs	0.23	13.23	1.00	1.00	3.21	1.00	1.00	0.82

B2	2011	1	PERIOD	AERC.RCALT	0.25	14.14	0.93	1.26	2.61	0.98	0.78	0.86
B2	2011	1	PERIOD	AERC.RCALF	0.19	15.97	1.20	1.92	2.05	0.96	0.64	0.75
B2	2011	1	PERIOD	MMIF.RCALF	0.23	12.24	1.00	1.61	2.23	0.96	0.62	0.82
B2	2011	1	PERIOD	MMIF.RCALT	0.27	12.90	0.87	1.23	2.63	0.99	0.82	0.87
B2	2011	2	PERIOD	obs	0.62	10.68	1.00	1.00	7.12	1.00	1.00	0.82
B2	2011	2	PERIOD	AERC.RCALT	0.65	13.20	0.95	1.48	5.66	0.97	0.64	0.81
B2	2011	2	PERIOD	AERC.RCALF	0.52	14.69	1.20	2.52	4.40	0.94	0.52	0.69
B2	2011	2	PERIOD	MMIF.RCALF	0.61	11.57	1.02	1.94	4.57	0.94	0.56	0.79
B2	2011	2	PERIOD	MMIF.RCALT	0.69	12.34	0.89	1.45	5.59	0.97	0.70	0.81
B2	2011	3	PERIOD	obs	0.84	8.55	1.00	1.00	8.93	1.00	1.00	0.83
B2	2011	3	PERIOD	AERC.RCALT	0.54	27.00	1.55	10.39	6.84	0.94	0.46	0.58
B2	2011	3	PERIOD	AERC.RCALF	0.28	67.10	3.04	1914.18	5.38	0.89	0.36	0.47
B2	2011	3	PERIOD	MMIF.RCALF	0.33	51.08	2.51	369.64	5.43	0.89	0.36	0.53
B2	2011	3	PERIOD	MMIF.RCALT	0.54	28.54	1.55	13.18	6.69	0.94	0.46	0.59
B2	2011	4	PERIOD	obs	0.13	47.63	1.00	1.00	3.73	1.00	1.00	0.83
B2	2011	4	PERIOD	AERC.RCALT	0.00	NA	NA	NA	2.83	0.92	0.68	NA
B2	2011	4	PERIOD	AERC.RCALF	0.00	NA	NA	NA	2.04	0.96	0.52	NA
B2	2011	4	PERIOD	MMIF.RCALF	0.00	NA	NA	NA	2.18	0.91	0.64	NA
B2	2011	4	PERIOD	MMIF.RCALT	0.14	39.11	0.94	1.46	2.75	0.99	0.72	0.83
B2	2011	5	PERIOD	obs	7.29	7.22	1.00	1.00	137.57	1.00	1.00	0.85
B2	2011	5	PERIOD	AERC.RCALT	12.39	5.44	0.59	1.44	162.48	1.00	0.66	0.76
B2	2011	5	PERIOD	AERC.RCALF	12.32	5.45	0.59	1.43	163.10	1.00	0.64	0.78
B2	2011	5	PERIOD	MMIF.RCALF	12.39	5.39	0.59	1.45	162.70	1.00	0.64	0.78
B2	2011	5	PERIOD	MMIF.RCALT	12.43	5.41	0.59	1.46	162.45	1.00	0.66	0.79
B3	2010	1	PERIOD	obs	0.19	12.99	1.00	1.00	2.24	1.00	1.00	0.81
B3	2010	1	PERIOD	AERC.RCALT	0.43	4.72	0.44	5.73	2.12	0.99	0.66	0.64
B3	2010	1	PERIOD	AERC.RCALF	0.41	4.75	0.48	5.36	1.90	0.99	0.68	0.65
B3	2010	1	PERIOD	MMIF.RCALF	0.34	6.24	0.56	2.66	1.95	0.99	0.70	0.72

B3	2010	1	PERIOD	MMIF.RCALT	0.35	6.79	0.55	2.31	2.17	1.00	0.68	0.71
B3	2010	2	PERIOD	obs	0.51	10.18	1.00	1.00	4.46	1.00	1.00	0.81
B3	2010	2	PERIOD	AERC.RCALT	1.00	4.45	0.50	3.59	4.28	0.98	0.64	0.67
B3	2010	2	PERIOD	AERC.RCALF	0.92	4.62	0.55	3.31	3.77	0.97	0.66	0.67
B3	2010	2	PERIOD	MMIF.RCALF	0.81	5.92	0.63	2.09	3.83	0.97	0.68	0.75
B3	2010	2	PERIOD	MMIF.RCALT	0.85	6.12	0.59	1.90	4.34	0.99	0.66	0.73
B3	2010	3	PERIOD	obs	0.51	9.99	1.00	1.00	4.17	1.00	1.00	0.81
B3	2010	3	PERIOD	AERC.RCALT	1.13	4.38	0.45	4.15	4.75	0.99	0.78	0.67
B3	2010	3	PERIOD	AERC.RCALF	1.04	4.68	0.49	3.37	4.23	0.98	0.78	0.69
B3	2010	3	PERIOD	MMIF.RCALF	0.83	7.01	0.61	1.68	4.27	0.98	0.80	0.80
B3	2010	3	PERIOD	MMIF.RCALT	0.93	6.32	0.55	1.97	4.86	0.99	0.86	0.76
B3	2010	4	PERIOD	obs	0.10	38.10	1.00	1.00	2.05	1.00	1.00	0.81
B3	2010	4	PERIOD	AERC.RCALT	0.41	5.23	0.23	517.88	2.37	0.99	0.60	0.54
B3	2010	4	PERIOD	AERC.RCALF	0.39	5.38	0.25	383.22	2.23	0.99	0.66	0.57
B3	2010	4	PERIOD	MMIF.RCALF	0.30	8.13	0.32	48.37	2.28	0.99	0.62	0.59
B3	2010	4	PERIOD	MMIF.RCALT	0.31	8.34	0.31	48.10	2.40	0.99	0.62	0.58
B3	2010	5	PERIOD	obs	6.66	6.43	1.00	1.00	118.96	1.00	1.00	0.85
B3	2010	5	PERIOD	AERC.RCALT	9.46	5.32	0.70	1.19	141.50	1.00	0.82	0.84
B3	2010	5	PERIOD	AERC.RCALF	9.46	5.29	0.70	1.19	141.72	1.00	0.82	0.87
B3	2010	5	PERIOD	MMIF.RCALF	9.54	5.32	0.70	1.19	143.29	1.00	0.84	0.87
B3	2010	5	PERIOD	MMIF.RCALT	9.54	5.34	0.70	1.19	143.07	1.00	0.84	0.88
B3	2011	1	PERIOD	obs	0.37	12.84	1.00	1.00	4.62	1.00	1.00	0.83
B3	2011	1	PERIOD	AERC.RCALT	0.42	7.45	0.90	1.62	4.27	0.98	0.78	0.84
B3	2011	1	PERIOD	AERC.RCALF	0.36	8.70	1.03	1.59	3.33	0.97	0.74	0.82
B3	2011	1	PERIOD	MMIF.RCALF	0.35	8.39	1.06	1.76	3.58	0.97	0.70	0.82
B3	2011	1	PERIOD	MMIF.RCALT	0.36	9.66	1.04	1.29	4.30	0.99	0.78	0.87
B3	2011	2	PERIOD	obs	0.96	11.15	1.00	1.00	10.22	1.00	1.00	0.83
B3	2011	2	PERIOD	AERC.RCALT	0.98	6.98	0.98	1.37	8.96	0.99	0.84	0.88

B3	2011	2	PERIOD	AERC.RCALF	0.84	8.44	1.13	1.44	6.96	0.97	0.80	0.83
B3	2011	2	PERIOD	MMIF.RCALF	0.85	8.13	1.12	1.52	7.42	0.97	0.72	0.84
B3	2011	2	PERIOD	MMIF.RCALT	0.88	8.94	1.09	1.18	8.75	0.99	0.92	0.90
B3	2011	3	PERIOD	obs	0.97	11.77	1.00	1.00	10.46	1.00	1.00	0.83
B3	2011	3	PERIOD	AERC.RCALT	1.11	8.68	0.87	1.26	11.86	0.99	0.90	0.89
B3	2011	3	PERIOD	AERC.RCALF	0.60	29.59	1.62	4.93	8.73	0.97	0.80	0.67
B3	2011	3	PERIOD	MMIF.RCALF	0.63	25.69	1.54	3.88	8.58	0.97	0.82	0.74
B3	2011	3	PERIOD	MMIF.RCALT	0.90	14.13	1.07	1.19	11.76	0.99	0.88	0.88
B3	2011	4	PERIOD	obs	0.00	NA	NA	NA	4.11	1.00	0.98	NA
B3	2011	4	PERIOD	AERC.RCALT	0.41	10.50	0.38	1135.41	5.17	0.94	0.70	0.56
B3	2011	4	PERIOD	AERC.RCALF	0.12	82.03	1.28	73.10	3.57	0.89	0.78	0.63
B3	2011	4	PERIOD	MMIF.RCALF	0.13	69.57	1.23	85.59	3.72	0.89	0.78	0.69
B3	2011	4	PERIOD	MMIF.RCALT	0.30	17.69	0.51	95.98	5.04	0.95	0.74	0.59
B3	2011	5	PERIOD	obs	12.83	6.29	1.00	1.00	201.86	1.00	1.00	0.88
B3	2011	5	PERIOD	AERC.RCALT	10.25	6.16	1.25	1.08	170.88	1.00	1.00	0.91
B3	2011	5	PERIOD	AERC.RCALF	11.27	5.35	1.14	1.07	159.27	1.00	1.00	0.95
B3	2011	5	PERIOD	MMIF.RCALF	11.16	5.48	1.15	1.07	164.49	1.00	1.00	0.95
B3	2011	5	PERIOD	MMIF.RCALT	10.41	6.14	1.23	1.07	172.76	1.00	1.00	0.94
B3	2012	1	PERIOD	obs	0.22	10.15	1.00	1.00	2.16	1.00	1.00	0.83
B3	2012	1	PERIOD	AERC.RCALT	0.22	7.39	1.00	1.29	1.64	0.98	0.76	0.86
B3	2012	1	PERIOD	AERC.RCALF	0.23	6.39	0.95	1.52	1.20	0.98	0.62	0.79
B3	2012	1	PERIOD	MMIF.RCALF	0.22	6.44	0.98	1.44	1.21	0.98	0.62	0.85
B3	2012	1	PERIOD	MMIF.RCALT	0.21	8.12	1.05	1.24	1.62	0.98	0.84	0.87
B3	2012	2	PERIOD	obs	0.56	7.99	1.00	1.00	4.54	1.00	1.00	0.82
B3	2012	2	PERIOD	AERC.RCALT	0.54	6.42	1.05	1.29	4.01	0.97	0.78	0.87
B3	2012	2	PERIOD	AERC.RCALF	0.51	6.31	1.12	1.42	2.89	0.96	0.76	0.81
B3	2012	2	PERIOD	MMIF.RCALF	0.50	6.53	1.13	1.35	3.01	0.97	0.74	0.86
B3	2012	2	PERIOD	MMIF.RCALT	0.51	7.21	1.11	1.27	4.13	0.97	0.80	0.84

B3	2012	3	PERIOD	obs	0.76	5.76	1.00	1.00	5.53	1.00	1.00	0.81
B3	2012	3	PERIOD	AERC.RCALT	0.65	8.68	1.17	1.34	6.15	0.99	0.84	0.87
B3	2012	3	PERIOD	AERC.RCALF	0.54	10.95	1.40	2.31	4.46	0.96	0.70	0.71
B3	2012	3	PERIOD	MMIF.RCALF	0.47	13.93	1.63	4.00	4.36	0.96	0.64	0.69
B3	2012	3	PERIOD	MMIF.RCALT	0.55	12.86	1.38	2.55	5.98	0.98	0.82	0.73
B3	2012	4	PERIOD	obs	0.15	22.98	1.00	1.00	2.49	1.00	1.00	0.82
B3	2012	4	PERIOD	AERC.RCALT	0.17	19.93	0.88	1.16	2.41	0.99	0.92	0.92
B3	2012	4	PERIOD	AERC.RCALF	0.00	NA	NA	NA	1.47	0.91	0.70	NA
B3	2012	4	PERIOD	MMIF.RCALF	0.14	24.87	1.02	1.31	1.47	0.99	0.80	0.91
B3	2012	4	PERIOD	MMIF.RCALT	0.00	NA	NA	NA	2.30	0.94	0.92	NA
B3	2012	5	PERIOD	obs	6.28	6.61	1.00	1.00	110.61	1.00	1.00	0.83
B3	2012	5	PERIOD	AERC.RCALT	6.43	6.24	0.98	1.01	115.19	1.00	1.00	0.98
B3	2012	5	PERIOD	AERC.RCALF	7.18	5.65	0.87	1.06	111.46	1.00	1.00	0.96
B3	2012	5	PERIOD	MMIF.RCALF	7.07	5.73	0.89	1.05	111.63	1.00	1.00	0.97
B3	2012	5	PERIOD	MMIF.RCALT	6.54	6.18	0.96	1.02	115.32	1.00	1.00	0.98
C1	2011	1	PERIOD	obs	0.40	5.93	1.00	1.00	4.26	1.00	1.00	0.83
C1	2011	1	PERIOD	AERC.RCALT	0.38	5.99	1.06	1.04	3.77	1.00	1.00	0.96
C1	2011	1	PERIOD	AERC.RCALF	0.35	6.70	1.14	1.14	3.62	0.99	0.90	0.92
C1	2011	1	PERIOD	MMIF.RCALF	0.31	8.26	1.29	1.41	3.76	0.98	0.82	0.85
C1	2011	1	PERIOD	MMIF.RCALT	0.33	7.84	1.22	1.26	3.89	0.99	0.86	0.89
C1	2011	2	PERIOD	obs	0.90	5.60	1.00	1.00	8.93	1.00	1.00	0.83
C1	2011	2	PERIOD	AERC.RCALT	0.85	5.66	1.07	1.04	8.00	1.00	1.00	0.96
C1	2011	2	PERIOD	AERC.RCALF	0.80	6.02	1.13	1.14	7.35	0.98	1.00	0.93
C1	2011	2	PERIOD	MMIF.RCALF	0.72	7.58	1.25	1.39	7.78	0.97	0.84	0.86
C1	2011	2	PERIOD	MMIF.RCALT	0.76	7.23	1.18	1.22	8.04	0.99	0.86	0.90
C1	2011	3	PERIOD	obs	1.09	5.25	1.00	1.00	10.55	1.00	1.00	0.84
C1	2011	3	PERIOD	AERC.RCALT	0.98	5.84	1.11	1.08	10.07	0.99	0.96	0.95
C1	2011	3	PERIOD	AERC.RCALF	1.00	5.66	1.10	1.15	8.87	0.98	0.98	0.92

C1	2011	3	PERIOD	MMIF.RCALF	0.81	7.73	1.34	1.61	8.74	0.97	0.78	0.82
C1	2011	3	PERIOD	MMIF.RCALT	0.79	8.59	1.39	1.71	9.90	0.97	0.82	0.80
C1	2011	4	PERIOD	obs	0.45	5.71	1.00	1.00	4.95	1.00	1.00	0.83
C1	2011	4	PERIOD	AERC.RCALT	0.40	6.99	1.13	1.13	4.81	0.99	0.94	0.93
C1	2011	4	PERIOD	AERC.RCALF	0.37	7.71	1.21	1.29	4.15	0.98	0.84	0.86
C1	2011	4	PERIOD	MMIF.RCALF	0.28	13.16	1.62	3.52	4.09	0.96	0.74	0.72
C1	2011	4	PERIOD	MMIF.RCALT	0.30	11.35	1.49	2.37	4.79	0.97	0.78	0.74
C1	2011	5	PERIOD	obs	7.32	7.93	1.00	1.00	138.69	1.00	1.00	0.83
C1	2011	5	PERIOD	AERC.RCALT	7.70	7.56	0.95	1.01	151.71	1.00	1.00	0.97
C1	2011	5	PERIOD	AERC.RCALF	8.46	6.91	0.86	1.05	148.98	1.00	1.00	0.96
C1	2011	5	PERIOD	MMIF.RCALF	8.28	7.05	0.88	1.04	148.19	1.00	1.00	0.97
C1	2011	5	PERIOD	MMIF.RCALT	7.65	7.61	0.96	1.01	150.82	1.00	1.00	0.99
C1	2012	1	PERIOD	obs	0.31	7.63	1.00	1.00	4.32	1.00	1.00	0.83
C1	2012	1	PERIOD	AERC.RCALT	0.22	6.90	1.41	1.18	2.49	1.00	0.88	0.80
C1	2012	1	PERIOD	AERC.RCALF	0.26	6.15	1.23	1.39	2.27	0.97	0.82	0.85
C1	2012	1	PERIOD	MMIF.RCALF	0.24	6.33	1.32	1.48	2.40	0.96	0.72	0.81
C1	2012	1	PERIOD	MMIF.RCALT	0.21	8.05	1.51	1.26	2.55	0.99	0.82	0.84
C1	2012	2	PERIOD	obs	0.73	6.71	1.00	1.00	8.68	1.00	1.00	0.83
C1	2012	2	PERIOD	AERC.RCALT	0.52	6.31	1.41	1.21	5.12	0.99	0.86	0.79
C1	2012	2	PERIOD	AERC.RCALF	0.56	6.13	1.30	1.47	4.69	0.96	0.70	0.80
C1	2012	2	PERIOD	MMIF.RCALF	0.52	6.49	1.39	1.54	4.96	0.95	0.72	0.80
C1	2012	2	PERIOD	MMIF.RCALT	0.49	7.27	1.47	1.30	5.28	0.99	0.78	0.83
C1	2012	3	PERIOD	obs	0.83	5.69	1.00	1.00	8.93	1.00	1.00	0.82
C1	2012	3	PERIOD	AERC.RCALT	0.53	8.59	1.57	1.90	5.77	0.96	0.86	0.73
C1	2012	3	PERIOD	AERC.RCALF	0.56	9.52	1.49	2.70	5.15	0.93	0.68	0.71
C1	2012	3	PERIOD	MMIF.RCALF	0.41	15.58	2.03	10.45	5.19	0.91	0.70	0.64
C1	2012	3	PERIOD	MMIF.RCALT	0.43	14.25	1.93	6.46	6.01	0.94	0.80	0.65
C1	2012	4	PERIOD	obs	0.27	11.61	1.00	1.00	4.41	1.00	1.00	0.83

C1	2012	4	PERIOD	AERC.RCALT	0.18	14.34	1.49	1.29	2.86	1.00	0.90	0.80
C1	2012	4	PERIOD	AERC.RCALF	0.18	17.24	1.46	1.82	2.51	0.98	0.72	0.76
C1	2012	4	PERIOD	MMIF.RCALF	0.13	29.22	2.02	6.36	2.48	0.97	0.62	0.65
C1	2012	4	PERIOD	MMIF.RCALT	0.14	23.91	1.96	3.15	2.82	0.99	0.78	0.70
C1	2012	5	PERIOD	obs	5.27	8.02	1.00	1.00	101.40	1.00	1.00	0.83
C1	2012	5	PERIOD	AERC.RCALT	4.35	7.11	1.21	1.07	97.07	1.00	1.00	0.94
C1	2012	5	PERIOD	AERC.RCALF	4.95	5.95	1.06	1.14	95.30	1.00	1.00	0.96
C1	2012	5	PERIOD	MMIF.RCALF	4.74	6.22	1.11	1.12	95.43	1.00	1.00	0.96
C1	2012	5	PERIOD	MMIF.RCALT	4.40	6.96	1.20	1.07	97.09	1.00	1.00	0.95
C2	2010	1	PERIOD	obs	0.29	9.19	1.00	1.00	2.27	1.00	1.00	0.81
C2	2010	1	PERIOD	AERC.RCALT	0.27	8.07	1.06	1.11	2.66	0.99	1.00	0.94
C2	2010	1	PERIOD	AERC.RCALF	0.21	10.77	1.40	1.36	2.22	0.98	0.78	0.81
C2	2010	1	PERIOD	MMIF.RCALF	0.23	9.88	1.28	1.30	2.43	0.98	0.82	0.85
C2	2010	1	PERIOD	MMIF.RCALT	0.27	8.56	1.05	1.09	2.72	0.99	1.00	0.95
C2	2010	2	PERIOD	obs	0.70	8.56	1.00	1.00	4.83	1.00	1.00	0.81
C2	2010	2	PERIOD	AERC.RCALT	0.67	6.98	1.05	1.16	5.59	0.99	0.96	0.93
C2	2010	2	PERIOD	AERC.RCALF	0.49	9.84	1.43	1.31	4.53	0.99	0.84	0.82
C2	2010	2	PERIOD	MMIF.RCALF	0.54	9.02	1.30	1.21	4.86	0.99	0.86	0.88
C2	2010	2	PERIOD	MMIF.RCALT	0.67	7.46	1.05	1.12	5.77	0.99	1.00	0.94
C2	2010	3	PERIOD	obs	0.64	11.75	1.00	1.00	5.64	1.00	1.00	0.81
C2	2010	3	PERIOD	AERC.RCALT	0.71	7.87	0.91	1.37	6.81	0.99	0.80	0.85
C2	2010	3	PERIOD	AERC.RCALF	0.46	16.61	1.40	1.34	5.48	1.00	0.86	0.82
C2	2010	3	PERIOD	MMIF.RCALF	0.48	15.72	1.34	1.22	5.31	1.00	0.88	0.88
C2	2010	3	PERIOD	MMIF.RCALT	0.62	11.34	1.05	1.12	6.79	0.99	1.00	0.92
C2	2010	4	PERIOD	obs	0.21	14.41	1.00	1.00	2.22	1.00	1.00	0.81
C2	2010	4	PERIOD	AERC.RCALT	0.20	15.00	1.04	1.08	2.79	1.00	1.00	0.94
C2	2010	4	PERIOD	AERC.RCALF	0.00	NA	NA	NA	2.13	0.95	0.70	NA
C2	2010	4	PERIOD	MMIF.RCALF	0.10	47.00	2.21	9.88	2.27	0.99	0.72	0.64

C2	2010	4	PERIOD	MMIF.RCALT	0.17	22.03	1.23	1.42	2.72	0.99	0.88	0.85
C2	2010	5	PERIOD	obs	8.28	5.40	1.00	1.00	124.53	1.00	1.00	0.85
C2	2010	5	PERIOD	AERC.RCALT	6.50	6.14	1.27	1.08	110.17	1.00	1.00	0.92
C2	2010	5	PERIOD	AERC.RCALF	7.02	5.79	1.18	1.04	108.08	1.00	1.00	0.96
C2	2010	5	PERIOD	MMIF.RCALF	7.07	5.77	1.17	1.03	107.79	1.00	1.00	0.96
C2	2010	5	PERIOD	MMIF.RCALT	6.54	6.13	1.27	1.08	110.04	1.00	1.00	0.94
C2	2012	1	PERIOD	obs	0.26	7.62	1.00	1.00	2.68	1.00	1.00	0.82
C2	2012	1	PERIOD	AERC.RCALT	0.21	7.48	1.24	1.12	2.15	0.99	0.94	0.89
C2	2012	1	PERIOD	AERC.RCALF	0.17	8.30	1.51	1.82	1.69	0.95	0.74	0.74
C2	2012	1	PERIOD	MMIF.RCALF	0.18	7.58	1.49	1.72	1.80	0.95	0.78	0.79
C2	2012	1	PERIOD	MMIF.RCALT	0.20	7.75	1.30	1.17	2.18	0.99	0.88	0.86
C2	2012	2	PERIOD	obs	0.63	6.84	1.00	1.00	5.82	1.00	1.00	0.82
C2	2012	2	PERIOD	AERC.RCALT	0.48	7.73	1.31	1.16	4.72	0.99	0.88	0.86
C2	2012	2	PERIOD	AERC.RCALF	0.41	8.01	1.54	1.71	3.55	0.96	0.80	0.75
C2	2012	2	PERIOD	MMIF.RCALF	0.42	7.34	1.52	1.55	3.74	0.97	0.82	0.81
C2	2012	2	PERIOD	MMIF.RCALT	0.47	7.87	1.34	1.20	4.68	0.99	0.88	0.85
C2	2012	3	PERIOD	obs	0.77	6.21	1.00	1.00	6.84	1.00	1.00	0.82
C2	2012	3	PERIOD	AERC.RCALT	0.47	12.60	1.64	2.51	6.71	0.98	0.76	0.75
C2	2012	3	PERIOD	AERC.RCALF	0.33	22.03	2.36	18.23	4.72	0.95	0.70	0.57
C2	2012	3	PERIOD	MMIF.RCALF	0.33	18.54	2.36	11.19	4.55	0.96	0.72	0.63
C2	2012	3	PERIOD	MMIF.RCALT	0.44	13.13	1.74	2.85	6.50	0.98	0.76	0.67
C2	2012	4	PERIOD	obs	0.22	13.24	1.00	1.00	2.88	1.00	1.00	0.82
C2	2012	4	PERIOD	AERC.RCALT	0.11	37.52	2.05	5.77	2.79	0.99	0.74	0.67
C2	2012	4	PERIOD	AERC.RCALF	0.00	NA	NA	NA	1.80	0.96	0.62	NA
C2	2012	4	PERIOD	MMIF.RCALF	0.06	63.53	3.87	234.87	1.84	0.95	0.64	0.56
C2	2012	4	PERIOD	MMIF.RCALT	0.10	37.13	2.24	7.13	2.65	0.99	0.72	0.60
C2	2012	5	PERIOD	obs	5.69	6.66	1.00	1.00	86.70	1.00	1.00	0.82
C2	2012	5	PERIOD	AERC.RCALT	5.31	6.68	1.07	1.01	85.23	1.00	1.00	0.98

C2	2012	5	PERIOD	AERC.RCALF	5.76	6.05	0.99	1.02	85.51	1.00	1.00	0.99
C2	2012	5	PERIOD	MMIF.RCALF	5.58	6.24	1.02	1.02	85.59	1.00	1.00	0.99
C2	2012	5	PERIOD	MMIF.RCALT	5.22	6.81	1.09	1.01	85.07	1.00	1.00	0.98

[Blank]

APPENDIX C: REPORT DISK

Volume 3 results can be requested from

Eric Wolvovsky
BOEM/OEP/DEA
Mail Stop: VAM-OEP
45600 Woodland Road
Sterling VA 20166
703-787-1719
Email: eric.wolvovsky@boem.gov